REDUCED SENSITIVITY OF GENOTYPE 3 HEPATITIS C VIRUS TO DIRECT ACTING ANTIVIRALS

Peter Alexander Cornelius Wing

A thesis submitted to Queen Mary, University of London in partial fulfilment of the requirements for the degree of Doctor of Philosophy

For My Family

ABSTRACT

Sofosbuvir is a uridine based nucleotide inhibitor of the hepatitis C viral (HCV) polymerase that is the backbone of many treatment regimens. In combination with drugs targeting other viral enzymes (including the poorly potent guanosine analogue ribavirin or highly potent inhibitors of viral NS5A or protease) most patients clear virus and resistance to sofosbuvir is rare, allowing effective retreatment with sofosbuvir. Patients with Genotype 3 HCV respond less well than other genotypes and response is reduced in those previously exposed to interferon. Here we show that patient-derived virus from patients with Genotype 3 HCV who relapse to sofosbuvir-based therapies have a reduced sensitivity to SOF in an *in-vitro* phenotyping assay. Analysis of viral sequencing data revealed two distinct polymorphisms (A150V and K206E) in the HCV polymerase that are associated with treatment failure and *in-vitro*; they reduce sofosbuvir sensitivity against genotype 3 hepatitis C virions. However both polymorphisms modify the cellular response to type I interferon and in cells lacking response to interferon the impact on sofosbuvir sensitivity is minimal. The A150V polymorphism reduces the response to interferon 70 fold whereas the K206E substitution has minimal effects on interferon in isolation but in combination with A150V reduces the response 100 fold. Preliminary data indicates that the A150V polymorphism interferes with the late response to type I interferons enabling the virus to overcome the induction of interferon-stimulated genes. These data indicate a complex interaction between direct acting antiviral drugs and the innate antiviral response.

Acknowledgements

Firstly, I would like to thank Professor Graham Foster for his encouragement, guidance, endless optimism and always persuading me to do just ‘one more experiment’ so that we might finally get to ‘fat city’. Also to Mel Jones, who throughout it all kept my enthusiasm in check on the days science was kind and helped me through days when science was not, usually by saying ‘Screw it! Lets go to the pub!’ Thanks also to Helen Heath for keeping me company in the lab, providing me with coffee when I needed it the most but also for our discussions on the interferon and STAT experiments. To everyone who worked in the Gastro Lab: Sam De Silva, Michelle Cheung, Upkar Gill, Jyoti Hansi, Jibran Mecci, Karen Hunt, Tanya Marchbank, Naheed Choudhry, Nick Bockett and Alistair Symonds. It was great fun working in the lab and I thoroughly enjoyed every minute, even on days when it looked like I didn’t.

I am extremely grateful to Professor John McLauchlan and Ana De Silva (Centre for Virus Research, University of Glasgow) for their help with the viral sequencing and critical discussions; to HCVRUK for the samples included in this study and to Professors Charles Rice (Rockefeller) and Jens Bukh (University of Copenhagen) for both the S52 and DBN clones. Also to Luke Gammon (Queen Mary, University of London) for his help and guidance with the INCELL automated microscope.

Finally, to my parents Christopher and Mary Wing, brother Edward Wing and girlfriend Laura Roberts, for their unwavering support, encouragement and help in both the write up and the ‘bad science’ days.

Communications Arising from Research

Papers

Jones, M., Cunningham, M. E., **Wing, P.,** DeSilva, S., Challa, R., Sheri, A., Padmanabhan, S., Iyer, R. P., Korba, B. E. & other authors. (2017). SB 9200, a novel agonist of innate immunity, shows potent antiviral activity against resistant HCV variants. *J Med Virol*.

Manuscripts in Preparation

Wing P, Jones M, Cunningham M E, DeSilva S, Cheung M, Filipe A, McLauchlan J, Barnes E, Foster G R. Reduction in Sofosbuvir sensitivity in Genotype 3 virus in Cirrhotic treatment failures. *N Engl J Med*

Oral Presentations

Wing P, Jones M, Cunningham M E, DeSilva S, Cheung M, Filipe A, McLauchlan J, Barnes E, Foster G R. Reduction in Sofosbuvir and Ribavirin sensitivity in Genotype 3 Hepatitis C Virus from patients who relapse to all oral therapy. **International Symposium for the study of Hepatitis C and related viruses 2016 Kyoto**. Registration bursary awarded.

Wing P, Jones M, Cunningham M E, DeSilva S, Filipe A, McLauchlan J, Barnes E, Foster G R. Reduction in sensitivity to Sofosbuvir and Ribavirin in patients with Genotype 3 Hepatitis C Virus who relapse following all oral antiviral therapy. **14th UK Meeting on the pathogenesis and study of the Hepatitis C virus 2016 Rydal Hall.**

Wing P, Jones M, Cunningham M E, DeSilva S, Filipe A, McLauchlan J, Barnes E, Foster G R. Resistance to sofosbuvir in Genotype 3 HCV – identification of novel mutations reducing response to therapy. **London Liver Meeting 2016**

Poster presentations

Wing P, Jones M, Cunningham M E, DeSilva S, Filipe A, McLauchlan J, Foster G R. Pre-Treatment Reduction in Sensitivity to Sofosbuvir and Ribavirin in Patients with Genotype 3 Hepatitis C Virus (HCV) Who Relapse Following All Oral Antiviral Therapy. **European Association for the Study of the Liver 2016 Barcelona.**

Wing P, Jones M, Cunningham M E, DeSilva S, Cheung M, Filipe A, Foster G R. Hepatitis C genotype 3 sensitivity to Ribavirin/Sofosbuvir investigated using capture fusion assay. **International Symposium for the study of Hepatitis C and related viruses 2015 Strasbourg.**

Table of Contents

List of Figures

List of Tables

Commonly used Abbreviations

BOC	Boceprevir
BSA	Bovine Serum Albumin
cDNA	Complementary deoxyribonucleic Acid
DAA	Direct Acting Antiviral
DAC	Daclatasvir
DMEM	Dulbreccos Modified Eagle Medium
DMSO	Dimethyl sulfoxide
DNA	Deoxyribonucleic Acid
ER	Endoplasmic reticulum
FACS	Fluorescence associated cell sorting
G	Genotype
FCS	Foetal Calf Serum
HCV	Hepatitis C Virus
HCVcc	Cell culture produced Hepatitis C Virus
IC_{50}	Inhibitory Concentration at 50%
IFN	Interferon
IRES	Internal Ribosome Entry Site
ISDR	Interferon Sensitivity Determining Region
ISG	Interferon Stimulated Gene
ISRE	Interferon Stimulated Response Element
IU	International Units
JFH	Japanese Fulminant Hepatitis
LD	Lipid Droplet
LDV	Ledipasvir
NTP	Nucleoside triphosphate
NS	Non-Structural protein
PBMC	Peripheral Blood Mononuclear Cell
PBS	Phosphate Buffered Saline
PCR	Polymerase Chain Reaction
PEG	Polyethylene Glycol
pegIFN	Pegylated Interferon

PFA	Paraformaldehyde
PMA	Phorbol 12-myrisate 13-acetate
qPCR	Quantitative Polymerase Chain reaction
RAV	Resistance Associated Variant
RBV	Ribavirin
RIG-1	Retinoic Acid Inducible Gene-1
RNA	Ribonucleic Acid
RPMI	Roswell Park Memorial Institute medium
RT-qPCR	Reverse Transcription-Quantitative Polymerase Chain Reaction
SD	Standard Deviation
SEAP	Secreted Alkaline Phosphatase
SEM	Standard Error
SOF	Sofosbuvir
STAT	Signal-Transducer and Activator of Transcription
SVR	Sustained Virological Response
UTR	Un-translated region
VEL	Velpatasvir
VSVG	Vesicular Stomatitis Virus G protein

1 Introduction

Hepatitis C Virus (HCV) remains a major human pathogen. Hepatitis C-related liver disease causes 300-500,000 deaths each year, with a further 150 million people infected worldwide; 3.2 million of these are within the European union (Razavi, 2017; World Health Organization, 2015). Infection with HCV causes both acute and chronic liver disease developing into cirrhosis of the liver and hepatocellular carcinoma. In recent years treatment of this virus has dramatically improved from sub-optimal pegylated-interferon (pegIFN) and ribavirin (RBV) therapy to a new age of direct acting antivirals (DAAs). The new DAA regimens achieve a high cure rate or sustained virological response (SVR) for the majority of the 6 main HCV genotypes. HCV genotype 3 (G3), which infects 58 million people globally (Gower *et al.*, 2014), remains difficult to treat with DAA therapy with relapse to new treatments more common than any other genotype. The virological reasons why G3 HCV is more refractory to new treatments remains unknown, yet there remains a clinical need to understand why relapse is more common in this genotype.

1.1 Discovery of HCV

HCV was initially classified as Non-A Non-B viral Hepatitis (NANBH) by two studies showing the majority of transfusion-associated hepatitis patients tested negative for specific serological tests for Hepatitis A and Hepatitis B (Alter *et al.*, 1975; Feinstone *et al.*, 1975). Both studies speculated that the aetiological origin of post-transfusion NANBH was likely viral in origin, triggering a search for the virus responsible for this condition. It was not until 1989 that the causative agent was identified and proved to be the aetiological origin by scientists working at the CDC, NIH and industry. The new virus was called hepatitis C. The process of discovery began with blind

immunoscreening of cDNA libraries with serum antibodies derived from infected patients revealing a positive clone. Further experiments revealed that cDNA from this clone hybridised to a 9600-nucleotide RNA molecule distally related to *Flaviviral* genomes. Additionally, circulating antibodies from this group of patients were shown to be specific for gene products of this clone providing further evidence for a viral aetiology of NANBH (Choo *et al.*, 1989; Reviewed in Houghton, 2009).

1.2 HCV genotypes

HCV like other RNA viruses encodes its own RNA-dependent RNA polymerase to replicate its genome. The lack of proof reading by this polymerase introduces mutations at a rate of $8.4x10^{-3}$-$1.4x10^{-6}$ per site with each round of replication (Powdrill *et al.*, 2011). This high level of genetic variability of HCV is a key element in HCV persistence, resistance to therapy and the development of genetically distinct genotypes (Figlerowicz *et al.*, 2003; Jackowiak *et al.*, 2014).

The seven known HCV genotypes vary in their geographical distribution. Genotype 1 is the most prevalent comprising approximately 83.4 million cases worldwide, with the majority of cases in North America. Genotype 3 is the next most prevalent comprising of an estimated 54.3 million cases worldwide most of which are located in South Asia. Genotypes 2,4 and 6 make up most the remaining of the global HCV cases with genotype 5 causing the fewest cases (Messina *et al.*, 2015). Several HCV subtypes have also emerged; specifically genotypes 1a, 1b, 2a and 3a in high-income HCV infected countries. These were thought to have spread rapidly in the days before the discovery of HCV by unscreened blood transfusions and intravenous drug use (Magiorkinis *et al.*, 2009; Pybus *et al.*, 2005)

1.3 Biology of the Hepatitis C Virus

HCV is an enveloped, single-stranded positive sense RNA virus from the *Flaviviridae* family (Lindenbach *et al.*, 2013). The 9.6 Kb genome of HCV consists of a single open reading frame flanked by a 5' and 3' un-translated region (UTR) (Fig 1.1). The 5'UTR contains 6 stem loop structures, which form the internal ribosome entry site (IRES), critical for the translation of the non-capped HCV RNA genome (Wang *et al.*, 1993). The 5'UTR also regulates HCV RNA replication and translation by interaction with the liver specific micro RNA-122 (miR122), which has been shown to increase levels of HCV replication when expressed in non-hepatic cells (Chang *et al.*, 2008). The 3' UTR contains a variable region followed by a (poly U/UC) tract ending with a highly conserved 3' tail shown to be essential for RNA replication (Kolykhalov *et al.*, 1996). The poly (U/UC) tract is one of the key molecular patterns recognised by the innate retinoic acid-inducible-gene-I (RIG-I) receptor during HCV infection (Saito *et al.*, 2008).

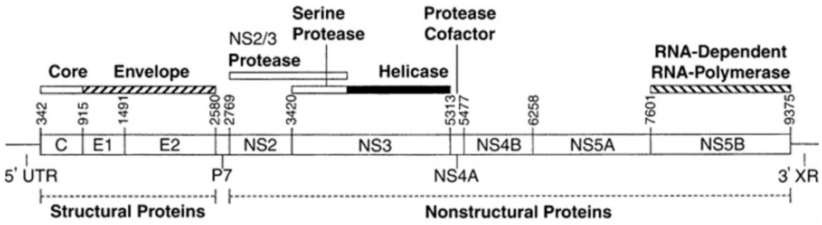

Gene	Protein Size	Function
Core (C)	21 kDa	• Forms the capsid that surrounds the HCV genome • The protein is transported to the site of HCV particle assembly in the endoplasmic reticulum (ER) and is essential for infectious virion production.
E1/E2	21 kDa (E1) 39 kDa (E2)	• E1 and E2 form the exterior envelope of the virus particle • Key for receptor binding and entry of HCV into the target cell.
P7	6 kDa	• Key for viral assembly • While discovered to be non-essential for replication is crucial for infectious virion production.
NS2	23 kDa	• Protease that forms a complex with NS3 to cleave the NS2/NS3 junction. • Essential for infectious virus production not replication.
NS3/NS4A	69 kDa (NS3) 5.6 kDa (NS4A)	• NS3 and NS4A form a the NS3-4A protein containing a serine protease and RNA helicase domains. • The serine protease domain cleaves the other HCV non-structural proteins. • The RNA helicase unwinds double stranded versions of the RNA genome during replication
NS4B	27 kDa	• Transmembrane protein that forms the 'membranous web compartment'; the supposed site of HCV replication
NS5A	56-58 kDa	• Exists in two forms: basally-phosphorylated (56 kDa) and hyper-phosphorylated (58 kDa) • Phosphorylation status is important in RNA replication as its inhibition promotes HCV replication. • Interacts with cellular proteins such as STAT1, key in the cellular IFN response to the virus.
NS5B	68 kDa	• Error-Prone RNA-dependent RNA polymerase • Synthesises acomplementary negative strand of the genome , which acts as the template for RNA genome replication.

Fig 1.1: HCV genome structure and protien functions
Schematic of the HCV genome adapted from (Liang *et al.*, 2000) showing the positions of the genes as well as the distinction between structural and non-structural proteins. The functional properties of the viral proteins are described in the table below the schematic.

1.3.1 Viral Particle

The HCV genome encodes a single poly-protein that is cleaved first by host and then viral proteases into 10 functional proteins that consist of structural proteins (those that comprise the viral particle) and non-structural proteins (involved in genome replication, particle assembly and immune interference) (Fig 1.1). The HCV structural proteins core, E1 and E2 as well as the RNA genome form the membrane enveloped HCV viral particle, which is approximately 40-50nm in diameter (Bradley *et al.*, 1985) (Fig 1.2). The interaction between the RNA genome and the core protein forms the viral

nucleocapsid. A lipid rich viral envelope shrouds the nucleocapsid with the E1/E2 glycoproteins displayed on the surface of the particle to mediate viral entry via host cell receptor binding (Nielsen *et al.*, 2004).

HCV viral particles derived from both patient sera and cell culture have a remarkably low buoyant density compared to other enveloped RNA viruses [Reviewed in (Lindenbach & Rice, 2013)]. This is due to the interaction of HCV particles with serum lipoproteins such as ApoA, ApoB, ApoC, and ApoE forming 'lipoviral particles' (LVPs) that are thought to facilitate entry and prevent antibody neutralisation (Grove *et al.*, 2007; Meuleman *et al.*, 2012). The exact structure of HCV within LVPs remains unknown and questions remain as to the interactions that mediate LVP formation as well as how the HCV glycoproteins are arranged to support viral entry.

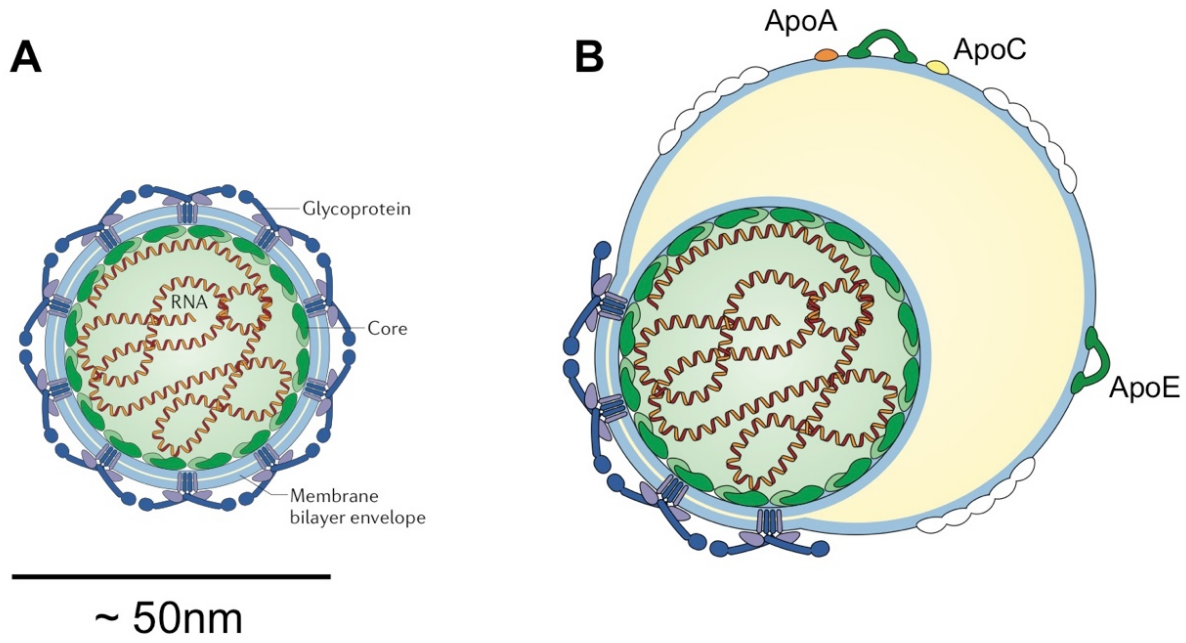

Fig 1.2: The HCV particle
(A) Schematic of a HCV particle. E1–E2 glycoproteins are located on the surface encompassing the viral nucleocapsid consisting of the core protein and viral RNA. (B) Proposed representation of a lipoviral particle, showing the virus sharing a lipid envelope with lipoprotein particles. Adapted from (Lindenbach & Rice, 2013).

1.3.2 Core

The HCV core protein is an integral component of the viral nucleocapsid, the mature form of which is a 21 kDa protein α-helical protein with RNA and lipid binding properties (Santolini *et al.*, 1994). Compared to other Flaviviruses such as West Nile and Dengue HCV core is unique in terms of size and increased hydrophobicity [reviewed in (Gawlik & Gallay, 2014)]. The protein itself is 191 amino acids in length consisting of two distinct domains in terms of amino acid composition and hydrophobic properties (McLauchlan, 2000). Domain 1 is hydrophilic comprised of basic residues located at the N-terminal region of the protein as well as RNA binding properties, thought to mediate packaging of the HCV genome into the viral particle during particle assembly (Cristofari *et al.*, 2004). Domain 2 comprises the C-terminal end of core and comprised of two-amphipathic α-helices separated by a hydrophobic loop. This motif is critical for interaction of the protein with lipid droplet (LD) membranes and the endoplasmic reticulum (Boulant *et al.*, 2006). Core association with LDs along with its RNA binding properties is thought to be the anchor around which the formation of the LVPs occurs. NS5A is thought to deliver the HCV genome to core anchored in the LD membrane to form the viral nucleocapsid, which is then fully immersed into the center of the LD subsequently forming the LVP [Reviewed in (Bartenschlager *et al.*, 2011; Lindenbach & Rice, 2013).

1.3.3 Envelope Glycoproteins E1 and E2

HCV has two envelope glycoproteins E1 and E2 that are heavily glycosylated and critical for entry. Both proteins have distinct functions; E1 forms the fusogenic subunit while interactions with cellular receptors during entry are mediated by E2.

Glycosylation sites on E1 and E2 are highly conserved and comprise of mannose based side chains which play a crucial role in folding of the glycoprotein as well as interactions with entry receptors (Goffard *et al.*, 2005). E1 and E2 are type I transmembrane proteins forming a non-covalent heterodimer within infected cells, however in the context of the viral particle they form large covalent complexes stablised by disulphide bonds (Vieyres *et al.*, 2010). The key role of the HCV glycoproteins is to interact with a range of receptors (critically CD81 and scavenger receptor type B class 1, discussed further in section 1.4.1) to gain entry of the circulating virus into the cell (Grove *et al.*, 2007; Scarselli *et al.*, 2002; Sharma *et al.*, 2011). E2 is central to this process as well as immune evasion due to the presence of two hypervariable regions, which have a particularly high rate of mutations driven by the constant targeting of E2 by neutralising antibodies (Boulestin *et al.*, 2002; Polyak *et al.*, 1998)

1.3.4 p7

p7, also known as the HCV viroporin, is a small 6kDa protein consisting of only 66 amino acids with two α helical transmembrane domains. During HCV polyprotein processing p7 is cleaved by host signal peptidases within the ER. Its transmembrane domains span the ER membrane with N- and C-terminus orientated towards the ER lumen (Carrere-Kremer *et al.*, 2002). While the precise function of p7 ion channel is unknown it is indispensable for virus particle assembly and release (Yu *et al.*, 2009). Studies have suggested that the transmembrane domain proximal to the C-terminus of p7 functions as a signal sequence for NS2 promoting its translocation to the lumen of the ER for cleavage by host signal peptidases (Tellinghuisen *et al.*, 2007). Additionally, p7 has been associated with suppressing acidification of intracellular

organelles thereby protecting newly formed virions from pre-mature acid inducted conformational changes (Wozniak *et al.*, 2010).

1.3.5 NS2

NS2 is a key non-structural protein essential for the HCV replication cycle. It is the first of two HCV proteases that process the HCV polyprotein into functional viral proteins. The 23 kDa protein consists of three transmembrane domains within the highly hydrophobic N-terminus of the protein, which insert into the ER membrane (Jirasko *et al.*, 2010). The C-terminal end of the protein however protrudes into the cytoplasm and contains the catalytic residues essential for the cysteine protease activity of NS2 the function of which is significantly enhanced by the N-terminal part of NS3 (Schregel *et al.*, 2009). Cleavage at the NS2/3 junction is a key stage of the viral lifecycle, critical to the release of the mature NS3 protein without which processing of further essential non-structural proteins such as the NS4-NS5B cannot occur.

1.3.6 NS3/4A protease

The NS3/4A protease is the largest viral protein complex in the HCV life with a range of functions mainly, but not limited to, processing of the HCV polyprotein. NS3 is a 67kDa protein with the serine protease active site located in the N-terminal region of the protein, while the C-terminus is associated with NTPase/helicase activity (Gallinari *et al.*, 1998). NS4A is a much smaller protein in comparison to NS3. Its highly hydrophobic N-terminus is responsible for targeting NS3 to the ER membrane and anchoring the NS3/4A complex to the ER membrane through a transmembrane helix (Bartenschlager *et al.*, 1993). The C-terminal region of the NS4 associates with the core of the NS3 activating the serine protease active site and increasing the efficiency

of protease cleavage (Kim *et al.*, 1996). In addition to cleavage of the HCV polyprotein the NS3 NTPase/helicase uses ATP hydrolysis in a “ratchet like fashion” to unwind double stranded or single stranded RNA with substantial secondary structure (Gu & Rice, 2010). The helicase activity is critical for HCV RNA replication and is also implicated in infectious viral particle assembly though the exact role remains elusive [reviewed in (Murray *et al.*, 2008)].

The sub-cellular localisation of NS3/4 is not just restricted to the ER membrane and HCV replication complexes but to a lesser extent the membranes of mitochondria (Horner *et al.*, 2011). This additional location of NS3/4A may explain how the protease is able to cleave the mitochondrial antiviral signalling protein (MAVS) a critical component of the RIG-I signalling pathway (Meylan *et al.*, 2005). In addition to MAVS cleavage NS3/4A also cleaves TIR-domain containing adaptor-inducing interferon-ß (TRIF) an essential adaptor in TLR3 signalling as well as blocking IRF-3 nuclear translocation of interferon-regulatory factor 3 (IRF-3) (Foy *et al.*, 2005; Foy *et al.*, 2003; Li *et al.*, 2005). These inhibitory events on the innate immune response impede the induction of IFN inducible genes blunting the ability of the cell to response effectively to HCV infection.

1.3.7 NS4B

The specific function of NS4B is relatively less-well characterised yet it is essential for the formation of the HCV replication complex. It is a small 27 kDa protein consisting of two amphipathic α-helices in the N-terminus, four transmembrane domains in the centre of the protein and a further two highly conserved α-helices in the C-terminus of the protein (Alexopoulou *et al.*, 2001; Lundin *et al.*, 2006; Meylan *et al.*, 2005). NS4B

localises to the ER membrane where it interacts with other viral RNA and non-structural proteins, inducing alterations to membranous vesicles that function as a scaffold for the HCV replication complex, referred to as the membranous web (Gosert *et al.*, 2003). Microscopy studies have shown that NS4B forms oligomers with the N- and C-terminal helices crucial for oligomerisation. Mutations that disrupt NS4B oligomerisation perturb membranous web formation demonstrating that NS4B complexes are essential for the induction of the HCV replication scaffold (Paul *et al.*, 2011). While the specific details of the various interactions NS4B has with the HCV non-structural proteins are still elusive, its pivotal role in the formation of the membranous web is a lynchpin in the establishment of HCV replication.

1.3.8 NS5A

Perhaps one of the most extensively studies HCV non-structural proteins; NS5A is a hydrophilic phosphoprotein with key roles in replication, assembly and viral-host interactions. Originally NS5A attracted considerable interest due to mutations within a specific region of the protein termed the interferon sensitivity determining region (ISDR) appearing to modulate response to IFNα therapy (Enomoto *et al.*, 1996) but it is now a key target for antiviral drugs. The structure of NS5A comprises of three domains separated by two low complexity sequences (LCS) (Tellinghuisen *et al.*, 2004). Domains I and II are primarily involved in RNA replication with crystal structure studies indicating that a dimeric form of domain I contains a basic groove in-between the dimers, which may form an RNA binding site (Lambert *et al.*, 2014; Love *et al.*, 2009). Domain I also contains a lipid biding motif critical for the association of NS5A with lipid droplets (Miyanari *et al.*, 2007). Domain III, while dispensable for RNA replication is essential for virion assembly (Appel *et al.*, 2008; Kim *et al.*, 2011;

Tellinghuisen *et al.*, 2008). Furthermore, deletions and insertions within domains II and III are relatively well tolerated and several reporter viruses and replicons have been generated with insertions of fluorescent genes. A recent example is the insertion of the nano luciferase gene in the c-terminal end of domain III in both a subgenomic replicon and infectious viral system (Eyre *et al.*, 2017). Surprisingly the authors uncovered the presence of NS5A in the extracellular environment in both cell culture models and then in a chimeric mouse model, implying that NS5A may have additional roles in the extracellular environment.

NS5A is extensively phosphorylated, existing in two forms, basally phosphorylated (56 kDa) and hyper-phosphorylated (58 kDa) with key phosphorylation residues mostly located within the LCS1 domain. Cell culture adaptive changes often occur in this region such as the S2204I mutation that increases replicon efficiency in almost all genotype specific replicons except JFH-1 [Reviewed in (Ross-Thriepland & Harris, 2015)]. In genotype 1 this mutation reduces NS5A hyper-phosphorylation which boosts replication efficiency (Blight *et al.*, 2000), yet this is not seen in JFH-1. While NS5A phosphorylation status is key to the functionality of the protein yet the molecular mechanisms as to how phosphorylation regulates NS5A function remains elusive.

In addition to its functions on the HCV life cycle NS5A also interacts with numerous cellular proteins to manipulate the host-cellular environment to favour HCV replication and assembly. A recent example of this defined the interaction of NS5A with a specific subset of host proteins nucleosome assembly protein 1-like protein 1 (NAP1L1), bridging integrator 1 (Bin1) and vesicle-associated membrane protein-associated protein A (VAP-A) as essential for HCV replication and NS5A dissemination

throughout the cellular cytoplasm (Goonawardane *et al.*, 2017). NS5A plays a key role in establishment of the HCV replication complex by stimulating phosphatidylinositol 4-kinase IIIα (PI4KIIIα) activity to increase the level of phosphatidylinositol 4-phosphate lipids, essential to the formation of the membranous web (Reiss *et al.*, 2013). It is through the many facets of the HCV lifecycle NS5A occupies that resulted in drugs such as daclatasvir, ledipasvir and more recently velpatasvir being such potent inhibitors of HCV. While all the functions and interactions of this protein are not yet defined, its extensive study has led to great advances in both HCV molecular biology and drug treatment.

1.3.9 NS5B

In a fashion typical to other Flaviviridae such as Dengue, West Nile and Yellow Fever virus, replication of the HCV positive sense RNA genome occurs through a synthesis of a negative strand intermediate, which serves as a template through which nascent genomes are synthesised. This process is performed by the virus encoded RNA-dependent-RNA polymerase (RdRp), which in the case of HCV is designated NS5B. The NS5B protein is 65 kDa in size and displays the 'fingers', palm and thumb motif common to all RdRps as well as signature motifs such as the GDD sequence within the catalytic domain which is critical to the functionality of the active site (Poch *et al.*, 1989). Studies on the 3D structure of the protein have revealed extensive interactions between the fingers and thumb domain, revealing a closed conformation of NS5B that completely encompasses the active site consistent with *de-novo* initiation of RNA synthesis (Moradpour & Penin, 2013; Simister *et al.*, 2009). The catalytic domain itself is located within the palm region where the two critical aspartic acid residues (D-220 and D-318) chelate two divalent metal ions (magnesium or manganese) as cofactors

for the polymerase reaction. The groove formed in between the fingers and thumb domain directs the RNA towards the active site [Reviewed in (Moradpour & Penin, 2013)]. NTPs enter from a specific tunnel to the rear of the protein leading to the active site for addition onto the newly synthesised RNA strand. Once initiated NS5B can elongate the nascent RNA along the entire length of the RNA genome without requiring a helicase to un-wind RNA secondary structures (Lohmann *et al.*, 1999). The mechanisms behind the termination of RNA synthesis remain poorly defined, however it may be that the NS5B simply disassociates from the genome once it has reached the end of the template.

The error-prone nature of RNA synthesis by NS5B is one of the most distinguishing features of HCV, giving rise to the high genetic diversity of clinical isolates. Powdrill and colleagues recently defined the error rate as 10^{-3} substitutions per site, with a strong preference for G:U/U:G mismatches in NS5B (Powdrill *et al.*, 2011). The mutation rate in HCV driven by NS5B is the highest reported for any RNA virus, resulting in HCV infection consisting of a diverse, closely related population of viruses or quasispecies (Martell *et al.*, 1992; Simister *et al.*, 2009). This feature of NS5B allows the virus to continuously adapt to immunological challenge, by providing beneficial mutations to avoid neutralising antibodies produced by the host in response to infection (Farci *et al.*, 1996). The constant mutating and adaption of viral epitopes also contributes to the host failing to mount an effective cytotoxic $CD8^+$ T-Cell response through failure in cells being able to recognise viral epitopes or present epitopes in the

context of major-histocompatibility-complex-class I (Bowen & Walker, 2005; Chang *et al.*, 1997; Erickson *et al.*, 2001; Tsai *et al.*, 1998).

The key role NS5B plays in the viral life cycle has resulted in it being a target for the development of therapeutic strategies to combat HCV replication. This has resulted in the development of the most effective HCV antiviral drug Sofosbuvir (SOF), a guanosine nucleotide analogue which binds to and inhibits the NS5B active site (Sofia *et al.*, 2010). The high barrier to resistance of SOF as well as combination with NS5A inhibitors Ledipasvir, Daclatasvir (discussed later) and weak antiviral Ribavirin has transformed clinical management of HCV replacing the old 'gold standard' of IFN based therapy achieving limited efficacy to a new highly effective regime with greatly improved response rates.

1.4 Viral life cycle

The lifecycle of HCV is typical of that expected from a member of the *Flaviviridae* family [Reviewed in (Gerold *et al.*, 2017; Mukhopadhyay *et al.*, 2005)]. Virions enter through receptor-mediated endocytosis, through interaction with a range of receptors with different binding affinities. Release of the RNA genome into the cytoplasm occurs through conformational changes of the virion brought about by acidification of the endosomal vesicle. Translation of the positive sense RNA genome yields a single polyprotein processed into functional domains by host and viral proteases. Virion assembly occurs on the surface of the endoplasmic reticulum (ER) with nascent virus particles transferred via the trans-Golgi network for release via exocytosis.

1.4.1 Entry

The first stage in HCV infection is attachment to the host cell surface. HCV entry to hepatocytes occurs on the basolateral surface beginning with a low affinity interaction with low-density-lipoprotein-receptor (LDLR) and with glycosaminoglycans (GAGs) (Germi *et al.*, 2002; Monazahian *et al.*, 1999). Both LDLR and GAGs interact with viron associated ApoE to bring the virus close to the cell surface to complete the early attachment phase. After the initial contact with LDLR and GAG further interactions between the HCV particle and additional surface receptors are essential for entry; the most crucial are CD81, scavenger receptor class B member 1 (SRB1), claudin 1 and occludin, their individual roles are summarised in **Error! Unknown switch argument.**.

The interaction between these receptors and lipoprotein-associated viral particles allow progression of the virus from cell surface attachment to entry into the hepatocyte. The lipid transfer ability is thought to be a key step in progression from initial contact by enabling the dissociation of the lipoproteins from the viral particle and exposing the CD81 binding domains of the HCV E2 glycoprotein (Dao Thi *et al.*, 2012; Zahid *et al.*, 2013). The CD81-bound viral particles are then transported laterally to the tight junctions of the cell to where the interaction with claudin-1 stimulates clatherin-mediated endocytosis (Farquhar *et al.*, 2012). This cell surface trafficking is dependent on the remodelling of cortical actin controlled by signal transduction pathways through epidermal growth factor receptor (EGFR) signalling and downstream RHO- and RAS-GTPase signalling (Lupberger *et al.*, 2011). While occludin is essential for HCV entry its precise role is unclear. Studies point to occludin binding directly to the HCV E2

glycoprotein in the tight junction region as well as being one of the last steps in HCV entry yet; the exact part occludin plays remains to be fully uncovered (Sourisseau *et al.*, 2013).

Table 1.1 Receptors essential for HCV entry into hepatocytes

Receptor	Role in HCV entry
CD81	• Tetraspanin binding protein • Necessary but not sufficient for HCV entry. • Binds HCV E2 glycoprotein and is one of the first HCV co-receptors discovered (Pileri *et al.*, 1998) • Indicated in post-attachment events, as HCV binding requires a conformational change in E2 (Petracca *et al.*, 2000). • Has also been shown to prime HCV glycoproteins for low-pH activation during entry (Sharma *et al.*, 2011)
SRB1	• Highly expressed on hepatocytes, binds high- and very-low-density lipoproteins. • Indicated as a HCV entry co-factor by increasing HCV permissiveness for CD81 deficient HepG2 cells • Interacts with virus associated lipoproteins • Lipid transfer activity of SRBI is important for HCV post binding entry (Zahid *et al.*, 2013) • Interaction with E2 causes a conformational change promoting CD81 binding (Scarselli *et al.*, 2002).
Claudin-1	• Tight junction protein found on the basolateral surface of hepatocytes • Indicated as HCV entry factor by cDNA library expression (Harris *et al.*, 2010). • Does not directly interact with HCV but is thought to stabilise virus internalisation by interacting with CD81 (Evans *et al.*, 2007).
Occludin-1	• Tight junction protein • Functions at a post attachment step of HCV entry (Sourisseau *et al.*, 2013). • Whether it directly interacts with the virus has yet to be elucidated. • Contributes to species tropism of HCV as mice become permissive for HCV when human Occulin -1 is expressed (Ploss *et al.*, 2009).

After clatherin-mediated endocytosis the virus is trafficked to an endosomal compartment were the lipid transfer activities of SRB1 are thought to modify the virus and the associated lipoproteins (Dao Thi *et al.*, 2012). This modification is possibly to expose the viral envelope to prime E2 by CD81 so that the glycoprotein can trigger

low pH induced membrane fusion between the endosomal membrane and the viral envelope (Sharma *et al.*, 2011). The fusion event between the endosomal compartment and the viral membrane releases the HCV genome into the cytosol where translation and replication can be initiated.

1.4.2 Translation/Replication

The site of HCV replication is the rough endoplasmic reticulum (rER). Here HCV faces a barrier to genome translation; the lack of a 5'-cap. All eukaryotic mRNA possess this modification allowing the recruitment of ribosome initiation factors to begin translation by scanning for the initiation codon. The virus overcomes this block by the presence of an internal ribosome entry site (IRES) in its 5'UTR region, which has been shown to be sufficient to induce the formation of an active 80S ribosome complex without the need for a 5'-cap (Wang *et al.*, 1993). This exhibits one of many mechanisms whereby the virus can subvert the host replication machinery for its own purposes.

Translation of the viral genome yields a single polyprotein approximately 3000 amino acids in length that is processed by cellular signal peptidases and viral serine proteases (NS2, NS3/4) to generate the 10 functional viral proteins. The HCV replication complex and subsequent polyprotein processing form a 'membranous web' within the rER (Miyanari *et al.*, 2003). This membranous web consists of double-membrane vesicles, HCV RNA, ER membranes and lipid droplets (Gosert *et al.*, 2003). Replication of the viral genome occurs within the membranous web by the NS5B RdRp using the positive strand RNA genome as a template to generate a negative strand intermediate that is used to produce further positive strand genomes

[reviewed in (Kim & Chang, 2013)]. The proposed model of this process is shown in Fig 1.3.

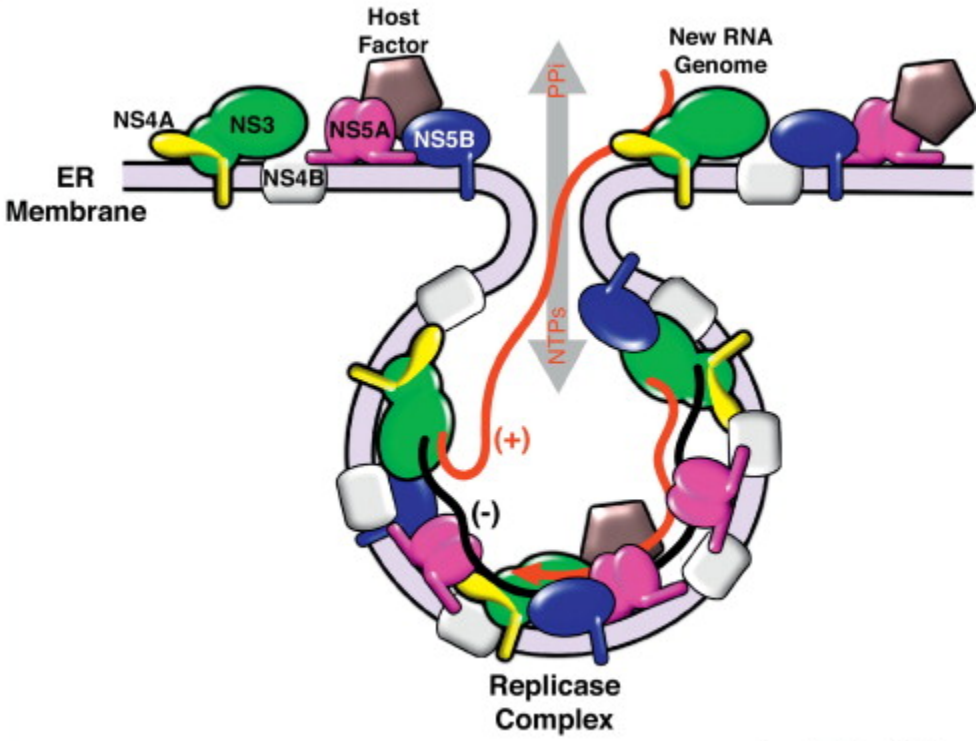

Fig 1.3 Model of the HCV Replication Complex
Schematic diagram adapted from Gu et al of the proposed model of the HCV RNA replication. After translation and cleavage of the HCV polyprotein non-structural proteins as well as host factors will form the HCV replication complex to replicate the positive strand RNA genome for packaging into new particles. Viral RNA is replicated through a negative strand RNA intermediate (Black) by the NS5B in this environment, which provides protection from proteases and nucleases. The positive strand RNA genome generated in this process is proposed to exit the complex for packaging and subsequent release of nascent particles.

Several host factors have been indicated in HCV replication, such as phosphatidylinositol-4 kinase-IIIα (PI4K-IIIα), cyclophillin A (CypA) and miR-122. PI4K-IIIα is a lipid kinase recruited to the membranous web by NS5A stabilising the HCV replication complex and promoting the integrity of the membranous web (Reiss *et al.*, 2011). Cyclophillin A is a peptidyl-prolyl isomerase that catalyses proline residue peptide bond isomerisation in protein folding and has been shown to be an essential cofactor for HCV replication and membranous web formation through interactions with NS5A and NS5B (Yang *et al.*, 2008). Finally the liver specific micro RNA miR-122

stimulates HCV RNA translation by binding to the 5'UTR promoting cap-independent translation in conjunction with the IRES (Roberts *et al.*, 2011).

1.4.3 Assembly and release

HCV assembly occurs at the surface of cytosolic lipid droplets (LD) and is highly dependent on the association between the core and these LDs. During HCV infection the core protein stimulates LD formation and recruits the viral non-structural proteins and the replication complex to the LD- associated membranes (Barba *et al.*, 1997). The association between the HCV replicase and LD appears critical for particle assembly as disruption of this interaction severely impairs virus production (Targett-Adams *et al.*, 2008)

The first step in viral assembly is the interaction between NS5A and LD-associated-core protein. Two further non-structural proteins p7 and NS2 interact with the NS3-4A serine protease to release the LD-associated-core to form the nascent viral particle and bring the E1 and E2 glycoproteins to the site of assembly (Jirasko *et al.*, 2010). Mutations in the RNA helicase domain of the NS3 protein have been shown to perturb HCV assembly, which may indicate a possible RNA genome-packaging role for the NS3 helicase during nucleocapsid formation (Pietschmann *et al.*, 2009). A recent study has highlighted an interesting role for the cellular factor heterogeneous nuclear ribonucleoprotein K (HNRNPK) in regulating the availability of the HCV RNA genome for virion packaging. HNRNPK was shown to bind to the HCV RNA genome thereby preventing its inclusion in new viral particles, demonstrating an interesting usurpation by HCV of host proteins to aid assembly (Poenisch *et al.*, 2015). Maturation of the HCV is dependent on VLDL synthesis as the mature particles are enriched with

proteins involved in VLDL assembly such as apoE, apoB and microsomal transfer protein (Huang *et al.*, 2007). The matured particles are then released from the cell through the secretory pathway during which the E1, E2 glycoproteins are post-translationally modified to prime them for pH-mediated fusion in the next infection cycle (Vieyres *et al.*, 2010).

1.5 *In vitro* methods to study HCV

Since the discovery of HCV several attempts have been made to propagate the virus in cell culture by infection with virus derived from patient sera. While replication can be detected in hepatoma cell lines and primary human hepatocytes, replication levels were often so low that detection relied heavily on highly sensitive reverse transcription (RT) qPCR [reviewed in (Bartenschlager & Lohmann, 2001)]. Since *in vitro* replication of patient derived HCV remains a considerable challenge the majority of the research into the biology of the virus has relied on replicon models that have been adapted for *in vitro* use.

1.5.1 The HCV subgenomic replicon system

Key discoveries that lead to the creation of the first HCV replicon were based on the observation that positive strand RNA viruses belonging to the flavi-and pestivirus family do not require their structural proteins for genome replication. This inspired the development of the first HCV subgenomic replicon, Con1, derived from viral cDNA of a patient with a chronic genotype 1b infection. The Con1 replicon is a bicistonic construct where the HCV IRES drives a G418 selectable resistance marker, while the HCV non-structural proteins, crucial for RNA replication, are expressed through a encephalomyocarditis virus (EMCV) IRES (Lohmann *et al.*, 1999). Stable replicon-

containing cell lines were generated through RNA transfection of the construct followed by antibiotic selection. This system does not produce infectious particles due to the lack of structural proteins only permitting study of the replication complex of HCV.

Several viral adaptive mutations were discovered from the replication of the HCV subgenomic replicons that have led to the selection of variants that have a higher replicative fitness. These mutations cluster in the NS3, NS4B, NS5A and NS5B regions with the bulk located in the NS5A just upstream of the interferon sensitivity-determining region (ISDR) (Blight *et al.*, 2000; Lohmann *et al.*, 2003). Mutations in NS4B also have a strong effect on the replicative ability of the Con1 replicon, however mutations in the NS3 and NS5B have a more moderate adaptive effect often being found in conjunction with other highly adaptive mutations in the NS5A (Lohmann *et al.*, 2003; Lohmann *et al.*, 2001). Adaptive mutations seen in replicon models are not observed in clinical HCV isolates therefore it is likely that they are specific to the Huh7 cell culture environment by modulating interactions between viral and cellular proteins to make a more favourable setting for HCV replication. The replicon system has now to date expanded beyond genotype 1b to include genotypes 1a (H77), 2a (JFH-1), 3 (S52), 4 (ED43), 5a and 6a [reviewed in (Catanese & Dorner, 2015)].

In addition to identification of mutations that boost replication efficiency, the subgenomic replicon lines lead to the development of cell lines with more permissive for HCV replication. This was based on the observation that cells 'cured' of the replicon using IFNα or a HCV specific drug had greatly improved rates of HCV replication. A clone of cured cells termed Huh7.5 cells were found to contain a mutation in the

retinoic-acid-gene I (RIG-I), an inducer of the interferon response through HCV RNA recognition, rendering it functionally non-viable (Blight *et al.*, 2002; Sumpter *et al.*, 2005). The high permissiveness of Huh7.5 to HCV replication has enhanced the study of HCV by providing a suitable platform to propagate both subgenomic replicons and cell culture derived HCV.

1.5.2 Genotype 3 sub-genomic replicons

Despite the efficient replicon models available for genotypes 1 and 2, replicons based on other genotypes generally replicate poorly in cell culture. For genotype 3 the most developed sub-genomic replicon model was developed by Saeed et al based on the consensus clone S52, which required several adaptive mutations namely P1226S, D1437H and S2210I to generate high numbers of stable colonies [ref Saeed et al]. While stable cell lines offer robust models for studying HCV replication, transient replicon assays are a preferable alternative for antiviral drug testing. These assays are well established in JFH-1 based sub-genomic replicons but replication levels in genotype 3 replicons are much lower. Recent work has looked to improve replication levels of G3 replicons by removal of the neomycin resistance cassette, reducing the CpG dinucleotide content of the replicon and overexpressing the recently described host factor SEC14L2 [wittevedlt et al]. From this study removal of the neomycin and over expression of SEC14L2 had the most positive impact on replication of the genotype 3 replicon.

1.5.3 Cell culture derived HCV

Inoculation of patient derived HCV in cell culture models do not result in productive infection. There is however one exception, a genotype 2a isolate obtained from a

Japanese patient who developed fulminant hepatitis as a result of HCV infection (a very rare outcome), designated JFH-1. This isolate is the only HCV virus that can infect and propagate within the Huh7 cell culture model, allowing our knowledge of HCV biology to be greatly enhanced (Kato *et al.*, 2003; Wakita *et al.*, 2005). JFH-1 has allowed the elucidation of novel factors in HCV entry, such as NPC1L1, EGFR and EphA2 as well as the development of a HCV humanised mouse model (Dorner *et al.*, 2013; Kelly *et al.*, 2017). Recently the use of the JFH-1 model system has uncovered a novel viral assembly mechanism mediated whereby an interaction between the p7 viroporin and NS5B regulates the morphogenesis of the viral particle enhancing infectivity (Aligeti *et al.*, 2015).

A recent development has been the creation of a robust model of infectious genotype 3 HCV termed DBN3a$_{cc}$ that can infect and propagate to similar levels as JFH-1 as well as producing high levels of infectious virus upon transfection (Ramirez *et al.*, 2016). This clone is a marked improvement on the S310 G3 infectious model, which took several weeks to propagate yielding low titre virus (Kim *et al.*, 2014). The adaption of this clone is extensive, 15 mutations were engineered across the length of the genome with mutations spanning core-NS5A critical to overcome the host barrier of Huh7.5 cells to achieve virus replication. In line with adaption of JFH-1, any reversion of adaptive mutations in the NS4A-NS5B regions significantly reduced viability of DBN3a however the authors note that they did not investigate the molecular mechanisms behind this.

This model may provide valuable insight into G3 HCV the study of which until now has been restricted to a poorly replicative infectious clone or subgenomic replicon. With

relapse to new antiviral therapy still a recurrent issue for G3 HCV use of this model could help to elucidate the mechanisms behind this. Though the considerable adaption this clone has undergone to make it viable *in-vitro* should be considered when drawing conclusions from its use. Yet, it remains an important and useful development for the study of the specifics of G3 HCV.

1.5.4 Limitations to replicons

The HCV replicon systems have allowed the dissection of various aspects of the viral life cycle. The development of cell culture derived HCV has confirmed early work through subgenomic replicon models on HCV RNA replication and expanded our knowledge of the various entry, assembly and release stages of the virus life cycle. However, one of the restrictions of the JFH-1 system is the heavy reliance on a single isolate that can produce infectious virus *in vitro*. While subgenomic replicons have been developed for other genotypes, robust infectious clones only exist for G2 and recently G3, making the study of any possible nuances in the viral life cycle between the 7 HCV genotypes especially in terms of assembly and release a challenge.

In terms of antiviral drug design HCV subgenomic replicons have been extensively used as they contain the primary direct acting antiviral drug targets, the NS3, NS5A and NS5B. Genetic manipulation of subgenomic replicons allows the construction of chimeras containing a non-structural gene of interest from HCV isolate. These can be then fused to a fluorescent or luminescent reporter system, which because of the robust and strong readout can be used in high-throughput drug screening assays (Bartenschlager, 2002; Gottwein *et al.*, 2011). For example, replacement of the NS5B

derived from clinical isolates in the Con-1 replicon has been used to develop phenotypic drug resistance assays to novel polymerase inhibitors (Middleton *et al.*, 2007). It has however been noted that the replacement of the NS3 or NS5B from different genotypes within JFH-1 can severely impair its replicative ability (Murayama *et al.*, 2007), making the study of antiviral drug resistance with the only full length viral model a challenge.

The use of the HCV replicon models has contributed enormously to the design of new powerful antiviral drugs for HCV and provided a robust model system to assess drug resistance. However, the replicon systems are unable to provide a system where patient derived HCV can be studied and phenotyped for drug resistance. Despite the new age of DAA therapy for HCV, which achieves high SVR rates, resistance to therapy remains a problem. While the generation of chimeric replicons derived from clinical isolates allow specific areas of the virus to be studied, they do not give the full picture in context with the rest of the natural virus. To accurately determine the mechanisms of relapse to the new DAA therapies, patient derived HCV must be studied.

1.5.5 Study of Clinical Isolates of HCV

Direct culture of HCV from clinical isolates has remained a constant challenge in HCV research with most isolates replicating at levels below well below detection of standard methods such as immunofluorescence and western blotting. While infection of primary human hepatocytes with clinical isolates is possible once the cells are in culture they have a limited life span and can down regulate factors characteristic of mature hepatocytes (Elaut *et al.*, 2006). With the recent development of techniques

associated with induced-pluripotent-stem-cells (iPSCs), a model that shows great promise is differentiation of hepatocytes like cells (HLCs) from these stem cell progenitors. The chief advantage of this system is the ability to obtain an unlimited supply of HLCs with without the variation of PHHs obtained from donors. Studies have demonstrated productive infection of HLCs with both cell-culture and patient derived HCV (Roelandt *et al.*, 2012; Schwartz *et al.*, 2012; Wu *et al.*, 2014). Although these cells do not recapitulate the full phenotype of mature hepatocytes they do robustly express key receptors such as CD81, SR-B1 and occludin as well as miR-122 (Sa-Ngiamsuntorn *et al.*, 2016b).

Improvements to the cell line based assays to replicate patient isolates have recently been enhanced by the discovery of SEC14L2 by Saeed *et al,* which in addition to boosting replicon replication could also support replication of clinical isolates from genotypes 1 and 3 albeit from clinical samples with high viral loads (Saeed *et al.*, 2015; Witteveldt *et al.*, 2016). The proposed mechanism as to how SEC14L2 promotes HCV infection is by inhibition of vitamin-E mediated lipid peroxidation though the authors note other mechanisms yet to be elucidated may exist. Although SEC14L2-expressing cell lines are a major step forward in our understanding of both cell-culture adaption and propagation of HCV clinical isolates, their abilities in resistance testing of virus to anti-viral agents remains largely untested.

1.5.6 The HCV 'Capture-Fusion' Assay

In an ideal scenario, being able to predict whether a patient infected with HCV was going to respond to the treatment prescribed would be the most effective and economical approach to drug selection. Deep sequencing of clinical isolates can

detect baseline resistant yet resistance with HCV are often complex and not entirely defined. Thus, being able to phenotypically determine the antiviral sensitivity of patient derived HCV would be of particular clinical benefit. Phenotypic assays using subgenomic replicons are time-consuming and often only focus on a specific region of the viral genome.

A technique developed by our research group represents a novel method by which the antiviral sensitivity of patient derived HCV genotypes 1-6 can be determined. The assay is based on the observation that HCV can associate with peripheral-blood-mononuclear cells (PBMCs) (Coquillard & Patterson, 2009; Ducoulombier *et al.*, 2004; Mellor *et al.*, 1998; Pham *et al.*, 2008) and although extra-hepatic replication of virus remains controversial, fusion of patient monocytes to Huh7.5 cells permits replication of virus albeit at a low level (Cunningham *et al.*, 2014). The assay was further developed to utilise a THP-1 monocyte cell line to 'capture' virus from patient serum when stimulated with phorbol 12-myristate 13-acetate (PMA) and IFNγ (Fig 1.4) and this form has been used to assess sensitivity of clinical isolates to a range of antiviral drugs including recently an experimental RIG-I agonist (Jones *et al.*, 2017). Questions remain as to the specific mechanisms of the capture fusion assay, namely why patient derived virus needs to be delivered to Huh7.5 cells via association with monocytes as opposed to direct infection. Additionally, the association of virus with THP-1 cells remains incomplete as it was shown to be independent of the classical HCV receptors such as CD81 and SR-B1. Though pre-treatment with PMA and IFNγ up-regulated Fc-receptor expression resulting in the hypothesis that THP-1 cells can associate with HCV antibody complexes to take up the virus (Marino *et al.*, 2005).

The capture fusion assay remains the only tested phenotypic assay that can determine the antiviral sensitivity of un-adapted clinical HCV isolates regardless of genotype. Replication in the assay is often low-level, relying on a sensitive RT-qPCR method to detect virus, yet the assay has been shown to correctly predict clinical response to Telaprevir where a NS3-based biochemical assay could not (Cunningham *et al.*, 2014). The phenotypic data that this assay can produce has the ability to determine virological causes of treatment failure in clinical HCV. Next-generation sequencing of clinical isolates can identify potential resistance variants but phenotypic assays such as capture fusion can define their effect on antiviral sensitivity.

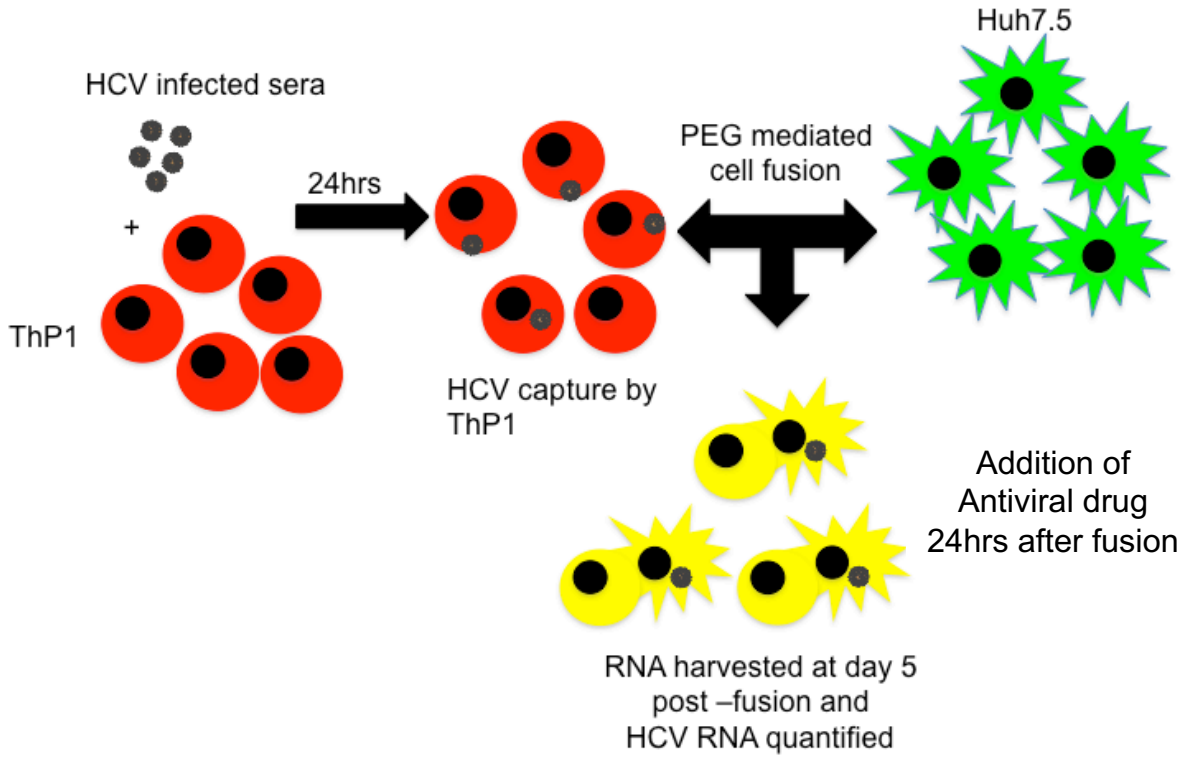

Fig 1.4 The HCV Capture Fusion Assay
Schematic representation of the key steps involved in the capture fusion assay. THP-1 cells pre-stimulated with phorbol 12-myristate 13-acetate (PMA) and IFNγ are inoculated with patient serum. Cells are then fused to the highly permissive Huh7.5 cell line using polyethylene-glycol (PEG). HCV can undergo a full replication cycle detected both by RT-qPCR and passage of virus onto naive Huh7.5 cells. Treatment of fused cells with antiviral drugs allow dose response curves to be generated and therefore determine the drug sensitivity of patient derived HCV.

1.6 IFN and RBV in the Treatment of chronic HCV

1.6.1 Interferon in HCV treatment

Treatment with type 1 interferon (IFN) and ribavirin (RBV) has been the gold standard of HCV treatment for many years, achieving around a 50% cure rate (Scheel & Rice, 2013). IFN alpha is an antiviral cytokine produced in response to infection. The binding of the IFNs (Table 1.2**)** to their respective receptors results in the activation of the signal transducer and activator of transcription complexes (STAT) via a cascade of signalling events.

Table 1.2: Classes of Interferon

Class	**Receptor**
Type I (IFNα, IFNβ, IFNω)	IFN-α receptor (IFNAR)
Type 2 (IFNγ)	IFN-**γ** receptor (IFNGR)
Type 3 (IFNλ 1-4)	Complex of IL10RB and IFNλ receptor (IFNLR)

The activation of STATs, specifically STAT1 and STAT2, cause a cascade of signals via the janus-kinase-STAT (JAK-STAT) pathway resulting in the transcription of IFN stimulated genes (ISG) such as IRF7, MX1 and OAS1 (Donnelly & Kotenko, 2010b). Failure in ISG activation can result in resistance to IFN treatment. The HCV core protein can interact with regulators of the IFN signalling cascade thereby preventing activation of ISGs and resulting in IFN insensitivity. However, the exact mechanisms and interactions between the all HCV proteins and the IFN pathway are not completely understood (Qashqari *et al.*, 2013).

1.6.1.1 The role of viral factors in IFN resistance

HCV viral proteins have been found to interfere with various stages of the IFN response. For example, the Core and NS5A inhibit transcription factor STAT1 by

preventing STAT1/STAT2 dimerization (Core) or decreasing the levels of phosphorylated STAT1 (NS5A) (Kumthip *et al.*, 2012). The HCV serine protease NS3-4A prevents ISG expression by cleaving TRIF a key adaptor protein in the stimulation of IFN response mediated by NFκB and TLR3. Additionally, both E2 and NS5A have been shown to interfere with the antiviral effects of the IFN-induced protein kinase R (PKR) by inhibiting PKR protein synthesis (Chayama *et al.*, 2000; Francois *et al.*, 2000).

1.6.1.2 Host factors in IFN resistance

Host factors such as age, body weight, obesity, diabetes and insulin resistance influence patient response to IFN therapy (Asselah *et al.*, 2010). Insulin resistance in particular has been shown to have an inhibitory effect on the IFN intracellular signalling pathway and increase steatosis and liver fibrosis progression (Romero-Gomez, 2006).

Genome-wide-association studies have revealed host genetic polymorphisms upstream of the IL-28B gene within the IFN-λ3 gene that can predict the outcome of IFN therapy. Specifically, two single nucleotide polymorphisms (SNP) designated rs12979860 and rs8099917 have been strongly associated with treatment outcome and spontaneous viral clearance (Tillmann *et al.*, 2010). The preferred variants rs12979860CC and rs8099917TT are associated with a favourable SVR where as

other variants such as rs12979860CT/TT or rs8099917TG/GG are more likely to fail IFN therapy (Fischer *et al.*, 2013).

1.6.1.3 Interferon Lambda (λ) in HCV infection

Type III IFNs (also referred to as IFNλs) are a key component of the innate antiviral response against HCV infection. The family consists of 4 members IFNλ1, IFNλ2, IFNλ3 and IFNλ4, which between them have a high degree of both similarity and size (Hamming *et al.*, 2013). The receptor for the IFNλs consists of 2 sub-units: IFN-lambda-receptor-1 (IFNLR1), the alpha sub-unit specific for IFNλs and IL10RB, the beta subunit, also shared with type II cytokine receptors for IL-10, IL-22 and IL-26 (Donnelly *et al.*, 2004). Not all tissues can respond to IFNλ since expression of the IFNLR1 is restricted to tissues with a high epithelial content such as the lungs and liver (Sommereyns *et al.*, 2008).

IFNλ signalling occurs through dimerisation of the IFNLR1 and IL10B1 subunits activating Janus Kinase-1 (JAK1) and tyrosine kinase-2 (TYK2), phosphorylating IFNLR1 resulting in the recruitment of STAT1 and STAT2. Phosphorylated STAT1/2 form a heterodimer with IRF9 to form IFN-stimulated gene factor 3 (ISGF3), which translocates to the nucleus where it binds the IFN-stimulated response element (ISRE) to drive IFN stimulated gene (ISG) synthesis (Donnelly & Kotenko, 2010a). ISGs induced by IFNα and IFNλ are largely similar resulting in a broadly similar antiviral effect, though it has been noted that IFNλ tends to induce a slower more sustained antiviral response (Bolen *et al.*, 2014; Kalie *et al.*, 2008). Among the many genes up regulated by IFNα and λ notable examples include myxovirus resistance gene 1 (MX1)

2’ -5’ - oligoadenylate synthetase 1–3 (OAS-1–3) and protein kinase R (PKR). A distinctive feature of IFNλ induction is the up-regulation of anti-inflammatory ISGs USP18 and suppressor of cytokine signalling (SOCS) 1-3, which obstructs STAT 1 and 2 phosphorylation causing the cell to lose sensitivity to the effects of type I and III IFNs (Francois-Newton *et al.*, 2011; Mahlakoiv *et al.*, 2012; Yoshimura *et al.*, 2007). In terms of inhibition of HCV, differences in the mechanisms of ISG induction between IFNα and λ have been shown to exist. Using knock out cells, both STAT-1 and STAT-2 were found to be essential for anti-HCV ISG expression by IFNλ, whereas IFNα was found to be able to induce ISG production in the absence of STAT-1 but not STAT-2 (Yamauchi *et al.*, 2016).

In addition to signalling through the phosphorylated form of ISGF-3 a second related factor exists consisting of un-phosphorylated STAT-1/STAT2 and IRF-9 termed U-ISGF3, which prolongs expression of a subset of ISGs such as MX1, 2’ -5’ – OAS and ISG-15 that can inhibit chronic HCV infection (Cheon *et al.*, 2014; Cheon *et al.*, 2013; Cheon & Stark, 2009). A recent study has shown that IFNλ produced as a result of HCV infection significantly up regulates levels of U-ISGF3, which subsequently render cells unresponsive to IFNα. The mechanism identified for this loss of type I IFN responsiveness was found to be ISG15-mediated stabilisation of USP18 a well-documented negative regulator of the IFN response as mentioned previously (Sung *et al.*, 2015).

1.6.2 Ribavirin in HCV treatment

RBV has been used in conjunction with IFN for HCV treatment since it was shown to improve SVR rates in patients with chronic HCV (Davis *et al.*, 1998). Randomised

clinical trials demonstrated that combination therapy improved SVR rates from 15% with IFN mono-therapy to 36% with IFN and RBV (Brillanti *et al.*, 1994; Poynard *et al.*, 1998). RBV is a synthetic guanosine analogue with a broad spectrum of antiviral activity against several RNA viruses such as respiratory syncytial virus and poliovirus. The similar chemical structure of RBV to guanosine allows the molecule to be incorporated into the viral genome causing errors in the coding sequence or directly inhibit the activity of the HCV polymerase (Fig 1.5). The addition of RBV to IFN increases antiviral effect but its greatest benefit is the prevention of relapse to therapy (Pawlotsky *et al.*, 2004).

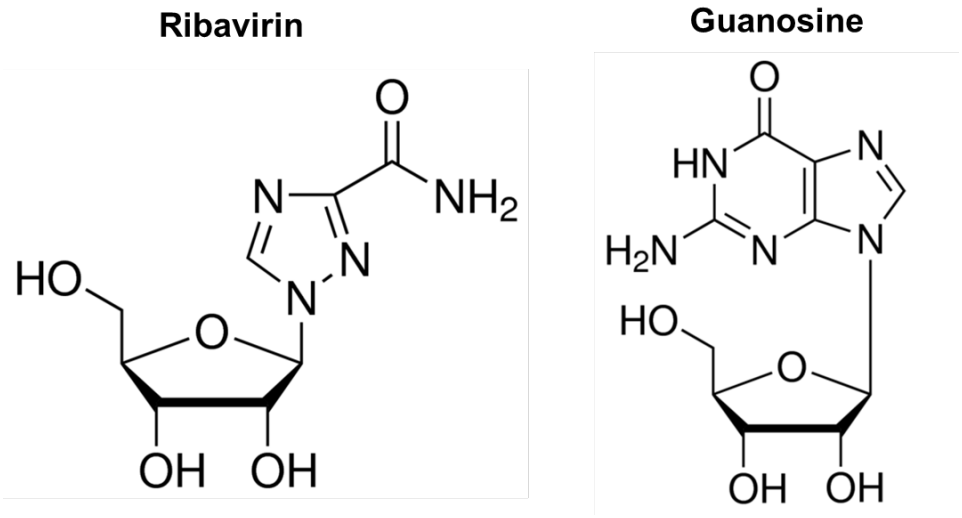

Fig 1.5 Chemical structure of Ribavirin
Schematic diagram of the chemical structure of Ribavirin and guanosine. RBV is a guanosine analog similar in structure but with alterations to the base group of the nucleotide. Upon entering the cell RBV is phosphorylated with RBV-triphosphate being the active compound that can bind to the active site of the polymerase. Specific details concerning the proposed mechanisms of action are discussed below. Chemical structures were adapted from Sigma Aldrich.

1.6.2.1 Mechanism of Action

RBV does not have one single mechanism of action. Since its discovery and clinical use as an antiviral a number of mechanisms have been identified. Even today the key overriding antiviral mechanism remains elusive. The reasons as to why this has remained unclear lie in the nature of the drug itself. RBV being a weak antiviral can

only exert a significant antiviral effect against HCV in combination with IFN, making the determination of the antiviral contribution of RBV among the highly complex IFN response a challenging task.

1.6.2.2 Inhibition of the HCV polymerase

Upon entry of RBV into the host cell it is phosphorylated into its active form RBV-triphosphate (Miller *et al.*, 1977). Since the HCV polymerases utilises the host nucleotide pool for genome replication RBV-triphosphate can be recognised by the HCV polymerase due to its similarity to guanosine. Once bound RBV may prevent further elongation by chain termination or sit in the active site of the polymerase preventing the binding of other nucleotides (Bougie & Bisaillon, 2003). Studies have shown *in vitro* that RBV can both bind to the active site of the HCV polymerase and inhibit chain elongation (Bougie & Bisaillon, 2003; Maag *et al.*, 2001). Clinical studies investigating the mutation rate of the NS5B in chronic HCV with RBV monotherapy identified mutations within the viral polymerase, which were shown *in vitro* not to confer resistance to RBV (Lutchman *et al.*, 2007). A possible explanation as to why RBV monotherapy did not yield any resistant mutations in the NS5B may be because RBV is not sufficiently potent antiviral to drive growth of resistant strains.

1.6.2.3 RNA mutagenesis

Another mechanism of action was proposed based on the observation that RBV could be incorporated into the HCV RNA genome and base pair with either cytosine or uracil. This would then result in an increase in the number of mutations within the HCV genome, perhaps to the point where the virus would be rendered non-viable (‘error catastrophe’). Studies investigating mutation rate upon exposure to RBV have

produced controversial data as to whether an increase in the mutation rate is either 'seen' or 'not seen' with RBV monotherapy [Reviewed in (Thomas *et al.*, 2013)]. As mutagenesis would occur randomly throughout the genome, a single resistant strain would not necessarily be selected for. An approach the virus could utilise to escape lethal mutagenesis would be the selection of a higher fidelity polymerase. This would not be necessarily a selective advantage for a virus such as hepatitis C as one of its strengths is its population diversity, allowing rapid selection of variants in response to the interventions both by the cell and antiviral drugs. The failure of RBV monotherapy and the controversy surrounding whether RBV does in fact increase mutation rates may suggest that this mechanism of action may occur at a rate below detection. Some evidence to support this comes from studies investigating RBV uptake into the HCV genome that show RBV is incorporated at best every 1/7000 nucleotides (Maag *et al.*, 2001).

1.6.2.4 Inosine Monophosphate Dehydrogenase (IMPDH) inhibition

The mechanisms of action of RBV discussed thus far target the virus directly, however additional indirect antiviral mechanisms have been shown such as the inhibition of the IMPDH enzyme. IMPDH converts inosine-5-monophosphate to xanthine-5-monophoshate, which is the rate-limiting step in the production of guanosine nucleotides. RBV has been shown to competitively bind to the active site of IMPDH blocking the access of inosine-5-monophosphate resulting in the downstream depletion of GTP pools (Malinoski & Stollar, 1981; Streeter *et al.*, 1973). As GTP is a critical requirement for viral genome replication its depletion would prevent efficient HCV genome replication. Trials with IMPDH inhibitors such as VX-497 showed an increased potency than RBV against hepatitis B virus (HBV), RSV and parainfluenza-

3 virus but not HCV (Markland *et al.*, 2000). The consequence of this has lead to IMPDH inhibition not being considered as a primary antiviral mechanism of RBV in HCV. However, IMPDH inhibition and the subsequent depletion of GTP pools may enhance the direct acting antiviral mechanisms of RBV of error catastrophe and RdRp inhibition by forcing the virus to incorporate RBV into its genome as an alternative to GTP. Therefore, it is possible that the summation of the relatively weak direct and indirect antiviral mechanisms of RBV that drive a significant antiviral response in HCV therapy.

1.6.2.5 Additional mechanisms

Work looking at the effect of RBV therapy on the immune system has revealed that RBV can drive the activity of the more cytotoxic T-helper-1 phenotype while supressing T-helper 2 cells. *In vitro* experiments demonstrated that RBV enhanced the Th1 cytokine by up-regulating both the mRNA and protein levels of IL-2, IFNγ and TNFα while down regulating cytokines associated with the Th2 response (IL-4, IL-5, IL-10) (Hultgren *et al.*, 1998; Ning *et al.*, 1998; Tam *et al.*, 1999). Skewing of the T-cell response towards a more cytotoxic phenotype by RBV would facilitate the clearance of virally infected cells and could enhance the antiviral effect of IFNα; this remains poorly defined. Studies examining the role of T-cells in IFN/RBV treated patients have not shown enhancement of HCV specific T-cell response in patients (Rahman *et al.*,

2004) therefore suggesting that this may not be a significant antiviral mechanism of RBV.

A final immune mediated mechanism implicated in RBVs activity is the augmentation of the IFN response when given in combination with IFNα. Gene expression studies performed on liver biopsies from HCV infected patients treated IFN/RBV revealed a higher ISG expression with the dual therapy. Furthermore, patients pre-treated with RBV displayed amplified induction of ISGs and down regulation of genes involved in IFN inhibition (Feld *et al.*, 2007). Further studies have confirmed *in vitro* and *in vivo* that RBV can promote the IFN response through several mechanisms such as PKR up-regulation (Liu *et al.*, 2007), activation of p53 and mTOR pathways (Su *et al.*, 2009) and heightened IFN-ß and IL-8 production (Tokumoto *et al.*, 2012).

1.6.2.6 Resistance

As RBV is an effective mutagen with error catastrophe being a suggested antiviral mechanism of action, resistant mutations are often found in the RdRp which cause an increased fidelity of the polymerase. Examples of this are found in the RBV resistant poliovirus where a G64A mutation within the polymerase increased the accuracy of replication (Vignuzzi *et al.*, 2008). Further examples can be found in foot and mouth disease virus and Coxsackie virus where RBV resistant variants identified in the RNA polymerase increase fidelity of replication (Gnadig *et al.*, 2012; Zeng *et al.*, 2014).

In HCV treatment RBV resistant mutations were identified by passage of HCV replicon cells in high concentrations of RBV. Sequencing of the RBV resistant replicon cells

revealed resistant mutations initially identified in the C-terminus of NS5A that conferred resistance to 300μM of RBV comparable to physiological concentrations (Pfeiffer & Kirkegaard, 2005a).

More recent experiments, which looked to develop RBV resistant JFH-1 by the serial passage in high RBV concentrations, resulted in a range of mutations throughout genome (Feigelstock *et al.*, 2011). Table 1.3 summarises currently known mutations associated with RBV resistance. The precise resistance conferring mutation as well as the mechanism of resistance remains unclear. A possible explanation could be increased replication fidelity conferred by RBV resistance associated variants, as these variants also have been shown to resist other mutagens such as 5-FU (Mihalik & Feigelstock, 2013).

Table 1.3 Identified RBV resistance mutations

Protein	RBV resistance associated change*
Core	R9S K78E Y81H G145S
E2	G64R V331I
P7	F43S
NS2	Y89H L195R
NS3	V36L T54S V55A D523N
NS5A	P402L G404S E442G T513A
NS5B	S13N A205V F415Y V449A

*** Table adapted from (Feigelstock *et al.*, 2011; Pfeiffer & Kirkegaard, 2005a)**

The contribution of all these changes to RBV resistance remains unclear, however mutations G404S and E442G NS5A were shown by Pfieffer and Kirkegaard to confer resistance to RBV in replicon cells. While they did not identify the mechanism of resistance, they speculated that these changes may affect the interaction between NS5A and NS5B making the polymerase less error-prone and thus less likely to incorporate RBV (Pfeiffer & Kirkegaard, 2005b). Mutations in the NS5B remain under characterised since their identification, with none of the sites located near the active site of the polymerase, their contribution to RBV resistance remains elusive. Indeed, the authors commented on the need for additional studies to fully characterise these

mutations (Feigelstock *et al.*, 2011).

1.6.3 Efficacy of peg-IFN/RBV treatment

The addition of RBV to peg-IFNα treatment was shown in three randomised clinical trials to significantly improve response rates compared to individual monotherapy (Fried *et al.*, 2002; Hadziyannis *et al.*, 2004; Manns *et al.*, 2001). The clinical benefit of RBV addition was shown to be higher on-treatment response rates and reduced incidences of virological relapse compared to RBV monotherapy (McHutchison *et al.*, 1998; Pawlotsky *et al.*, 2004). Efficacy of pegIFN/RBV varied across different HCV genotypes resulting in genotype specific recommendations for treatment (Ghany *et al.*, 2009). Treatment duration for patients infected with HCV G2 and 3 was 24 weeks of pegIFN/RBV, which achieved SVR in 75-85% of patients. However, this treatment regimen was less effective for those infected with genotype 1 and 4 HCV achieving SVR rates between 40-50% and 55-65% respectively even with an increased duration of treatment to 48 weeks (Fried *et al.*, 2002; Hadziyannis *et al.*, 2004; Manns *et al.*, 2001)

Patients who fail to respond to IFN based therapy either show a null-response, where no appreciable drop in serum HCV RNA is observed (most common with G1 infection), or relapse where viral RNA levels drop but return after cessation of treatment (most common in G3) (Fig 1.6). In either case further treatment options are limited. Re-treatment with the same course of therapy is not recommended resulting in SVR in less than 5% of cases (Cheruvattath *et al.*, 2007). Treatment with a different pegIFNα-subtype such as 2A to 2B only improves SVR rate if patients had received IFN mono-

therapy and not infected with genotype 1 HCV (Jacobson *et al.*, 2004; Shiffman *et al.*, 2004; Taliani *et al.*, 2006). Patients who experience virological relapse (resurgence of virus after 12 weeks), while likely to respond to the same treatment regime a second time still face high rates of relapse even with higher doses of pegIFN (Cheruvattath *et al.*, 2007).

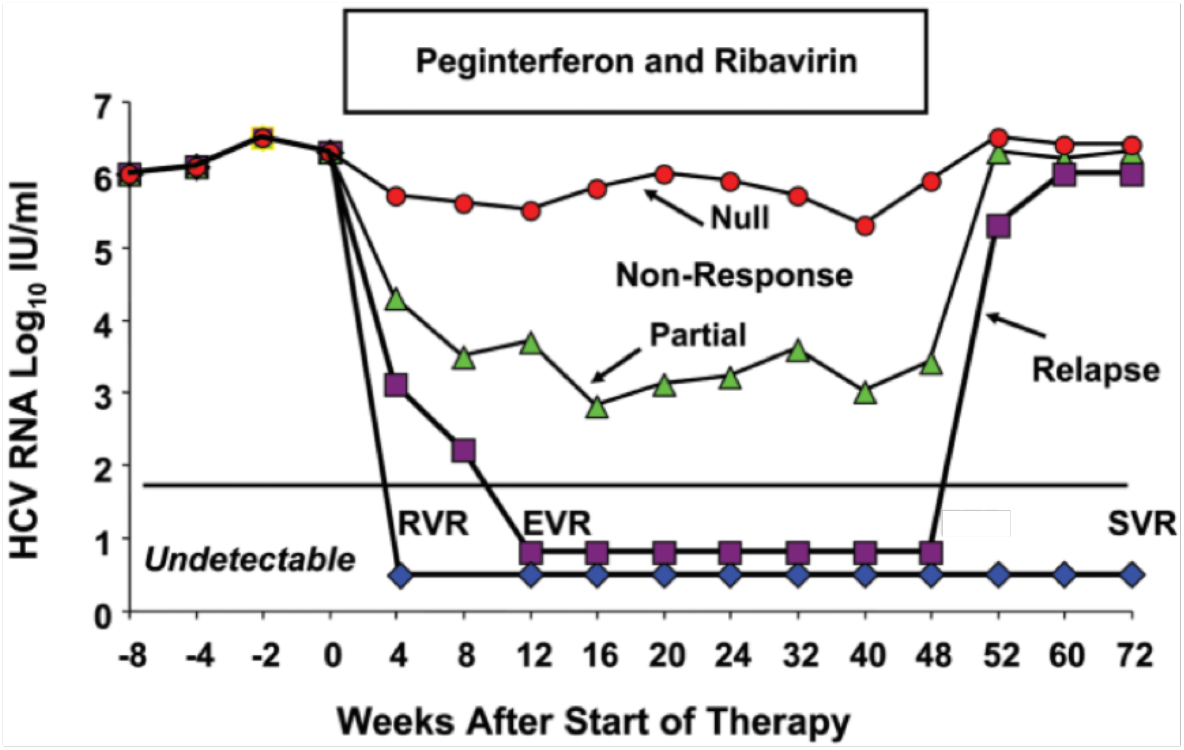

Fig 1.6 Virological responses to pegIFN/RBV treatment
Rapid virological response (RVR) defined as clearance of the virus detected by qPCR 4 weeks after the start of therapy. A ≥2-log drop in serum RNA at week 12 is referred to as early virological response (EVR) and if patients continue to be HCV RNA negative 24 weeks after the cessation of therapy this is described as a sustained virological response (SVR). Non-response is categorised as: null-response where treatment shows no substantial drop in HCV RNA after 24 weeks treatment and partial non-response where a ≥2-log drop is observed but patients are still HCV RNA positive at week 24. Virological relapse occurs when HCV RNA in the serum reappears after the end of treatment. Adapted from (Ghany *et al.*, 2009).

Several factors can influence response to pegIFN/RBV therapy. Of these factors, none can robustly predict treatment outcome but only indicate the probability of achieving SVR. The presence of advanced liver fibrosis or cirrhosis is one of the strongest negative influences on the achievement of an SVR regardless of genotype. Response

rates with cirrhosis are reduced from 41%-34% in genotype 1 and 79%/71% to 66%/44% for genotypes 2 and 3 respectively (Lee *et al.*, 2006). To a lesser extent the presence of co-morbidities such as obesity, insulin resistance, intra-venous drug use, alcoholism and co-infection with HIV also have a negative impact on SVR rates (Ghany *et al.*, 2009). HCV genotype as alluded to earlier, is also a major indicator of treatment response. G1 infection is intrinsically more resistant to pegIFN/RBV therapy, characterised by a delay in the clearance of infected cells compared to genotypes 2 and 3. The mechanism for this lack of response to IFN treatment in G1 remains relatively unknown but it is noteworthy that treatment does not select for viruses that are inherently resistant to IFN (Pawlotsky *et al.*, 1998a; Pawlotsky *et al.*, 1998b).

1.7 Recent advances in HCV treatment

The field of HCV treatment has changed dramatically in the last few years. The classical pegIFN/RBV regime, fraught with adverse effects and low SVR rates has been replaced with a new class of drugs, the direct acting antivirals (DAAs). The DAAs have raised the cure rate of chronic HCV from 50% to almost 90% especially in genotype 1 infection (Kowdley *et al.*, 2014). First generation DAAs were inhibitors of the NS3 protease such as telaprevir, boceprevir and more recently simeprevir. Since 2011 protease inhibitors have been introduced as the primary treatment regime for genotype 1 infection in combination with pegIFN/RBV, however adverse effects were still observed with this regime (Jacobson *et al.*, 2011; Poordad *et al.*, 2011). Second generation DAAs included a pan-genotypic NS5B polymerase inhibitor sofosbuvir (SOF) as well as NS5A inhibitors daclatasvir (DAC), ledipasvir (LDV) and more recently velpatasvir (VEL), which present a much more potent treatment regime with reduced side effects.

1.7.1 Protease Inhibitors (-previrs)

Cleavage of the HCV polyprotein by the NS3/4 serine is an essential part of the viral life cycle. Its blockage therefore would seriously disrupt the viral replication cycle and ultimately prevent the generation of new infectious viral particles. The first drugs shown to inhibit NS3 by binding to the active site of the protease approved for clinical use were telaprevir (TEL) and Boceprevir (BOC). Triple therapy with TEL or BOC in combination with pegIFN/RBV showed up to 75% SVR rates in naïve G1 infection when given over 24-48 weeks (Jacobson *et al.*, 2011; Poordad *et al.*, 2011). May 2014 saw the approval of a second-generation protease inhibitor simeprevir (SIM), which was regarded as a superior drug to TEL and BOC in terms of dosing (single 150mg tablet) and reduced side effects. In a clinical trial setting SIM achieved improved SVR rates (up to 80%) compared to TEL and BOC when used in combination with pegIFN/RBV (Jacobson *et al.*, 2014).

The treatment algorithms for regimes with TEL and BOC differed. BOC regimes consisted of a 4-week lead in with pegIFN/RBV followed by an additional 4 weeks of pegIFN/RBV/BOC. If viral RNA was detected at week 8 then therapy was continued for 48 weeks, if not therapy was stopped after 24 weeks. TEL based regimes consisted of an initial 12 weeks of pegIFN/RBV/TEL with viral RNA levels monitored at 4 and 12 weeks. Detection of HCV RNA ≥1000IU/ml at either week 4 or 12 resulted in subsequent treatment of pegIFN/RBV for 48 weeks otherwise patients were only given an additional 12 weeks of pegIFN/RBV (Barritt & Fried, 2012; Marks & Jacobson, 2012). The addition of protease inhibitors significantly improved SVR rates among patients with cirrhosis, however these rates were reduced compared to patients with

mild fibrosis. Furthermore, response rates were markedly reduced in response guided regimes compared to longer fixed dose courses of therapy, resulting in 48 weeks therapy being recommended for cirrhosis to maximise the potential to achieve high SVR rates (Bacon *et al.*, 2011; Jacobson *et al.*, 2011; Poordad *et al.*, 2011; Zeuzem *et al.*, 2011).

BOC and TEL are strong inhibitors of CYP3A, which can affect the plasma concentration of certain drugs metabolised by this pathway. For this reason, TEL and BOC are contraindicated with the drugs given in birth control, anti-cholesterol drugs and antidepressants. Additionally, the antiretroviral drug efavirenz decreases the plasma concentration of BOC making this drug combination unfavorable in patients infected with HIV. In terms of adverse events, patients receiving BOC were more likely to discontinue therapy due compared to control groups. Common adverse events were anemia, rash, flu like symptoms and nausea for BOC treatment, whereas gastrointestinal disorders such as nausea and diarrhea were more common in TEL regimens (Jacobson *et al.*, 2011; Poordad *et al.*, 2011; Wilby *et al.*, 2012; Zeuzem *et al.*, 2011).

A low genetic barrier to resistance has hindered use of protease inhibitors. Specifically, the pre-existence of resistance-associated mutations such as the Q to K polymorphism at position 80 in NS3 severely comprises the efficacy of protease inhibitors such as SIM in G1a infection (Jacobson *et al.*, 2014; Manns *et al.*, 2014). EASL and AASLD 2015 guidelines recommend the use of viral sequencing to exclude patients with the Q80K polymorphism from receiving protease inhibitor regimes.

1.7.2 NS5A inhibitors (-asvirs)

The NS5A protein plays a key role in several aspects of the viral life cycle such as replication complex formation and viral packaging as well as interacting with several cellular functions [Reviewed in (Pawlotsky, 2013)]. NS5A is believed to exist as a dimer and is commonly found on ER-derived membranes in HCV infection existing in a basally phosphorylated and hyper-phosphorylated form. Precisely how NS5A regulates viral replication or assembly is unknown. As a result the exact impact NS5A inhibitors have on the HCV replication cycle is not completely understood however, it is thought that they disrupt NS5A dimerisation, preventing replication complex formation (Ascher *et al.*, 2014). NS5A inhibitors have been found to have a much wider more potent activity against the various HCV genotypes than the protease inhibitors, inhibiting HCV replication at picomolar concentrations (Gao *et al.*, 2010). Since NS5A inhibitors also have a low genetic barrier to resistance they are used in combination with other antivirals. Recently, they have been approved for use as part of the all-oral treatment regime for G1 HCV infection.

1.7.2.1 Daclatasvir

Daclatasvir (DAC) was the first NS5A inhibitor discovered. It has since demonstrated pan-genotypic antiviral activity with a minimal side-effect profile. When combined with pegIFN/RBV, DAC is a well-tolerated treatment regime achieving 80% SVR rates in genotype 2 and above 60% in genotype 3. The frequency of post-treatment relapse was higher in patients with cirrhotic genotype 3 infection (Dore *et al.*, 2015). Phase III

studies have shown that in non-cirrhotic genotype 3 infection the combination of DAC plus sofosbuvir (SOF) can achieve 98% SVR rates after 12 weeks of therapy without the need for RBV (Nelson *et al.*, 2015). Several mutations in the NS5A cause resistance to DAC including M28T, Q30E/H/R, L31M, H58D, and Y93H/N. The mutations found in the majority of G1 infected patients who did not achieve SVR were L31M/V and Y93H/N (Lontok *et al.*, 2015; Nelson *et al.*, 2015).

1.7.2.2 Ledipasvir

Since 2014 ledipasvir (LDV) with SOF has been available as a fixed dose combination oral therapy (HARVONI) for the treatment of genotypes 1, 3 and 4. SVR rates of 99% have been achieved with LDV in combination with SOF in genotype 1-treatment naïve patients without the need for RBV. Use of LDV also demonstrated high SVR rates of 94% in previous G1 non-responders after only 12 weeks of therapy, which increased to 99% with and extension to 24 weeks (Afdhal *et al.*, 2014). Overall data from several clinical trials suggest that 12 weeks of therapy with LDV/SOF achieve SVR rate of 96% with genotype 1 infection. This drops to 90% in treatment experienced patients suggesting that these patients may require a longer duration of therapy [reviewed in (Thiagarajan & Ryder, 2015)]. Mutations identified to confer resistance to LDV are similar to those for DAC including Q30E/R, L31M, and Y93C/H/N [reviewed in (Lontok *et al.*, 2015)]. This is not surprising as both drugs have the same NS5A binding site.

1.7.3 NS5B inhibitors (buvirs)

The HCV NS5B RNA-dependent-RNA-polymerase is critical for replication of the viral genome. The inhibition of this enzyme will stall viral replication and prevent the formation of infectious virons. NS5B inhibitors exist in two types; nucleoside and non-

nucleoside analogues. Nucleoside analogues bind to the active site of the enzyme causing premature chain termination, while non-nucleoside inhibitors bind to allosteric sites resulting in conformational changes inactivating the enzyme. Due to necessity to conserve the active site across the HCV genotypes gives the potential for pan-genotypic activity for nucleoside inhibitors. Recent years has seen the development of one of the most effective anti-HCV drugs to date, sofosbuvir (SOF) a nucleoside analogue that has dramatically improved SVR rates across all HCV genotypes (Fig 1.7).

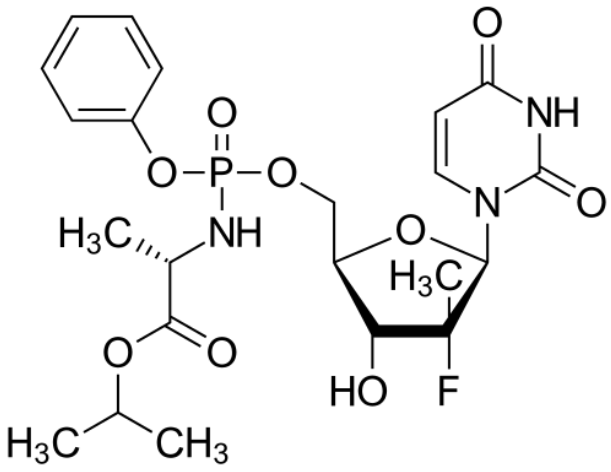

Fig 1.7 Chemical structure of Sofosbuvir
Sofosbuvir is a nucleoside analog that upon entering the cell is phosphorylated into its active triphosphate form. This then acts as a defective substrate for the polymerase binding to the active site preventing chain elongation. Chemical structre was adapted from Sigma Aldrich

1.7.3.1 Sofosbuvir

SOF has recently been approved for treatment of all HCV genotype. Data from phase III clinical trials FISSION and VALENCE revealed that SOF/RBV is effective for all genotypes. However reduced SVR rates were observed with G3 achieving 85% SVR compared to 93% for G2, 90% for G1 and 96% for G4 (Lawitz *et al.*, 2013; Zeuzem *et al.*, 2014b). NEUTRINO revealed that SOF with pegIFN/RBV for 12 weeks achieved a 90% response rate in patients infected with genotypes 1, 2 and 4. Notably SVR rates

for genotype 3 infections were markedly reduced compared to genotype 2 (56% vs 97%) with 12 weeks of SOF/RBV treatment as part of the FISSON study (Lawitz *et al.*, 2013). Increasing treatment duration to 24 weeks increased SVR at week 12 (SVR12) to 92% in treatment naïve non-cirrhotic G3 patients (Zeuzem *et al.*, 2014a). Previous treatment experience with IFN in G3 resulted in low SVR12 rates of only 30% when treated with 12 weeks of SOF/RBV, this however was found to double to 60% when treatment duration was extended to 16 weeks (Jacobson *et al.*, 2013). Presence of cirrhosis in treatment experienced patients was found to negatively impact SVR rates with 12 and 16 weeks of SOF and RBV treatment alone. Two further clinical trials BOSON and LONESTAR tested adding pegIFN to SOF and RBV regimens which, subsequently achieved SVR12 of 83% and 85% respectively amongst G3 treatment experience cirrhotic patients (Foster *et al.*, 2015b; Lawitz *et al.*, 2015). The BOSON trial in particular contained a high proportion of patients with both advanced liver disease and previous treatment failure.

The combination of SOF plus LDV in the ION clinical trial series for genotype 1 revealed that high SVR rates (95%) could be achieved after just 8 weeks of therapy compared to 12 weeks (Afdhal *et al.*, 2014). Treatment of genotype 3 with SOF remains sub-optimal. Data from the ELECTRON-2 clinical trial shows SVR rates in treatment naive genotype 3 patients with SOF/LDV are improved by the addition of RBV (100% compared to 64% without RBV) after 12 weeks of therapy. The reasons why RBV improves SVR rates are unknown.

NS5B variants have been identified that confer resistance to SOF therapy. These were first identified in laboratory studies of the HCV replicon where they emerge relatively

frequently. However in patients these mutations are much less common, perhaps indicating that they are less replication competent. The first SOF resistance associated variant found was S282T and was isolated in a genotype 2 patient who was treated with SOF monotherapy thought its subsequence occurrence in patients is rare (Gane *et al.*, 2013). Other mutations have been found by a combination of sequence analysis and replicon selection. Substitutions such as L159F and V321A have been identified form collated data from phase 3 SOF trials treating G3 infection (Svarovskaia *et al.*, 2014). When these mutations have been engineered into replication models they only cause a modest reduction in SOF sensitivity (Lontok *et al.*, 2015). The mechanism as to how these substitutions contribute to virological relapse to SOF remains unknown.

1.7.3.2 Modern HCV treatment regimens

All oral therapy for HCV is based on three classes of DAAs: protease inhibitors, NS5A inhibitors and NS5B inhibitors (Table 1.4). DAA treatment regimens are always given in combination to achieve effective inhibition of HCV replication and a high barrier to resistance. While most DAA therapy potently represses HCV replication they have a low barrier to resistance when given in monotherapy. The only exception to this is SOF, which can be given in monotherapy with RBV, but higher SVR rates are achieved when SOF is coming with a protease or NS5A inhibitor. Additionally, a treatment combination of three DAAs with low barriers of resistance such as

Paritaprevir/Ombitasvir plus Dasabuvir can achieve a high barrier of resistance when given together (Welzel *et al.*, 2014).

Table 1.4 Direct Acting Antivirals

Protease Inhibitors	NS5A Inhibitors	NS5B Inhibitors
Simeprevir Grasoprevir Paritaprevir	Daclatasvir Ledipasvir Ombitasvir Elbasvir Velpatasvir	Sofosbuvir Dasabuvir

At the time of writing the international guidelines for treatment of HCV G1 and G4 are SOF combined with an NS5A inhibitor with or without RBV (Table 1.5). The most recent EASL guidelines recommend three treatment options: SOF with LDV, DAC, or Velpatasvir (VEL) all of which achieve high SVR rates (EASL, 2017). Treatment for 12 weeks with either of those combinations is sufficient to treat G1b patients regardless of the presence of cirrhosis. RBV is still recommended for treatment experienced G1a with and without cirrhosis (Afdhal *et al.*, 2014; Feld *et al.*, 2015; Poordad *et al.*, 2016; Sulkowski *et al.*, 2014). Additionally, as an alternative to non-SOF based regimens the non-nucleoside inhibitor Dasabuvir combined with Paritaprevir and Ombitasvir achieve SVR rates of 98% when given for 8 weeks (Ara & Paul, 2015). Treatment for G4 follows

the guidelines for G1a with SIM still having a role in treatment experience patients with RBV.

Table 1.5: Summary of HCV treatment options by Genotype

Genotype	Treatment Rationale	Drugs	Duration
1	SOF with NS5A inhibitor – RBV if treatment experienced	SOF+ LDV, DAC, VEL	12 weeks
2	SOF with NS5A inhibitor – RBV if previously treated with IFN	SOF and VEL, RBV if decompensated cirrhotic	12 weeks
3	SOF with NS5A inhibitor – RBV if previously treated with IFN	SOF and VEL, RBV if decompensated cirrhotic	12 weeks
4	SOF with NS5A inhibitor – RBV if treatment experienced	SOF+ LDV or DAC	12 weeks

For G2 and G3 SOF in combination with DAC or VEL has largely replaced SOF/RBV or SOF/pegIFN/RBV as treatment options (EASL, 2017). RBV is no longer required to treat naïve non-cirrhotic patient with SOF/DAC or SOF/VEL representing an equivalent treatment option. For patients receiving SOF and DAC regimens RBV is still recommended for the treatment of patients with previous exposure to IFN based regimens as well as patients with cirrhosis regardless of treatment experience, although for the SOF/VEL regimen ribavirin is only recommended in patients with decompensated cirrhosis (Foster *et al.*, 2015a; Leroy *et al.*, 2016; Nelson *et al.*, 2015). SVR rates for G3 even with these regimens are still lower compared to other genotypes, for reasons yet unknown.

1.8 Project Aims/Hypothesis

Therapy for G3 HCV remains sub-optimal with relapse to treatment occurring at a clinically significant rate. The virological reasons for relapse remain poorly defined due to the inability to study patient derived HCV. Interestingly the use of RBV appears to boost SVR rates in cirrhotic G3 HCV. Why this occurs is unknown. The establishment of a novel HCV phenotyping assay in our lab has permitted the study of the drug phenotype of clinical HCV samples across all HCV genotypes (Cunningham *et al.*, 2014). It is the aim of this study to use this assay to examine the antiviral drug sensitivity of G3 HCV to determine if a virological insensitivity exists in patients who relapse compared to those who achieve SVR. The hypotheses for this study are:

1. A reduced sensitivity to antiviral drugs in pre-treatment G3 samples is associated with treatment failure
2. Antiviral-drug sensitivity is reduced in post treatment samples from relapse samples
3. Mutations in HCV are associated with antiviral drug ‘resistance’

2 Materials and Methods

2.1 Materials

2.1.1 Molecular Biology buffers

TAE Buffer	50X stock: 2M Tris Base (Trizma) with 57.1ml Glacial Acetic acid and 0.05M EDTA (pH 8.0). Make up to 1L with ddH_2O.
10X MOPS	0.2M MOPS, 0.05M sodium acetate, 0.01M EDTA, pH 5.5-7. For 1L: 41.86g MOPS, 4.102g sodium acetate, 3.72g EDTA in 800ml of DEPC ddH_2O. Adjust pH with NaOH.
10X TBS	Tris 100mM, NaCl 1.5M. For 1L: 12.11g TRIS, 87.66g NaCl in 1L of ddH_2O
TBS-T wash buffer	TBS diluted to 1X supplemented with 0.05% (vol/vol) Tween20
Blocking solution	TBS-T supplemented with 5% Non-Fat-Dry-Milk (weight/vol)
SDS-PAGE Running buffer	25mM Tris, 192mM Glycine, 0.1% SDS. For 1L: 3g Tris, 14.5g Glycine, 1g SDS in 1L H_2O.
Transfer Buffer	24mM Tris, 1.92mM Glycine, 10% Methanol. For 1L: 2.9g Tris, 1.45g Glycine, 100ml Methanol.
DEPC-Water	1ml DEPC to 1L ddH_2O, Leave overnight at room temperature and autoclave to sterilise.

RIPA Buffer	20mM Tris pH 7.5, 2mM EDTA, 150mM NaCl, 1% NP40 (IGEPAL)

2.1.2 Buffers for Bacterial Culture and to generate competent cells

Luria-Bertani Broth (LB)	For 1L, 10g Tryptone 5g Yeast extract and 10g of Sodium Chloride were dissolved in 1L of water and sterilised by autoclave
RF1	100mM Rubidium Chloride, 50mM Manganese (II) chloride tetrahydrate, 30mM Potassium acetate, 10mM Calcium chloride dihydrate, 15% (v/v) glycerol, buffered to pH 5.8 with glacial acetic acid
RF2	10mM MOPS, 10mM Rubidium Chloride, 75mM Calcium chloride dihydrate, 15% Glycerol (v/v), Buffered to pH 6.8 with NaOH
SOC	2%(w/v) tryptone, 0.5% (w/v) yeast extract, 20mM glucose, 10mM NaCl, 2.5mM MgCl2, 10mM MgSO4
XL-10 Recovery media	80mM of Magnesium Chloride, 80mM Magnesium Sulphate dissolved in LB broth supplemented with 0.4% (w/v) glucose

.

2.1.3 Mini Prep buffers

P1 (resuspension buffer)	50 mM Tris-HCL, 10mM EDTA pH8, supplemented with 50µg/ml RNase A (Sigma).
P2 (Lysis Buffer)	0.2M NaOH with 1% SDS.
P3 (Neutralisation Buffer)	4M Guanidine Hydrochloride with 0.5M potassium acetate buffered to pH 4.2 with glacial acetic acid.
PB (wash buffer I)	5M Guanidine Hydrochloride, 20 mM Tris-HCL (pH 6) 38% ethanol (final concentrations after the addition of ethanol).
PE (wash buffer II)	20mM NaCl, 2mM Tris-HCL (pH 7.5), 80% ethanol (final concentrations after the addition of ethanol).

2.1.4 Primers for HCV taqman expression assay

Primer Name	Sequence 5'-3'
HCV F	GCCTTGTGGTACTGCCTG
HCV R	CACGGTCTACGAGACCTCC
HCV Probe	ATAGGGTGCTTGCGAGTGCCCCGGG

2.1.5 Primers for Sybr Green qPCR

Primer Name	Sequence 5'-3'
HCVneg F	GCGAACCGGTGAGTACAC
HCVneg R	TACCACAAGGCCTTTCGC
5S F	TGTGATTTCCGCTGGTACGG
5S R	AGCCATCTCGAACCAGACAC
MxA F	AACAACCTGTGCAGCCAGTA
MxA R	AAGGGCAACTCCTGAGAGTG

2.1.6 Primers used for amplification of VSVG

Primer Name	Sequence 5'-3'
VSVG-Xba-F	TCTAGACACCATGAAGTGCCTTTTGTACT
VSVG-Xho-R	CGTAGCTCGAGTTACTTTCCAAGTCGGTTCATCT

2.1.7 Primers used for PCR mutagenesis of the S52-Subgenomic replicon and DBN3acc constructs

Outer NS5B primers encoding *XhoI* and *XbaI* restriction sites at the 5' and 3' end of NS5B	
S52-5B XhoI F	TGCCTCCTCTCGAGGGAGAG
S52-5B XbaI R	GGTCGACTCTAGACATGATCTGC
Overlapping primers designed to introduce the specified amino acid change in NS5B	
S52-5B-K100R-F	GTCCCTCCTCACTCTGCCCGGTCGAGGTTCGGGTATAGTGCGAAGG
S52-5B K100R-R	CCTTCGCACTATACCCGAACCTCGACCGGGCAGAGTGAGGAGGGAC
S52-5B-G188D-F	GTCAATTGAGACGATGGATTCCGCTTATGGATTCCAATACTC
S52-5B-G188D-R	GAGTATTGGAATCCATAAGCGGAATCCATCGTCTCAATTGAC
S52-5B-A150V-F	GTTTTGTGTGGACCCCGTTAAAGGGGGCCGC
S52-5B-A150V-R	GCGGCCCCCTTTAACGGGGTCCACACAAAAC
S52-5B-K206E-F	CGGGTCGAACGTCTACTGGAGATGTGGACCTCAAAG
S52-5B-K206E-R	CTTTGAGGTCCACATCTCCAGTAGACGTTCGACCCG
S52-5B-T213N-F	GAAGATGTGGACCTCAAAGAAAAACCCCTTGGGGTT
S52-5B-T213N-R	AACCCCAAGGGGTTTTTCTTTGAGGTCCACATCTTC
S52-5B-N244I-F	GGAGATATATCAATGCTGTATCCTTGAACCGGAGGC
S52-5B-N244I-R	GCCTCCGGTTCAAGGATACAGCATTGATATATCTCC

2.1.8 Primers used for NS5B amplification

Primer Name	Sequence 5'-3'
NS5B-F2	ATAGGATCCACCATGGTCTATGTCATACTCCTGGACC
NS5B-R2	TCATAGAATTCTTAGTAGAAGGAGGAAGGTCGAGCTAC

2.1.9 Primary antibodies

Mouse anti B-Actin (Abcam-8224)	Western Blot 1:5000
Mouse anti STAT-1 (BD-61085)	Western Blot 1:1000
Mouse STAT-2 (BD-61087)	Western Blot 1:1000
Mouse anti NS5A (Millipore)	Western Blot 1:2500
Sheep anti NS5A (Kind Gift from Mark Harris)	Western Blot 1:2500
	Immunofluorescence 1:1000
Rabbit anti-VSVG (Millipore)	Western Blot 1:2500
Rabbit anti NS5B (Abcam 65410)	Immunofluorescence (1:100)

2.1.10 Secondary antibodies

Sheep anti Mouse (VWR NA931)	Western Blot 1:5000
Donkey anti-Rabbit (Stratatech-711-036-152-JIR)	Western Blot 1:25,000
Donkey anti-sheep Alexa 488 (Life technologies A11015)	Immunofluorescence 1:1000
anti-sheep Alexa 488 (Life technologies A11015)	Immunofluorescence 1:1000

2.1.11 Plasmid Vectors

pGEMT-Easy	TA Cloning vector from PROMEGA. T7 promoter, Antibiotic resistance: Ampicillin
pTRIP-VSVG	Lentiviral expression vector expressing the G protein from VSVG, CMV promoter, Antibiotic resistance: Ampicillin
pcDNA3.1	Mammalian expression vector CMV promoter, Antibiotic resistance: Ampicillin
pRetroX	Lentiviral expression vector (Kindly Donated by Dr Richard Sloan, Queen Mary University of London), CMV promoter, Antibiotic resistance: Ampicillin
pDBN3acc	Plasmid construct encoding the full length DBN genotype 3 infectious isolate. (Kindly Donated by Prof Jens Bukh, University of Copenhagen) HCV genome under control of HCV IRES, Antibiotic resistance: Ampicillin
pS52-(SHI)-SG	Genotype 3 subgenomic replicon encoding the NS3-NS5B non-structural proteins. Structural proteins were replaced with a Firefly luciferase/Neomycin cassette driven by HCV IRES (Kindly donated by Prof Charlie Rice, Rockefeller Institute). HCV non-structural proteins driven by EMCV promoter.
pVSVG	Lentiviral envelope plasmid. CMV promoter, Antibiotic resistance: Ampicillin
pMD1.1	Lentiviral packaging plasmid encoding Gag and Pol accessory proteins. CMV promoter, Antibiotic resistance: Ampicillin
pNL1.1	Expression vector driving expression of the Nano luciferase reporter (Promega). CMV promoter, Antibiotic resistance: Ampicillin
pGL4.45	Reporter vector containing the interferon-stimulated response element driving transcription of the luciferase reporter gene *luc2P*. (Promega) CMV promoter, Antibiotic resistance: Ampicillin.

2.1.12 Competent cells

XL-10-Gold Ultracompetant cells	TetR Δ(mcrA)183 Δ(mcrCB-hsdSMR-mrr)173 endA1 supE44 thi-1 recA1 gyrA96 relA1 lac Hte [F´ proAB lacIqZΔM15 Tn10 (TetR) Amy CamR]
JM109	recA1, endA1, gyrA96, thi, hsdR17 (rK–,mK+), relA1, supE44, Δ(lac-proAB), [F´, traD36, proAB, lacIqZΔM15] (4).

2.1.13 Cell lines used in this study

Cell line	Description
THP-1	Monocyte cell line
Huh7	Hepatoma cell line
Huh7.5	Permissive hepatoma cell line for HCV infection due to non-functional RIG-I pathway
Huh7 Lunets	Hepatoma line generated from cured HCV replicon cells. Kindlty donated by Gilead Sciences
Huh7.5-SEC14L2	Huh7.5 cells over expressing the SEC14L2 gene, kindly donated from Peter Simmonds (University of Oxford)
Huh7.5-VSEC	Huh7.5 cells overexpressing both SEC14L2 and PIV5-V protein/ Kindly Donated from Mark Harris (University of Leeds)
S52-Wt	Huh7.5-cells stably expressing the S52-SG replicon
S52-K100R	Huh7.5-cells stably expressing the S52-SG replicon with a K-R mutation at amino acid position 100 in NS5B
S52-G188D	Huh7.5-cells stably expressing the S52-SG replicon with a G-D mutation at amino acid position 188 in NS5B
S52-K206E	Huh7.5-cells stably expressing the S52-SG replicon with a K-E mutation at amino acid position 206 in NS5B

2.1.14 Antiviral drugs used in this study

Sofosbuvir – Stock 10mM kindly donated by Gilead Sciences

Ribavirin- Stock 20mM, Sigma

Daclatasvir- Stock 10mM Kindly Donated by Bristol-Myers-Squib

IFNα-2A –Stock 10^7 IU/ml PeproTech

2.2 Methods

2.2.1 Clinical material

HCV patient sera were obtained from the HCV Research UK national bio-bank under tissue transfer agreement TR00335. Ethical approval for the study was given by London – City Research Ethics Committee and informed consent was obtained from all patients for the use of their samples in laboratory research.

2.2.2 Cell Culture

2.2.2.1 Passage of adherent cell lines

Media was aspirated and cells were washed with 1XPBS. Cells were removed from the flask surface with 2mL 1XTrypsin-EDTA, incubated at 37˚C for 5 minutes. Cells were then collected by adding DMEM supplemented with 10% fetal calf serum (FCS) and centrifuged at 200x*g* for 5mins. The cell pellet was re-suspended in 10mls DMEM 10% FCS, then split at a 1:3-1:10 ratio into a new T75cm^2 flask and maintained at 37˚C with 5% CO_2. Cells were passaged approximately every 3-4 days or when they reached 80-90% confluence.

2.2.2.2 Passage of suspension cell lines

The contents of a confluent flask were transferred into a 50mL falcon tube and centrifuged at 250x*g* for 5 min. Media was discarded and cell pellet re-suspended in 10ml RPMI 10% FCS. Cells were split 1:10 and maintained at 37˚C with 5% CO_2.

2.2.3 HCV Capture Fusion Assay

2.2.3.1 THP-1 Stimulation/infection

$1x10^6$ THP-1 cells were seeded in 6 well plates and stimulated overnight with 200ng/ml of PMA and 10ng/ml of IFNγ. Cells were washed in RPMI containing 2%FCS before inoculation with HCV sera at a multiplicity of infection (MOI) of 1. 24hrs post infection THP-1 cells were washed in PBS twice before removing from the plastic with a cell scraper.

2.2.3.2 Fusion of infected THP-1 and Huh7.5 cells

Huh7.5 cells were combined with the THP-1 cells at a ratio of 1:1 and centrifuged at 200x*g* for 5mins. Supernatant was removed and polyethylene glycol (PEG-Roche) was added drop wise directly to the THP-1/Huh7.5 cell pellet and incubated at 37ºC for 2mins. PEG was diluted out with serum free DMEM and incubated for a further 5min recovery period before centrifuging at 200x*g* for 5min. Fused cells were seeded at a density of $5x10^5$ in 6 well plates and maintained at 37ºC for a maximum of 5 days before harvesting into TRIzol (Invitrogen). For antiviral drug experiments media was replaced 24hrs after fusion with drug-containing media at a range of concentrations. This was subsequently replenished 3 days post fusion.

2.2.3.3 Cell Colouring

Cells were typsinised, pelleted by centrifugation at 200xg and washed in 1XPBS. Working solutions of the cytoplasmic dyes were made by diluting the Cell trace violet (Invitrogen) and CMRA orange (Invitrogen) to 1μM and 10μM respectively. Cells were

then re-suspended in 1ml of the either dye working solution and incubated at 10mins at 37˚C. To assess staining intensity, cells were fixed in 4% paraformaldehyde for 10mins at room temperature and then analysed by flow cytometry with a LSRII (Becton Dickenson)

2.2.4 RNA Extraction

RNA was extracted from capture fusion experiments using TRIzol reagent (Invitrogen) according to manufacturer's protocols. 1ml of TRIzol was added to each well of a 6 well plate and transferred into a 1.5ml eppendorf tube. To this 200µl of chloroform (Sigma) was added to and spun at 12,000*xg* for 15mins at 4ºC. The upper aqueous layer was removed into 0.5ml of isopropanol (Sigma) and incubated at room temperature to precipitate the RNA. This was re-spun at 12,000x*g* for 15mins at 4ºC before washing with 75% molecular grade ethanol (Sigma). A further spin was performed at 7500x*g* before re-suspension in 30-50µl of RNase free ddH_20. All RNA was stored at -80ºC

2.2.5 Quantitation of RNA by Ribogreen

To determine accurate RNA concentrations for PCR all RNA from capture fusion was quantified using the Quant-IT RiboGreen assay (Invitrogen). 1ug of RNA was DNase treated in a 10µl reaction containing 10x buffer and 1U of DNase (Promega) at 37ºC for 30mins. This was diluted 1:50 in 1XTE buffer and added in equal volume to the RiboGreen dye on a 96 well plate in duplicate and incubated for 5mins at room temperature. Fluorescence intensity at 485nm was recorded on a BMG FLUOstar optima plate reader. RNA concentrations were determined from a standard curve of known 16S RNA standard (Fig 2.1).

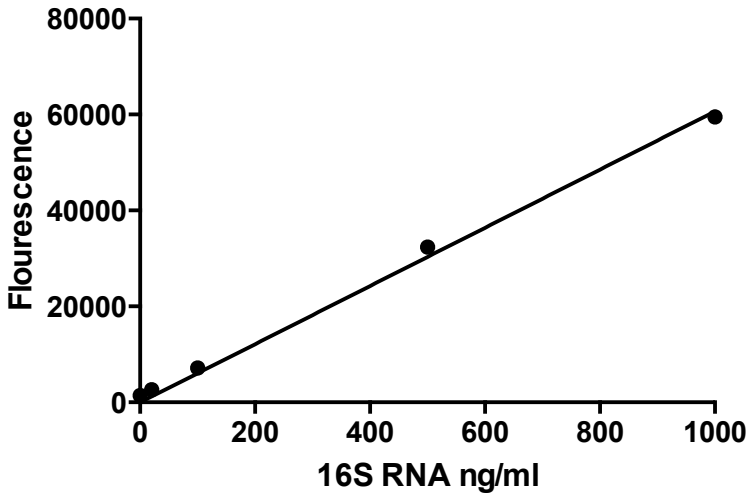

Fig 2.1 RiboGreen Standard Curve.
To enable RNA quantification a set of known RNA concentrations was prepared with each RiboGreen assay. Each standard was run in duplicate

2.2.6 Quantitative PCR

HCV RNA copy number was quantified using a one-step reverse transcription qPCR with the QuantiTect Viral Nucleic Acid detection kit according to manufacturer's instructions in 20µl reactions. Each reaction contained:

Reagent	Amount per 20µl Reaction
5X QuantiTect virus master mix	4µl
Primer/Probe mix	1µl
QuantiTect Virus RT mix	0.2µl
RNA template	50ng
RNase/DNase-free ddH_2O	Volume to 20µl

For HCV F/R Primer and HCV probe sequences see section 2.1.4. Each sample was run in triplicate with a standard curve of known amounts of *in-vitro* transcribed JFH-1 RNA in every PCR run (Fig 2.2). PCR steps consisted of Reverse transcription 20mins 50ºC, Hot-start activation step 95ºC 5mins, 40 cycles of denaturation 15secs at 95ºC

and annealing/extension 45secs at 58ºC. PCR runs were performed on a Rotorgene 6000 (Corbett Biosciences)

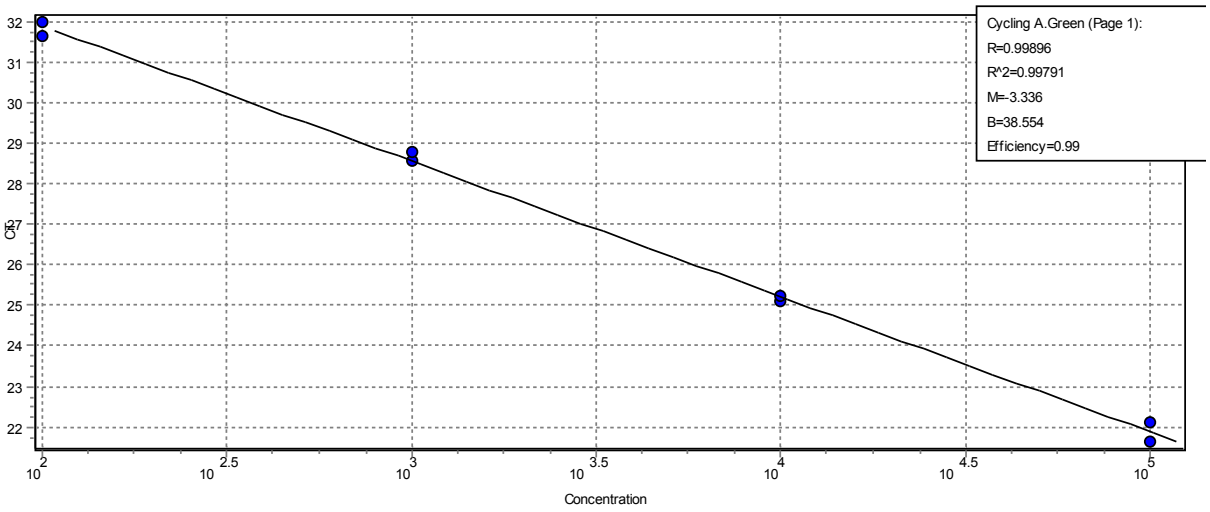

Fig 2.2 HCV qPCR standard curve
Standard curve generated by serial dilutions of JFH-1 RNA.

2.2.7 cDNA Synthesis

In a sterile RNase free 1.5ml eppendorf tube 1µg of DNase digested RNA was added to 0.5µg of random primers (Promega) in a volume of <14µl of water. This was heated to 70ºC for 5mins to melt any secondary structure within the RNA template. The tube was cooled to 4ºC immediately to prevent the secondary structure from reforming. To this mixture the following was added: M-MLV 5X Reaction buffer, dNTP 10mM mix (Final concentration 0.5mM/NTP), 200U M-MLV RT, Nuclease free water to a volume of 50µl. The reaction was incubated at 37ºC for 60mins after which cDNA yield was quantified.

2.2.8 Quantification of mRNA expression by SYBR green qPCR

Quantification of mRNA expression was performed using the QuantiTect- SYBR-Green real time PCR system (Qiagen). cDNA was diluted to a concentration of 250ng/ul with 500ng added per reaction. Each reaction contained: 12.5µL 2x

QuantiTect SYBR-Green PCR MasterMix 1µL forward and 1µL reverse primer (final concentration 0.5µM). Cycling conditions were: Hot-Start Activation: of 95ºC for 15 minutes, followed by 35 cycles of denaturation of 94ºC for 15 sec, annealing at 58ºC for 30 sec and extension of 72ºC for 30 sec. Data acquisition was performed during the extension step. Melt curve analysis was performed to check quality of product and to exclude presence of primer-dimers from the analysis. Results were normalised to expression of 5S from the sample, and expressed as relative gene expression using the Pflaffl method ($2^{-\Delta\Delta CT}$).

2.2.9 PCR amplification with High-fidelity polymerase

For amplification of DNA where a high degree of accuracy is required such as molecular cloning a high-fidelity polymerase with proof reading activity was used. The Q5 polymerase system by NEB was used for all high-fidelity PCR reactions as it has an error rate 280 fold lower than *Taq* polymerase. Reactions with this polymerase contained 5X reaction buffer, a final concentration of 0.2mM dNTPs, 0.5µM forward and reverse primers, 5X GC enhancer and Q5 polymerase at 0.02U/µl. < 10ng of plasmid DNA was used as a template. Cycling conditions were based on Initial denaturation of 98ºC for 30 seconds 25-30 cycles of denaturation at 98ºC for 30 seconds, primer annealing at 60ºC (optimised for primer set used) for 30 seconds and extension at 72ºC for 1 minute. A final extension of 72ºC for 30secs/kb was also performed.

2.2.10 Agarose gel electrophoresis

Agarose powder (1% w/v) was dissolved in 1XTAE buffer by heating in a microwave. Molten agarose was cooled to a safe temperature after which Ged-Red DNA dye 10,000X (Biotium). The gel was poured into a cast with a comb and left to set at room temperature. After the gel had set it was immersed in 1XTAE with DNA samples loaded in 6X loading dye. Gels were run at 5V/cm to allow separation of the DNA bands visualised with a UV-trans-illuminator. A DNA ladder was run in parallel with samples so that DNA band size could be estimated.

2.2.11 TA-Cloning into pGEMT

2.2.11.1 PCR amplification

PCR was carried out using the NEB Phusion DNA polymerase. Samples were prepared on ice and placed in a Bio-Rad thermocycler. Cycling conditions were an initial denaturation at 95ºC for 30 minutes. Amplification steps consisted of 30 cycles of denaturation at 95ºC for 15 seconds, primer annealing at 57-65ºC (depending on primer set used) for 30 seconds and extension at 72ºC for 30 seconds/kb of amplicon. A final primer extension was carried out at 72ºC for 2 minutes. Due to the proof reading activity of the high-fidelity Phusion polymerase a subsequent A-tailing step was performed using Go-Taq DNA polymerase (Promega). Reactions consisted of 5X Go-taq buffer, 400µM dATP, 1.5mM $MgC1_2$ and 1.25U of Go-Taq polymerase in a total reaction volume of 50µl. The reaction as incubated at 70ºC for 30 minutes. The A-tailed PCR product was purified using the QiaSpin PCR purification kit (Qiagen) before use in the ligation reaction. Ligation reactions consisted of 2X Rapid ligation reaction buffer, 50ng of the pGEM-T easy vector and 3 units of T4 DNA ligase. The A-tailed PCR product was added to the reaction in a 3:1 molar ratio of insert to vector.

Reactions were incubated for 1 hour at room temperature. Positive control DNA was provided by the supplier and a negative control that contained neither control nor PCR insert DNA was also used.

2.2.11.2 Transformation of ligation reaction JM109 Chemically competent cells with blue white/screening

5µl of the ligation reactions was added to chemically competent JM109 cells and incubated on ice for 30 minutes. The cells were heat shocked at 42ºC for 30 seconds to permeabilise the cells for the uptake of DNA and returned to ice. 250µl of sterile SOC medium was added to each transformation, which was subsequently incubated at 37ºC for 1 hour with agitation. The transformed cells were spread onto LB plates containing ampicillin (100µg/ml) supplemented with 0.1mM IPTG and 1mg/ml X-Gal and left overnight at 37ºC. White colonies were picked, inoculated into fresh LB media containing ampicillin (100µg/ml) and the plasmid DNA was extracted by mini-prep for sequencing to confirm the successful cloning of the desired fragments into the pGEM-T vector.

2.2.11.3 Preparation of plasmid DNA

Overnight cultures of *E. coli* were grown in LB broth with an appropriate selective antibiotic. Plasmid DNA was extracted using a QIAprep® Mini-prep kit (Qiagen). The overnight culture was centrifuged at 3,000x*g* and re-suspended in 250µl of buffer P1 (with RNase added). 250µl of buffer P2 was then added to lyse the cells and was neutralised after 3-5 minutes by the addition of 350µl of buffer N3. The solution was centrifuged at ~17,500x*g* for 10 minutes to pellet cell debris from the lysis reaction. The supernatant was added to a QIAprep spin column and centrifuged at ~17,500x*g*

for 1 minute and the flow through discarded. Two wash steps then occurred with buffers PB and PE, discarding the flow through each time. An extra spin was performed with the PE wash to remove any residual traces of ethanol. 50µl of molecular grade water was added to the centre of the QIAprep spin column filter and spun at ~17,500xg for 1 minute to elute the plasmid DNA.

2.2.11.4 Restriction digestion

5µg of plasmid was digested in 50µl reaction containing 10X cut-smart buffer, 20U restriction enzyme and water to 50µl. The reaction was incubated overnight at 37ºC. The resulting digest was separated on a 1% agarose TAE gel and purified using the Qiaspin Agarose gel extraction kit (QIAGEN) according to manufacturer's protocol.

2.2.11.5 Dephosphorylation of plasmid vectors

Digested plasmid vectors typically will possess a 5' phosphate group that may cause the vector to self-ligate. To prevent this and minimise any background activity of the cloning process the 5' phosphate was removed before ligation. 1µg of the digested vector was dephosphorylated in a 20µl reaction containing 10x rAPid alkaline phosphatase buffer and 1U of alkaline phosphatase enzyme (Roche). The reaction was incubated at 37ºC for 10min before inactivation at 72ºC for 2min.

2.2.11.6 Ligation of DNA fragments into plasmid vectors

The purified digested DNA fragment was ligated into the dephosphorylated vector at a insert:vector ratio of 3:1. Vector and insert were diluted in a 5X DNA dilution buffer and added to the ligation reaction containing 2X ligation buffer and 5U of T4 DNA ligase (Roche). The reaction was incubated for 5min at room temperature before

transformation into JM109 cells. Optimum colony numbers were however observed at an overnight incubation at 16ºC.

2.2.12 Generation of chemically competent XL-10 gold cells

XL10 gold cells were streaked from frozen glycerol stock onto an LB agar plate supplemented with tetracycline and incubated overnight at 37˚C for 16hrs. Colonies were picked into 10ml of LB and incubated overnight at 37˚C with shaking. The overnight culture was then used to inoculate a larger 500ml culture, which was grown throughout the day until an optical density at 600nm between 0.4 and 0.9 was reached. At this point cultures were transferred to 50ml falcon tubes and chilled on ice for 20mins before centrifugation at 3800x *g* for 20mins at 4˚C. Pellets were re-suspended in 0.8ml of RF1 (see 2.1.2) after which the volume was made up to 20ml with RF1 and incubated on ice for 10min. Cells were pelleted by centrifugation at 1000x*g* for 20mins, combined into one 50ml falcon tube and incubated on ice for a further 15mins in 20mls of RF2. Cells were aliquoted into sterile eppendorf tubes and left on ice for 2hrs. After incubation cells were snap frozen in liquid nitrogen and stored at -80˚C until needed.

2.2.13 Transformation of XL-10 Gold competent cells

Up to 50ng of DNA/5µl of a ligation reaction were added to a 25µl aliquot of frozen cells. This was incubated for 20mins on ice before heat shocking at 42ºC for 45 seconds. Cells were incubated on ice for 2 mins and recovered in 250µl of XL-10 recovery media and incubated at 37ºC for 1hr. Transformed cells were then streaked on LB agar with appropriate selection media and incubated at 37ºC for 16hrs to so that transformed colonies could growth through selection.

2.2.14 PCR based, Site directed mutagenesis of the S52-(SHI)-SG replicon construct

To incorporated mutations into the NS5B of the G3-S52-Subgenomic replicon an overlapping PCR mutagenesis technique was employed using PCR primers containing the desired mutation. This process requires two steps; first the generation of two overlapping fragments with primers containing the mutation of interested, the second step is then the creation of the full-length insert with the mutation by denaturing and then annealing the overlapping fragments. This insert was then cloned into the S52-replicon by restriction digestion and ligation. Steps involved in this process are described graphically in Fig 2.3.

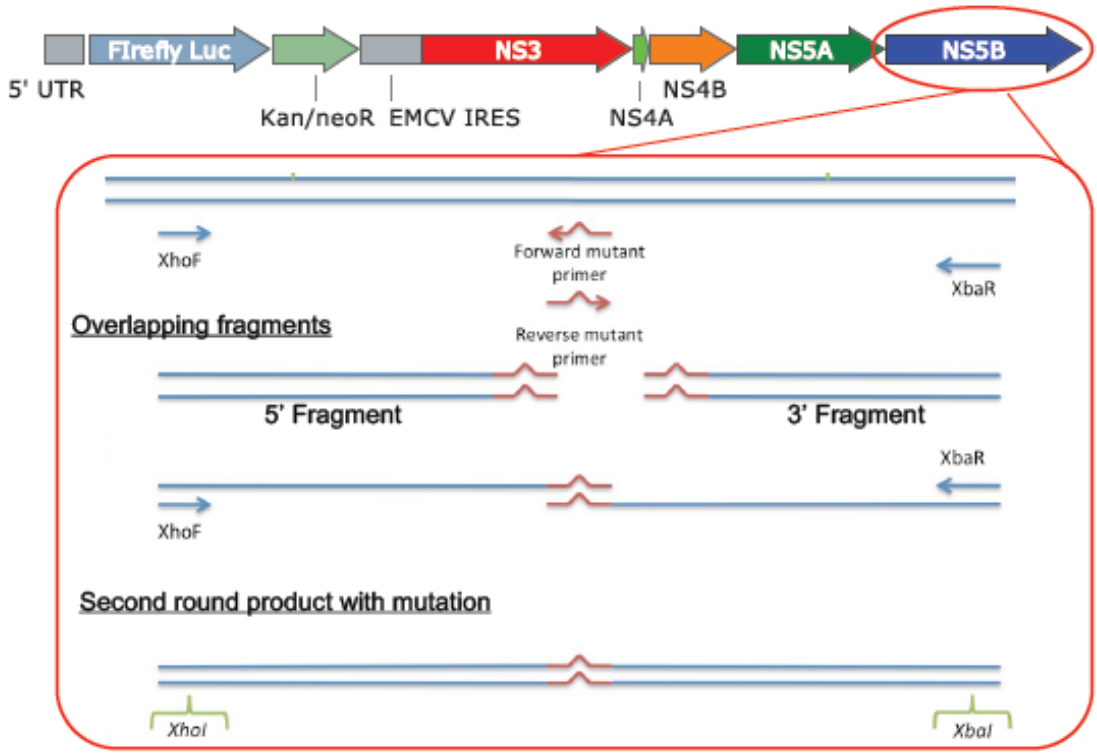

Fig 2.3 Schematic of PCR mutagenesis
Mutagenic primers encoding the mutation to be introduced were used to generate two overlapping PCR fragments, subsequently used in a second PCR reaction to generate the full length insert. Outer primers

used to generate this insert included *XbaI* and *XhoI* restriction sites allowing it to be cloned back into complementary sites in the replicon.

For each mutation, two first round fragments were generated using the Q5 high-fidelity polymerase using a combination of the S52-5B-XhoI forward and mutagenic reverse primer and mutagenic forward and S52-5B-XbaI-Rreverse primer (See 2.1.7). Reactions were set up containing a final concentration of 0.2mM dNTPs, 0.5µM of each forward and reverse primer, G/C enhancer (5µl/25µl reaction), 5X Q5 reaction buffer and 10 units of Q5 polymerase. 10ng of the S52-SG replicon plasmid was used as a template. Cycling conditions were carried out as follows: initial denaturation of 98ºC for 30 seconds and 30 cycles of denaturation at 98ºC for 30 seconds, primer annealing at 58ºC for 30 seconds and extension at 72ºC for 30 seconds/kb of amplicon. A final primer extension was carried out at 72ºC for 2 minutes.

To generate a full-length insert with the engineered mutation purified fragments were used in a second-round reaction with both the S52-XhoI-forward and S52-XbaI reverse primers. Before the primers were added, an initial 4 rounds of cycling were carried out containing the reaction mix as above as well as both fragments in an equimolar ratio. The overlapping regions of both fragments would anneal and extend to the end of the fragment generating a small amount of the full-length amplicon. The S52-XhoI-forward and S52-XbaI reverse primers were then added to the reaction to amplify the insert. Cycling conditions for the entire reaction were as follows: Initial denaturation of 98ºC for 30 seconds 4 cycles of denaturation at 98ºC for 30 seconds, primer annealing at 60ºC for 30 seconds and extension at 72ºC for 1 minute. The reaction paused as the primers were added and then a further 29 cycles of 98ºC for 30 seconds, 58ºC for 30

seconds and extension at 72ºC for 2 minutes, ending with a final extension of 72ºC for 5mins.

The full-length insert containing the mutation was digested with *XbaI* and *XhoI* and ligated into the pre-digested S52-replicon plasmid. Colonies containing successful recombinants were obtained by transformation of chemically competent XL-10 gold cells as above.

2.2.15 Site directed mutagenesis of the DBN3acc construct

Nucleotide changes were introduced into the genotype 3 DBN3acc infectious clone using the Quick-Change II XL site-directed-mutagenesis kit (Agilent) according to manufacturers instructions. Reactions consisted of 10x reaction buffer, 10ng of plasmid template, 125ng of each mutagenesis primer (see2.1.7), 1µl of Agilent dNTP mix, 3µl of Quick solution, 2.5U of PfuUltra HF DNA polymerase and water to a volume of 50µl. Cycling conditions were 95ºC for 1min followed by 18 cycles of 95ºC for 50secs, 60ºC for 50secs, 68ºC for 1min/kb of plasmid length and a final extension of 68ºC for 7mins. 10U of *DpnI* was added to reaction and incubated for 1hr at 37ºC to digest the parental DNA template after which 5µl of the reaction was transformed into the XL-10 Ultracompetant cells as above. Colonies were screened for mutagenesis by Sanger sequencing (Source Bioscience, Cambridge).

2.2.16 *In vitro* transcription

Replicon plasmids were linearised by restriction digestion with *XbaI* for 3hrs at 37ºC. Reaction volume was then made up to 300µl with ddH20 to which 1 volume of Phenol:Chloroform pH 8 was added. Samples were inverted at least 6 times and

centrifuged at >15,000x*g* for 3mins at 4ºC. The upper aqueous layer was removed to a fresh eppendorf tube to which 1 volume of chloroform was added, which was then re-centrifuged as above. The upper aqueous layer from the chloroform spin was removed, placed in a new tube and precipitated by the addition of 0.3M sodium acetate (final concentration) and 2.5 volumes of ice-cold ethanol. To achieve maximum precipitation samples were incubated at -20ºC for at least 1hr. The overhang from the *XbaI* was cleaved by digestion with Mung bean nuclease. 1ug of purified DNA was incubated at 30ºC for 30 minutes in a reaction containing 10 units of nuclease and 10X reaction buffer. DNA was then re-purified as above.

In vitro transcription of replicon RNA was performed by use of the T7-Megascript kit (Ambion). Reactions were prepared at room temperature to prevent precipitation of the spermidine in the 10X reaction buffer. Each 20µl reaction contained 2µl of ATP, GTP, CTP UTP, 2µL of 10X reaction buffer, 1µg of linearised template DNA and water to make up the volume to 20µl. Reactions were incubated at 37ºC for 3hrs after which they were stopped by the addition of 115µl of DEPC-treated water and 15µl of ammonium acetate stop solution. RNA was then extracted by addition of an equal volume of acidic phenol:chloroform, followed by chloroform. RNA was precipitated from the subsequent aqueous layer by the addition of 1 volume of isopropanol followed by chilling at -20ºC for at least 1 hr. RNA was pelleted by centrifugation at 16,000x*g* for 15mins, quantified by nanodrop and stored at -80ºC in 10µg aliquots.

2.2.17 Electroporation of HCV replicon constructs

For electroporation, cells were washed X2 with ice cold PBS and diluted to a concentration of $5x10^6$ cells/ml. 5µg of purified RNA was mixed with 400µl of the cell

suspension and electroporated using a BioRad Genepulser II on the exponential setting (pulse settings: 250V and 950μF). For antiviral drug assays, cells were transferred to complete medium and seeded into 96 well plates at a density of $5x10^3$ cells/well and left to recover for 24hrs. Antiviral drugs were added for 72hrs after which cells were lysed in 1Xpassive lysis buffer in a volume appropriate to the size of culture dish they were seeded in. Lysates were added to an opaque white 96well luciferase plate with the luciferase substrate (promega) added in a 3:1 ratio. Luminescence was recorded using a BMG FlouStar plate reader (Optima).

2.2.18 Transfection of DBN replicon construct to generate infectious G3 virus

Transfection of the DBN3acc construct and generation of Genotype 3 infectious HCV Huh7.5-SEC14L2 cells were seeded in a 6 well plate at a density of $4.2x10^5$ cells/well 24hrs before transfection. For transfection 3.75μl of Lipofectamine 3000 was diluted in 125μl of OptiMEM and 5μg of DBN3acc RNA was diluted in 250μl of OptiMEM. Both mixes were incubated at room temperature for 5mins before combining after which the reaction mixture was incubated for a further 20mins at room temperature and then added drop wise to the cells. Cells were washed once with PBS before transfection and placed in 2ml of OptiMEM for at least 20mins before transfection. After 24hrs cells were placed in DMEM 10% FCS and expanded into T25 then T75cm^2 flasks. At 7 days post transfection a sample of transfected cells were seeded on to coverslips to assess presence of HCV replication complexes by NS5A immunofluorescence (see 2.2.21). Once >50% of cells were deemed to be positive for HCV, supernatants from the

transfected cells were filter-sterilised using a 0.45μm syringe filter, aliquoted and stored at -80ºC.

2.2.19 Focus Forming assay to titre cell culture derived HCV

Huh7.5-SEC14L2 cells were seeded in 96 well plates at a density of $3x10^3$ cells/well. After 24hrs cells were exposed to 1:3 serial dilutions of supernatants from cells transfected with the DBN3acc virus. Cells were then incubated for a further 4 days and then washed in 1XPBS before fixation in ice-cold methanol. To visualise HCV foci, wells were blocked in PBS 3%FCS for 30mins and then incubated with sheep anti-NS5A (kind donation from Mark Harris) diluted at 1:1000 for 1hr at room temperature. Unbound primary antibody was removed by 3 washes with 1XPBS before incubation with AlexaFlour 488 donkey anti-sheep secondary antibody diluted to 1:1000 for 1hr at room temperature. Wells were then incubated with DAPI (1:1000) for nucleus visualisation.

2.2.20 Quantification of HCV Foci using a INCELL automated microscope

Huh7.5-SEC14L2 cells were infected, maintained and stained as above for a focus-forming assay. After secondary antibody incubation cells were stained with a 1:100,000 dilution of HCS Cell Mask Deep Red Stain (Invitrogen), which uniformly stains the cell plasma membrane for 1.5hrs. HCV foci were then quantified using a GE High throughput INCA2200 automated microscope with 9 fields taken per well using a X20 objective. Images were analysed using the high content analysis software Developer toolbox (GE, Version 1.9.2). Raw images were processed to define nuclear and cytoplasmic borders based on DAPI and cell mask staining. Acceptance criteria for NS5A foci included size and pixel intensity. Targets were linked to quantify

nucleated cells containing foci. Workflow is described in Fig 2.4.

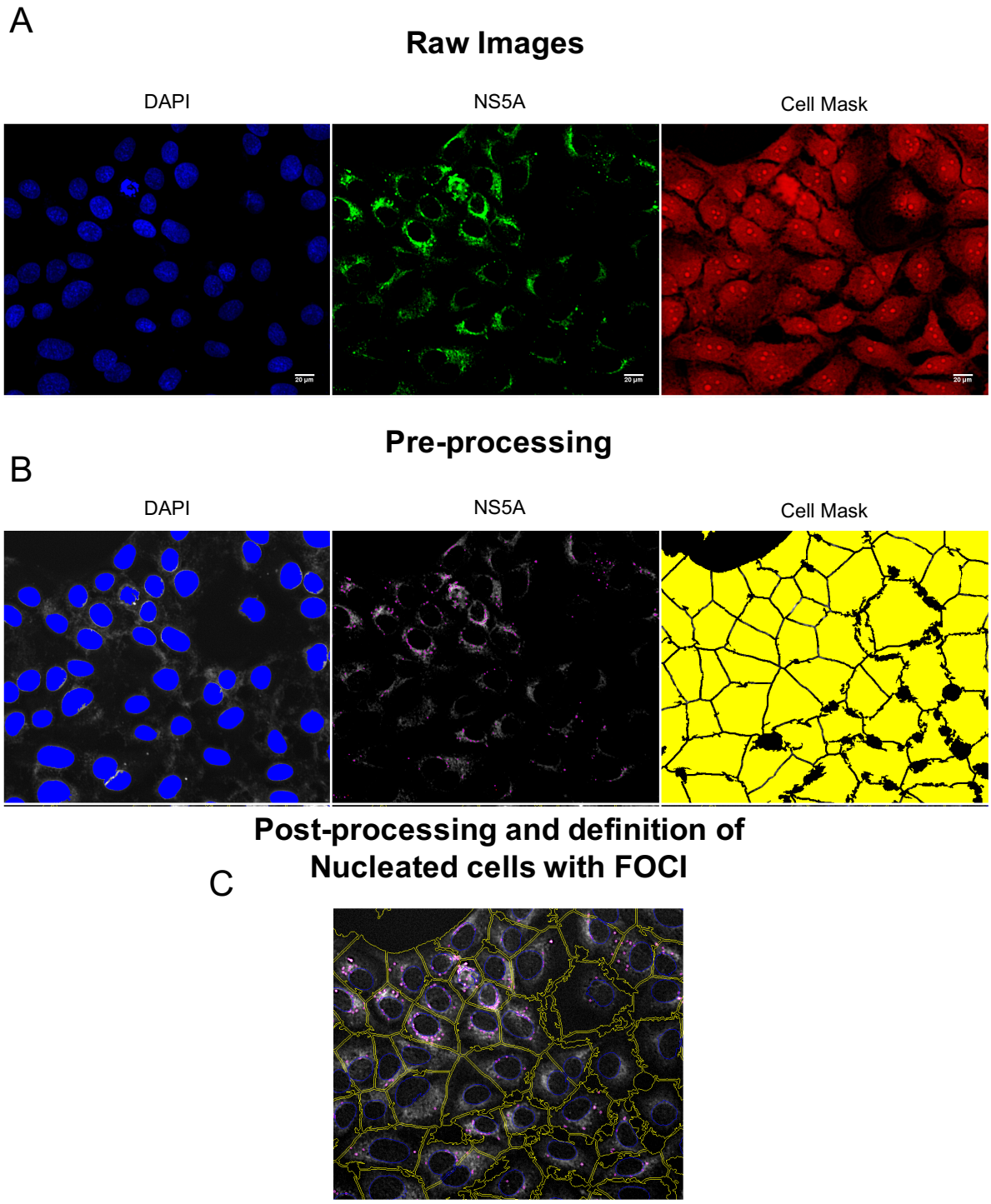

Fig 2.4 Quantification of HCV foci by the INCELL automated microscope
(A) Raw images taken before processing showing NS5A staining as well as nuclear and cell membrane staining. (B) Pre-processing of each image to define the nuclear and cell border. Acceptance criteria for HCV foci were set based on size of foci and cellular localisation. (C) Post processing of images.

Nuclear, foci and cell mask images were linked to quantify the number of nucleated cells containing foci per field and then per well.

2.2.21 Indirect immunofluorescence

Cells were plated on coverslips and fixed with 4% paraformaldehyde for 20mins. The cells were permeabilised in PBS 0.25% (v/v) Triton-X then non-specific binding was blocked by incubation in PBS/3% BSA. Coverslips were incubated with the primary antibody for 1hr at room temp, before washing and then further incubating with an appropriate secondary fluorescent antibody for 1hr. Coverslips were counterstained with 4',6-diamidino-2-phenylindole and mounted with Prolong Gold (Invitrogen). Slides were viewed on a Leica MM fluorescence microscope (Leica Microsystems, Milton Keynes, UK).

2.2.22 Plasmid Transfection

Cells were seeded in 6 well plates at a density of $1x10^5$ cells/well and incubated overnight at 37ºC. Transfection mixes containing plasmid and Lipofectamine 3000 (Invitrogen) were prepared including a mock transfection control. 3µl of Lipofectamine was first diluted in 125µl Opti-MEM and incubated for 5mins at room temperature (tube A). In a separate tube 1µg of plasmid was also diluted in 125µl of Opti-MEM supplemented with 3µl of P3000 (tube B). Tubes A and B were combined and incubated for a further 20 mins at room temperature. The ratio of Lipofectamine:DNA was 3:1. The mixture along with a mock transfection control was added drop wise directly to the plated cells and incubated overnight at 37ºC. After 24hrs media was changed and cells were place under antibiotic selection, specific to the construct used.

2.2.23 Lentiviral preparation and transduction

293FT cells were seeded in a 10cm plate so that they would be 50% confluent on the day of transfection. Plasmid mix containing 8µg of the pTRIP-VSVG plasmid, 2µg of the pMLV gag/pol plasmid and 0.15µg of the pVSVG envelope plasmid was added to 25µl Fugene diluted in 500µl of Optimem. The transfection mix was incubated at room temperature for 45mins and then added drop wise on to the cells. Lentiviral supernatants were harvested at 24 and 48hrs. These were centrifuged at 3000x*g* for 10mins to remove cell debris, passed through a 0.45µm filter and stored at -80˚C.

2.2.24 Protein extraction

Cells were washed with PBS, trypsinised and pelleted by centrifugation at 200x*g.* Cell pellets were resuspended in RIPA buffer supplemented with 1XHALT protease and phosphatase inhibitor cocktail (Invitrogen) and incubated on ice for 30mins. Protein samples were then centrifuged for 30mins at 16,000x*g* at 4˚C to pellet DNA and nuclear debris. Supernatants containing protein were stored at -20˚C until used.

2.2.25 Protein Quantification by bicinchoninic (BCA) assay

Copper II Sulphate was diluted 1:50 with the BCA reagent and 200µl aliquoted on a clear flat bottom 96-well plate. To this 5µl of protein sample or standard were added and the plate incubated at 37ºC to catalyse the colour change to purple. This colour change is based on the reduction of Cu^{+2} to Cu^{+1} by protein in an alkaline environment. The chelation of two BCA molecules with one Cu^{+1} forms the purple colour, which

exhibits a strong absorbance at 562nm. Protein concentrations were determined with reference to a standard curve derived from serial dilutions of known concentrations of bovine serum albumin.

2.2.26 Western Blotting

Protein samples were separated by SDS-PAGE using a NuPAGE Novex 4-12% Bis-Tris Protein Gels at 200V. A protein size marker was included in every run (Amersham-Full rage molecular weight marker). After electrophoresis the stacking gel was removed and the running gel was rinsed in protein transfer buffer. A sheet of nitrocellulose membrane (BioRad) was cut to size and then incubated briefly in transfer buffer. The NuPage transfer cassette was assembled and the transfer process is carried out at 25V for an hour. Following transfer, the membrane was removed and rinsed briefly in blocking solution (see section 2.1.1). Non-specific binding sites were blocked by immersing the membrane in 1XTBS supplemented with 5% (w/v) non-fat-dry-milk for 1hr at room temperature. Primary antibody was diluted in blocking solution and incubated on the membrane overnight at 4ºC. Membranes were washed with TBST for 4x5mins and then incubated with an HRP secondary antibody diluted in blocking solution (supplemented with IGEPAL final concentration of 0.1%). A final wash step was performed and blots left in wash buffer for 1hr before detection of protein bands with ECL (Amersham). After 5min incubation in ECL, the membrane was wrapped in clingfilm and exposed to a sheet of autoradiography film (Amersham) for 30secs-5minutes before being developed on a Xograph film developer machine

2.2.27 Next-generation sequencing of HCV genomes

Full HCV genome sequencing was performed by the University of Glasgow Centre for Virology research using a Metagenomic-Illumia RNA-seq method of total plasma RNA as previously described (Thomson *et al.*, 2016).

2.2.28 Interferon Stimulated Response Element Luciferase assay

Cells were seeded onto a 96well plate at a density of $5x10^3$ cells/well. The luciferase reporter plasmid pGL4.45 was mixed 2:1 with the Nanoluc expression plasmid pNL1.1(see 2.1.11) as a transfection control in a volume of 10µl of OptiMEM. Plasmid mixes were then combined with Lipofectamine 3000 in a ratio of 3:1 and allowed to complex at room temperature for 5mins. The transfection mix was added to the cells so that the final amount of plasmid per well was 150ng of pGL4.45 and 75ng of pNL1.1. After 16hrs cells were incubated with 10-1000IU/ml of IFNα-2A for a further 24hrs after which cells were lysed in 1X passive lysis buffer. Firefly luciferase corresponding to the ISRE reporter was measured as before. To account for transfection efficiency, nanoluciferase was measured using the Nanoglo luciferase kit (Promega) according to manufacturer's instructions.

3 RESULTS: Optimisation of Methods to Study Patient Derived HCV

One of the challenges HCV researchers face is the inability to effectively propagate clinical virus *in vitro*. In the face of constant development of HCV direct acting anti-viral (DAA) treatment, relapse to treatment is becoming increasingly infrequent, yet endures, particularly with genotype 3 (G3) infection. The reasons for the increased relapse rates in G3 remain unsolved and study of clinical samples derived from patients who have relapsed may help to clarify why this genotype remains refractory to DAA therapy. Recent studies such as the discovery of SEC14L2 and the use of stem cell derived hepatocyte like cells have helped to unravel key host factors that hepatocyte cell lines such as Huh7.5 may lack to enable patient derived HCV to replicate in cell culture (Sa-ngiamsuntorn *et al.*, 2016a; Saeed *et al.*, 2015; Schwartz *et al.*, 2012). However, despite these advances propagation of patient derived hepatitis C virus remains problematic, hampering a full understanding of factors that influence treatment response. The capture fusion assay developed by our group is an established method, which can determine sensitivity of clinical HCV isolates to a range of antiviral drugs (Cunningham *et al.*, 2014; Jones *et al.*, 2017). The assay itself is a labour intensive, complex procedure with its key component consisting of fusion between viral infected THP-1 cells and Huh7.5 by treatment with polyethylene glycol (PEG). PEG fusion is an intricate technique causing high levels of cell toxicity resulting in a sufficient but relatively low frequency of hybridoma formation (Golestani *et al.*, 2007; Lovy *et al.*, 2012; Schneiderman *et al.*, 1979). To this end we conducted experiments to assess whether the PEG fusion technique could be either enhanced or replaced to increase the efficiency of fusion formation between THP-1 and Huh7.5 cells. We established a simple FACS based assay to provide an indication of the level

of cell fusion, which permitted a range of different conditions to be rapidly assessed. Our strategy was to identify potential improvements to the assay and then confirm them in formal assessments of viral replication from clinical isolates.

The recent publication by Saeed and colleagues uncovered SEC14L2 as a key host factor that could permit limited replication of patient-derived HCV when over expressed in Huh7.5 cells (Saeed *et al.*, 2015; Witteveldt *et al.*, 2016). Given the potential value of cell lines expressing this protein to enhance our understanding of HCV replication we assessed the potential of SEC14L2 expressing cell lines to allow replication of patient derived viral isolates and compared their ability to determine sensitivity to antivirals to that of the capture fusion assay. The aim of these experiments was to establish whether SEC14L2 expressing cells were a sufficient model system for HCV replication in isolation or if they could be incorporated into the capture fusion model.

3.1 Determining the level of cell fusion in the capture fusion assay

3.1.1 FACS analysis of fused cells

Previous studies of PEG mediated cell fusion used FACS based assays to determine levels of fusion between two cell populations by staining each with a different fluorescent dye (Hoffman *et al.*, 2017; Li *et al.*, 2014). Here we sought to establish a FACS assay to measure the efficiency of PEG cell fusion between THP-1 and Huh7.5's. PEG fusion between two cells types amalgamates the cytoplasmic membranes between the cells to form a multi-nucleated heterokaryon from both cells [Reviewed in (Lentz & Lee, 1999)]. Therefore, staining the two cell types with distinct cytoplasmic dyes and then performing PEG fusion should allow the detection of fused cells that share dual fluorescence for each cytoplasmic dye.

Stimulated THP-1 and Huh7.5 cells were coloured with Cell-Trace-Violet and CMRA orange respectively before fusion. Subsequent FACS analysis of the stained THP-1 and Huh7.5 cell populations revealed that the cytoplasmic dyes achieved discrete staining of the THP-1 and Huh7.5 cell populations when compared to the non-stained control (Representative examples are shown in Fig 3.1 A-D). Stained THP-1 and Huh7.5 cells were then fused by PEG and analysed by FACS to determine the proportion of cells that had dual fluorescence (Fig 3.1 H). To account for any background in dual fluorescence caused by adherence between the THP-1 and Huh7.5 cells, a non-PEG treated fusion control was also included (Fig 3.1 G). FACS analysis of fusion control showed the Huh7.5 and THP-1 cells as distinct populations. In non-treated cells around 6% of the total cell population were found to contain dual fluorescence (Fig 3.1 G). When the cells were treated with PEG the percentage of cells with dual florescence rose to approximately 13% (Fig 3.1 H). Statistical analysis of 4 independent fusion experiments revealed that this increase in dual fluorescence was significant in cells treated with PEG compared to the non-PEG control (Fig 3.1 J).

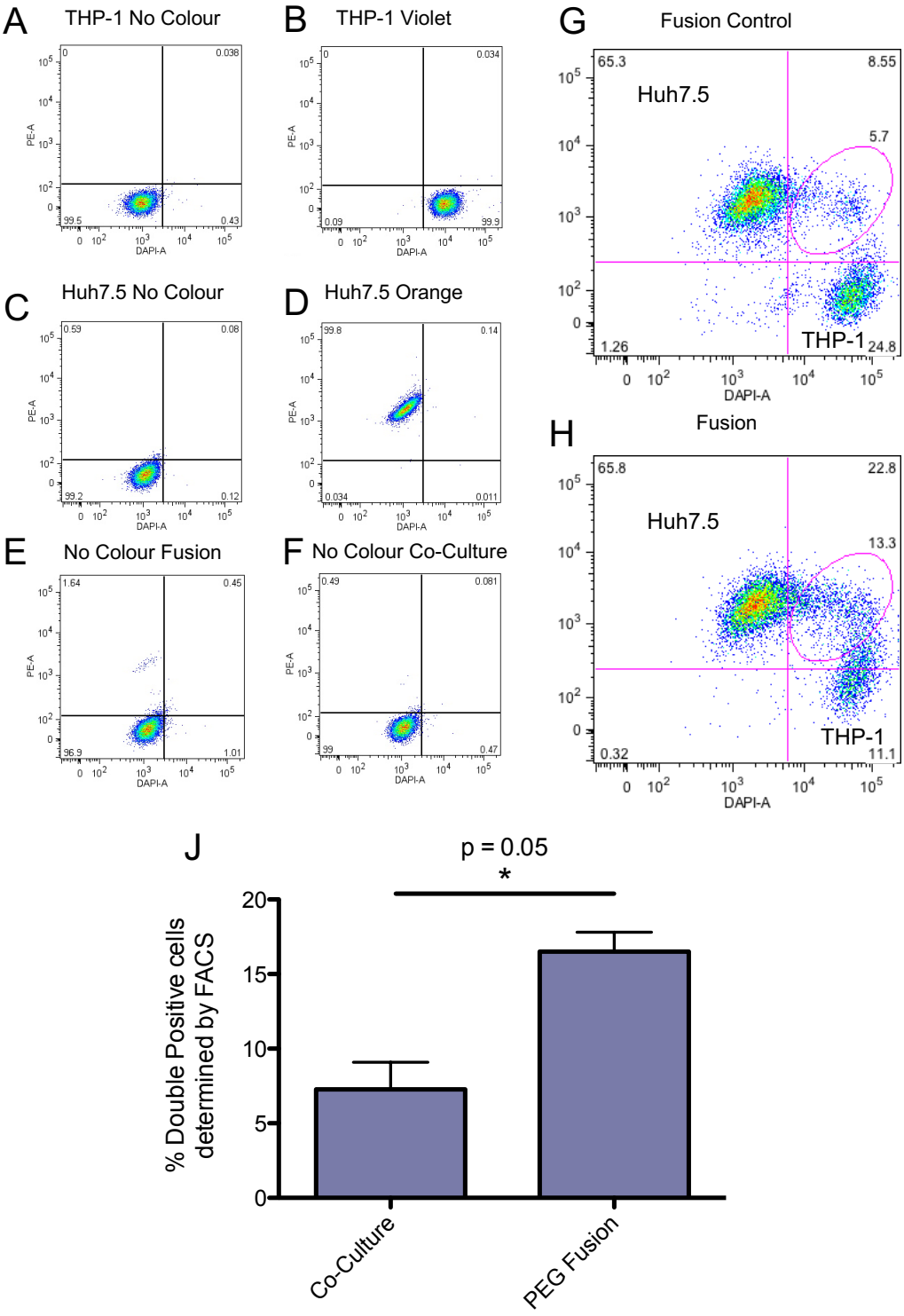

Fig 3.1 FACS analysis of Capture Fusion
FACS plots of THP-1 and Huh7.5 cells stained with Cell Trace Violet (B) and CMRA Orange (D) cytoplasmic dyes. Non-coloured cell populations were included as controls (A, C, E, F). To assess the levels of fusion coloured THP-1 and Huh7.5 cells were fused with PEG and analysed by FACS for dual fluorescence (H). The oval gate in the upper right quadrant defines cells as fluorescent for both dyes. A fusion control was included by co-culturing coloured THP-1 and Huh7.5 cells without exposure to PEG to account for dual fluorescence caused by adherence between the two cell types (G). The plots presented above are representative of 4 independent experiments. Comparison of the co-culture control

and PEG fusion with this assay revealed a significant increase in dual fluorescence with PEG fused cells. Statistical analysis was performed using a Man-Whitney U test (J).

3.1.2 Analysis of Fusion by immunofluorescence

To demonstrate that PEG resulted in fusion events between Huh7.5 and THP-1 cells we sought to visualise fused cells by fluorescent microscopy. An alternative staining strategy to that used in the FACS experiments was employed due to difficulties encountered detecting the cell-trace violet stain with the fluorescent microscope. THP-1 cells were stained with CMRA orange before fusion to Huh7.5 cells, while Huh7.5 cells were stained by immunofluorescence for the liver specific protein albumin post-fusion. Examination of the PEG fused cells revealed multinucleated cells with orange staining in the cytoplasm likely due to amalgamation of the two cytoplasmic membranes characteristic of PEG fusion (Fig 3.2). This staining pattern was not observed in the fusion control however the THP-1 cells were seen to be in close proximity to the Huh7.5 cells indicating that these cells adhere to one another when co-cultured in the absence of PEG. The direct immunofluorescence experiments confirmed the results from the FACS experiments that cell fusion is relatively uncommon but given the complexity of this technique we continued to use the FACS based assay to analyse cell fusion.

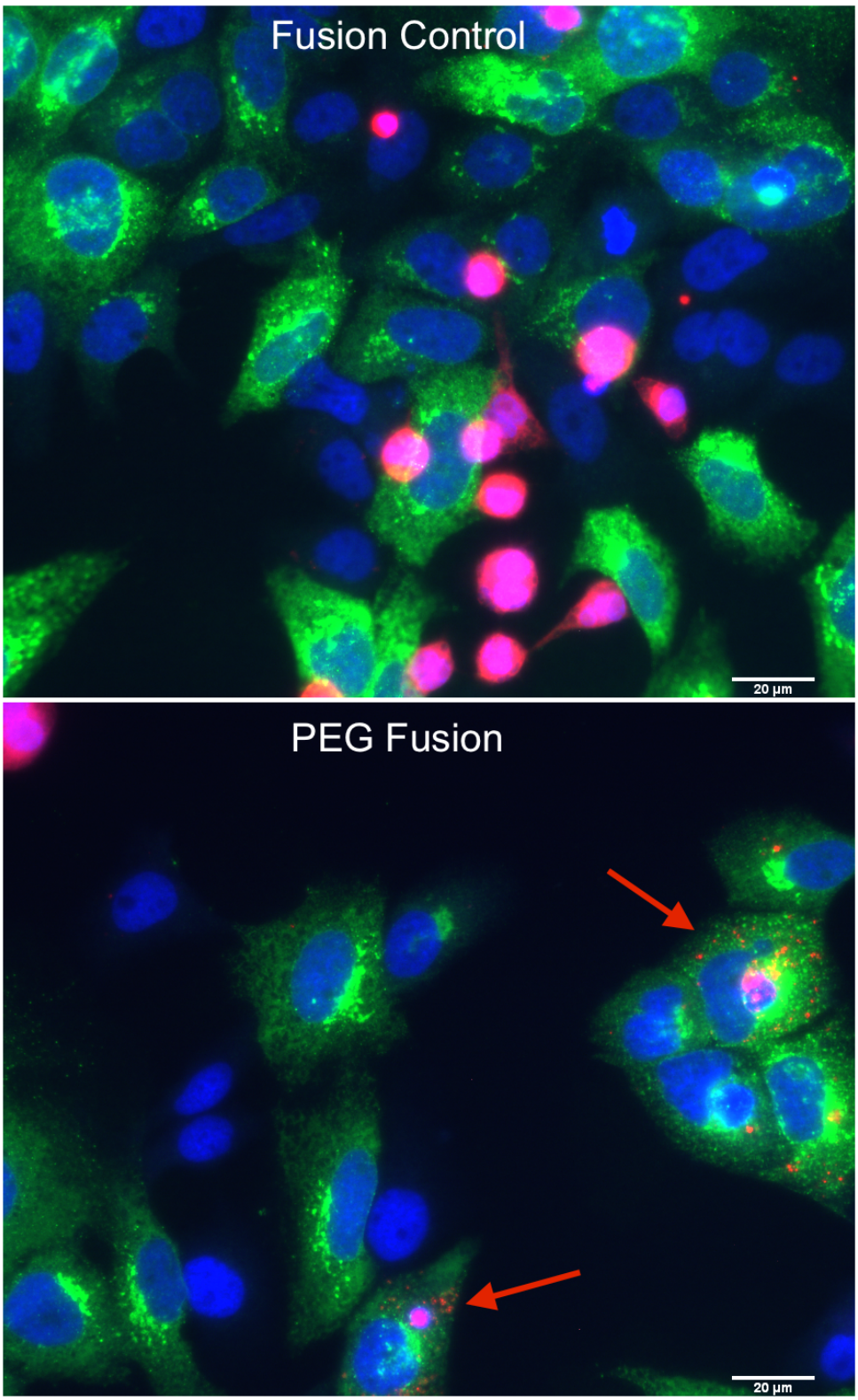

Fig 3.2 Immunofluorescence of PEG fusion
THP-1 cells were stained with CMRA orange before PEG fusion to Huh7.5 cells. A non-PEG treated control for fusion was also included. Cells were left to recover for 24hrs post-fusion and then fixed in 4% PFA. Huh7.5 cells were then stained for the liver specific protein albumin by an anti-albumin monoclonal antibody and all cells were counter stained with DAPI. Red arrows indicate fused cells. Representative images were taken by a Leica DM5000 fluorescent microscope.

PEG-fusion between THP-1 and Huh7.5 cells is critical for replication of patient-derived HCV in the capture fusion assay (Cunningham *et al.*, 2014). These experiments illustrate that the efficiency of PEG fusion between THP-1 and Huh7.5 cells is low. The FACS based assay employed here allows an estimation of the degree of fusion between THP-1 and Huh7.5 cells despite the presence of cell to cell adherence between THP-1 and Huh7.5 cells, as evidenced by the non-PEG-treated fusion control and fluorescent microscopy images. Including a no fusion control when using this assay to account for the level of cell-to-cell adherence between THP-1 and Huh7.5 cells is therefore essential to obtaining a more precise assessment of the level of PEG-fusion.

3.2 Improving PEG fusion using a Biotin-Streptavidin-Biotin Bridge.

A recent study claimed to improve the rate of PEG-mediated fusion by creating a Biotin-Streptavidin-Biotin (BSB) bridge between cells before fusion, (Li *et al.*, 2014). The principle of the method is to coat both cell types with biotin; one of the cell types is then further treated with streptavidin (SA), which will covalently bind to the biotin coating the cell's surface. The biotin-SA coated cells then act like 'hooks' to form a biotin-SA-biotin bridge with the other cell type, treated with biotin only, to bring both cell types within close proximity enhancing PEG fusion.

This method was applied to the capture fusion assay. THP-1 and Huh7.5 cells were treated with biotin before PEG fusion, with the Huh7.5 cells being further treated with SA to form the biotin-SA 'hook'. Cells were then combined to allow the formation of the biotin-SA-biotin-bridge between the Huh7.5 and THP-1 cells and then fused as before with PEG.

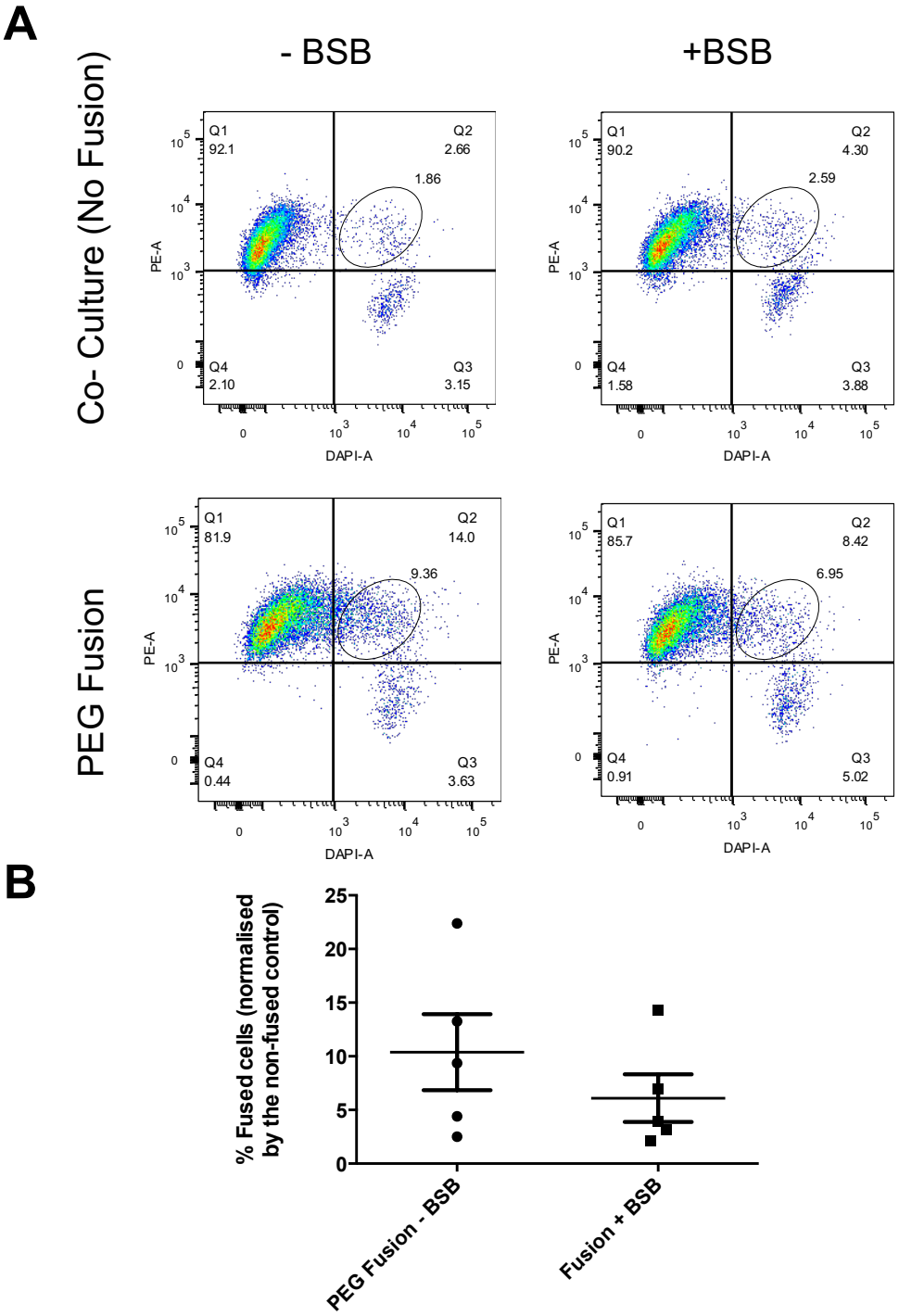

Fig 3.3 PEG fusion with Biotin-Streptavidin-Biotin Bridge
(A) FACS analysis of THP-1/Huh7.5 PEG fusion either with or without Biotin-SA-Biotin (BSB) bridge formation. THP-1 (Cell-trace Violet) and Huh7.5 (CMRA-orange) cells were first coated with biotin; Huh7.5 cells were further treated with Streptavidin before being incubated with biotin-treated THP-1 cells. PEG fusion was performed as before and cells analysed by FACS. Background non-fused double positive cells were accounted for by a non-fused co-culture control. Representative FACS plots are shown. (B) Comparison of PEG fusion +/-Biotin-SA-Biotin bridge in PEG fusion. 5 PEG fusions performed without BSB bridge formation was compared to 5 fusions with the BSB bridge. Values obtained from the fusion control were deducted from the values obtained for PEG fusion to account for cell-to-cell adherence.

FACS analysis of PEG fusion with the BSB-bridge revealed no improvement in the degree of cell fusion, in fact presence of the BSB-bridge appeared to cause a reduction in the percentage of fused cells compared to fusion in the absence of the bridge (Fig 3.3B). Though this reduction was not significant (p=0.095) this method does not appear to have a beneficial effect on fusion between THP-1 and Huh7.5 cells. Only a slight increase in dual positivity (fused cells) was observed in the FACS plot indicating that the BSB Bridge was having a minimal effect on increasing cell adherence between THP-1 and Huh7.5 cells. As the BSB-bridge did not appear to enhance THP-1/Huh7.5 cell fusion alternative approaches were examined.

3.3 pH Dependent Cell Fusion Using Viral Fusion Proteins

Entry of enveloped viruses into cells often involves fusion of the viral and cellular membrane by viral proteins with fusogenic properties [Reviewed in (Podbilewicz, 2014)]. These proteins undergo conformational changes when confronting various cellular environments such as a low pH, exposing hydrophobic fusion peptides and fusion loops causing membrane destabilisation and fusion (Harrison, 2008). The properties of viral fusion proteins can be utilised to cause fusion between cells in *in vitro* models, a notable example being the treatment of cells with inactivated Sendai-virus which causes cell fusion via the fusogenic-F protein (Okada, 1993).

Gottesman and colleagues published a method of cell fusion which exploited the pH sensitive fusion properties of the G protein from the Vesicular Stomatitis Virus (VSVG) (Gottesman *et al.*, 2010). The method relied upon stable expression of VSVG in human fibroblasts, which resulted in cell fusion as observed by time-lapse microscopy.

We speculated that VSVG expression on Huh7.5 cells might facilitate a better method of cell fusion in the HCV capture fusion assay.

3.3.1 Lentiviral transduction of Huh7.5

Lentiviral constructs expressing VSVG with a GFP tag (pHeGFP-VSVG) were donated by Y. Lazebnik, Cold Spring Harbour Laboratories. To ascertain the lentiviral titre Huh7.5 cells were transduced with a range of lentiviral dilutions and then assayed for GFP fluorescence by FACS (Fig 3.4A). Transduction with un-diluted lentivirus achieved 100% GFP positivity in Huh7.5 cells, which decreased with increasing dilutions of the virus. To achieve a population of cells stably expressing VSVG, Huh7.5 cells were re-transduced with an MOI of 1 and cell sorted into a GFP positive population (Fig 3.4C). The cell-sorted population was placed under puromycin selection with resistant Huh7.5 colonies observed after 2 weeks of antibiotic selection. Colonies were grown to confluency at which point a sample was taken for RNA extraction. Expression of the VSVG construct was examined in the cDNA by PCR, however no band corresponding to size of VSVG was observed in the cDNA from the transduced Huh7.5 cells (Fig 3.4C).

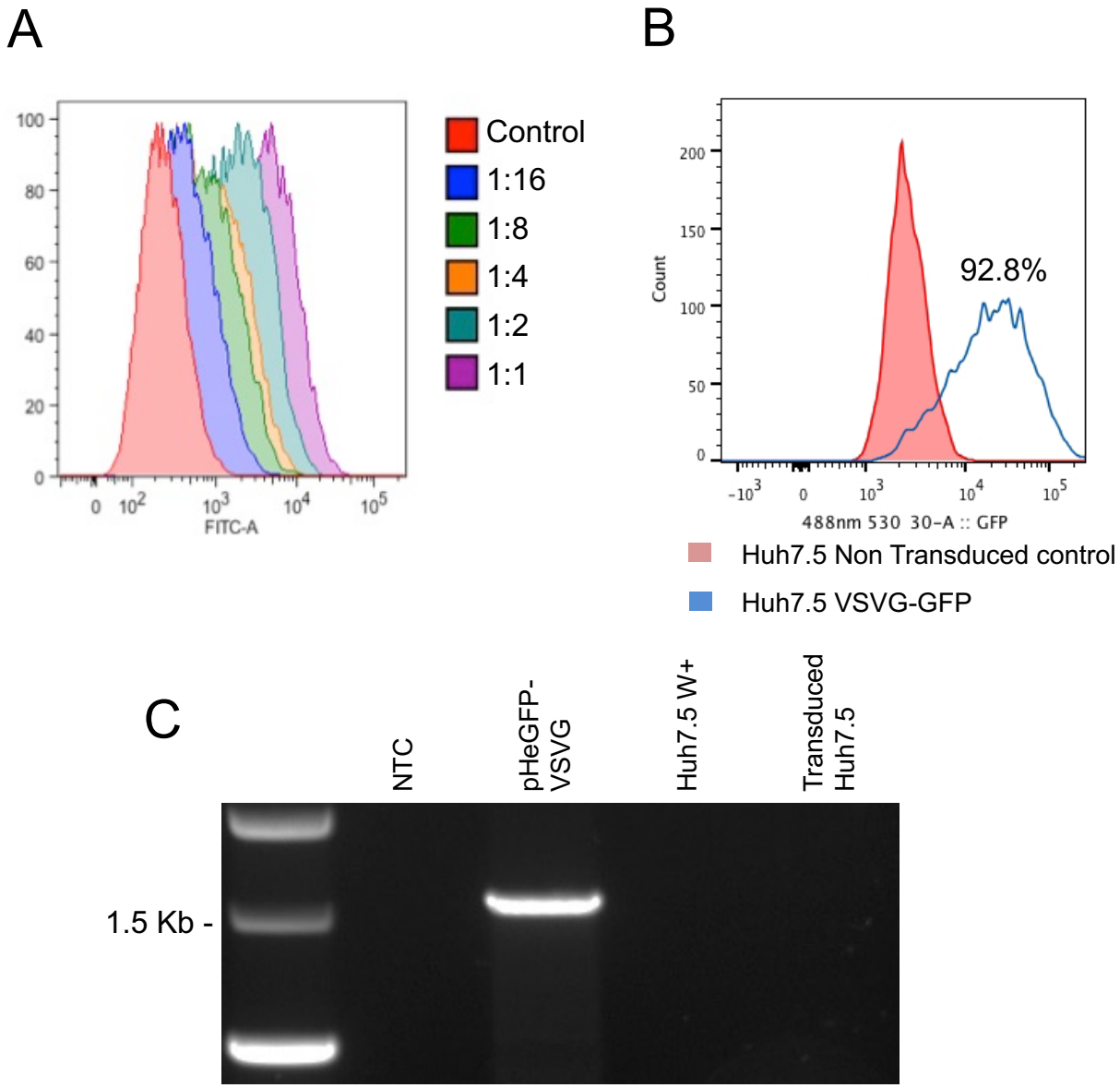

Fig 3.4 Huh7.5 transduction with pHeGFP-VSVG lentivirus
(A) Huh7.5 cells were transduced with a 1:2 serial dilution series of the pHeGFP-VSVG lentivirus to establish a titre. After 48 hrs cells were assessed for GFP positivity by FACS. Lentiviral titre was determined to be 1.03x10^6 transducing units/ml. The FACS plot is representative of 2 independent experiments (B) Transduced Huh7.5 cells were cell sorted for GFP and placed under puromycin selection. (C) Puromycin resistant colonies were assessed for VSVG expression by PCR. The proviral pHeGFP-VSVG plasmid containing the 1.5 Kb VSVG gene was used as a positive control in the PCR reaction. The above is a representative example from 3 independent transductions.

Transduction of the Huh7.5 cells with the pHeGFP-VSVG construct was repeated thrice with the same outcome. It was postulated that the Lentiviral vector used in these experiments was unable to express VSVG despite conferring puromycin resistance. The pHeGFP-VSVG was a bicistronic construct with the puromycin resistance (*pac*)

gene under control of a PGK promoter while VSVG expression was driven by IRES. It is possible that the IRES driven VSVG expression is impaired in some way in the Huh7.5 cells despite being previously used to express VSVG in human fibroblasts (Gottesman *et al.*, 2010). It was therefore decided to re-clone VSVG into the pTRIP lentiviral system that had been previously used to transduced Huh7.5 cells to create a fluorescence based HCV cell reporter assay (Jones *et al.*, 2010).

3.3.2 Cloning of VSVG into the pTRIP lentiviral vector

The RFP-NLS-IPS cassette was first excised from the pTRIP plasmid by restriction digestion with *XhoI* and *XbaI* (Fig 3.5A). The 1.5kb VSVG gene was then amplified by PCR with *XhoI* and *XbaI* restriction sites designed into the forward and reverse primers respectively to ensure the gene was cloned into the pTRIP vector in the correct orientation (Fig 3.5B). Transformed pTRIP colonies were screened for the presence of VSVG by PCR and restriction digestion with *XbaI/XhoI*. A 1.5Kb product consistent with the size of VSVG was observed in both restriction digestion and PCR of the pTRIP-VSVG plasmid (Fig 3.5C, D). Orientation of the VSVG gene as well as the start codon was validated by sanger sequencing.

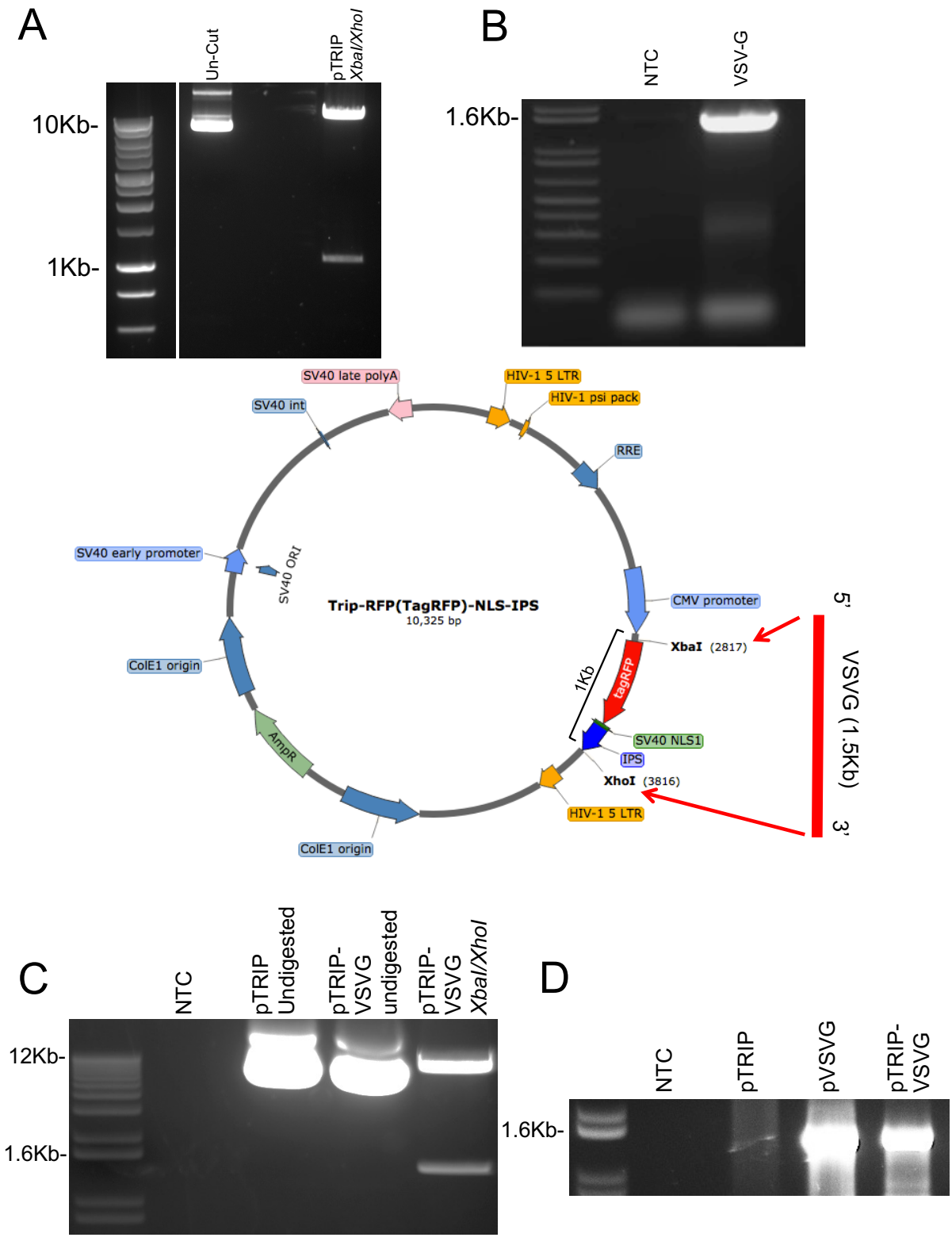

Fig 3.5 Cloning of VSVG into the pTRIP vector
(A) The pTRIP vector was digested with *XbaI* and *XhoI* to remove the 1Kb HCV fluorescence reporter cassette from the plasmid backbone. (B) VSVG was amplified by PCR from a lentiviral pVSVG envelope plasmid with complementary *XbaI*/*XhoI* restriction sites allowing the gene to be directionally cloned into the pTRIP backbone. (C) Resulting colonies were shown to contain a 1.5Kb band consistent with the size of VSVG when digested with *XbaI/XhoI.* (D) Presence of VSVG in the pTRIP vector was also

confirmed by PCR. The pVSVG used as the initial template for *VSVG* was included as a positive control. The original pTRIP plasmid was also included as a negative control.

3.3.3 pTRIP-VSVG lentiviral transductions

The pTRIP-VSVG was used to make lentiviral particles for subsequent transduction into Huh7.5 cells. As an additional control to test the viability of the lentivirus a sample of the 293FT cells used to make the pTRIP-VSVG lentivirus was also transduced. RNA and protein samples were taken 48 hours post-transduction to establish VSVG expression. Immunoblot analysis of protein extracted from transduced Huh7.5 confirmed VSVG expression (Fig 3.6). A 56 KDa protein band consistent with the size of VSVG was observed in cell lines transduced with this lentivirus.

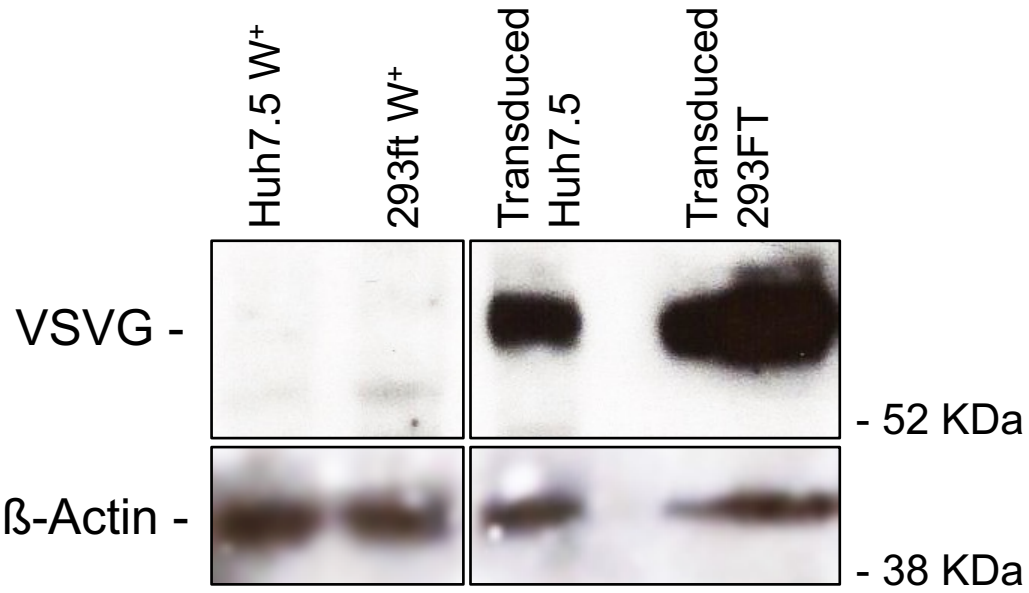

Fig 3.6 Transduction of Huh7.5, THP-1 and 293FT with pTRIP-VSVG
VSVG expression in transduced Huh7.5 and 293FT cells was assessed by immunoblotting, with bands consistent with the size of VSVG observed in cells transduced with the pTRIP-VSVG lentivirus compared to controls. ß-Actin was used as a loading control in this experiment.

Huh7.5-VSVG cells were then tested for the ability to fuse cells when exposed to an acidic pH as shown in (Gottesman *et al.*, 2010). THP-1 cells and Huh7.5-VSVG cells were stained with violet and orange cytoplasmic dyes respectively (Fig 3.7A, B). Both cell lines were co-cultured and briefly exposed to an acidic buffer to induce the fusogenic property of VSVG. After a 24-hour recovery period cells were analysed by FACS as before for the presence of fused cells with dual fluorescence. No noticeable increase in double positive cells was observed between THP-1/Huh7.5-VSVG cells treated with an acidic buffer (6.2%) (Fig 3.7D) compared to the non-treated control (6.09%) (Fig 3.7C). Cell fusion with the Huh7.5-VSVG cells was compared to PEG fusion of Huh7.5 and THP-1 cells. FACS analysis of the two fusion methods revealed that PEG fusion caused a 2-fold increase in double positive cells whereas comparable levels of double positive cells were observed between VSVG fusion and the no-fusion control (Fig 3.7E). These experiments indicate that while VSVG is expressed in Huh7.5–VSVG cells the acid treatment does not cause any detectable fusion events as assessed by FACS, certainly not at the levels seen with PEG fusion.

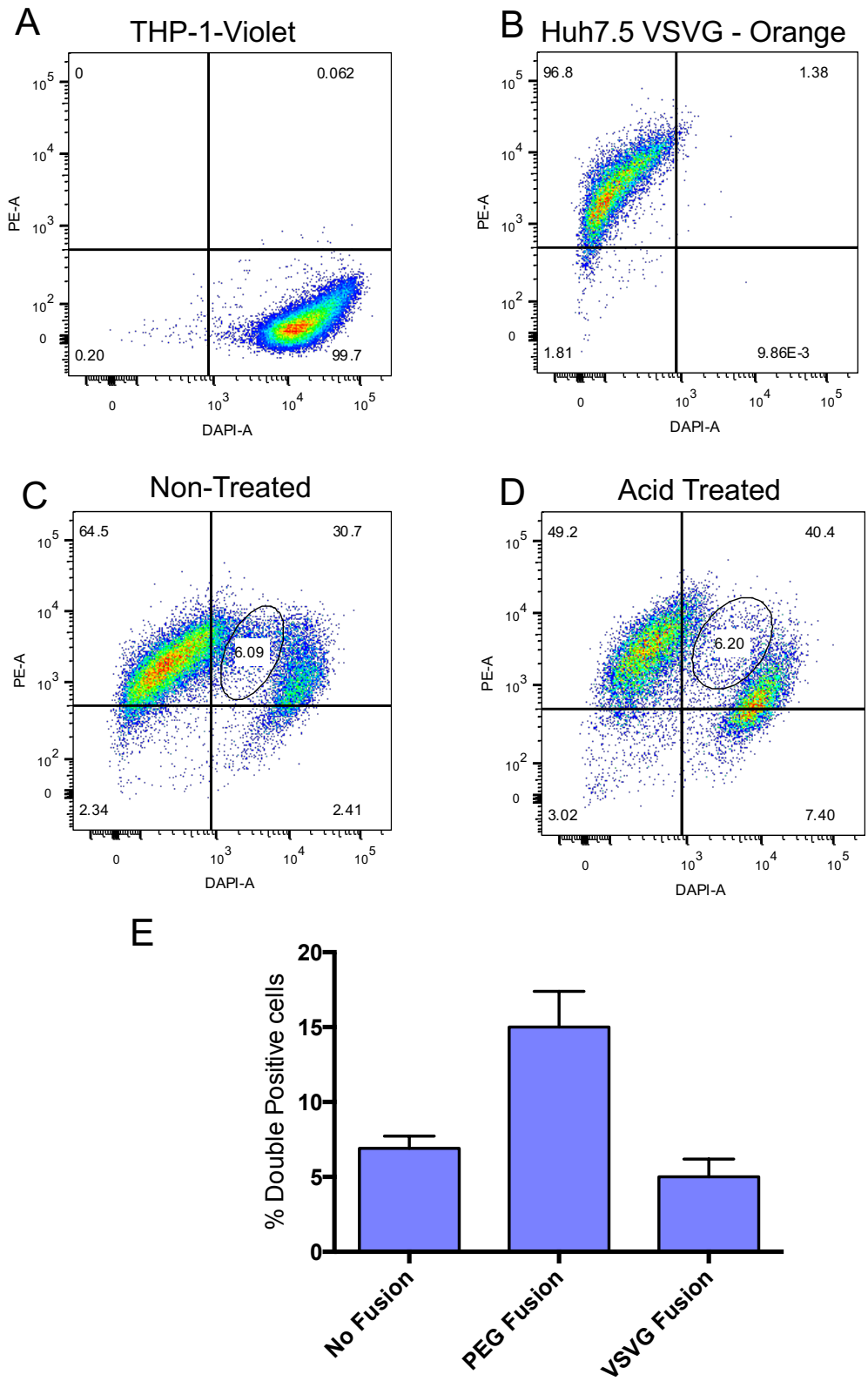

Fig 3.7 Ability of Huh7.5-VSVG cells to fuse with THP-1 cells
THP-1 (violet) (A) and transduced Huh7.5 (orange) (B) were co-cultured then treated with an acidic buffer to induce VSVG fusion (D). Non-Acid treated cells were used as a non-fusion control (C). Cells were analysed by FACS to determine the amount of cell fusion by measuring the percentage of cells with dual fluorescence for both cytoplasmic dyes. (E) VSVG fusion was compared to PEG fusion of

THP-1 and Huh7.5 cells with double positive cells measured by FACS analysis. Data presented is representative of 2 independent experiments.

3.3.4 HCV RNA levels are higher in PEG fusion compared to VSVG fusion

Despite the lack of cell fusion with the Huh7.5-VSVG cells, we speculated that the quality of fusion may be improved with VSVG expression and therefore performed functional experiments with these cells. We compared the ability of VSVG mediated fusion to replicate patient derived HCV to standard PEG fusion. Stimulated THP-1 cells were incubated with patient-derived HCV sera and either fused using PEG or fused by incubating with Huh7.5-VSVG cells and exposed to a low pH buffer. After incubation for 5 days HCV RNA levels were quantified by qPCR.

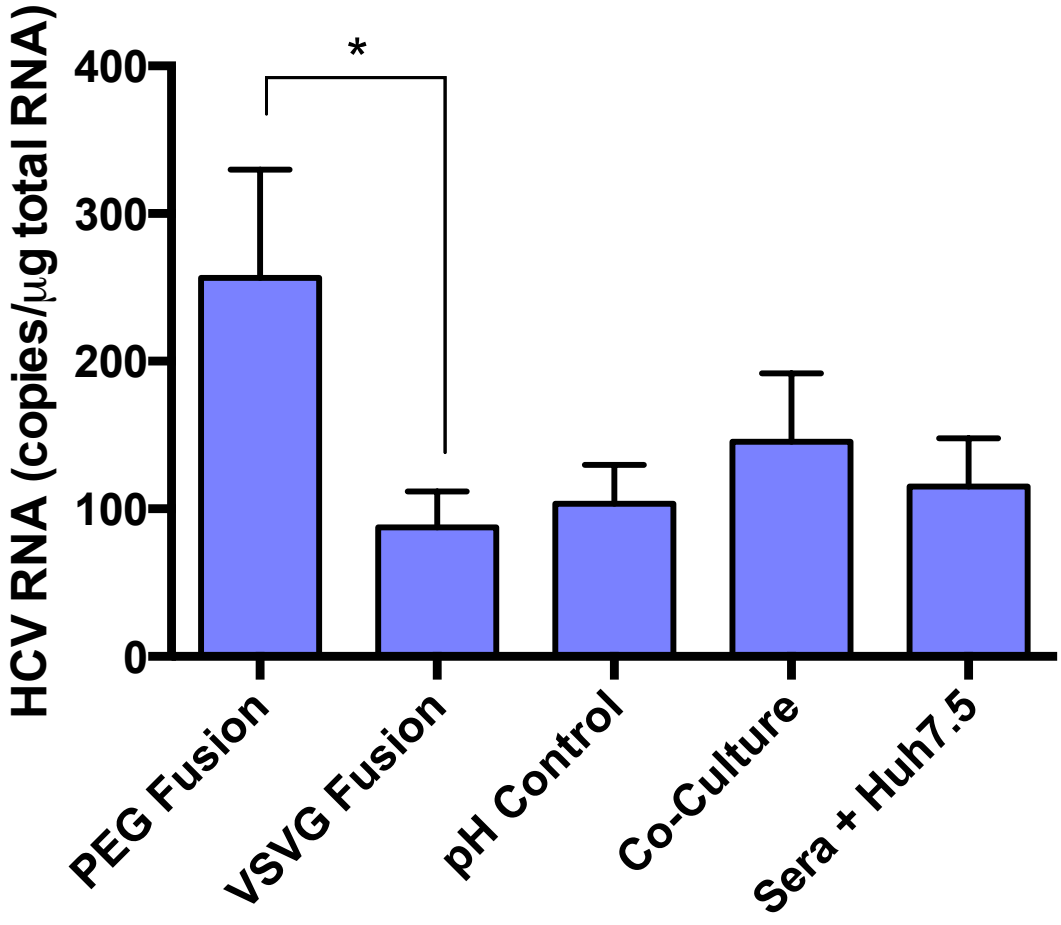

Fig 3.8 HCV replication in Huh7.5-VSVG cells
THP-1 cells challenged with patient derived HCV sera were either fused to Wt Huh7.5 cells by PEG or fused using the VSVG transduced Huh7.5 cells by low pH exposure for 60 secs. Controls included were: Wt Huh7.5 mixed with HCV exposed THP-1s exposed to the low pH buffer (pH Control), Wt

Huh7.5 cells co-cultured with infected THP-1 cells with no fusion (Co-Culture) and finally Wt Huh7.5 exposed directly to patient sera (Sera + Huh7.5). Experiment was left for 5 days before harvesting and HCV RNA was quantified. Above represents pooled data (mean ± SEM) obtained from experiments performed with 5 different HCV sera. Statistical analysis was performed using a Mann-Whitney U-Test

Significantly higher levels of HCV were obtained from PEG fusion compared to VSVG fusion (p=0.048) (Fig 3.8). HCV RNA levels were comparable between VSVG fusion, non-VSVG expressing Huh7.5 exposed to the same low pH buffer (pH Control), co-cultured HCV-sera-exposed THP-1 and Huh7.5 cells exposed directly to sera. Together these data indicate that the Huh7.5-VSVG cells are not a functional replacement for replicating patient derived HCV in the HCV capture fusion assay

3.3.5 Summary of VSVG experiments

Transduction of Huh7.5 cells with the pTRIP-VSVG lentiviral construct enabled expression of VSVG within this cell line as determined by western blot and PCR. Functional FACS based experiments assessing the ability of the Huh7.5-VSVG cells to fuse with THP-1 cells revealed an apparent lack cell fusion when compared to cells treated with PEG. Finally, when the Huh7.5-VSVG cells were used to fuse THP-1 cells exposed to patient-derived HCV, viral RNA levels were significantly higher in cells fused by PEG compared to VSVG fusion. It was concluded that VSVG expression was not a viable replacement for PEG fusion in the capture fusion model and further work to replace the method of fusion in the capture fusion model was not continued.

3.4 Expression of SEC14L2 to study HCV replication

A recent advance in the *in vitro* study of HCV by Saeed et al has been the development of a cell culture system which is reported to permit the propagation of patient derived HCV without the need for culture adaptive mutations. This is achieved by the overexpression of SEC14L2, also known as tocopherol-associated protein 1 (TAP1) a cytosolic lipid binding protein, expressed in primary human hepatocytes but not human hepatoma or non-hepatoma cell lines. SEC14L2-expressing Huh7.5 cells displayed higher replication levels of HCV replicons such as Con-1, H77, J6 and JFH-1. Notably SEC14L2 cells were able to propagate G1 and G3 HCV derived from patient sera, which was attenuated by the addition of the NS5A inhibitor daclatasvir (Saeed *et al.*, 2015). To create a system whereby these cells could be used to phenotype drug sensitivity of patient derived HCV, the length of time HCV could be propagated in SEC14L2 expressing cells first needs to be established. Saeed et al cultured patient derived HCV for a total of 7 days with the addition of drugs on day 5 resulting in a 10-fold reduction in HCV RNA levels. In capture fusion drugs are added 24 hours after fusion and maintained for 7 days. It was therefore of interest to establish whether a similar time scale could be utilised with the SEC14L2 cell system.

3.4.1 Assessing HCV replication in SEC14L2 expressing cells by PCR

SEC14L2 expressing Huh7.5 cells were kindly donated by P. Simmonds and used to examine their utility in the detection of antiviral drug sensitivity in patient derived HCV. The SEC14L2 cells clearly have the potential to obviate the need for the capture fusion

technique and we therefore examined the ability of these cells to replicate virus from our patients. The time course of replication in these cells was first examined.

SEC14L2-Huh7.5 cells were infected at an MOI of 1 with sera from 2 G1 and 2 G3 patients with high viral loads. HCV RNA levels were then quantified over a period of 10 days. A decline in HCV RNA from day 0 was observed for both genotypes between days 3-5. For the 2 G1 sera (JW060 and MJ018) a further decline was observed up to days 7 and 10. However HCV RNA levels for the two genotype 3 sera (JW057 and MJ018) was seen to increase slightly on day 7 and then continued to decline on day 10 to levels comparable to the G1 serum (Fig 3.9). These data do not provide robust evidence of HCV replication in these cells and further attempts were made to determine whether or not these cells are of value in viral phenotyping assays.

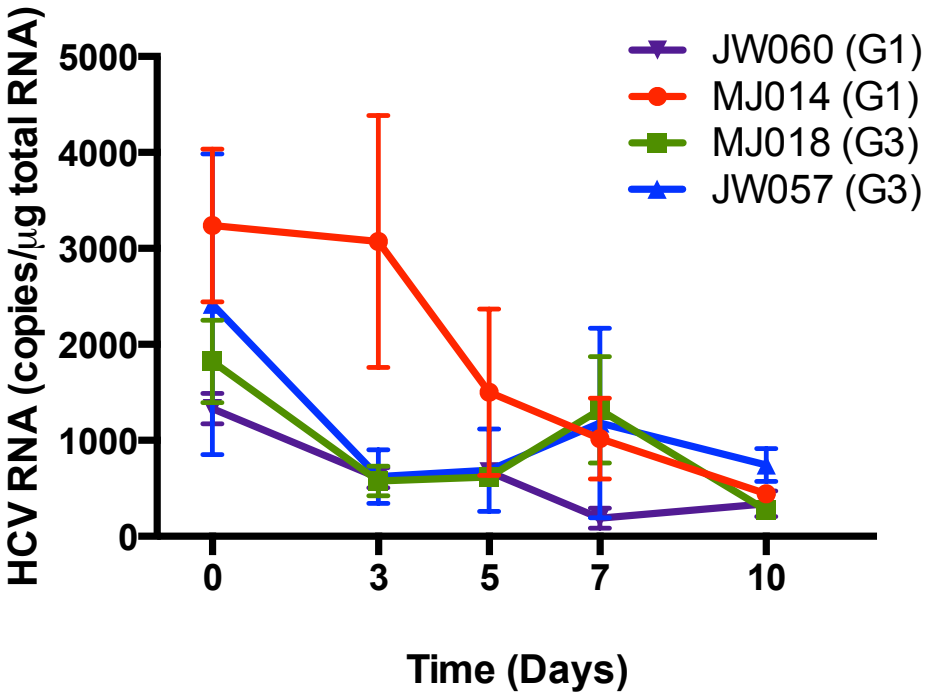

Fig 3.9 HCV replication in SEC14L2 expressing cells.
Sera from 2 G1 and 2 G3 patients were used to infect SEC14L2 expressing huh7.5 cells at an MOI of 1. HCV RNA was quantified by RT-qPCR in triplicate at indicated time intervals. Data presented is representative of 2 independent experiments. Graph shows mean ± SEM.

3.4.2 Using a SEAP reporter system to detect HCV replication in SEC14L2 expressing cells

The SEC14L2 cells have the potential to propagate HCV at similar levels to capture fusion. In both methods detection of HCV relies upon RNA extraction and RT-qPCR, which is a time consuming and labour intensive process. Other methods of HCV detection that do not rely upon HCV RNA quantification but rather the mechanics of HCV replication do exist but have been discounted for use in capture fusion due to the limited level of HCV replication and the complex nature of the fusion process (Cunningham *et al.*, 2014). One such method developed by Iro and colleagues describes a cell-based secreted alkaline phosphatase (SEAP) reporter assay to detect *in-vitro* HCV replication. This system consists of the SEAP reporter construct containing a recognition sequence for the HCV NS3/4 serine protease that, when

present, will release SEAP into the extracellular medium which is then detected via chemiluminescence (Iro *et al.*, 2009). Huh7-J20 cells containing the SEAP reporter were kindly donated by A. Patel, Glasgow University, and were stably transfected with a SEC14L2 expression plasmid. J20-SEC14L2 cells were tested for their ability to detect HCV by infection with increasing MOIs of JFH-1 and sera from a G3 HCV patient. SEAP levels in J20-SEC14L2 cells were observed to be considerably higher than the J20 mock-transfected cells when exposed to JFH-1 and patient sera. The chemiluminescent signal appeared to reflect the amount of virus used as relative SEAP activity increased with an MOI of 0.3 compared to 0.1 of JFH-1 (Fig 3.10A). For this system to be a viable alternative to capture fusion it would need to be able to detect a dose-response to anti-viral drugs from patient derived sera. To this end J20-SEC14L2 and J20-Wt cells were infected with JFH-1 and MJ018 sera for 24hrs and then treated with SOF for 5 days after which SEAP activity was measured. Treatment with increasing doses of SOF did decrease luminescence in both the JFH-1 and patient-sera infected cells (Fig 3.10B). The effect of SOF was more prominent in the JFH-1 infected cells causing only a very slight decrease in luminescence in cells infected with MJ018 HCV sera. Despite several attempts, a robust response to SOF could not be attained using patient-derived sera. Additionally, difficulties were encountered achieving reproducible data with these cells due to a high background signal resulting in the decision not to continue with the development of this system to evaluate antiviral phenotype.

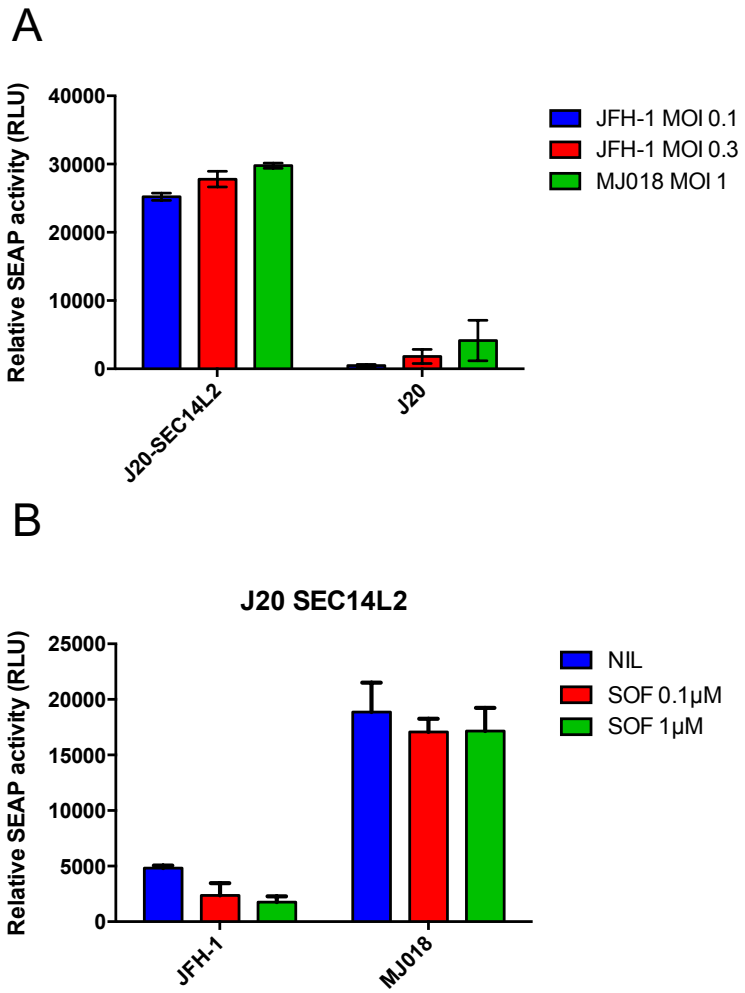

Fig 3.10 Detection of HCV replication in J20-SECL14L2 cells
(A) J20 Wt and J20-SEC14L2 cells were seeded in a 96 well format and infected with either JFH-1 or a G3 patient sera (MJ018) at the indicated MOI. SEAP activity in the culture medium was detected 5 days post infection. Relative SEAP activity was normalised to uninfected cells to account for background luminescence. (B) J20-SEC14L2 were infected with JFH-1 (MOI 0.1) and MJ018 (MOI 1) for 24 hours and then treated with the indicated doses of SOF for 5 days after which chemiluminescent SEAP activity was measured. Above data is representative of 2 independent experiments with graphs depicting mean ± SEM.

3.4.3 Using SEC14L2 Cells to Evaluate Antiviral Sensitivity of HCV Sera by qPCR

Experiments thus far have not confirmed the data from Saeed et al showing general replication of virus in SEC14L2 expressing cells (Fig 3.9). However, there was an indication that for the two samples containing G3 HCV some replication did occur after 7 days. We therefore sought to determine whether inhibition of replication could be observed in this system. Five G3 HCV sera were used to infect SEC14L2 cells at an

MOI of 1. Cells were then treated with a range of SOF and DAC doses either day 3 or day 5 post-infection with HCV RNA quantification performed 7 days post-infection in both cases. However consistent data could only be obtained with two of these sera, MJ018 and JW057 as RNA levels were too low in the others to detect reliably. Both periods of drug treatment caused a decline in HCV RNA in response to increasing doses of SOF and DAC, indicating replication in these cells (Fig 3.11A-D). IC_{50} values calculated from HCV RNA were observed to increase slightly with drug treatment at 5 days post infection compared to 3 days post infection (0.011-0.045μM and 0.017-0.026μM for SOF and DAC respectively). This is likely due to the virus having more time to propagate in cell culture combined with a shorter duration of antiviral treatment when drug treatment is performed 5 days post-infection compared to 3 days.

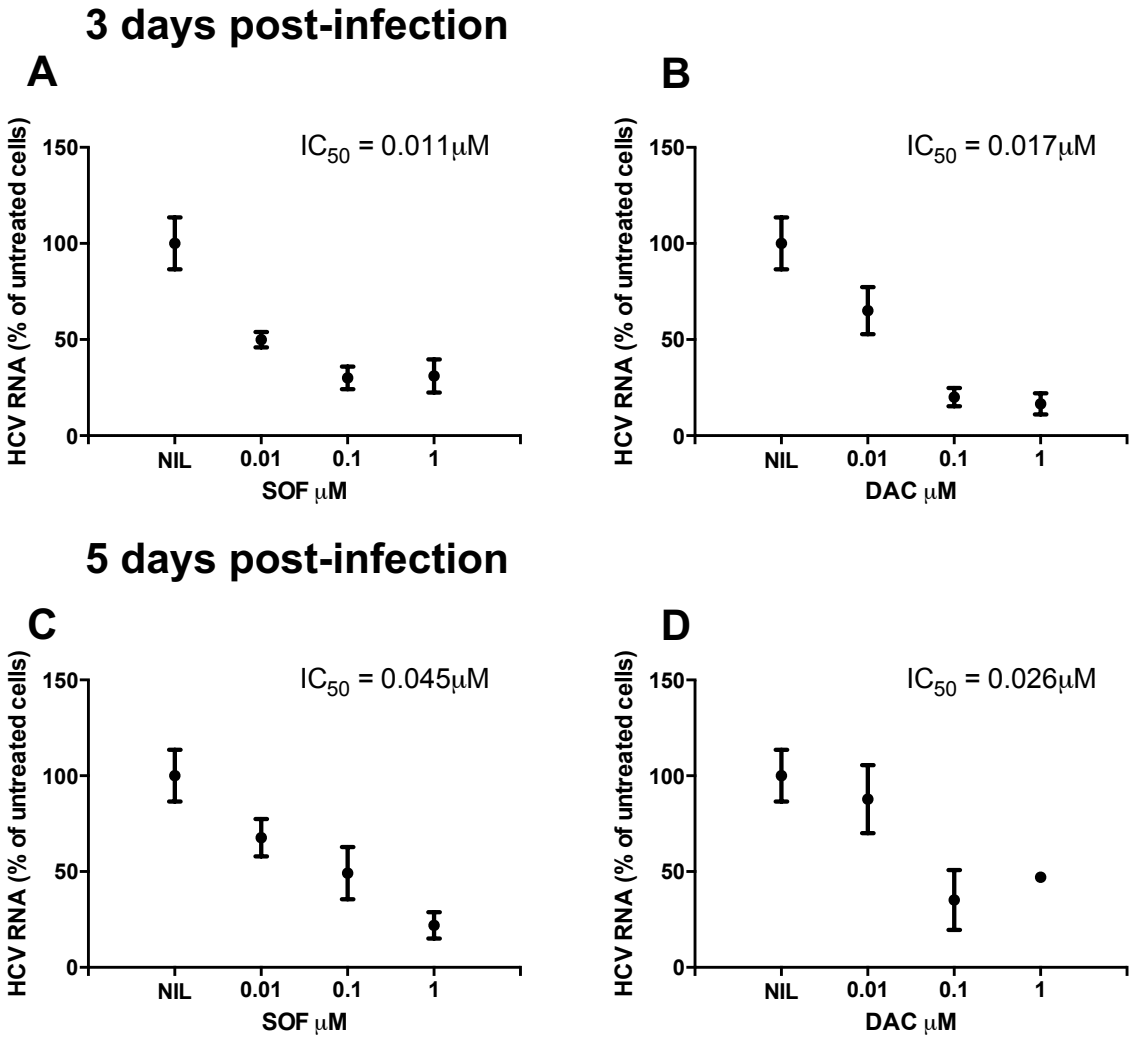

Fig 3.11 Drug inhibition in SEC14L2 cells.
SEC14L2 cells infected with G3 sera were treated with either sofosbuvir (SOF) or daclatasvir (DAC) 3 days post infection (A/B), or 5 days post infection (C/D) at indicated doses. HCV RNA in both experiments was quantified 7 days post infection and IC_{50} values calculated. Data presented for each drug at day 3 and 5 is pooled data from 2 patient sera MJ018 and JW057. Graphs depict mean ± SEM.

These experiments suggest that for these two G3 viral samples infection and replication within the SEC14L2 cells could be observed and this model could be used to assess drug sensitivity. We therefore examined the impact of drug treatment in these cells using time courses that were similar to those previously used in the capture-fusion experiments (Cunningham *et al.*, 2014). We tested SOF on these sera with treatment applied to the SECL4L2 cells 24 hours after infection. Cells were incubated with SOF for a total of 7 days with medium and drug being replaced after 3

days. Capture fusion experiments with the same sera using Huh7.5 cells were also performed alongside direct infection of SEC14L2 expressing cells.

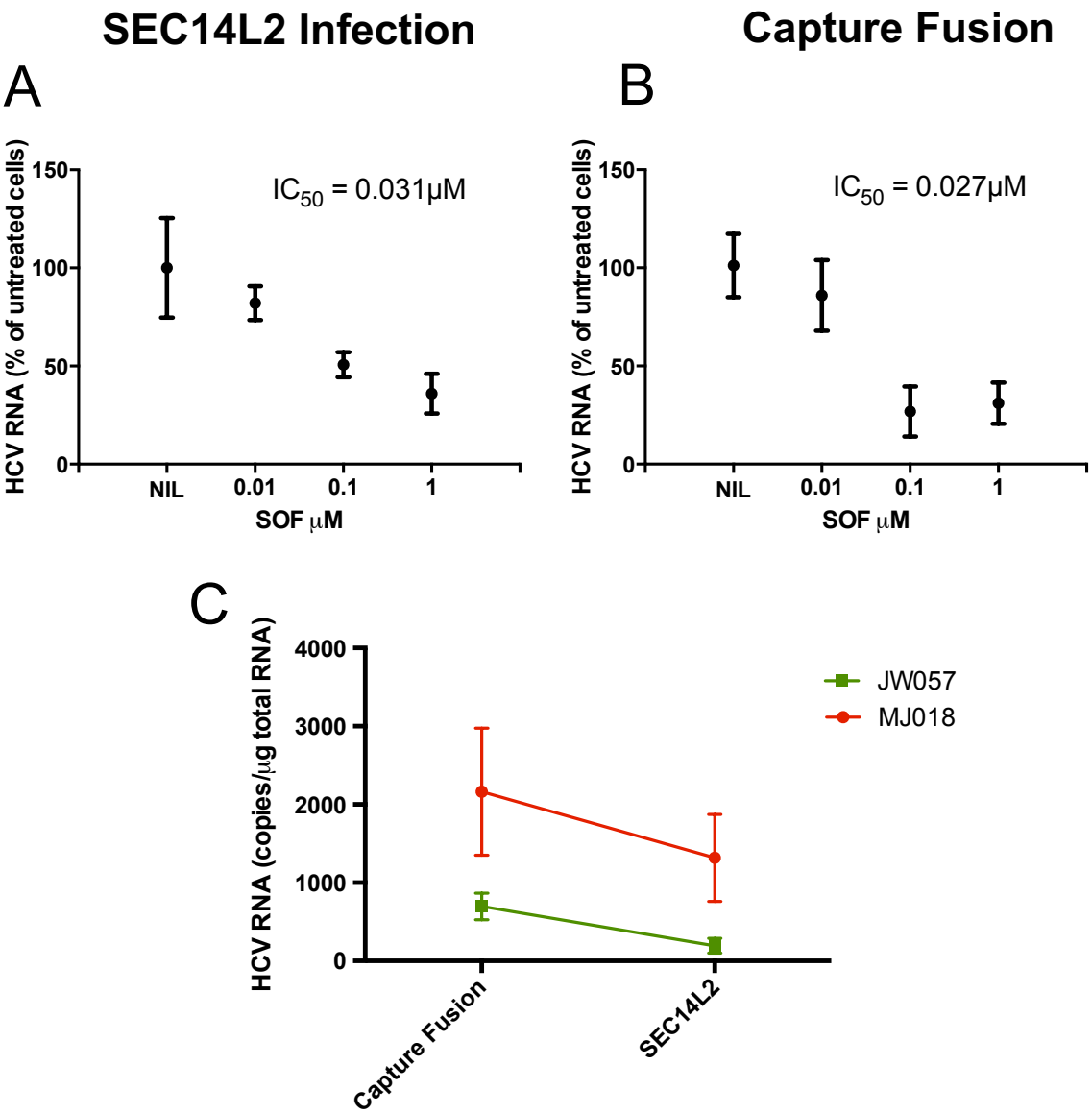

Fig 3.12 Drug inhibition with SEC14L2 cells 24 hours after infection.
(A) SEC14L2 cells were infected with G3 sera JW057 and MJ018 respectively at an MOI of 1. Cells were treated with indicated doses of SOF 24 hours post infection with drug replacement on day 3. (B) Capture fusion experiments were performed with the same sera with the same time scale of drug inhibition as the SEC14L2 cell infections. For both experiments, HCV RNA was quantified 7 days post infection from which IC_{50} values were calculated. (C) HCV copy numbers obtained at day 7 from capture fusion and infection of SEC14L2 cells with MJ018 and JW057 sera. Data presented is pooled from experiments with both sera. Graphs depict mean ± SEM.

Similar IC_{50} values for SOF were obtained with direct infection of the SEC14L2 cells to that of capture fusion Fig 3.12A, B). This suggests that the timescale of drug

inhibition post infection with the SEC14L2 cells can be done in a similar fashion to capture fusion and the output IC_{50} is similar to that of experiments with a different duration of drug exposure. Additionally, this set of experiments demonstrates the potential of the SEC14L2 cells to be used as a system to phenotype the sensitivity of G3 HCV sera to antiviral drugs. HCV copy numbers at day 7 were compared between capture fusion and direct infection of SEC14L2 cells as a relative measure of the amount of HCV replication in each system (Fig 3.12C). For both sera HCV copy numbers were reduced in direct infection of SEC14L2 cells compared to capture fusion. The impact of this reduction in these experiments was minimal due to the reasonably high replication rates and viral load of the sera used. However, not all patient derived HCV replicates equally well in the capture fusion model with drug phenotypes to 'low replicators' being challenging to determine. We tested five serum samples and HCV replication was only detected in the two samples illustrated here. Therefore as validation of these cells could only be determined with two G3 sera and as the replicative abilities of these cells may be dependent on the relative fitness of the patient derived virus used to infect them we decided not to continue with this approach.

3.4.4 Using SEC14L2 cells in the HCV Capture Fusion Assay

We speculated that the Huh7.5-SEC14L2 cells might serve as a more favourable platform for the replication of patient sera than Huh7.5 cells in the capture fusion assay. To this end we compared the HCV copy number in capture fusion experiments with matched G3 sera performed with either Huh7.5 cells or Huh7.5—SEC14L2 cells. For all samples tested HCV RNA levels were found to be significantly higher (p=0.016) in capture fusion experiments using Huh7.5-SEC14L2 cells compared to Huh7.5 cells,

indicating that the Huh7.5-SEC14L2 cells may be more beneficial to the replication of patient-derived HCV in the capture fusion assay.

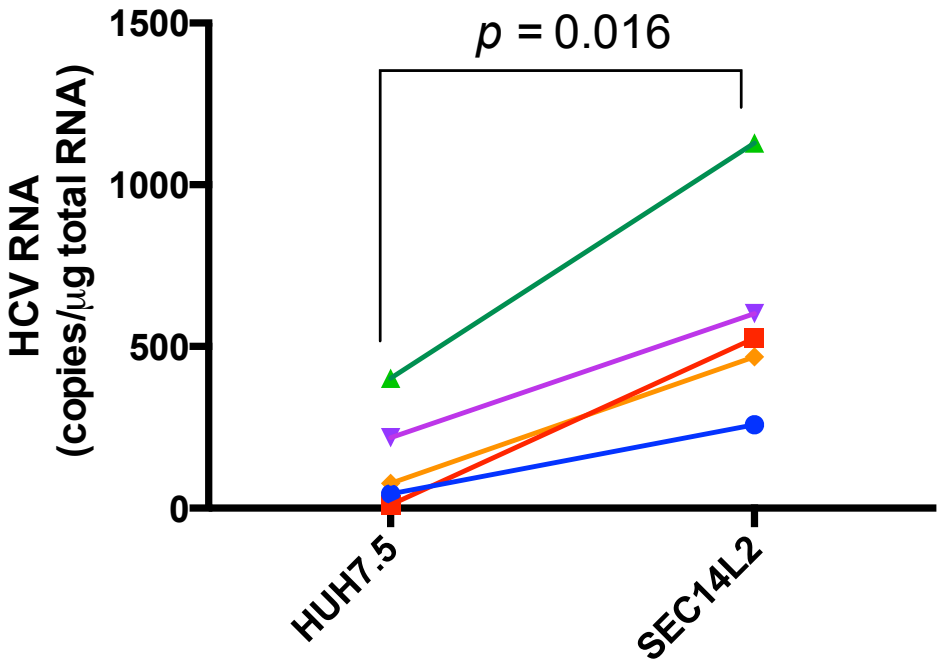

Fig 3.13 Comparison of Huh7.5 to Huh7.5-SEC14L2 cells in Capture Fusion
THP-1 cells infected with sera from 5 genotype 3 clinical isolates were fused to either Huh7.5 or Huh7.5-SEC14L2. After fusion cells were incubated for 5 days after which RT—qPCR quantified HCV RNA levels. Each patient isolate was assayed in quadruplicate for fusion experiments with both Huh7.5 and Huh7.5-SEC14L2 cell lines. Statistical analysis was performed using a Mann-Whitney U-test.

3.5 Discussion

This chapter describes my attempts to improve upon our current viral phenotyping assay, the 'capture-fusion' model of HCV replication. The development of the FACS based assay allowed the efficiency of different approaches to fusion to be evaluated. The assay revealed a large amount of self-adherence between THP-1 and Huh7.5 cells that could overestimate the proportion of cells deemed fused. To account for this THP-1 and Huh7.5 cells that had been co-cultured but not fused were an essential control in these experiments. PEG fusion between THP-1 and Huh7.5 cells occurs at a low efficiency, with efforts to improve the technique using a BSB bridge not resulting

in a significant increase in the efficiency of THP-1/Huh7.5 hybridoma formation. Given the additional time and resources to form the bridge in an already complex procedure, further study into this method was deemed impractical. Adaption of an alternative fusion method by the over-expression of the VSV-G protein was performed in an attempt to replace PEG-fusion with a seemingly better alternative. Despite overcoming difficulties in expressing VSV-G in Huh7.5 cells FACS based assessment of fused cells revealed that these cells were unable to fuse THP-1 cells when exposed to a low pH and were subsequently shown in a viral replication setting to be a non-viable alternative to PEG fusion. Finally, the Huh7.5-SEC14L2 cells were considered as an alternative to capture fusion due to their reported ability to replicate patient-derived HCV (Saeed *et al.*, 2015). Time course assays showed the two G3 sera tested were able to modestly replicate at 7 days post infection. Comparable SOF IC_{50} values to capture fusion were obtained with these cells implicating their ability to determine antiviral sensitivity in patient isolates. Higher HCV copy numbers however, were observed in capture fusion compared to direct infection of Huh7.5-SEC14L2 cells with the same sera. Replacing Huh7.5 cells with Huh7.5-SEC14L2 cells in the capture fusion yielded significantly higher HCV levels with matched patient-derived G3 sera. This may be due to the fusion process being a better delivery method for virus into the Huh7.5-SEC14L2 cells than direct infection. The improvement attained by the Huh7.5-SEC14L2 cells in HCV copy number, may permit the antiviral phenotyping of clinical isolates that were previously unable to be defined by capture fusion due to low replication rates. It was therefore decided to use the Huh7.5-SEC14L2 cells as the standard liver cell line in the capture fusion assay.

4 RESULTS: Sofosbuvir and Ribavirin sensitivity in genotype 3 relapse and SVR samples

With the changing face of HCV treatment to 'IFN-free' regimes where the NS5B inhibitor Sofosbuvir (SOF) dominates, treatment relapse has become less common especially in G1 infected patients. Cirrhotic G3 infection remains difficult to treat despite these new highly potent regimes, achieving SVR rates of 68%, most often due to relapse after treatment discontinuation (Zeuzem *et al.*, 2014a). Ribavirin (RBV) appears to retain a key role in G3 treatment as SVR rates are boosted with its inclusion in treatment regimes, particularly in those with difficult to cure characteristics, such as cirrhosis (Foster *et al.*, 2015b).

The virological reasons for relapse within cirrhotic G3 patients are poorly understood. One possible explanation is that relapse to G3 HCV is due to selection of mutations which enable the virus to resist the mode of action of these new direct acting antivirals. Direct sequence analysis of samples from patients who have relapsed could identify potential resistance associated variants (RAVs), although given the heterogeneity of HCV and the rarity of relapse this may be technically challenging. Host factors such as poor compliance with medication, presence of cirrhosis may also contribute to treatment failure and analysis of sequences from patients who have failed antiviral therapy will therefore involve a heterogeneous group of patients with a variety of different mechanisms of treatment failure. Identification of samples from patients where primary viral resistance was responsible for treatment failure would allow more informed sequence analysis of samples. Currently the capture fusion model is the only system that can determine the anti-viral drug phenotype of patient derived HCV.

Previous work with the assay has indicated that a reduced sensitivity to RBV exists in pre-treatment samples isolated from G3 infected patients who relapsed after treatment with pegIFN/RBV (Cunningham *et al.*, 2014).

Here we examine the hypothesis that:

1) Failure to respond to all oral antiviral treatments is associated with a reduced sensitivity to ribavirin and/or other drugs involved in therapy.

4.1 Sensitivity to SOF/RBV in G3 SVR samples

To establish a suitable dose response curve for both SOF and RBV initial experiments used HCV sera from patients who cleared virus were obtained from The Liver Unit at the Royal London Hospital. Samples were taken after informed consent in line with ethical approval granted to Dr Morven Cunningham. Sera from 3 G3 patients were used in the capture fusion assay to determine sensitivity to a range of SOF and RBV doses. Patient serum used in this experiment was selected based on high viral load and clinical outcome (Table 4.1).

Table 4.1 Details of G3 patient serum used in capture fusion

Patient ID	Genotype	Viral load (x10^6 IU/ml)	Clinical outcome
A	3a	1.2	SVR
B	3k	10.1	SVR
C	3	2.3	SVR

Sensitivity of these 3 sera to SOF and RBV is shown in Fig 4.1. The dosage of RBV has been previously established for the capture fusion assay (Cunningham *et al.*, 2014). The SOF dose range was recommended by Hongmei Mo, Gilead Sciences Ltd. Average IC_{50} values of 0.54μM and 0.028μM were obtained for RBV/SOF respectively (Fig 4.1). These are comparable to values previously obtained by Cunningham et al

from G3 SVR samples indicating sensitivity to these drugs. The dose range of both drugs appears to be of suitable scope to show drug sensitivity in these patient sera with the 'capture fusion' assay.

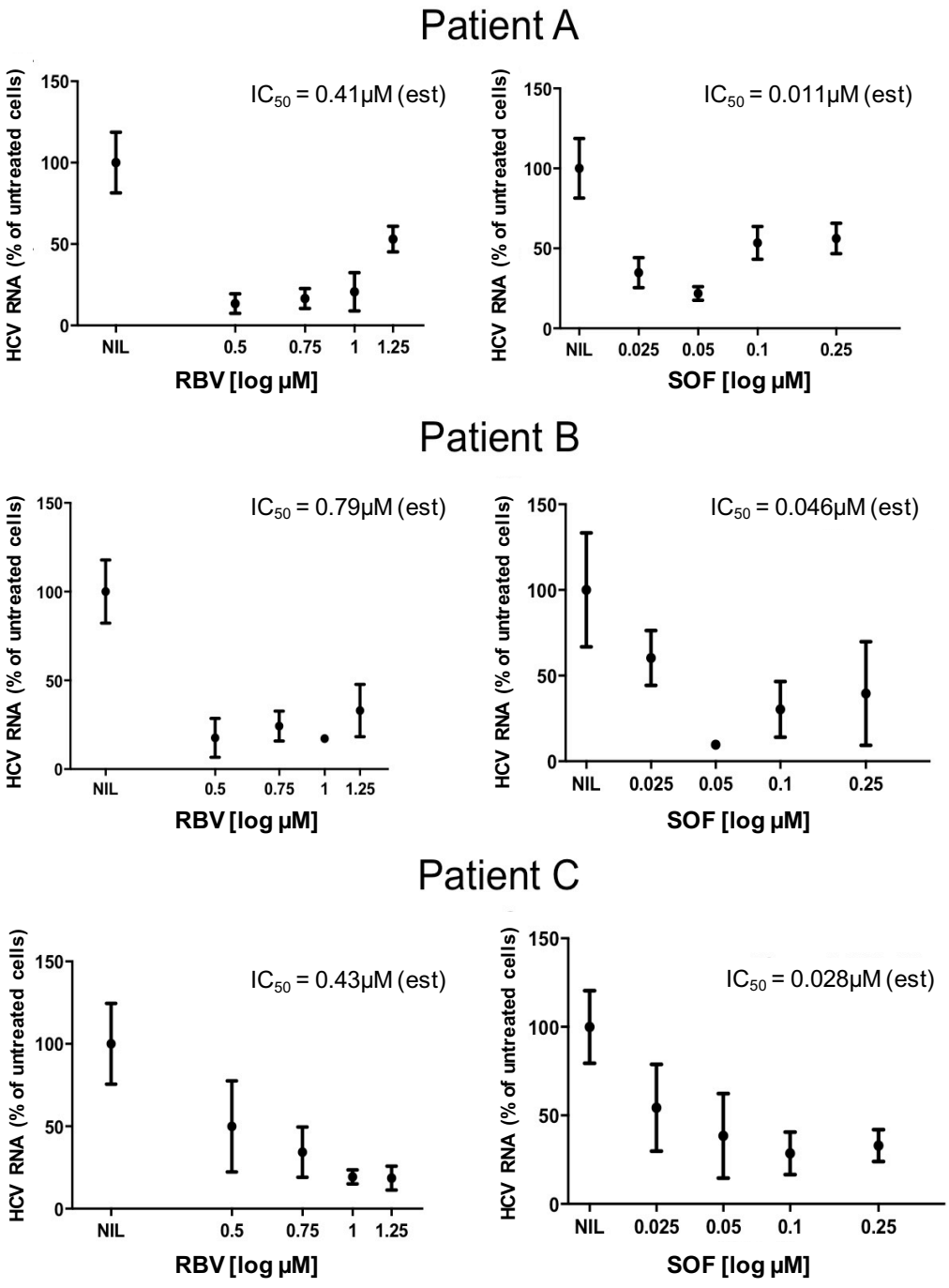

Fig 4.1 Sensitivity to SOF/RBV in G3 patient derived HCV.
Sera from 3 individual G3 HCV patients were used in capture fusion to determine sensitivity to SOF and RBV. Stimulated THP-1 cells were infected with sera at an MOI of 1 then fused 24hrs later to Huh7.5 cells. SOF or RBV was then added at indicated concentrations 1-day post fusion and replaced 3 days post fusion. Cells were harvested on day 5 and HCV RNA quantified by RT-qPCR. IC_{50} values were calculated from dose response curves. Graphs show mean ± sem for each drug concentration. For experiments with ribavirin high concentrations (1 -1.25 μM) were often associated with cell toxicity

resulting in paradoxical increases in HCV RNA)

4.2 Comparisons of SOF and RBV sensitivity in pre-treatment samples from patients who did, or did not, achieve a sustained virological response.

To assess whether a reduced sensitivity to SOF/RBV is present in patients who relapsed following antiviral therapy the capture fusion assay was used to assess sensitivity of HCV obtained from patients who relapsed to SOF based direct acting antiviral therapy. Samples were sourced from the English expanded access program, which was a compassionate use program to treat patients with the most severe liver disease with SOF based treatment regimens. As part of this program the HCV national biobank HCV Research UK (HCVRUK) collected serum samples from all patients participating in the UK expanded access program with samples taken throughout their treatment course. Patients gave informed consent to donate their samples to the biobank and samples were made available to us after approval by the designated tissue access panel, in line with ethics approval granted to Professor Irving. Patient samples used in this work were obtained from the HCVRUK national biobank, with key criteria for patient selection consisting of:

- Infection with G3 HCV
- Viral load sufficiently high to provide $2x10^6$IU, (due to difficulties sourcing patients with high viral loads in the cohort with advanced cirrhosis these criteria was subsequently relaxed)
- Treatment with SOF/LDV or SOF/DAC and RBV
- Full genome viral sequencing either performed or underway
- Sample taken pre-treatment.

As a control samples were also requested from G3 patients who had achieved SVR and we included two samples from our Royal London HCV patient cohort, which had high viral loads and were known to replicate well in the capture-fusion assay system.

28 samples were received from HCVRUK with the clinical details relating to outcome blinded. ‘Capture fusion’ experiments were performed on 12 out of the 28 highly viraemic samples to determine sensitivity to SOF and RBV. Limitations on serum volume and low viral loads prevented capture fusion experiments being performed on the remaining 16 samples.

Capture fusion experiments of each serum sample to ascertain response to SOF and RBV were performed in quadruplicate for each concentration of drug. Sensitivity to both drugs was assayed at the same time with analysis of the phenotyping data performed with no prior knowledge of the clinical outcome status of the sample tested. Response to drugs was determined by a highly sensitive taqman-RT-qPCR assay, which calculated HCV copy-numbers/µg for each sample tested. Of the samples tested, 8 exhibited sensitivity to SOF with an average IC_{50} of 0.039µM, comparable to earlier experiments performed with SOF (Fig 4.2A). The same samples were also found to exhibit RBV sensitivity although the average IC_{50} was noted to be higher than observed previously (Fig 4.2C). 6 samples however did not show the same reduction in HCV RNA levels in response to SOF and RBV treatment (Fig 4.2B, D). IC_{50} values for this group of samples were found to exceed the maximum dose of each drug used in the assay indicating a loss in sensitivity to both drugs.

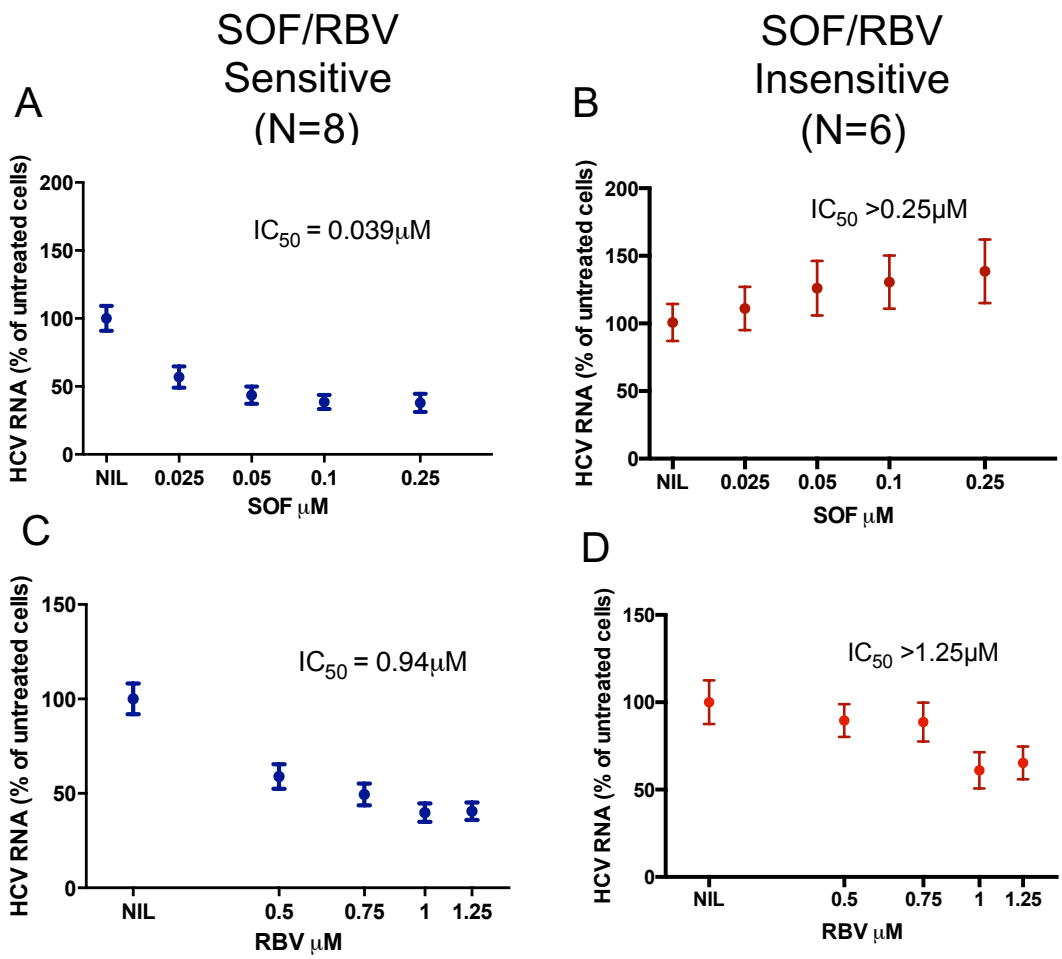

Fig 4.2 Sensitivity of Patient serum to SOF and RBV
14 pre-treatment samples were assayed for sensitivity to SOF and RBV by capture fusion. 8 samples of the exhibited sensitivity to SOF and RBV (A, C) while 6 samples exhibited a loss of sensitivity defined as an IC_{50} < 0.25μM for SOF and 1.25μM for RBV (B, D). Each serum sample was tested in quadruplicate. Graphs depict mean ±SEM .

Only after analysis of capture fusion data was complete was the clinical outcome of these samples revealed. Of the samples tested 2/12 achieved an SVR, 2 were from previous 'good replicators' (patients 2 and 3) and 10/14 were from patients who relapsed. All SVR samples and most relapse samples were treated with SOF/LDV/RBV while the remaining 3 relapse samples received DAC instead of LDV (Table 4.2).

Table 4.2 Clinical Data of the 14 patients used in capture fusion

Patient	Therapy	Outcome	age (yrs)	Gender	Cirrhosis	Previous IFN treatment	Baseline viral load (iu/mL)	Retreatment therapy (24 weeks)	Outcome
1	Sof/DCV/RBV	SVR	59	m	decompensated	yes	2,178,912		
2	Sof/vel	not yet available	32	f	compensated	no	5,992,729		
3	ombitasvir/ paritaprevir/ ritonavir + sofosbuvir	SVR	61	f	non cirrhotic	yes	2,301,777		
4	Sof/DCV/RBV	SVR	59	F	non cirrhotic	no	2,663,854		
5	Sof/LDV/RBV	Relapse	47	m	decompensated	no	2,321,679	Sof/LDV/ RBV	SVR
6	Sof/DCV/RBV	Relapse	49	m	decompensated	yes	1,913,455	Sof/DCV/ RBV	Relapse
7	Sof/LDV/RBV	Relapse	52	m	decompensated	yes	808,776	Sof/LDV/ RBV	SVR
8	SOF/LDV	Relapse	49	m	decompensated	no	3,100,000	Sof/LDV/ RBV	SVR
9	Sof/DCV/RBV	Relapse	48	m	decompensated	no	1,585,601	Sof/DCV/ RBV	SVR
10	Sof/LDV/RBV	Relapse	54	m	decompensated	no	255,934	Sof/LDV/ RBV	Relapse
11	Sof/LDV/RBV	Relapse	56	m	non cirrhotic (transplant graft)	yes	2,362,045	Sof/LDV	SVR
12	Sof/DCV/RBV	Relapse	58	m	decompensated	yes	902,000	Sof/DCV/ RBV	SVR
13	Sof/LDV/RBV	Relapse	43	m	decompensated	no	5,670,819	not retreated	
14	Sof/LDV/RBV	Relapse	50	m	decompensated	yes	570,000	Sof/LDV/ RBV	SVR

Drug sensitivity data from the capture fusion assay was re-grouped by clinical outcome data. Individual IC_{50} values obtained for SOF and RBV for each sample tested were divided into samples that achieved an SVR and those who relapsed. Comparison of IC_{50} values between SVR and relapse samples revealed a significant overall increase in IC_{50} for both SOF and RBV (p=0.022 for SOF and p=0.088 for RBV) (Fig 4.3A, B).

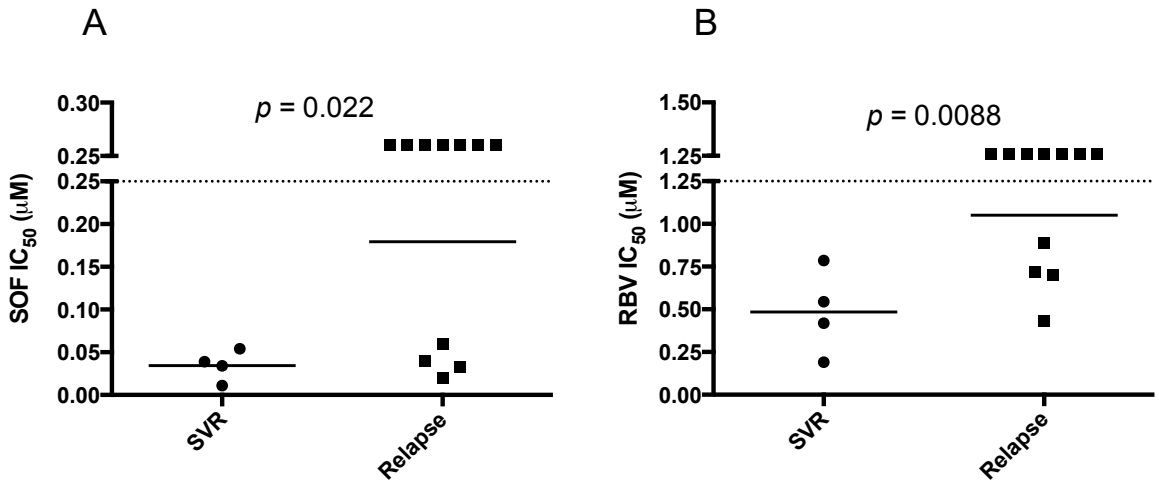

Fig 4.3 Grouping of Capture fusion data by clinical outcome
Individual IC_{50} values for SOF (A) and RBV (B) obtained by capture fusion were grouped into samples that achieved and SVR compared to samples that relapsed to therapy. A significant difference in IC_{50} vales for both drugs was found between SVR and relapse samples. Statistical analysis was performed using a Mann-Whitney U-test.

It was noted that a group of relapse samples retained comparable IC_{50} values for both SOF and RBV to SVR samples. To highlight this dose response curves for both drugs were re-grouped into: SVR-drug sensitive, relapse-drug sensitive and relapse drug insensitive (Fig 4.4). Dose response curves from SVR patients were comparable to the 4 relapse patients who exhibited SOF and RBV sensitivity (Fig 4.4A-B, D-E) whereas the 6 relapse samples defined as drug insensitive showed little reduction in HCV RNA levels in response to both SOF and RBV treatment in comparison to SOF/RBV sensitive samples (Fig 4.4C, F).

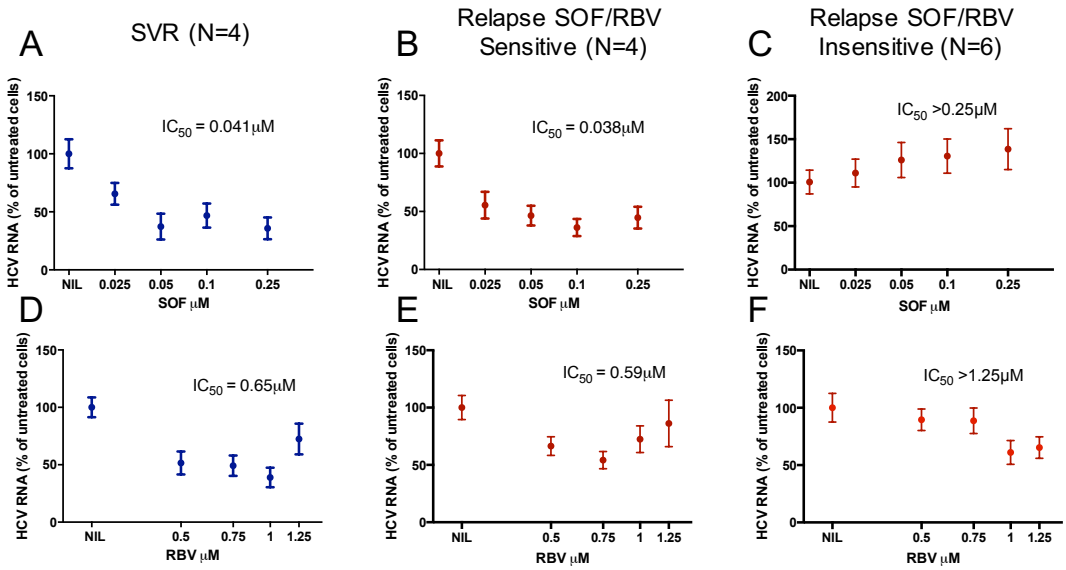

Fig 4.4 Dose response curves to SOF and RBV grouped by clinical outcome and drug sensitivity. Capture fusion data for SOF and RBV were grouped by clinical outcome into patients who achieved SVR (A, D) or relapsed (B, C, E, F). Relapse samples were further divided in to SOF and RBV sensitive (B, E) and insensitive (C, F). IC_{50} values for each drug represent the average of the indicated number of patients in each group. Graphs display mean ± sem

Together, these data indicate that a differential sensitivity to SOF and RBV exists in virus from G3 cirrhotic patients before the start of treatment. The majority of samples from patients in this cohort who went on to relapse to DAA therapy had a reduced sensitivity to both these antivirals implicating viral-drug sensitivity as a possible cause for relapse. However not all relapse samples were observed to be drug insensitive, implying that for those patients there may be alterative factors that caused relapse to therapy.

4.3 Sensitivity of G3 SVR and relapse samples to NS5A inhibitors and a novel RIG-I agonist

All patient samples studied were treated with NS5A inhibitors such as Ledipasvir (LDV) or Daclatasvir (DAC) in addition to SOF and RBV. We therefore performed additional experiments to establish if a difference in sensitivity to LDV or DAC existed in any of

the relapse samples. We also tested a novel agonist of the innate immunity SB 9200 that potently amplifies the host antiviral response by the activation of the retinoic acid inducible gene (RIG-I) and nucleotide oligomerisation domain protein 2 (NOD2) signalling cascades (Iyer *et al.*, 2010). This compound was recently used in a phase I clinical trial setting and shown to reduce HCV viral load with no serious adverse events with a similar antiviral effect to interferon (Thompson *et al.*, 2015).

We analysed, in a blinded fashion, response to DAC and LDV. However due to limitations in the volume of patient sera not all the previously tested relapse samples could be used in this experiment. In those that could be tested there was insufficient sample for a full dose response curve, so we developed a modified assay. Drug sensitivity was assessed in capture fusion by treating the infected-fused cells with a single concentration of LDV, DAC or SB 9200. Fold change in HCV RNA calculated from the non-treated control was performed to determine drug response. A significant fold reduction in HCV RNA was seen with LDV and SB 9200 treatment for both SVR and relapse samples (Fig 4.5). No significant reduction in HCV was observed with DAC treatment with the samples tested. Of the relapse samples tested it was discovered that one sample contained the well-described Y93H mutation, which confers resistance to NS5A inhibitors. The presence of this resistance variant may contribute to the reduced response of the relapse group to DAC.

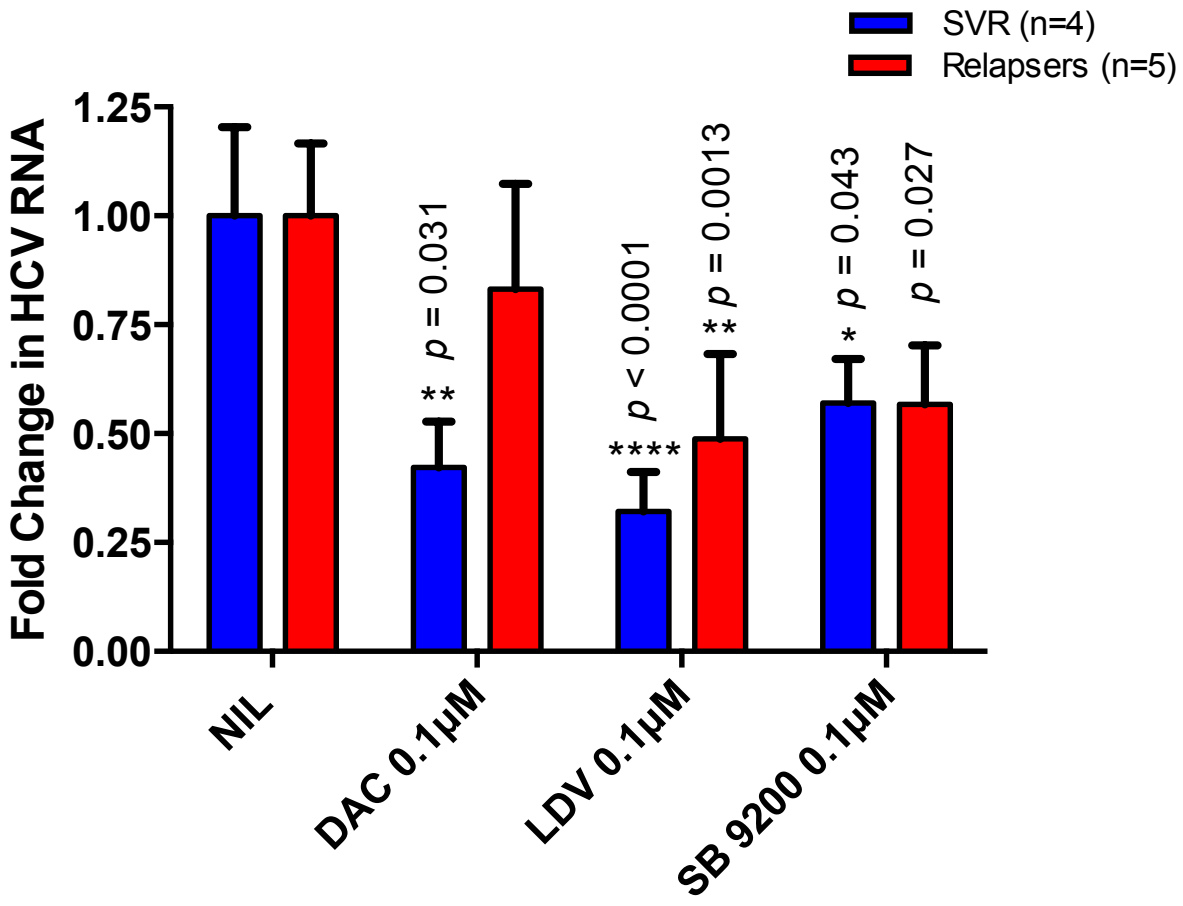

Fig 4.5 Sensitivity of G3 EAP samples to Daclatasvir, Ledipasvir and SB 9200.
Capture fusion assay was performed on sera from 9 of the previously studied G3 patients who had either achieved an SVR or relapsed to DAA treatment. All SVR samples and 3 of the relapse samples were treated with SOF/DAC/RBV and the remaining 2 relapse samples were treated with SOF/LDV/RBV. Fused cells were treated with a single dose in quadruplicate of either Daclatasvir (DAC), Ledipasvir (LDV) or SB 9200 and the fold change in HCV RNA compared to the no drug control ± sem plotted. Statistical analysis was performed using the Mann-Whitney U-test.

In summary, the data presented thus far show a subset of G3 patient-derived viruses possesses a refractory phenotype to SOF and RBV. Subsequent experiments assaying response of relapse samples to NS5A inhibitors showed that relapse samples had a reduced response to DAC likely due to the presence of the Y93H mutation in NS5A. However these experiments can only be used as an indication of response as serum limitations prevented full dose response curves to drugs being generated, which would have given a more representative indication of the response of these sera to LDV and DAC. Additionally, these experiments demonstrate the

potential of SB 9200 as alternative to DAA's for 'difficult to treat' genotype 3 HCV as comparable significant reductions in HCV RNA levels were observed in both SVR and relapse samples.

4.4 Sequence analysis of SOF/RBV insensitive samples

Samples used in capture fusion experiments underwent next-generation HCV viral genome sequencing (performed by Ana De Silva Filipe) as part of the HCVRUK study. Next-generation sequencing reads were analysed as previously reported (Thomson *et al.*, 2016). Substitutions present in fewer than 15% of the sequencing reads were discarded and only considered sequences with a read frequency of >16%. All samples were initially screened for known DAA resistance associated substitutions (RAS). Further analysis however compared drug sensitive to drug insensitive sequences with the aim of identifying unique sequence motifs within the NS5B region.

4.4.1 Identification of known resistance associated substitutions in samples assayed by capture fusion

Consensus files obtained for each phenotyped sample were aligned by ClustalW using the Geneious™ Bioinformatics and Alignment program (Kearse *et al.*, 2012). Samples were screened for the presence of RAS that confer resistance to DAAs in the NS3-NS5B regions (summarised in (Lontok *et al.*, 2015)). No well-characterised NS3 RAS such as Q80K or R155K were detected in any patient sample. At position 175 all patients were found to have the M-L mutation that has been previously reported to confer resistance to Boceprevir (Lauck *et al.*, 2012). This mutation was however only reported in <10% of patients who did not achieve an SVR. Its impact is also limited, as patients in the EAP were not given protease inhibitors as part of their treatment

regime. Additional RAS were detected in the NS5A region. Patient 3 had a T at position 30 which is implied as a possible RAS but shown not to affect sensitivity to DAC in a genotype 3a subgenomic replicon system (Wang *et al.*, 2013). Patients 9 and 14 were found to have H at position 93, which confers resistance to ledipasvir, daclatasvir and ombitasvir (Fridell *et al.*, 2011; Gao, 2013). Of particular relevance to this work, no mutations previously indicated in resistance to sofosbuvir (such as S282T) were found in any relapse samples shown to be drug insensitive. This suggests that novel; previously un-identified mutations may exist in the NS5B region of samples affecting sensitivity to sofosbuvir.

Table 4.3. Resistance associated substitutions in phenotyped samples

			NS3												NS5A									NS5B			
Patient	Clinical Outcome	Assay Outcome	V36	T54	V55	Q80	V107	S122	L132	R155	A156	Q168	I170	M175	M28	P29	A30	L31	P32	P58	S62	E92	Y93	L159	S282	C316	V321
1	SVR	Sensitive	L	T	V	Q	V	S	L	R	A	Q	V	L	M	P	A	L	P	P	S	E	Y	L	S	C	V
2	-	Sensitive	L	T	V	Q	V	S	L	R	A	Q	I	L	M	P	A	L	P	P	I	E	Y	L	S	C	V
3	SVR	Sensitive	L	T	V	Q	V	S	L	R	A	Q	V	L	M	P	T	L	P	P	L	E	Y	L	S	C	V
4	SVR	Sensitive	L	T	V	Q	V	S	L	R	A	Q	I	L	M	P	A	L	P	P	S	E	Y	L	S	C	V
5	Relapser	Sensitive	L	T	V	Q	V	S	L	R	A	Q	I	L	M	P	A	L	P	P	I	E	Y	L	S	C	V
6	Relapser	Sensitive	L	T	V	Q	V	S	L	R	A	Q	I	L	M	P	A	L	P	P	S	E	Y	L	S	C	V
7	Relapser	Sensitive	L	T	V	Q	V	S	L	R	A	Q	I	L	M	P	A	L	P	P	S	E	Y	L	S	C	V
8	Relapser	Sensitive	L	T	V	Q	V	S	L	R	A	Q	I	L	M	P	A	L	P	P	M	E	Y	L	S	C	V
9	Relapser	Insensitive	L	T	V	Q	V	S	L	R	A	Q	I	L	M	P	A	L	P	P	S	E	H	L	S	C	V
10	Relapser	Insensitive	L	T	V	Q	V	S	L	R	A	Q	I	L	M	P	A	L	P	P	S	E	Y	L	S	C	V
11	Relapser	Insensitive	L	T	V	Q	V	S	L	R	A	Q	I	L	M	P	A	L	P	P	S	E	Y	L	S	C	V
12	Relapser	Insensitive	L	T	V	Q	V	S	L	R	A	Q	I	L	M	P	A	L	P	P	T	E	Y	L	S	C	V
13	Relapser	Insensitive	L	T	V	Q	V	S	L	R	A	Q	I	L	M	P	A	L	P	P	V	E	Y	L	S	C	V
14	Relapser	Insensitive	L	T	V	Q	V	S	L	R	A	Q	I	L	M	P	A	L	P	P	S	E	H	L	S	C	V

4.4.2 Phylogenetic analysis of NS5B sequences in drug-sensitive and insensitive samples

NS5B sequences from all patient samples were used to plot a phylogenetic tree to establish if insensitive samples show any distinctive changes in their NS5B sequence (Fig 4.6). All samples cluster into 4 distinct clades, with drug sensitive samples comprising most of clades A and D and drug insensitive samples comprising clades B and C. Two insensitive samples do not fit this pattern. Patient 9 shows more similarity with the sensitive samples in clade A and patient 13 does not fit into any of the 4 clades.

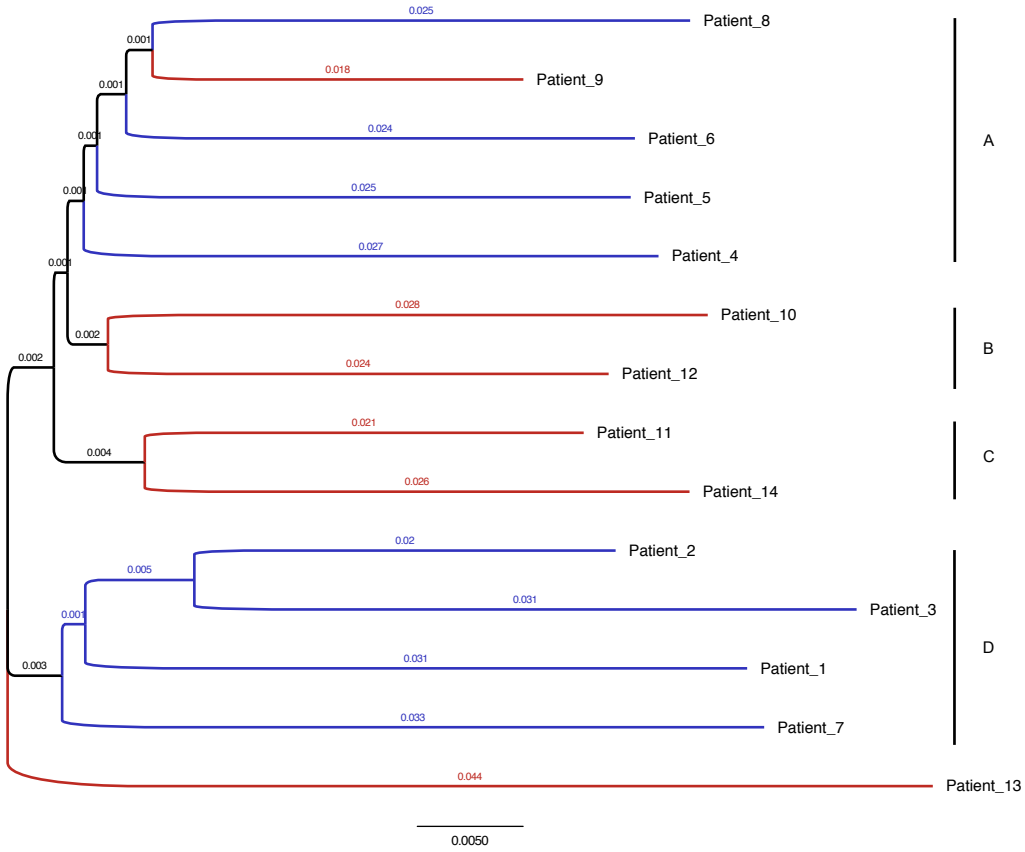

Fig 4.6 Phylogenetic tree based on the NS5B sequences of phenotyped samples
Phylogenetic tree constructed using the Neighbour-Joining method. The tree is drawn to scale, with branch lengths next to the branches. The differences in NS5B sequences were calculated using the Jukes-Cantor method and are in the units of the number of base substitutions per site. The analysis involved 14 nucleotide sequences. All positions containing gaps and missing data were eliminated. There were a total of 1796 positions in the final dataset. Red branches indicate drug insensitive

samples; blue branches indicate drug sensitive samples Tree was constructed using the MEGA7 program (Kumar *et al.*, 2016).

This analysis illustrates that the NS5B sequence from insensitive samples possess a similarity that distinguishes them from drug sensitive samples. It is possible that insensitive samples may have a unique substitution or set of substitutions in the NS5B that account for this distinctive phylogenetic grouping. However, the number of samples studied is too small for a definitive conclusion to be drawn.

4.4.3 Identification of unique substitutions within the NS5B of drug insensitive samples

NS5B sequences from SVR and relapse samples defined as SOF and RBV sensitive by capture fusion were collated to form a 'drug sensitive' consensus sequence (see appendix). This was used to identify unique changes within the NS5B of drug insensitive samples. Results of this analysis are summarised in Table 4.4. We noted two distinct mutation patterns with either five (K100R, A150S, G188D, K206E, T213N and N244I - patient 9) or two amino acid changes (A150V and K206E – patients 10-14). These patterns were not seen in patients who were 'sensitive' to sofosbuvir although individually the A150V and K206E substitutions were observed. These changes have not been previously observed as natural polymorphisms within NS5B of genotype 3 HCV (Di Maio *et al.*, 2014).

In patients whom pre- and post-treatment viral sequencing data was available, no significant change in the frequency of the substitutions of interest was observed (Table 4.4). The only notable change was observed in-patient 10, where the frequency of 150V and 206E increased from 54% and 89% respectively to 99% for both positions

post-treatment.

Table 4.4 Mutations within NS5B unique to drug insensitive samples

Patient	Therapy	Outcome	Drug sensitivity§		Relevant polymorphisms (Frequency (%) pre →post therapy) †						
			Sof IC50 (μM)*	RBV IC50 (μM)*	K100R	A150V	A150S	G188D	K206E	T213N	N244I
1	Sof/DCV/ RBV	SVR	0.039	0.786		V(98%)					
2+	Sof/vel	not yet available	0.034	0.545							
3+	ombitasvir/ paritaprevir/ ritonavir + sofosbuvir	SVR	0.011	0.419							
4	Sof/DCV/ RBV	SVR	0.054	0.19					E(98%)		
5	Sof/LDV/ RBV	Relapse	0.06	0.43					E(99%)		
6	Sof/DCV/ RBV	Relapse	0.033	0.886					E(99%)		
7	Sof/LDV/ RBV	Relapse	0.04	0.72		V(98%)					
8	SOF/LDV	Relapse	0.02	0.701							
9	Sof/DCV/ RBV	Relapse	0.26	>1.26	R (65→98%)		S (98→99%)	D (98→97)		N (98→99%)	I (94→99%)
10	Sof/LDV/ RBV	Relapse	0.26	>1.26	R (97→98%)	V (54→98%)			E (89→99%)		
11	Sof/LDV/ RBV	Relapse	0.26	>1.26		V (98→95%)			E (98→99%)		
12	Sof/DCV/ RBV	Relapse	0.26	>1.26		V (98→97%)			E (100→99%)		
13	Sof/LDV/ RBV	Relapse	0.26	>1.26		V (98→99%)			E (98→99%)		
14	Sof/LDV/ RBV	Relapse	0.26	>1.26		V (99%)*			E (100%)*		

* IC_{50} values for SOF and RBV were calculated from capture fusion.
§ Samples were deemed SOF and RBV sensitive if the IC_{50} was <0.25 and 1.25μM for each drug respectively and insensitive if the IC_{50} exceeded those values.
† Variants were identified by comparison of NS5B next generation sequencing data from drug sensitive versus insensitive samples. % Values indicate the frequency each variant was present in the viral population. No data was obtained for sample 14 due to low viral load post-relapse.
\+ Samples were not from the EAP but were previous responders to SOF/RBV in capture fusion assay

4.4.4 Location of identified substitutions in NS5B

To establish any possible effect of the identified substitutions on the activity of NS5B we sought to plot their location on a 3D model of the polymerase. To date the crystal structure of the G3 NS5B has not been determined. The most recent report of an NS5B crystal structure used the NS5B from the G2a JFH-1 (Appleby *et al.*, 2015). While not ideal due the significant sequence variation between HCV genotypes, our substitutions

were plotted on this structure.

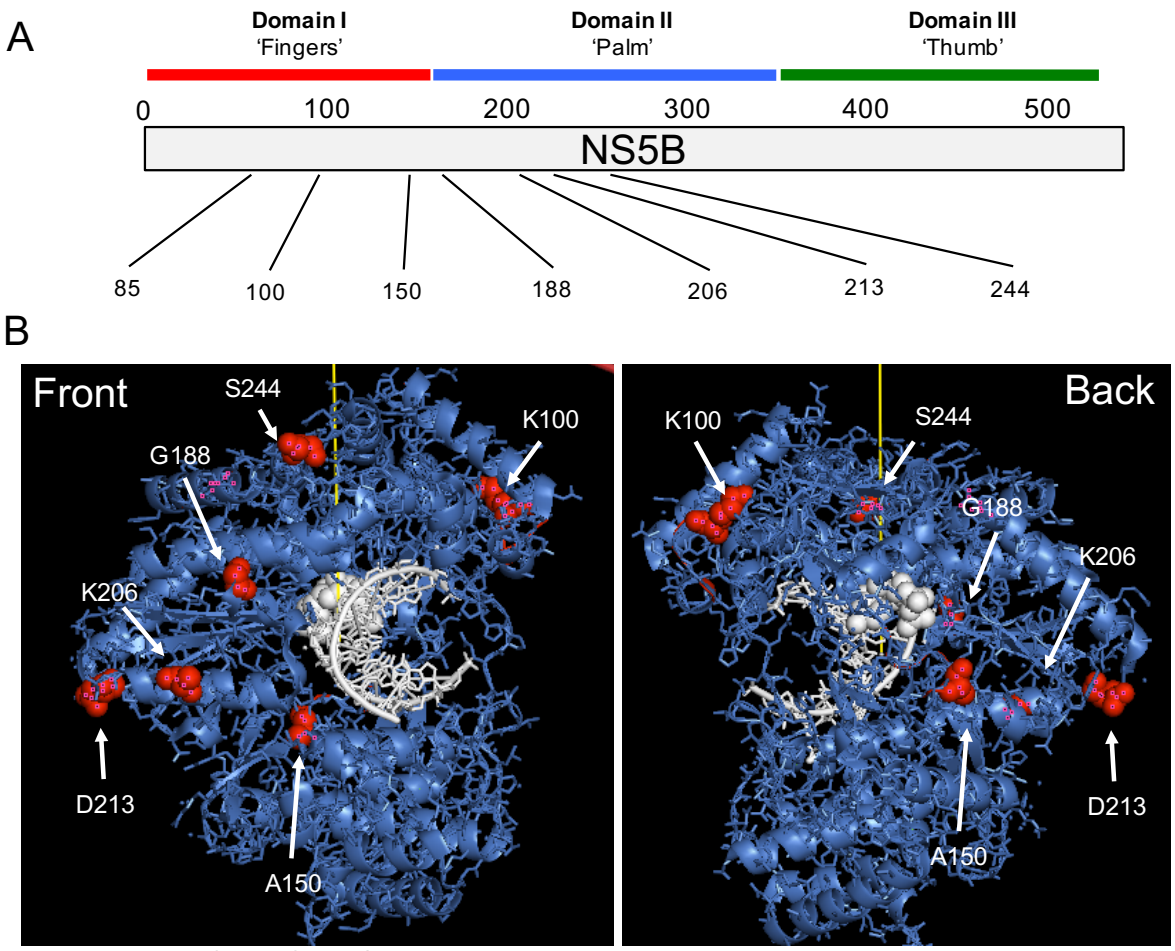

Fig 4.7: 3D model of identified NS5B substitutions
(A) Linear schematic representation of the locations of the substitutions of interest within NS5B. (B) 3D model of NS5B derived from a crystal structure with the positions of interest coloured red with white labelling.. The white structure in the centre represents a bound RNA strand. PDB crystal structure ID: 4WTG. Structure was annotated using the PyMOL software.

Most substitutions were located within domains I ("fingers") and II ("palm") of the NS5B protein (Fig 4.7A). The palm domain contains the catalytic triad that forms the RdPp active site. Highly conserved residues, crucial for the active site are D220, D225, G317, D318 and D319 (Hagedorn, 1999; Waheed *et al.*, 2012). While none of our identified positions are part of or next to residues of the active site, two are close, K206E and T213N. The 3D structure shows that K206 (LYS-206) forms part of an alpha helix close to the RNA binding cleft but not directly within (Fig 4.7). This residue is also close to a domain previously reported crucial to the RNA binding capacity of NS5B (Qin *et al.*, 2001). Thr-213 (ASP-213 in the above structure) however, is shown

in the 3D structure to some distance from the catalytic site of the polymerase.

The catalytic activity the NS5B is modulated by a direct interaction with NS5A (Shimakami *et al.*, 2004; Shirota *et al.*, 2002). This interaction stimulates activity of the polymerase but can also inhibit activity in a dose dependent manner (Shirota *et al.*, 2002). Specific domains on the NS5B are crucial for this interaction these are residues 143-145, 149-155, 365-371 and 382-388. A150V is located within one of these domains, which may affect NS5A binding and potentially modulate of the NS5B catalytic activity through NS5A.

4.5 Prevalence and impact of NS5B mutations in a second patient cohort

To further examine the impact of the substitutions we examined their frequency in a second, independent cohort of patients with genotype 3 HCV receiving sofosbuvir based therapies. We studied sequences from pre-treatment genotype 3 samples from the BOSON trial (Foster *et al.*, 2015b). This cohort consisted of 522 genotype 3 patients of which approximately 50% had previous experience with pegIFN/RBV therapy. Approximately 37% of the entire cohort had cirrhosis. The frequency of our identified mutations in patients who did, or did not, achieve an SVR was examined by Dr Azim Ansari (University of Oxford) (Fig 4.8). Individually, each of the identified variants associated with reduced sofosbuvir sensitivity was not present in the cohort at a high prevalence making robust statistical analysis difficult (Fig 4.8A). The exception was the A150V variant which was present in 47% of patients and in the 204 samples with the V residue an SVR was achieved in 153 patients (75%) compared to a response rate of 168 of 191 (88%) patients with the A variant (p=0.0012) (Fig 4.8B).

The combination of A150V and K206E was uncommon (22 patients, 6%) and was associated with a SVR of 82%.

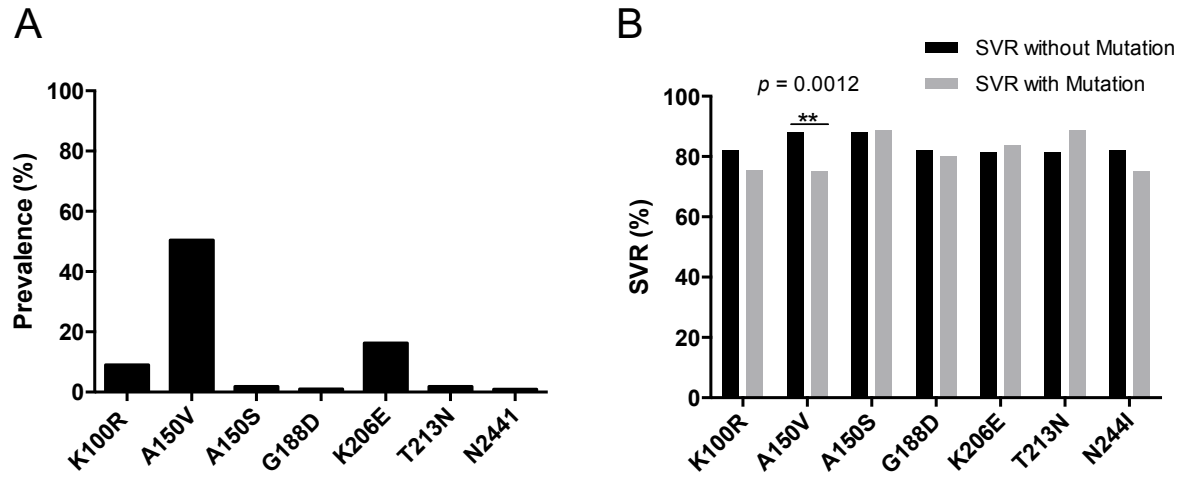

Fig 4.8 Analysis of identified NS5B mutations in the BOSON patient cohort
(A) The prevalence of identified NS5B mutations was assessed from >500 viral sequencing samples obtained from the BOSON cohort. (B) Each mutation was tested to assess whether the frequency was significantly different between SVR and Non-SVR samples. Frequencies were analysed using a fisher's exact test.

4.6 Summary

Using the 'capture fusion' assay, a set of G3 patient-derived viral samples were identified with a reduced sensitivity to both SOF and RBV. Analysis of next-generation viral sequencing data revealed that none of the drug insensitive samples contained any RAS previously associated with resistance to SOF or RBV, however 2 samples did contain the well-characterised Y93H mutation in the NS5A protein. Phylogenetic analysis of NS5B sequencing data indicated that SOF and RBV insensitive samples contained distinctive differences in their polymerase region compared to drug sensitive samples. By comparison of the NS5B sequences from samples defined as drug insensitive to those defined as sensitive to SOF and RBV we identified two a combination of mutations, A150V and K206E, unique to the majority of drug insensitive samples. Additionally a pattern of multiple NS5B mutations consisting of K100R,

A150S, G188D, T213N and N244I was identified in a single isolate. To establish how these mutations affect SOF and RBV sensitivity they will have to be studied in the context of a subgenomic or infectious HCV replicon assay.

5 RESULTS: Using HCV replicon systems to assess the impact of identified NS5B mutations on antiviral sensitivity

5.1 Introduction

Study of the HCV lifecycle has been greatly enhanced by the development of subgenomic and fully infectious replication systems. These systems have furthered our understanding of HCV replication as well providing useful screening tools for antiviral resistance testing [reviewed in (Catanese & Dorner, 2015)]. The highly variable nature of the HCV genotypes in terms of both sequence and behaviour has led to the development of genotype specific replicons such as con-1 (G1), JFH-1 (G2), S52 (G3), ED45 (G4) (Kato *et al.*, 2003; Lohmann *et al.*, 1999; Saeed *et al.*, 2012).

We hypothesised that the unique NS5B motifs identified in drug insensitive patient samples (listed in Table 5.1) affect sensitivity to SOF and RBV. To test our hypothesis, we used two *in vitro* models of G3 HCV. The first was the S52 based subgenomic replicon developed by Saeed and colleagues (Saeed *et al.*, 2012), which can be used either in a transient replication assay or to make stable replicon cells by virtue of the G418 resistance marker embedded in the construct (Witteveldt *et al.*, 2016). The second was a recently described infectious model of G3 HCV developed by (Ramirez *et al.*, 2016), which can produce G3 virus at titres comparable to JFH-1. These systems allowed us to study of the effects of these mutations on the viral replication enzymes (subgenomic replicon) and the complete viral life cycle (G3 infectious virus).

Table 5.1 NS5B mutations identified from drug insensitive patient samples

NS5B sites to be mutated	*Nucleotide change*
K100R	AAG – A**G**G
A150V	GCT – G**T**T
G188D	GTT – G**A**T
K206E	AAG – **G**AG
T213N	ACC – A**A**C
N244I	AAC – A**T**C

5.2 Engineering NS5B mutations into the S52-Subgenomic replicon construct

A PCR mutagenesis method was employed to introduce the mutations listed in Table 5.1 into the S52-subgenomic (SG) replicon construct. Two overlapping fragments covering the entire NS5B region were amplified from the S52-SG plasmid using a set of primers with the desired mutations and a set off outer primers encoding unique restriction sites (see Methods 2.1.7). Once amplified, these fragments were used in a second-round PCR to create the full NS5B amplicon containing the desired mutation (Fig 5.1C). Using *XhoI* and *XbaI* restriction sites, mutated NS5B products were cloned back into the S52-SG construct, which was confirmed by restriction digestion Fig 5.1D).

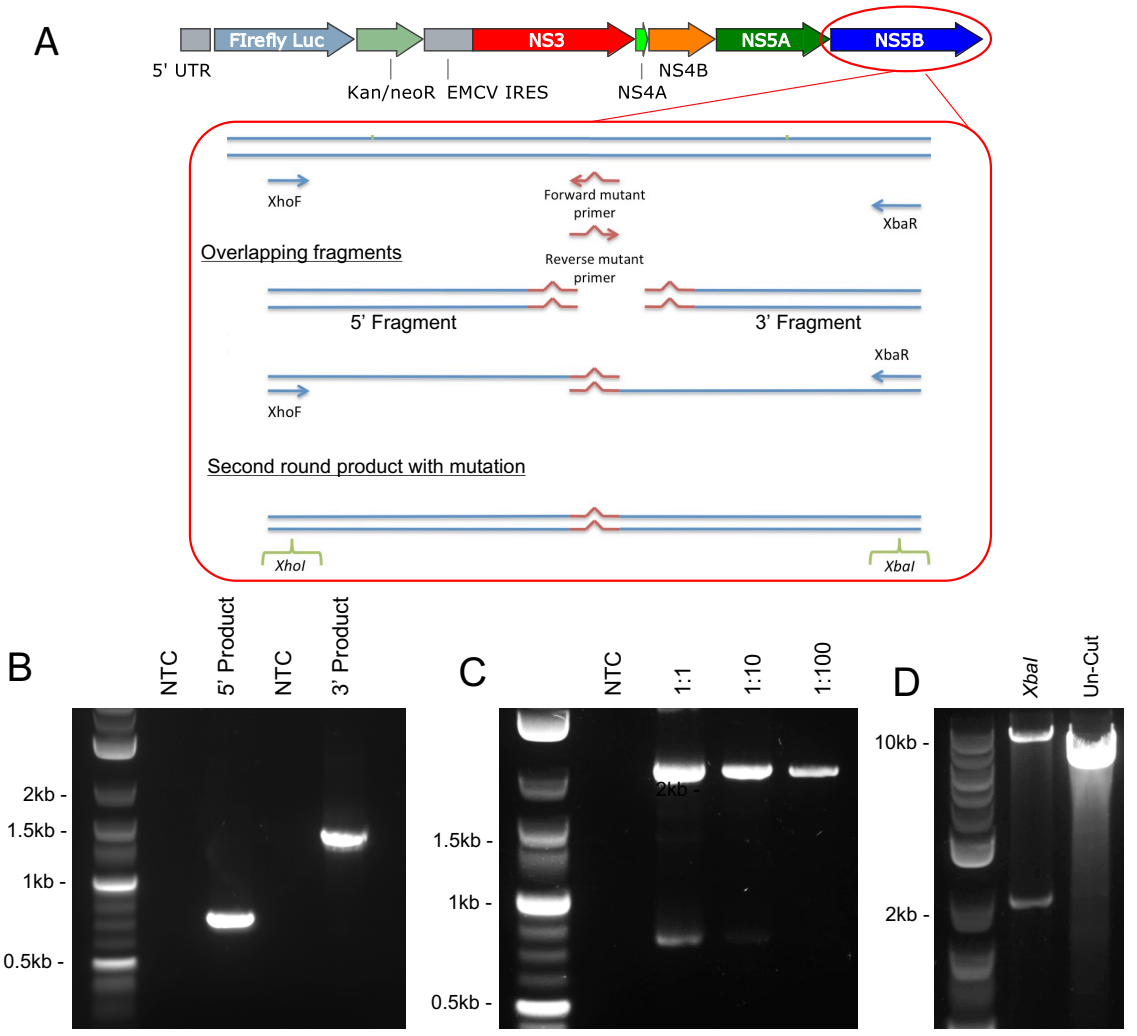

Fig 5.1 PCR mutagenesis of the S52-SG replicon
(A) Schematic overview of the PCR mutagenesis experiments to engineer the listed NS5B mutations into the S52-SG replicon. (B) Amplification of the overlapping NS5B fragments by PCR. The XhoF outer primer was used with the mutation specific reverse primer to amplify the 5' fragments and the mutation specific forward primer was used with the XbaR primer to amplify the 3' fragment. Size of fragments varied according to the location of the target mutation. (C) Second round PCR to create the entire NS5B amplicon contained the desired mutation. 5'and 3' fragments were mixed in an equimolar ratio and serially diluted 10 fold to create a single 2.1kb product. This product was then subsequently cloned back into the S52-SG construct using *XbaI*/*XhoI* restriction sites. (D) *XbaI*/*XhoI* restriction digest of colonies after ligation showing a 2.1kb product consistent with the size of the NS5B insert PCR results and restriction digests presented are representative examples for all cloning experiments

Mutated constructs were validated by Sanger sequencing (Source Bioscience) confirming that NS5B mutations were correctly engineered and the reading frame had not been altered (Fig 5.2). All mutations were engineered individually and the A150V and K206E changes were also made in combination, as the most common sequence motif in SOF/RBV insensitive patients.

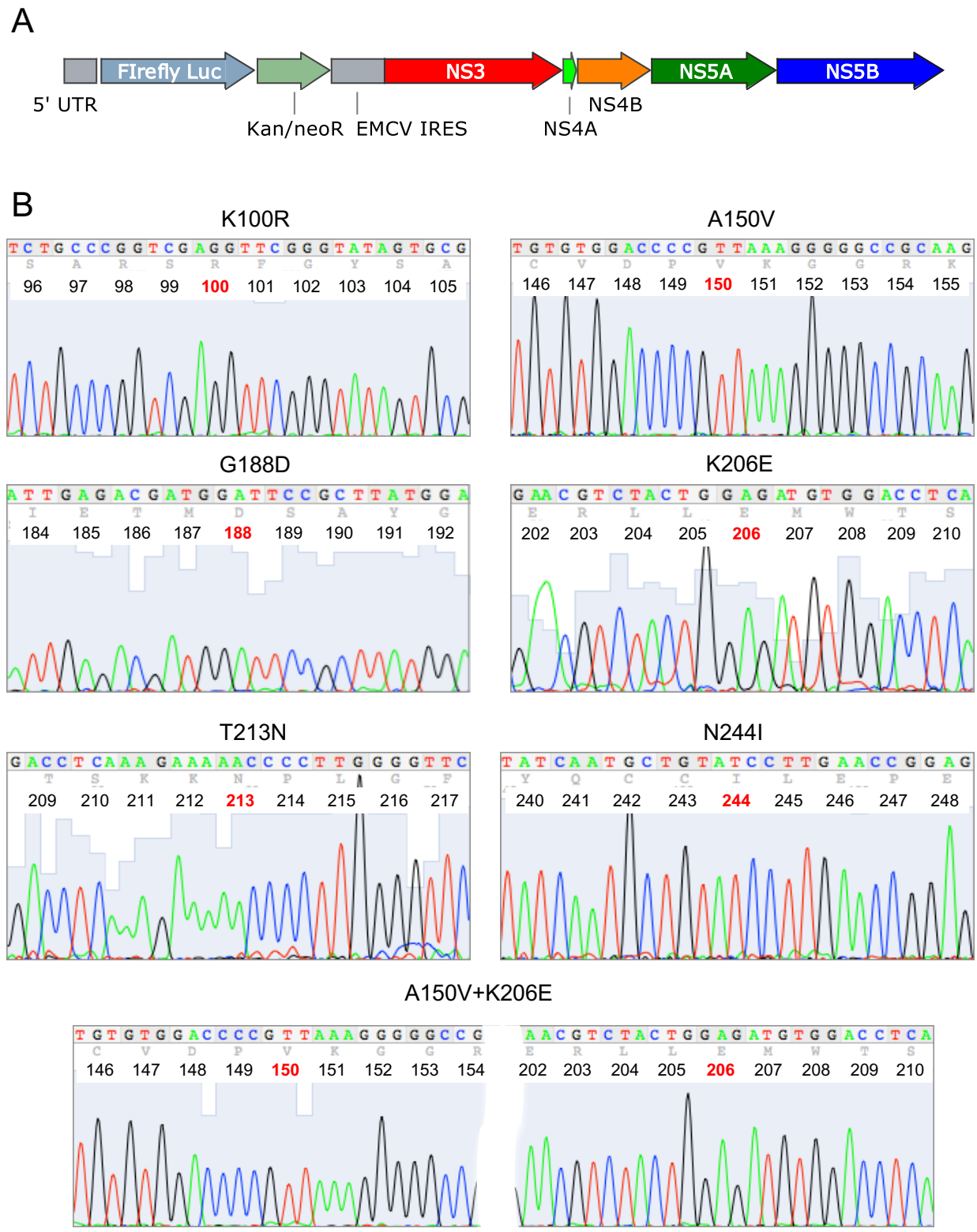

Fig 5.2 Sequencing of mutated NS5B sites within the S52-SG-replicon
(A) Schematic representation of G3 S52-SG replicon. (B) Sanger sequencing traces from S52-constructs with indicated mutations engineered in the NS5B by PCR-mutagenesis. Mutated amino acid is highlighted in red, with numbering referring to the start of NS5B

5.3 Analysis of mutations in cells stably expressing the S52-SG replicon

One of the properties of the S52-SG replicon is the presence of a firefly luciferase/neomycin resistance cassette driven by the HCV IRES (Fig 5.1A). This allows cells stably expressing the replicon to be obtained through G418 selection, generating a robust cell culture model to investigate any effect the identified NS5B mutations may have on drug sensitivity.

Mutated S52 constructs were electroporated into Huh7.5 SEC14L2 cells and placed under G418 selection for 3 weeks to obtain stable replicon colonies. Despite several attempts (N= 3 on different occasions using different RNA preparations and cells) stable colonies were not obtained from constructs expressing the A150V mutation. Wild type (Wt) constructs or those containing K100R, G188D and K206E mutations only were generated. Functionality of the luciferase reporter was established by treatment of the cells with 1000IU/ml of IFNα-2A, which caused a significant reduction in luciferase activity in all replicon cells tested (Fig 5.3A). HCV protein expression and was confirmed in these cells by staining for NS5A, which was found to form characteristic punctate structures in the cytoplasm of the replicon cells (Fig 5.3B).

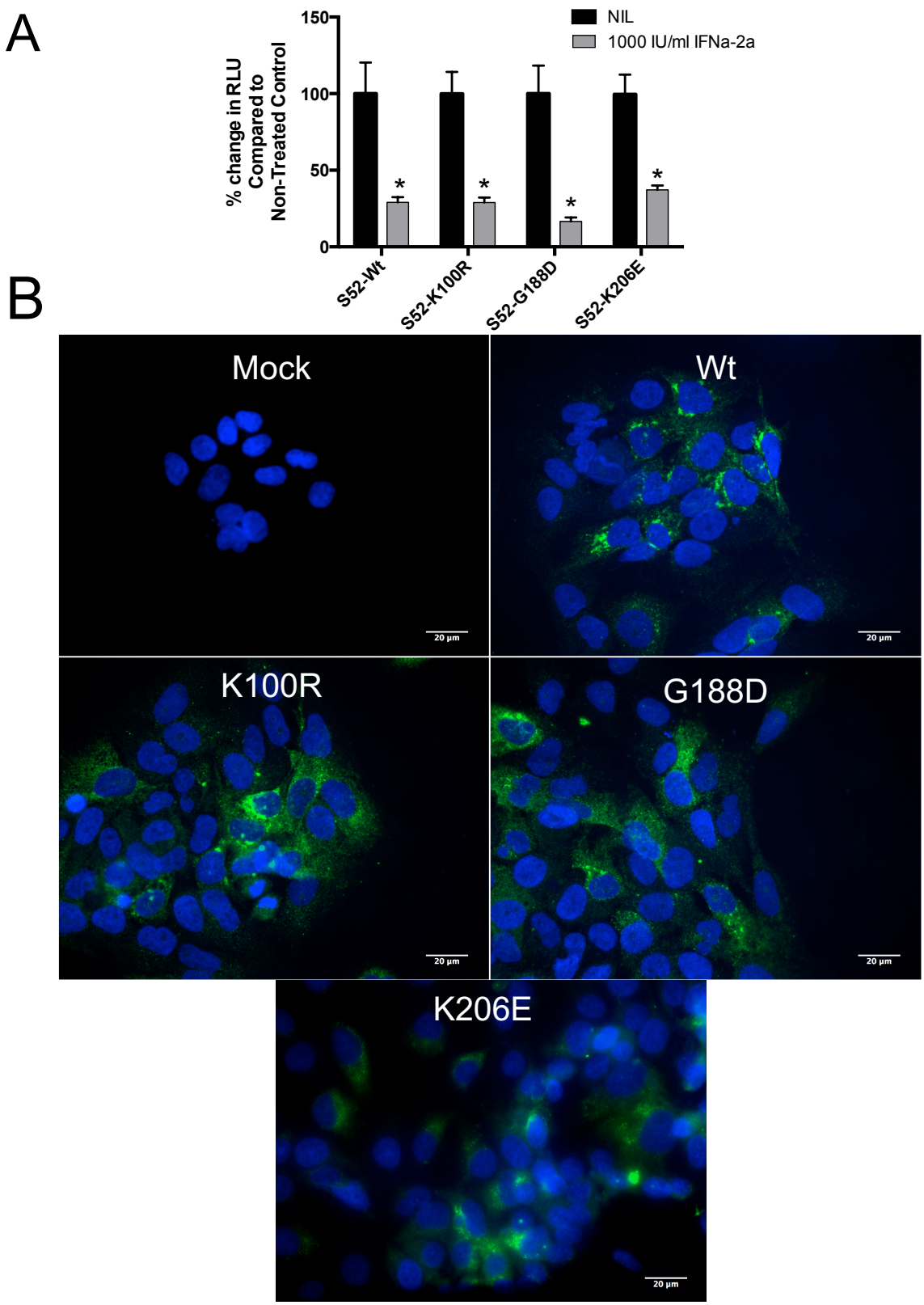

Fig 5.3 Validation of S52-SG replicon cells
(A) Replicon cells were treated for 72hrs with 1000 IU/ml IFNα-2A after which cells were lysed to measure luciferase activity. Data was normalized to the un-treated control to calculate % change in

luciferase activity. (B) Replicon cells were fixed in methanol to visualise NS5A by fluorescent microscopy. Cells were also counterstained with the nuclear specific dye DAPI.

5.3.1 Response of stable replicon cell lines to sofosbuvir and ribavirin

Despite only obtaining stable lines for three NS5B mutations, drug sensitivity experiments were performed to assess any effect of K100R, G188D or K206E may have on SOF and RBV sensitivity. Luciferase activity was used as a measure of RNA replication in response to SOF and RBV treatment as has been previously established with the S52-replicon (Saeed *et al.*, 2012). Replicon cells were treated with serial dilutions of SOF and RBV for 48hrs after which luciferase expression was quantified. Treatment of Wt replicon cells with SOF and RBV resulted in a decrease in luciferase activity in a dose dependent manner (Fig 5.4A, B). The K100R mutation had a negligible effect upon sensitivity to SOF with a comparable IC_{50} obtained to the Wt replicon. G188D and K206E had more of a pronounced effect on SOF sensitivity affecting a 3.6 and 10-fold increase in SOF IC_{50} respectively (Fig 5.4A). These mutations appeared to have more of an effect on RBV sensitivity than SOF. A 5- and 14-fold increase in RBV IC_{50} was observed with the K100R and K206E replicon cells respectively, though the greatest effect was observed in replicon cells with the G188D mutation where a loss of sensitivity to RBV was observed (Fig 5.4B).

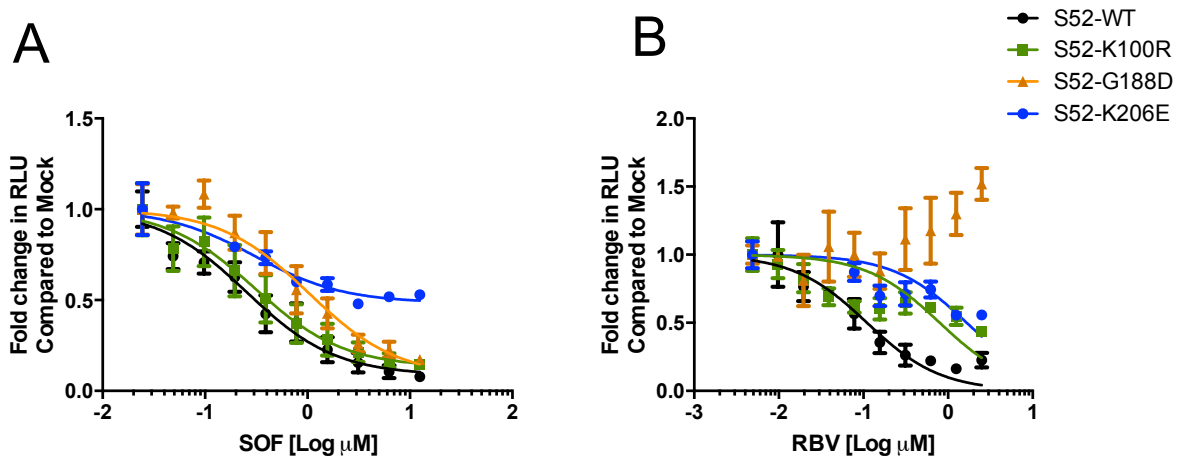

S52 Cell line	SOF IC_{50} [μM] (CI_{low}-CI_{high})	RBV IC_{50} [μM] (CI_{low}-CI_{high})	Fold change in SOF IC_{50}	Fold change in RBV IC_{50}
Wt	0.35 (0.25-0.47)	0.11 (0.074-0.16)	1	1
K100R	0.47 (0.31-0.71)	0.79 (0.47-1.355)	1.34	4.6
G188D	1.27 (0.89-1.80)	>10	3.63	-
K206E	3.5 (2.15-5.70)	1.64 (1.08-2.57)	10	14.9

Fig 5.4 Sensitivity of Stable replicon cells to sofosbuvir and ribavirin
Replicon cells expressing the K100R, G188D and K206E mutations were treated with serial dilutions of SOF (A) and RBV (B) for 48hrs. IC_{50} values for both drugs shown with 95% CI were calculated from the reduction in luciferase activity compared to the no-drug control. Fold change in SOF and RBV IC_{50} were calculated from the IC_{50} value obtained from the unmodified Wt replicon line. The above represents 2 independent experiments. Values plotted are mean ± SEM.

5.4 Analysis of mutations in a transient replicon assay

As stable replicon lines expressing all NS5B mutations of interest could not be obtained an alternative approach was deployed to assess their effect on SOF and RBV sensitivity. Transient HCV replicon assays are well defined (Kato *et al.*, 2003; Saeed *et al.*, 2012; Targett-Adams & McLauchlan, 2005; Witteveldt *et al.*, 2016) and have the advantage of being unlikely to acquire cell culture adaptive mutations through the process of antibiotic selection that enhance replication and subsequently may affect antiviral resistance testing (Blight *et al.*, 2000; Lohmann *et al.*, 2001).

5.4.1 Replication of G3 S52-SG replicon in a transient assay

The G3 S52-SG replicon was transfected into Huh7.5-SEC14L2 cells, with luciferase expression measured at various time points. Luciferase levels peaked between 24 and 48hrs post-electroporation and were seen to drop after 72hrs levelling out at 125hrs post electroporation

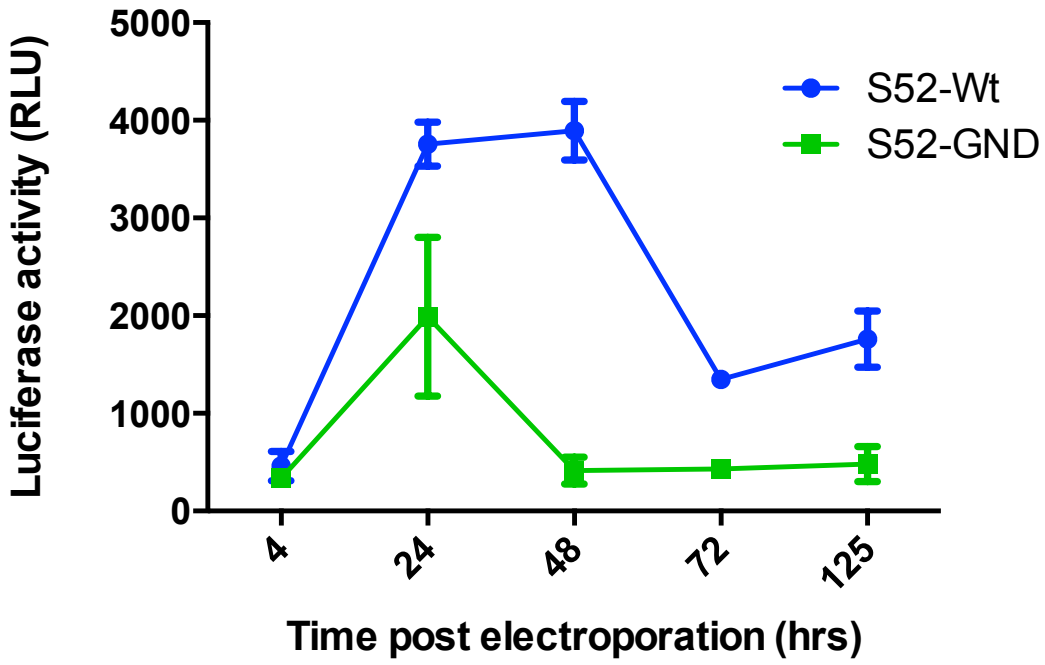

Fig 5.5 Replication of the S52-SG replicon
The S52-SG Wt construct was electroporated into Huh7.5 SEC14L2 cells with samples taken at the time intervals indicated to measure luciferase expression. A modified version of the replicon with a mutation in the NS5B active site impairing activity of the enzyme (S52-GND) was included as a replication control. Data plotted is mean±SEM.

5.4.2 Effect of mutations in a transient replicon assay

S52-SG constructs were transiently transfected into Huh7.5-SEC14L2 cells to assay response to SOF and RBV (Fig 5.6). Cells were recovered for 24hrs and then treated with serial dilutions of SOF and RBV for 72hrs. Luciferase expression was then quantified to evaluate the effect of the antiviral treatment. The unmodified Wt replicon acted as a control for drug sensitivity while a replicon containing the well-described S282T SOF resistance mutation was created using PCR mutagenesis to serve as a control for SOF resistance (Svarovskaia *et al.*, 2014). Due to the high degree of

variability experienced with electroporation three independent antiviral assays were performed with each mutated replicon.

In line with data previously obtained from the stable replicon assays, K100R had a modest effect on SOF inducing a 2 shift in IC_{50} for each drug respectively (Fig 5.6A, C). Yet for RBV, this mutation was observed to have a much greater effect causing a 32-fold increase in IC_{50} than the 4-fold increase observed with the stable replicon (Fig 5.6B, C). G188D was shown to cause a greater shift in SOF IC_{50} in this assay (11 fold IC_{50} shift compared to 3.6) than was previously shown in the stable cell line but retained its effect on RBV inducing up to a 15-fold increase in IC_{50}. The effect of K206E on SOF was similar in this assay (fold shift of 8.3) than was observed with the stable cells (fold shift 10) (Fig 5.6A, C). Likewise, with RBV K206E induced an 11- fold increase in IC_{50}, which was similar but slightly reduced to the 14-fold shift observed with the stable cells (Fig 5.6B, C).

A

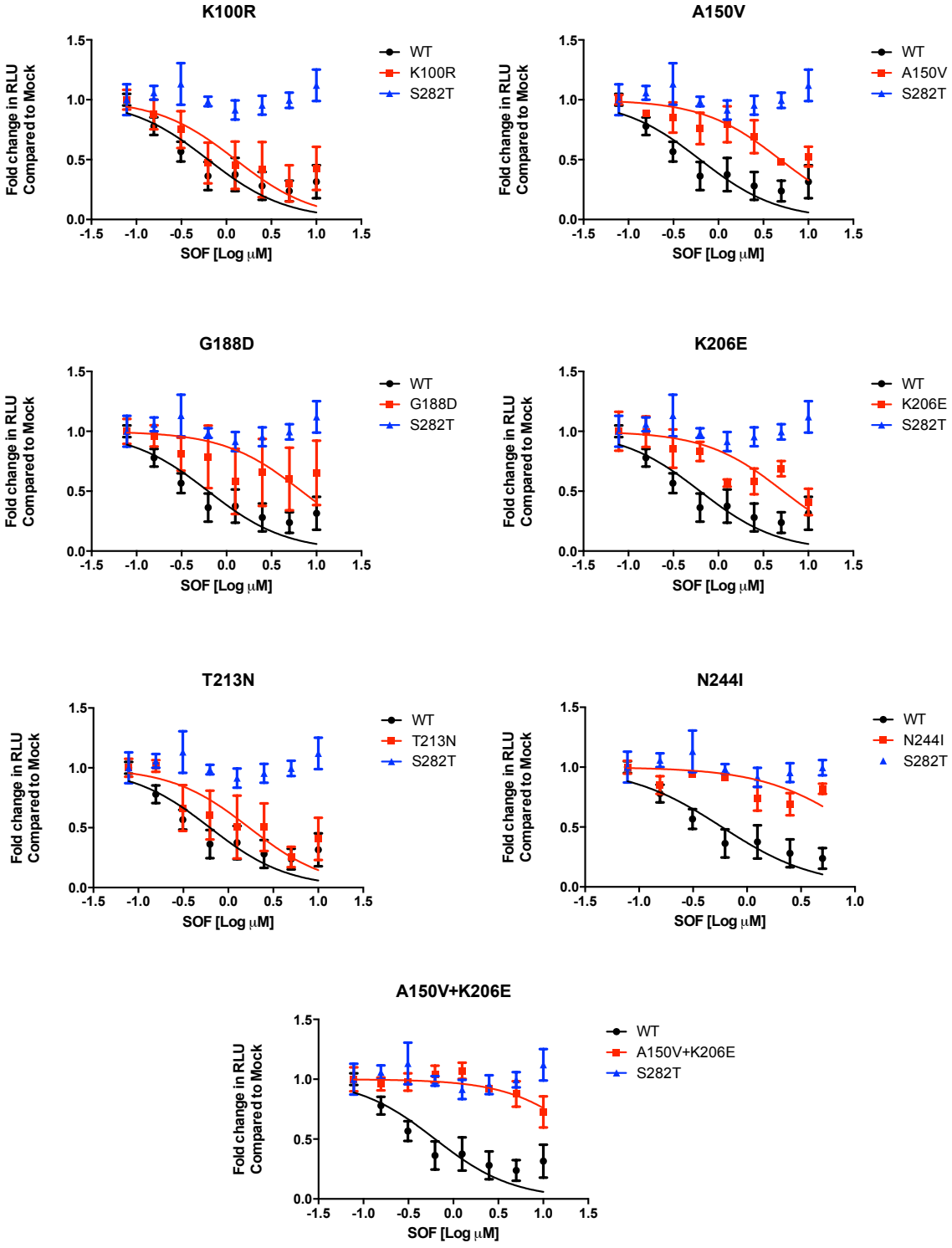

Fig 5.6: Sensitivity of NS5B mutations in transient replicon assay

B

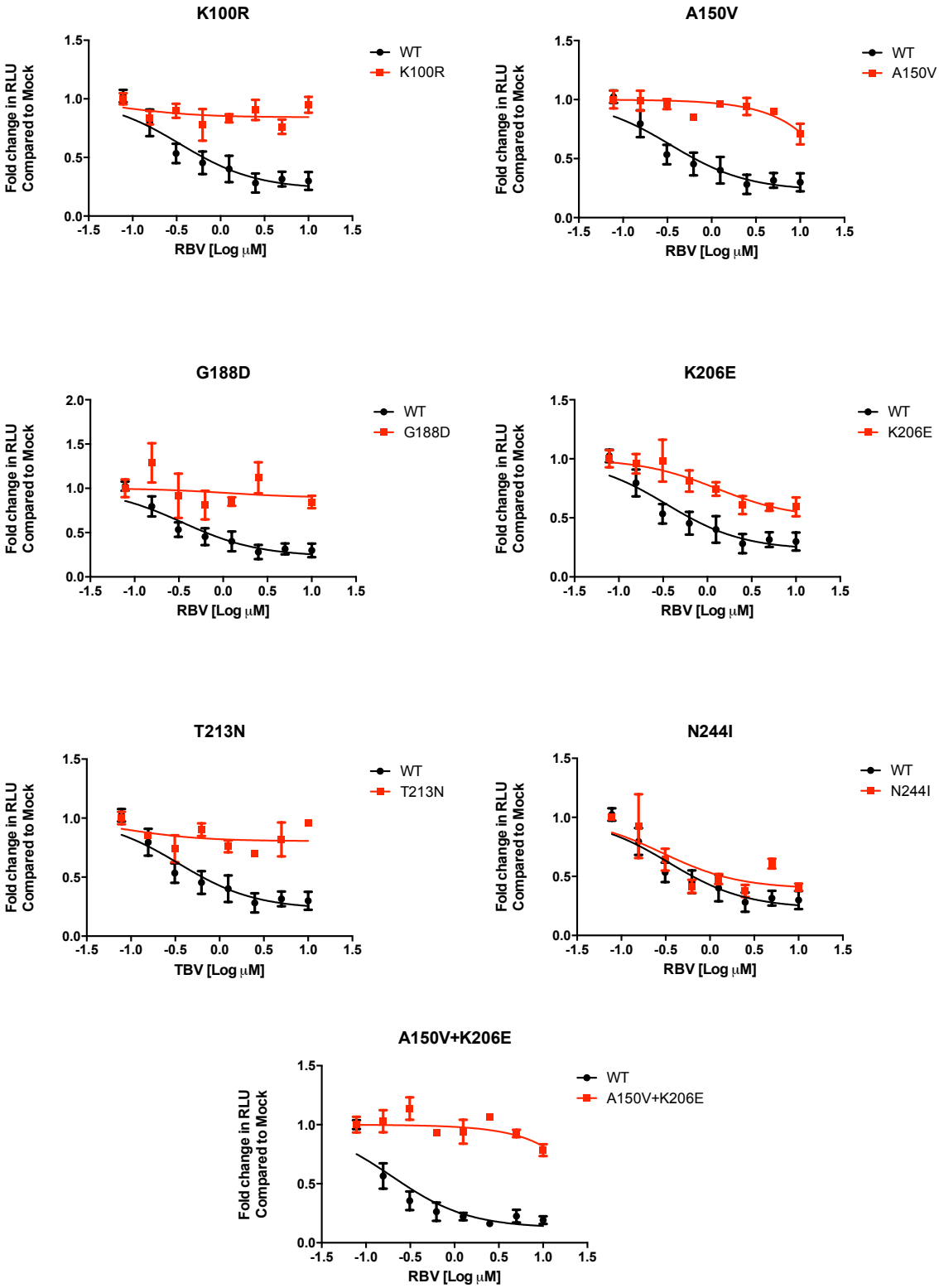

Fig 5.6 Continued

C

S52-Replicon	SOF IC_{50} [µM] (CI_{low}-CI_{high})	Fold change in SOF IC_{50}	RBV IC_{50} [µM] (CI_{low}-CI_{high})	Fold change in RBV IC_{50}	Luciferase levels as % of Wt (mean ±SEM)
Wt	0.63 (0.40-0.99)	1	0.70 (0.47-1.05)	1	100.00 (±10.33)
K100R	1.26 (0.64-2.50)	2.00	23.61 (9.96-55.95)	32.85	72.45 (±13.18)
A150V	4.88 (2.70-8.827)	7.75	28.03 (17.14-45.83)	40.04	98.17 (±11.59)
G188D	6.84 (2.47-18.90)	10.86	15.19 (4.94-46.67)	21.70	74.02 (±17.11)
K206E	5.25 (2.96-9.33)	8.34	7.40 (4.66-11.75)	10.57	59.35 (21.05)
T213N	1.71 (0.85-3.43)	1.27	6.12 (3.58-10.54)	8.74	108.20 (±18.19)
N244I	10.32 (5.28-20.16)	16.38	1.49 (0.78-2.86)	2.13	55.95 (±13.01)
A150V+K206E	22.54 (12.47 to 40.74)	35.77	48.69 (20.81-113.9)	69.55	120.40 (±17.75)
S282T	45.15 (6.04-161.6)	71.67	-	-	67.85 (±18.88)

Fig 5.6 Sensitivity of NS5B mutations in transient replicon assay
Huh7.5-SEC cells transiently transfected with S52-replicon constructs with indicated NS5B mutation were assayed for their response to SOF (A) and RBV (B). Cells were treated with SOF for 72hrs after which luciferase expression was quantified. Luciferase values were normalised to a sample taken 4hrs post-electroporation for each construct. As a control for SOF resistance a replicon containing the SOF resistant S282T NS5B mutation was included in all transient SOF sensitivity experiments. (C) IC_{50} values for SOF and RBV for each replicon construct are shown with 95% confidence intervals. Fold change in IC_{50} for SOF and RBV was calculated for each mutated construct using the unmodified wild type S52-replicon as a baseline. Relative luciferase levels compared to the Wt replicon construct for each mutated replicon were also included. The above is representative of at least 3 independent experiments.

The main advantage of the transient replicon assay was that it allowed the effect of the additional NS5B mutations for which stable cells lines could not be established to be assessed such as T213N, N244I and A150V). T213N had a comparable IC_{50} to the Wt replicon for SOF but reduced sensitivity to RBV by approximately 9-fold. N244I

however had more of an impact on SOF sensitivity causing a 16-fold increase in IC_{50} but had almost no effect on RBV sensitivity. The most informative finding from the transient replicon experiments was the combination of two mutations found most frequently in the SOF/RBV insensitive samples (A150V/K206E). Presence of each mutation individually had relatively minor effects on SOF sensitivity, causing a 7.75 and 8.12 -fold increase in IC_{50} respectively. When both mutations were engineered in the same replicon a more dramatic effect in drug sensitivity was observed, resulting in the highest fold shift in SOF IC_{50} than any of the other mutations. This increase in IC_{50} was not as marked as that seen in the replicon containing S282T but indicates a notable loss in sensitivity to both SOF and RBV. Similarly, the combination of these mutations caused the greatest loss in RBV sensitivity compared to their individual expression (Fig 5.6B, C).

5.5 Analysis of mutations in G3 Infectious clone

Use of subgenomic replicons, which contain only the HCV non-structural proteins allow studies of viral genome replication but no other part of the lifecycle can be studied. In this context, transient subgenomic replicon assays have demonstrated that possession of both NS5B mutations A150V and K206E impact the sensitivity of the polymerase to both SOF and RBV. We sought to confirm our findings in an infectious HCV model, which covers all stages of the viral lifecycle and is thus more representative of the situation *in vivo*. Most infectious HCV models are focused on the genotype 2a JFH-1 clone, which is a robust model of HCV infection [reviewed in (Catanese & Dorner, 2015; Ortega-Prieto & Dorner, 2016)]. The variability between HCV genotypes makes the study of genotype 3 specific NS5B mutations in a genotype 2a infectious unsuitable as there are significant differences between the genotypes. A

recent study by (Ramirez *et al.*, 2016) created a genotype 3a based infectious clone (designated DBN3a$_{cc}$) with 15 cell culture adapted mutations that could generate high titre viral stocks and infect naïve Huh7.5 cells. Here we used this infectious clone to test whether the loss of sensitivity to SOF observed in our subgenomic replicon experiments caused by A150V and K206E is also recapitulated in an infectious model of genotype 3 infections.

5.5.1 Creating genotype 3 HCVcc with the A150V and K206E mutations

A150V, K206E and the combination of both was introduced into the NS5B of the DBN3a construct by a one-step site-directed mutagenesis reaction using overlapping primers encoding the desired mutation. This approach was favoured over using PCR mutagenesis due to unfavourable restriction sites in the DBN plasmid as well as being a faster more efficient method of introducing the mutations.

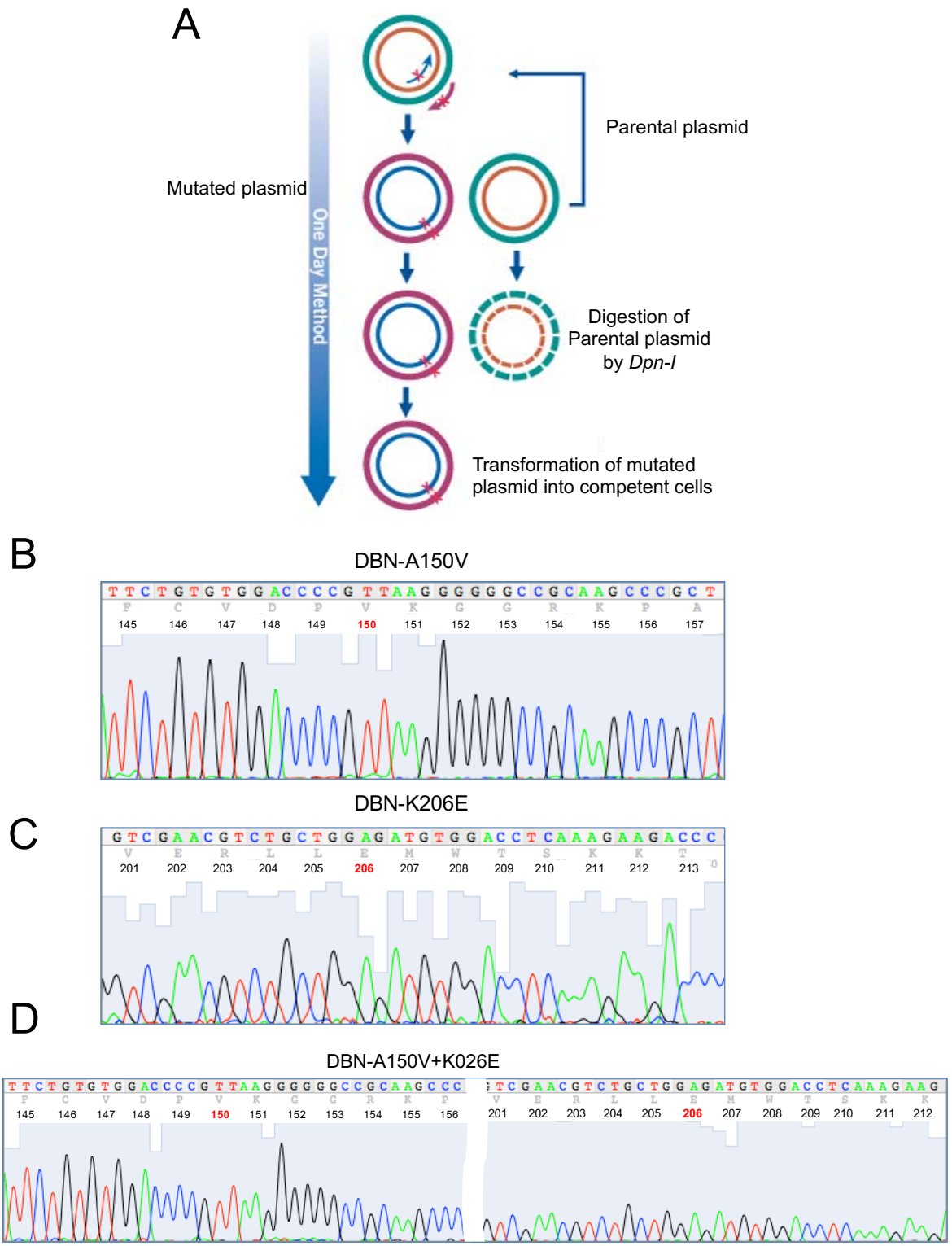

Fig 5.7 Site-directed mutagenesis of DBN3a$_{cc}$ Plasmid Construct
(A) Schematic representation of the site-directed mutagenesis reaction (Adapted from the QuickChange II lighting kit manual, Agilent). Each mutation was introduced into the plasmid construct using overlapping mutagenic primers that annealed to the template and are extended by a high-fidelity polymerase to create a new plasmid construct with the desired mutation. The parental DNA is then degraded by digestion with *Dpn-I,* a restriction enzyme specific for methylated DNA. (B-D) Sanger sequencing traces showing the presence of the A150V, K206E and combination of both mutations in

the DBN3a$_{cc}$ construct. Numbers depict amino acid positions from the start of NS5B, with mutated position highlighted in red.

Overlapping mutant oligonucleotides were designed to introduce the A150, K206E and their combination into the DBN3a$_{cc}$ construct. Site-directed-mutagenesis reactions were carried out for each mutation with the produce of the reaction transformed into competent cells to obtain bacterial colonies of the mutant constructs (Fig 5.7A). Colonies were screened for the presence of the mutation by Sanger sequencing with constructs harbouring the A150V, K206E and dual mutation obtained (Fig 5.7B-D).

Huh7.5-SEC14L2 cells were transfected with the unmodified Wt, A150V, K206E and A150V+K206E constructs to generate stocks of each virus. After 7 days, transfected cells were shown to be positive for HCV determined by indirect immunofluorescent staining of NS5A (Fig 5.8A). It was at this time point that virus-containing supernatants were harvested. The presence of A150V and K206E did not appear to affect the infectivity titre of the DBN virus as comparable infectivity titres were observed for the A150V, K206E and combination viruses to the un-modified DBN-Wt between days 7-20 post-transfection (Fig 5.8B).

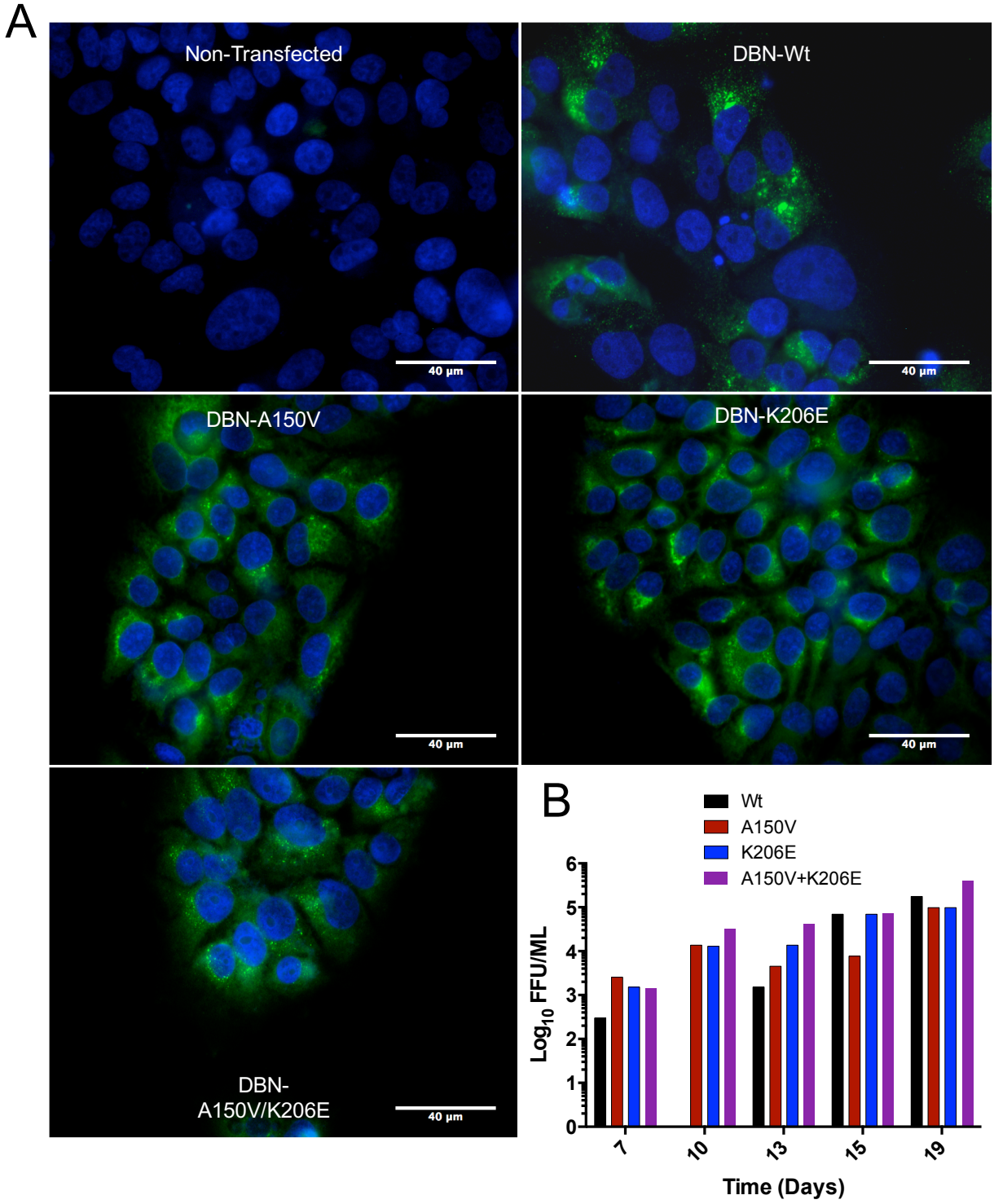

Fig 5.8 Validation of DBN virus stocks
(A) Huh7.5-SEC14L2 cells transfected with the DBN viral constructs were stained for NS5A by immunofluorescence 7 days post-transfection (B) Infectivity titre of DBN viruses was determined by focus forming assay and compared between virus stocks containing the A150V, K206E and dual mutation. Time in days refers to the number of days post-transfection the virus containing supernatants were harvested.

5.5.2 Effect of the A150V and K206E mutation on the viral growth curve

As the presence of the A150V and K206E mutations were within the active site of the polymerase protein we sought to assess whether these changes altered the propagation of virus in culture. To this end we infected naïve Huh7.5-SEC14L2 cells with a low MOI of Wt and mutant virus and monitored HCV RNA levels over a period of 6 days. After 2 days of infection RNA levels between the viruses were comparable, however between Days 2-3 RNA levels for the Wt DBN virus still increased by approximately 1-log whereas RNA levels for the mutated viruses begin to plateau (Fig 5.9). At day 6 RNA levels of the WT were significantly higher (p=<0.001) than levels observed for the mutated viruses. This indicates that the A150V and K206E mutations may confer a slight fitness cost to the DBN3a$_{cc}$ infectious clone. This cost may be due to a reduction in replication efficiency as viral levels were still observed to increase but not to such a high level as the Wt virus.

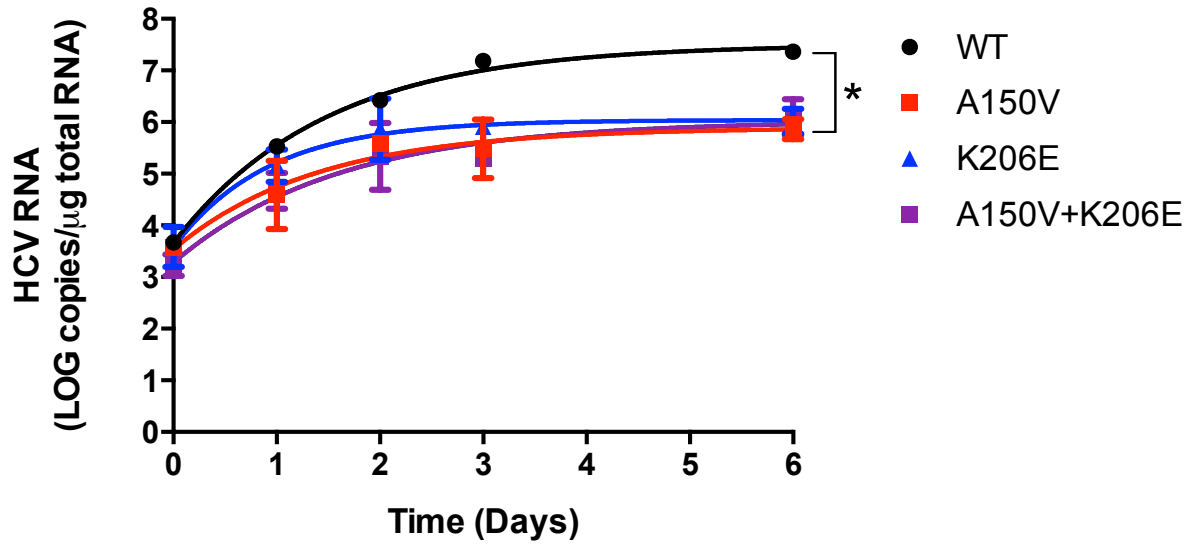

Fig 5.9: Effect of A150V and K206E on growth of the DBN3a$_{cc}$ virus
Naïve Huh7.5-SEC14L2 cells were infected with Wt and mutated DBN virus at an MOI of 0.05. Samples were taken at the indicated time points for quantification of HCV RNA by RT-qPCR. Data presented is representative of 2 independent experiments. Graph depicts mean ±SEM.

5.5.3 The effect of A150V and K206E on Antiviral sensitivity in an infectious system

The creation of viruses bearing A150V, K206E and the combination of both allowed us to assess whether the effect on SOF sensitivity seen in the G3 subgenomic replicon was maintained in an infectious system. The DBN viruses with the A150V and K206E substitutions were used to infect Huh7.5-SEC14L2 cells and their response to antiviral treatment assessed by RT-qPCR and focus forming assay (FFA). A recent genome wide association study identified a strong association between the A150V mutation and the human interferon lambda 4 gene indicating a possible interaction between this position and the host innate immune response (Ansari *et al.*, 2017) and we therefore tested the anti-viral effects of type I interferons on these viruses.

Using the un-modified DBN-Wt virus we performed initial experiments to establish the timing and dosage of antiviral treatment on infected Huh7.5-SEC14L2 cells. Cells were infected with DBN-Wt virus at a multiplicity of infection (MOI) of 0.5 for 24hrs before treatment with a range of SOF and IFN doses. Infected cells were kept under drug treatment for 48hrs and then harvested for HCV RNA quantification by qPCR. Analysis of HCV RNA levels revealed an acute sensitivity of the DBN-WT to both SOF and IFN. Treatment with the lowest doses of each drug caused a >60% decrease in HCV RNA, which continued until levels were virtually undetectable (Fig 5.10A, B). IC_{50} values calculated for SOF and IFN reflected the acute sensitivity of the DBN-WT virus yielding a value for SOF 100 times less than that observed for the G3 subgenomic replicon (see Fig 5.6). This experiment demonstrated that treatment of infected cells for 48hrs with either SOF or IFN was sufficient to see the antiviral effect of both drugs. Yet the

severe effect the lowest dose of both drugs had on HCV RNA levels indicated that the doses used were too high. It was therefore decided to expand the range of concentrations of both drugs so a more dynamic dose response curve could be attained.

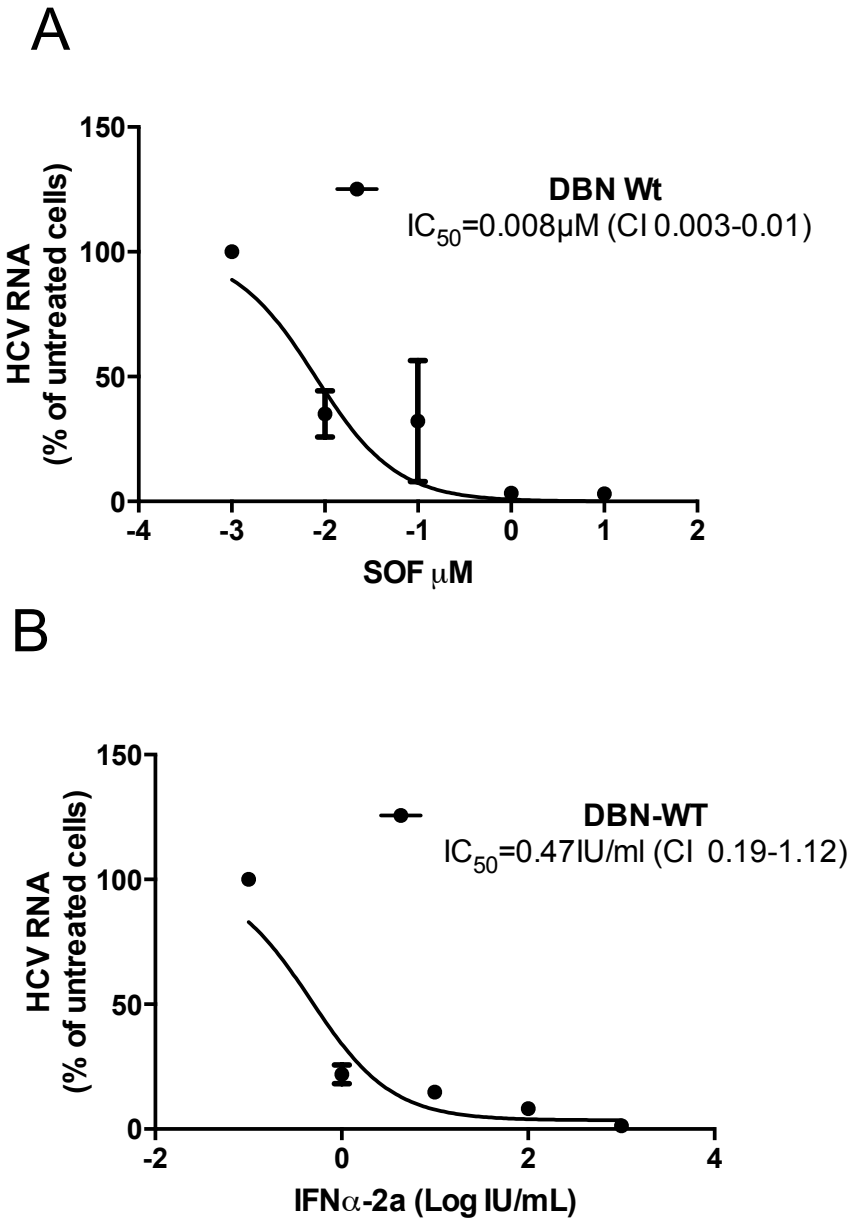

Fig 5.10 Establishing the SOF and IFN dose response with the DBN virus
Huh7.5-SEC14L2 cells were infected with DBN–WT at an MOI of 0.5. After 24hrs cells were treated with a range of SOF and IFN for a further 48hrs and then harvested in Trizol for HCV RNA quantification by RT-qPCR. IC_{50} values were calculated from % change in HCV RNA levels compared to the non-treated control. Values are shown with 95% confidence intervals. The above is representative of 2 independent experiments. Graphs depict data mean ±SEM.

The antiviral infection experiments were repeated with the A150V, K206E and

A150V+K206E viruses with an extended dose range for both SOF and IFN. The length of drug treatment and MOI were kept the same as the previous experiments. The presence of the A150V mutation had a minimal impact on SOF sensitivity (IC_{50} 0.033μM) but caused an approximate 100-fold increase in IFN IC_{50} (109.5IU/ML compared to 0.73IU/ml for WT virus) (Fig 5.11A, B). The presence of K206E conversely caused a more notable effect on SOF sensitivity, causing an approximate 5-fold increase in IC_{50} (0.10μM compared to 0.018μM for WT virus) but had only a minimal impact on IFN with an IC_{50} comparable to the WT virus (Fig 5.11A, B). Virus containing the combination of A150V+K206E was observed to decrease sensitivity to SOF and IFN in a similar manner to K206E and A150V in isolation. The SOF IC_{50} obtained for the combination virus was higher but comparable to the K206E virus, whereas the IC_{50} for IFN was found to be slightly higher (109.50IU/ml) than that observed for A150V alone (70.95IU/ml) (Fig 5.11E). The effect of these mutations on RBV sensitivity was also assessed. While the presence of A150V and K206E did reduce sensitivity to RBV the fold change observed with the infectious virus was not as marked (Fig 5.11C). Additionally, obtaining a dose response curve to RBV was achieved with some difficulty due to high concentrations used of the drug having a cytotoxic effect on the infected cells, which may explain the overlapping confidence intervals observed with the various viruses (Fig 5.11E). Viruses were also treated with a range of doses of the NS5A inhibitor DAC as a control to show that the A150V and K205E mutations had a specific effect to NS5B inhibitors. Treatment even with the lowest concentration of DAC resulted in a dramatic reduction in DBN RNA for all viruses indicating an acute sensitivity to DAC. IC_{50} values obtained were comparable even in the presence of A150V and K206E indicating that these mutations did not impact upon sensitivity to NS5A inhibitors.

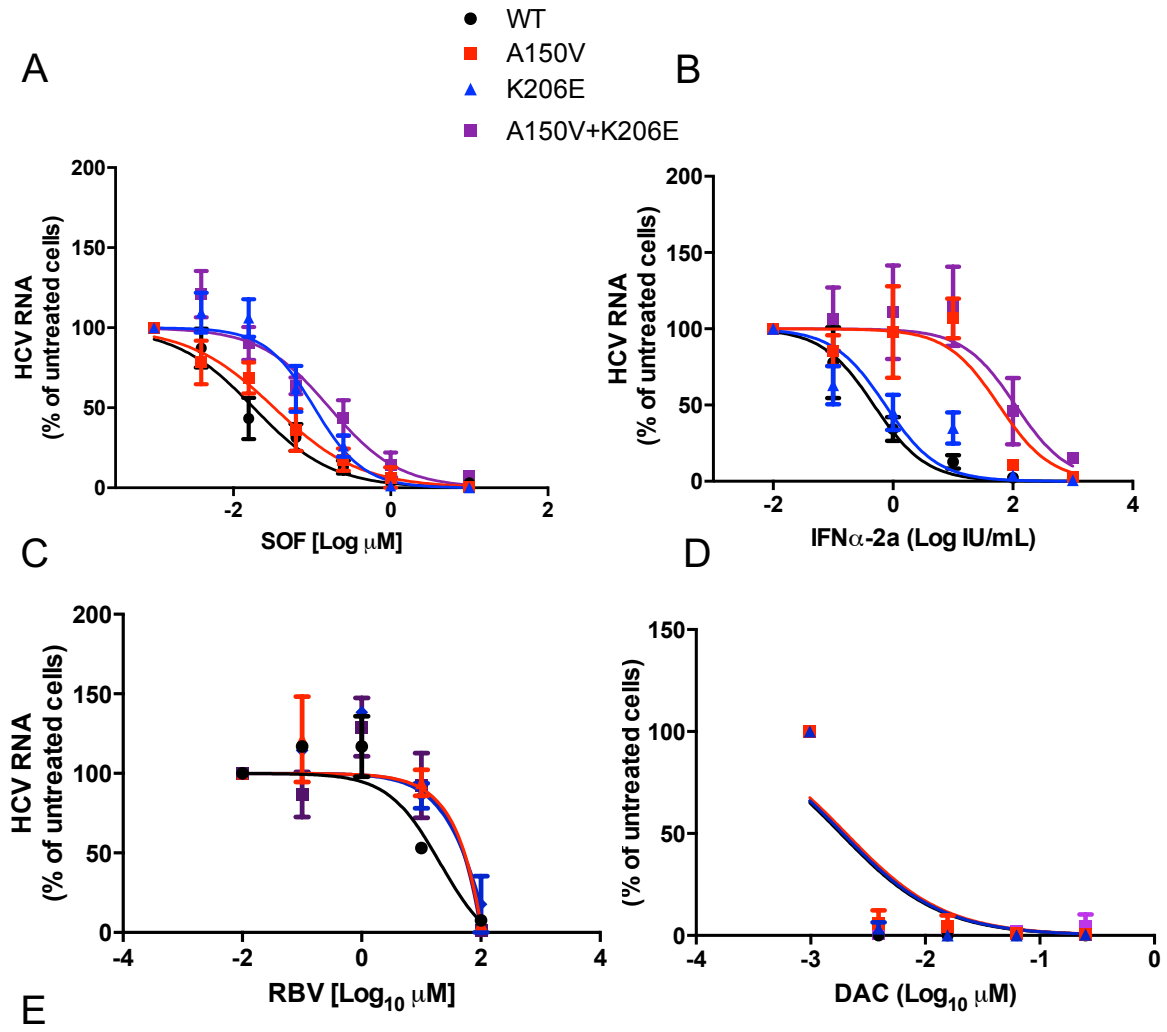

	Wt	A150V	K206E	A150V+ K206E
SOF IC_{50}, μM (CI_{low}-CI_{high})	0.018 (0.010-0.031)	0.033 (0.018-0.060)	0.10 (0.071-0.16)	0.17 (0.094 to 0.30)
Fold Change	**1**	**1.83**	**5.56**	**9.44**
IFN IC_{50}, IU/ml (CI_{low}-CI_{high})	0.7307 (0.3751 to 1.423)	70.42 (20.61 to 240.7)	0.95 (0.4647 to 1.951)	109.50 (21.65 to 453.50)
Fold Change	**1**	**96.46**	**1.30**	**149.31**
RBV IC_{50}, μM (CI_{low}-CI_{high})	14.89 (3.648 to 60.74)	31.53 (6.838 to 145.4)	36.63 (9.804 to 136.9)	28.68 (8.032 to 102.)
Fold Change	**1**	**2.12**	**2.46**	**2.02**
DAC IC_{50}, μM (CI_{low}-CI_{high})	0.0018 (0.00060 to 0.0055)	0.0020 (0.00075 to 0.0055)	0.0019 (0.00066 to 0.0055)	0.0019 (0.00064 to 0.0056)
Fold Change	**1**	**1.11**	**1.06**	**1.06**

Fig 5.11 Sensitivity of DBN viruses to SOF, IFN, RBV and DAC
Huh7.5-SEC14L2 cells were infected with an MOI of 0.5 for 24 hrs before treatment with a serial dilution series of SOF (A), IFN (B), RBV (C) or DAC (D). After 72hrs cells were harvested for quantification of HCV RNA by RT-qPCR. IC_{50} values for SOF, IFN, RBV and DAC were calculated from % change in HCV RNA levels compared to the no drug control (E). Values are presented with 95% confidence intervals. Fold change in IC_{50} was calculated by comparison of IC_{50} values obtained from the mutant

viruses to that of the Wt. The above is representative of at least 3 independent experiments. Graphs depict is mean ±SEM.

In addition to drug sensitivity experiments performed with qPCR we also used a modified focus-forming assay to confirm the impact of these mutations on SOF and IFNα sensitivity. Using the percentage of cells positive for HCV antigen was the technique that Ramirez and colleagues used in antiviral sensitivity assays with the DBN clone. We sought to replicate that technique with regard to our mutated A150V and K206E containing viruses to confirm our findings on the effect these mutations have on SOF and IFNα treatment. Cells were infected as before and drug treatment duration was the same as for qPCR assays. Percentage of cells positive for HCV antigen was determined by NS5A staining and quantified using an INCELL automated microscope. Fold change in SOF IC_{50} using this method showed a comparable shift with the A150V, K206E and combination viruses (1.08, 6.44 and 10.38 respectively) as determined by qPCR. Correspondingly, viruses containing the A150V mutation caused the largest change in IFN IC_{50} >70-fold in this assay, which again was similar to that shown by qPCR. SOF and IFN IC_{50} confidence intervals were noted to be wider in this assay than shown by qPCR. Though despite this effect of A150V and K206E on drug sensitive assay corroborated data obtained by qPCR.

A

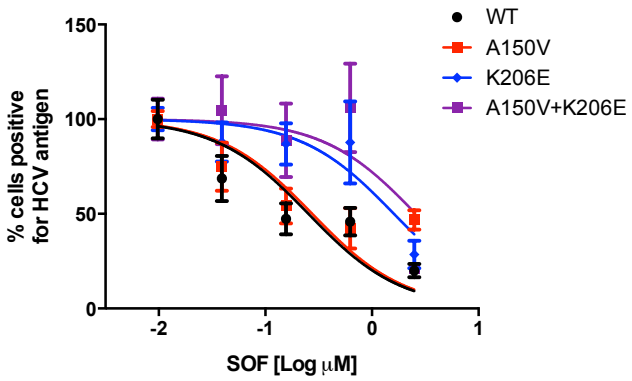

B

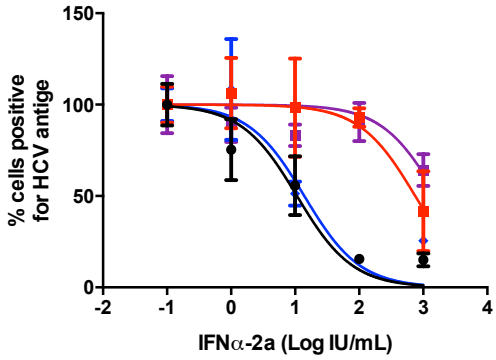

C

	Wt	A150V	K206E	A150V+ K206E
SOF IC_{50}, μM (CI_{low}-CI_{high})	0.25 (0.15-0.44)	0.27 (0.15-0.52)	1.61 (0.64-4.06)	2.58 (0.55-12.18)
Fold Change	**1**	**1.08**	**6.44**	**10.32**
IFN IC_{50}, IU/ml (CI_{low}-CI_{high})	10.48 (3.33 to 34.21)	750.40 (242.40-2323.00)	13.91 (2.81-68.90)	1662.00 (423.70-6560)
Fold Change	**1**	**71.60**	**1.34**	**159.81**

Fig 5.12 Sensitivity of DBN viruses to SOF and RBV using a FFU based assay
Huh7.5-SEC14L2 cells were infected with DBN virus at the same MOI and timing as for previous drug sensitivity experiments. Infected cells were seeded on a 96 well plate and treated with SOF (A) and IFNα (B) for 72hrs after which cells were fixed and stained for NS5A. Number of cells per well positive for NS5A was quantified using an INCELL 2200 automated microscope (GE). Dose response curve were calculated by comparison of NS5A levels between the un-treated control and wells that were treated with a serial dilution of each drug. (C) Fold change in IC_{50} was calculated by comparison of IC_{50} values obtained from the mutant virtues to that of the Wt. The above is representative of at least 3 independent experiments. Graphs depict is mean ±SEM.

These data confirm the contribution of the A150V and K206E on drug sensitivity. While A150V has little effect on SOF in isolation it has a major effect on sensitivity to IFN. Conversely K206E has almost no effect on IFN but a greater effect on SOF. The combination of these mutations in the same virus (most commonly found in drug insensitive patients) causes the greatest effect on sensitivity to SOF and IFN.

5.5.4 Reduced potency of SOF in cells lacking an IFN response

Data obtained thus far from the infectious clone indicates that in isolation A150V has a negligible effect on SOF sensitivity but a greater effect on IFN. K206E however has a much greater effect on SOF but almost no effect on IFN in isolation. When these two mutations are combined the greatest reduction in both SOF and IFN is observed. This led us to hypothesise that to achieve maximum potency SOF may require an intact type I IFN response to effectively clear a virally infected cell.

To test this hypothesis we used a Huh7.5-SEC14L2 cell line expressing the V protein from the parainfluenza virus 5 (PIV5-V), which degrades STAT-1 causing this cell line to be unable to mount an IFN response (kind gift from Professor Mark Harris). Huh7.5-SEC14L2 cells expressing PIV5-V (Huh7.5-VSEC) were infected as before with the DBN Wt and mutant viruses and their sensitivity to SOF compared to assays performed with Huh7.5-SEC cells. A dose response to SOF was still obtained in these cells indicating that the loss of the IFN response did not totally blunt the effectiveness of SOF (Fig 5.13A). Yet, IC_{50} values calculated from treatment of Huh7.5-VSEC cells infected with Wt and mutant virus with SOF were found to be on average 10-fold higher than values calculated from infection of Huh7.5-SEC cells. Additionally infection of the Huh7.5-VSEC cells with viruses containing the A150V mutations had no effect on SOF sensitivity resulting in a comparable SOF IC_{50} to Wt virus (Fig 5.13B). However, response to SOF with the K206E and the combination virus did cause a small fold change in SOF IC_{50} albeit to a much lesser degree than seen from infection with Huh7.5-SEC cells. Data from these experiments indicate that in IFN-unresponsive cells the antiviral effect of SOF is less effective but not completely diminished. This

indicates, that to achieve maximum antiviral potency SOF requires cells to have an intact STAT-1 mediated IFN response.

A

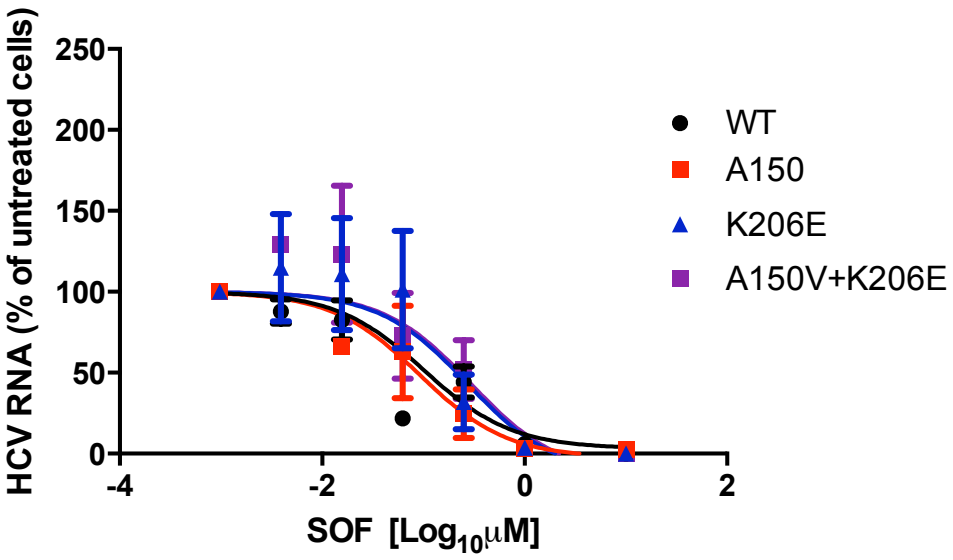

B

		Wt	A150V	K206E	A150V+K206E
SEC	SOF IC_{50}, μM (CI_{low}-CI_{high})	0.018 (0.010-0.031)	0.033 (0.018-0.060)	0.10 (0.071-0.16)	0.17 (0.094 to 0.30)
	Fold Change	**1**	**1.83**	**5.56**	**9.44**
VSEC	SOF IC_{50}, μM (CI_{low}-CI_{high})	0.10 (0.042-0.25)	0.091 (0.035-0.24)	0.27 (0.061-1.21)	0.29 (0.056-1.53)
	Fold Change	**1**	**0.91**	**2.7**	**2.9**

Fig 5.13 Sensitivity of DBN viruses to SOF in an IFN unresponsive cell line
(A) Huh7.5-VSEC cells were infected with DBN-WT, A150V, K206E and A150V+K206E for 24hrs before treatment with SOF serial dilutions of SOF. After 72hrs cells were harvested and HCV RNA levels were quantified by RT-qPCR. (B) IC_{50} values obtained for these cells were compared to those obtained from assays performed with Huh7.5-SEC cells. Data is representative of 3 independent experiments. Graph indicates mean ±SEM.

5.6 Summary

Together data presented in this chapter indicate that the NS5B mutation K206E has an impact on sensitivity to SOF in isolation and in combination with A150V. While in isolation A150V has a minimal effect on SOF sensitivity and it appears to slightly

enhance the anti-SOF effect of K206E when present in combination in the NS5B. These findings were consistent in both a transient subgenomic replicon assay and in the context of a fully infectious G3 virus. In addition although a stable replicon cell line could only be established for the K206E mutation alone, this also showed a reduction in SOF and RBV sensitivity. Differences in the relative fold shift in SOF and RBV IC_{50} were found between assays performed with the subgenomic replicon assay and the DBN infectious clone. While both assays indicate that the combination of A150V and K206E cause the largest reduction in sensitivity to SOF, the subgenomic replicon indicates this change is a 35-fold increase in SOF IC_{50} compared to the wild type, whereas the infectious virus indicates this causes only a 10-fold change in SOF IC_{50}. The fold changes in SOF sensitivity for the DBN virus were confirmed both by qPCR and viral antigen expression level, which are both direct measures of viral replication. The luciferase measurement of the activity of the subgenomic replicon while representative of the relative replication of the construct may not be as accurate a measure as qPCR for example. Furthermore the virus allows consideration of the impact of these mutations on the entire viral life cycle whereas only viral replication can be considered with the subgenomic replicon, making the DBN virus more a representative model of HCV infection *in vivo*.

The cause for this difference may be due to both systems having different baseline sensitivities to SOF implied by the IC_{50} for the WT DBN-virus being approximately 10-fold lower than the Wt S52 subgenomic replicon. Both systems are derived

A surprising finding was the significant impact of A150V upon sensitivity to IFN. Presence of this mutation in isolation or in combination with K206E substantially

reduced sensitivity of the DBN virus to IFNα. Furthermore it was shown that in cells unresponsive to IFN through a lack of STAT-1 the antiviral effects of SOF on DBN infection were less potent. Together this suggests while K206E has the greatest effect of SOF sensitivity in isolation, the anti-IFN effects of A150V, reduce the potency of the drug when this mutation is present in combination, therefore reducing the sensitivity to SOF even further. Possible mechanisms as to how A150V causes such a dramatic reduction in IFN sensitivity are considered in the subsequent chapter.

6 RESULTS: Analysis of the effect of the A150V polymerase polymorphism on Interferon Signalling

We investigated the mechanism behind the loss of responsiveness to IFNα of DBN viruses bearing the A150V mutation in the NS5B protein. We hypothesised that the A150V mutation either disrupted the cellular response to IFNα through the signal transduction pathway or allowed the virus to evade the IFN antiviral state. To this end we designed experiments to investigate if infection of Huh7.5-SEC14L2 cells with DBN-A150V virus impaired the ability of the cell to respond to IFNα through interferon-stimulated-gene (ISG) production. We also overexpressed the NS5B with the A150V mutation in Huh7 cells to assess whether exogenous expression of the protein without the rest of the non-structural proteins could affect IFN signalling.

6.1 MxA induction in cells infected with DBN-A150V

We set out to determine whether infection with DBN-A150V impaired induction of crucial antiviral ISGs such as MxA when cells were treated with IFNα. Huh7.5-SEC14L2 were infected with DBN-Wt, A150V and K206E viruses and allowed to propagate for 3 days to allow the virus to establish infection. Cells were then challenged with 10 and 100IU/ml of IFNα-2A with samples taken 24hrs post IFN treatment to quantify MxA and HCV levels by RT-qPCR. Comparable levels of MxA induction were observed at 100IU/ml of IFNα between uninfected cells and infected cells, though a high degree of variation was observed between each virus infection. A slight but not significant (p>0.05) reduction in MxA was observed at 100 IU/ml IFN with the A150V+K206E virus (Fig 6.1B). MxA fold induction with 10IU/ml of IFNα was comparable between un-infected cells and cells infected with the DBN Wt and DBN-

K206E virus (Fig 6.1B). These levels however did drop in cells infected with the DBN-A150V virus and the dual mutant though neither approached significance (p>0.05). Viral levels for the DBN-Wt and K206E decreased in a dose dependent manner with IFNα treatment (Fig 6.1C). While levels did drop with the DBN-A150V and DBN-A150V+K206E virus, the reduction was not as marked as observed with the Wt or K206E virus.

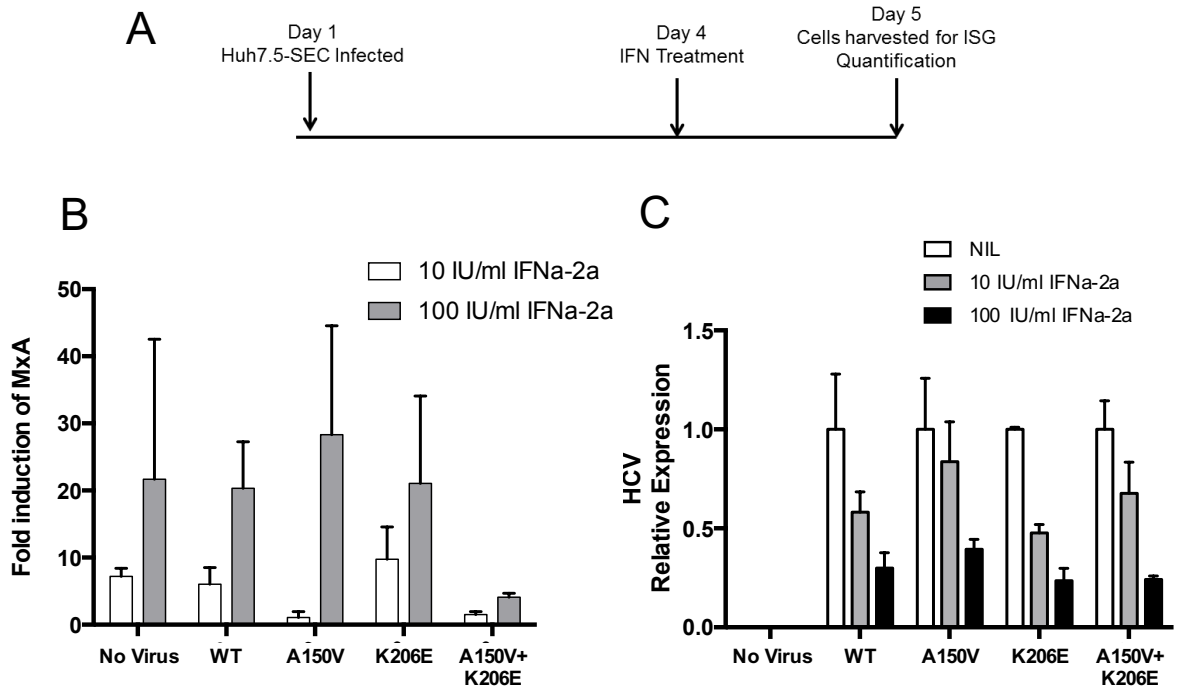

Fig 6.1 MxA expression in Infected Huh7.5-SEC14L2 cells
(A) Schematic of the timings of the experiment. Huh7.5-SEC14L2 cells were infected with an MOI of 0.5 with the infection allowed to propagate for 3 days. Cells were then treated with 10 and 100IU/ml for 24hrs before harvesting in Trizol. Relative expression of MxA (B) and HCV (C) was quantified by RT-qPCR using the pflaffl method to normalise gene expression to the 5S housekeeping gene. Data is representative of 2 independent experiments. Graphs depict mean ±SEM.

6.1.1 Effect of the DBN-A150V virus on the Interferon Stimulated Response Element

To assess whether the slight reduction in MxA levels observed in the previous experiments reflected a reduced activation of MxA transcription by factors that drive gene expression we examined ISG promoter activity in cells containing HCV. Control

of ISG expression, including MxA, is directed by the IFN-Stimulated-Response-Elements (ISRE), which are activated when bound by IFN-stimulated gene factor 3 (ISGF-3), formed as a result of the JAK-STAT signalling pathway in response to IFN (Kanazawa *et al.*, 2004). Using a reporter plasmid containing firefly luciferase under the control of the 6-16 canonical ISRE sequence the relative activity of the ISRE within a cell can be evaluated. Huh7.5-SEC14L2 cells infected with the DBN viruses for 72hrs were transfected with the luciferase reporter plasmid prior to treatment with a range of IFNα doses with Luciferase levels quantified 24hrs after IFNα treatment. ISRE activity was comparable between infected and un-infected cells increasing in a dose dependent manner with IFNα treatment. Infection of cells with the DBN-A150V or the DBN-A150V+K206E virus did not have an observable impact on ISRE activity in comparison to the DBN-WT (Fig 6.2A). Infection of cells was confirmed by quantification of HCV RNA levels by RT-qPCR (Fig 6.2B). These data indicate that the effect of A150V on the cellular response to interferon may not be mediated via the classical Stark-Kerr-Darnell ISGF3 signal transduction pathway. However, recent work (Sung *et al.*, 2015) has indicated that alternative signalling pathways do exist and it is possible that A150V interacts with one of the alternative pathways.

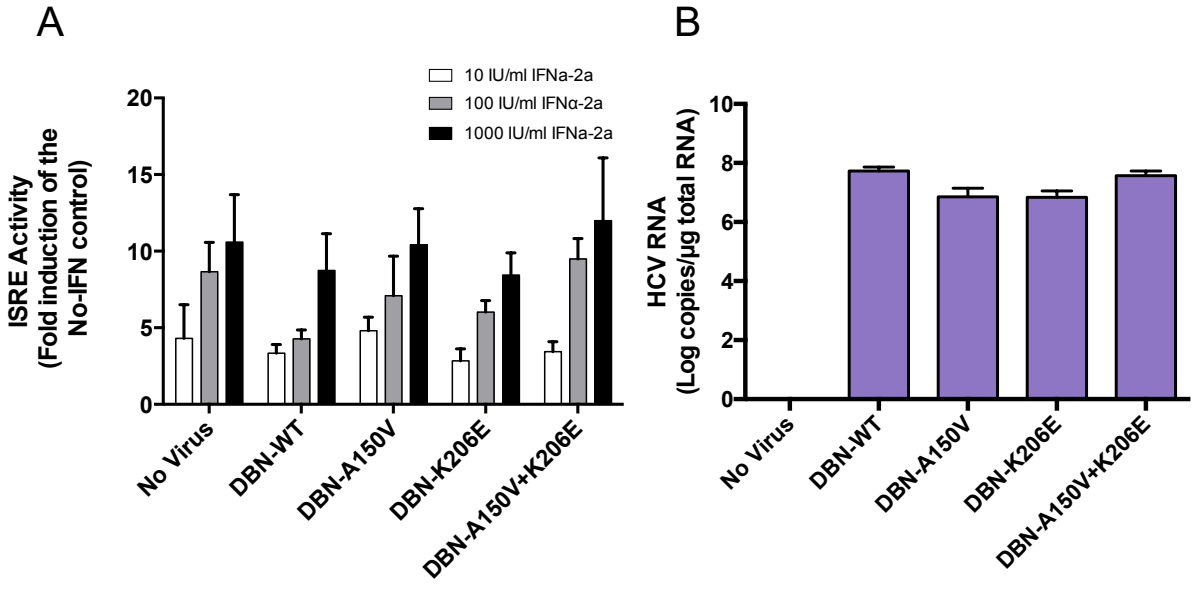

Fig 6.2 ISRE activity in DBN infected cells
(A) Huh7.5-SEC14L2 cells were infected with virus 3 days prior to transfection with the pGL4.45 ISRE-Firefly reporter plasmid along with the pNL1.1 Nanoluc reporter plasmid to account for transfection efficiency. After transfection cells were treated with indicated doses of IFNα-2A for 24hrs then harvested to quantify luciferase activity. Firefly luciferase levels were normalised to Nanoluc luciferase to account for transfection efficiency. Fold induction of ISRE activity was calculated from the no-IFN control. (B) To confirm cells were infected HCV RNA levels were quantified from the non-treated control by RT-qPCR. Data presented is representative of 3 independent experiments. Graphs depict mean ±SEM.

6.1.2 Virus with A150V can overcome the Type I IFN mediated antiviral state

Data thus far indicates that cells infected with DBN-A150V can result in a slight suppression of MxA induction when treated with a low dose of IFNα yet has no effect on the classical interferon signalling pathway. We speculated that A150V might enable the virus to resist the cellular antiviral state that occurs by the activation of the type I IFN response or interact with the recently described 'late' U-ISGF3 signal transduction pathway. To examine this we pre-treated Huh7.5-SEC14L2 cells with IFNα for 24hrs to activate the classical signal transduction pathway and induce ISGs. Cells were then infected with DBN-WT, A150V, K206E and A150V+K206E viruses and allowed to propagate for 3 days after which viral levels were quantified.

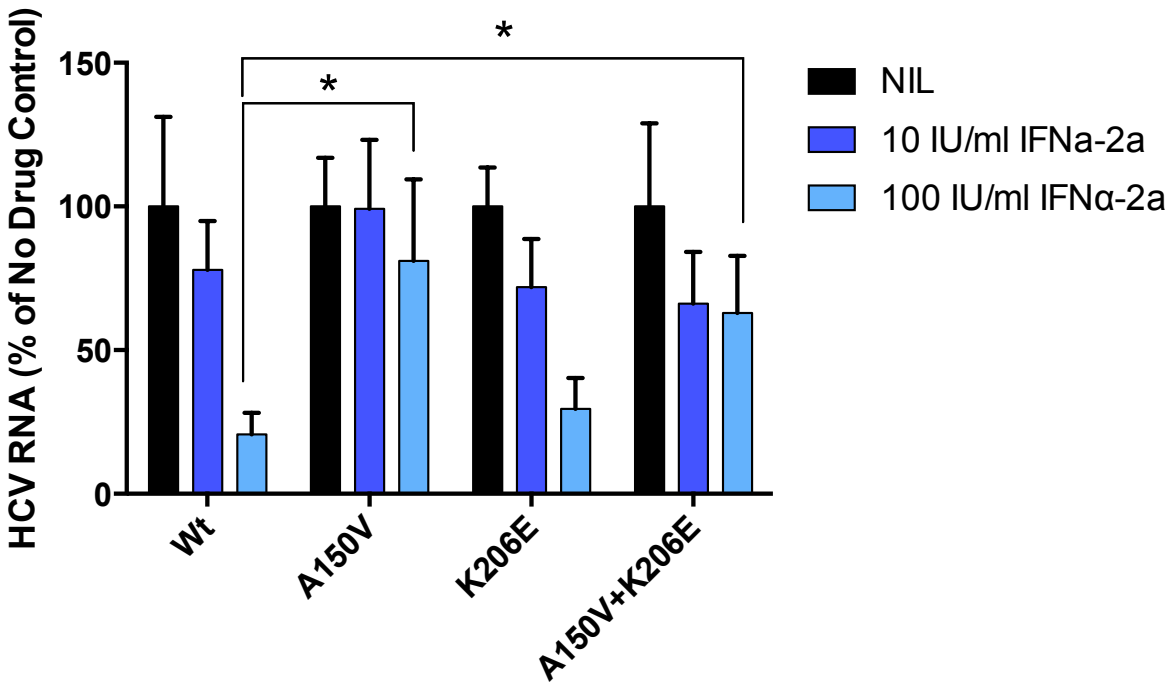

Fig 6.3 Infection of cells pre-treated with IFNα
Huh7.5-SECL14L2 cells were pre-treated with 10 and 100 IU/ml of IFNα-2A for 24hrs before infection with the DBN viruses at an MOI of 0.5. Infected cells were incubated for a further 3 days before harvesting and quantification of HCV RNA levels by RT-qPCR. Data is representative of 3 independent experiments. Statistical analysis was performed using Graphpad Prism 7, $p<0.05$ = ∗. Graphs depict mean ±SEM.

A marked decrease in HCV RNA was observed in cells pre-treated with 10 and 100 IU/ml of IFNα when infected with the DBN-Wt and K206E viruses compared to the non-treated control (Fig 6.3). In contrast, comparable levels of virus were obtained with infection of the pre-treated cells to the non-treated control with the DBN-A150V virus. A slight decrease was observed with infection of cells pre-treated with 100 IU/ml IFNα however this was not as striking as that observed with the Wt or K206E virus. The impact of IFN pre-treatment was also reduced with the DBN-A150V+K206E virus with higher viral levels observed compared to the DBN-Wt. Though not as distinct as observed for the DBN-A150V virus, statistical analysis of viral levels obtained from

cells pre-treated with 100 IU/ml IFNα revealed significantly higher levels of HCV RNA with the DBN-A150V and DBN-A150V+K206E viruses (p=0.015 and 0.029 respectively). These experiments suggest that the A150V mutation interferes with the cellular response to IFN downstream of the classical signal transduction pathway.

6.1.3 Generation of a cell line overexpressing NS5B-A150V

We next sought to develop a stable platform to conduct experiments to dissect any potential interference of the NS5B-A150V mutation on IFN signalling. As we were unable to generate a stable G3 replicon cell line harbouring the A150V mutation we decided to clone the DBN-NS5B with A150V, K206E and A150V+K206E into the pRetroX expression vector to generate stable cell lines expressing the mutated NS5B protein. This system would be complementary to our infectious model, but have the advantage of constitutively expressing the NS5B-A150V mutation minimising variable rates of infection between the different viruses.

The 1.7Kb NS5B gene was amplified from the original DBN plasmids used to generate the infectious virus. NS5B amplicons were obtained from the WT, A150V, K206E and A150V+K206E DBN constructs (Fig 6.4A). Each amplicon was engineered to contain a *BamHI* and *EcoRI* restriction sites at the respective 5' and 3' ends to allow directional cloning into complementary sites within the pRetroX vector as well as a start and stop codon.

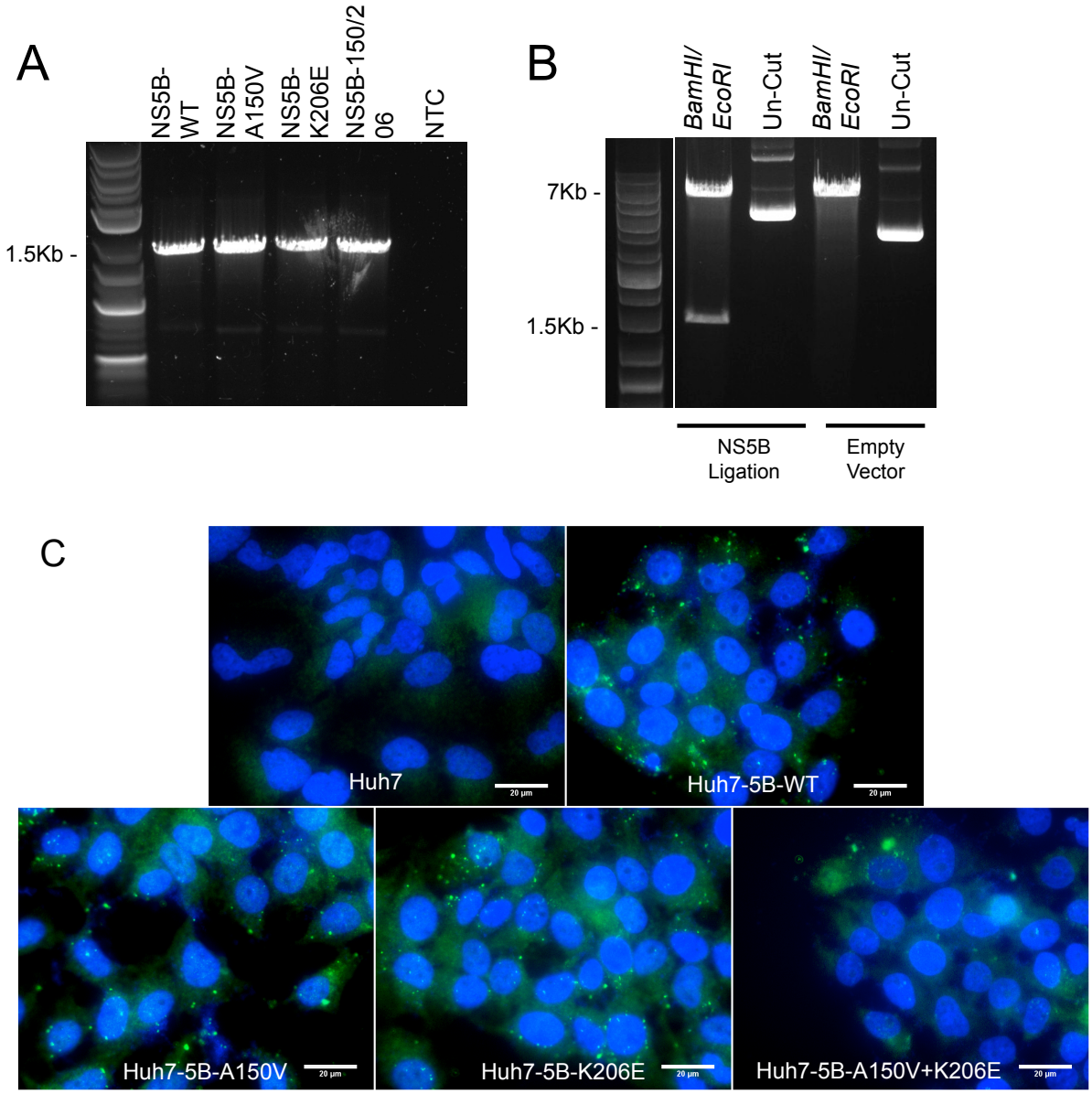

Fig 6.4 Cloning of NS5B into pRetroX
(A) NS5B was amplified from the DBN plasmids with the indicated mutations. Each amplicon was engineered to contain a Kozak sequence, start and stop codon as well as *BamHI* and *EcoRI* restriction sites at either end of the amplicon. (B) Bacterial colonies obtained from the ligation of NS5B into pRetroX were digested with *BamHI* and *EcoRI* to screen for the presence of the 1.7Kb NS5B gene. Vectors found to contain the correct size product were sent for sanger sequencing for confirmation. Representative images of each step are shown. (C) Plasmid constructs were transfected into Huh7 cells with stable colonies selected for by puromycin. NS5B expression was confirmed by immunofluorescence.

Presence of NS5B in the vector was confirmed by detection of a 1.7Kb band when digested with *BamHI* and *EcoRI* (Fig 6.4B). All vectors were subsequently sequenced by a commercial group, (Sanger sequencing, Bioscience), which confirmed the

presence of the A150V and K206E mutations in the respective vectors. Constructs were transfected into Huh7 cells with stable colonies obtained after 2 weeks of puromycin selection. Expression of NS5B was confirmed in these cells by fluorescence microscopy with NS5B found to localise mainly to the cytoplasm. Staining was observed to be less prominent in the Huh7-5B-A150V+K206E cells, possibly reflecting an impact of these mutations upon NS5B expression.

With NS5B expression confirmed in these cells we looked at the affect this had on response of these cells to IFNα. We first assessed the activity of the ISRE by transfecting the cells with the ISRE reporter plasmid as before and challenging them with a range of IFN doses for 24hrs. ISRE activity was observed to be greater in un-transfected Huh7 cells with 1000 IU/ml compared to those expressing NS5B (Fig 6.5). No substantial difference in ISRE activity was observed between the Huh7-5B-Wt cells and those expressing A150V, K206E or A150V+K206E when treated with 10, 100 and 1000 IU/ml of IFNα. Despite a slight reduction in ISRE activity when cells expressing NS5B with the K206E and double mutation where treated with 100 and 1000 IU/ml IFNα, this was not significant at either concentration when compared the Huh7-5B-Wt cells (p=0.32 and p=0.13 for 100 IU/ml and p=0.33 and 0.22 for 1000 IU/ml respectively). These data confirm the data in virally infected cells showing that the classical ISRE promoter is not inhibited by the A150V mutated HCV G3 polymerase.

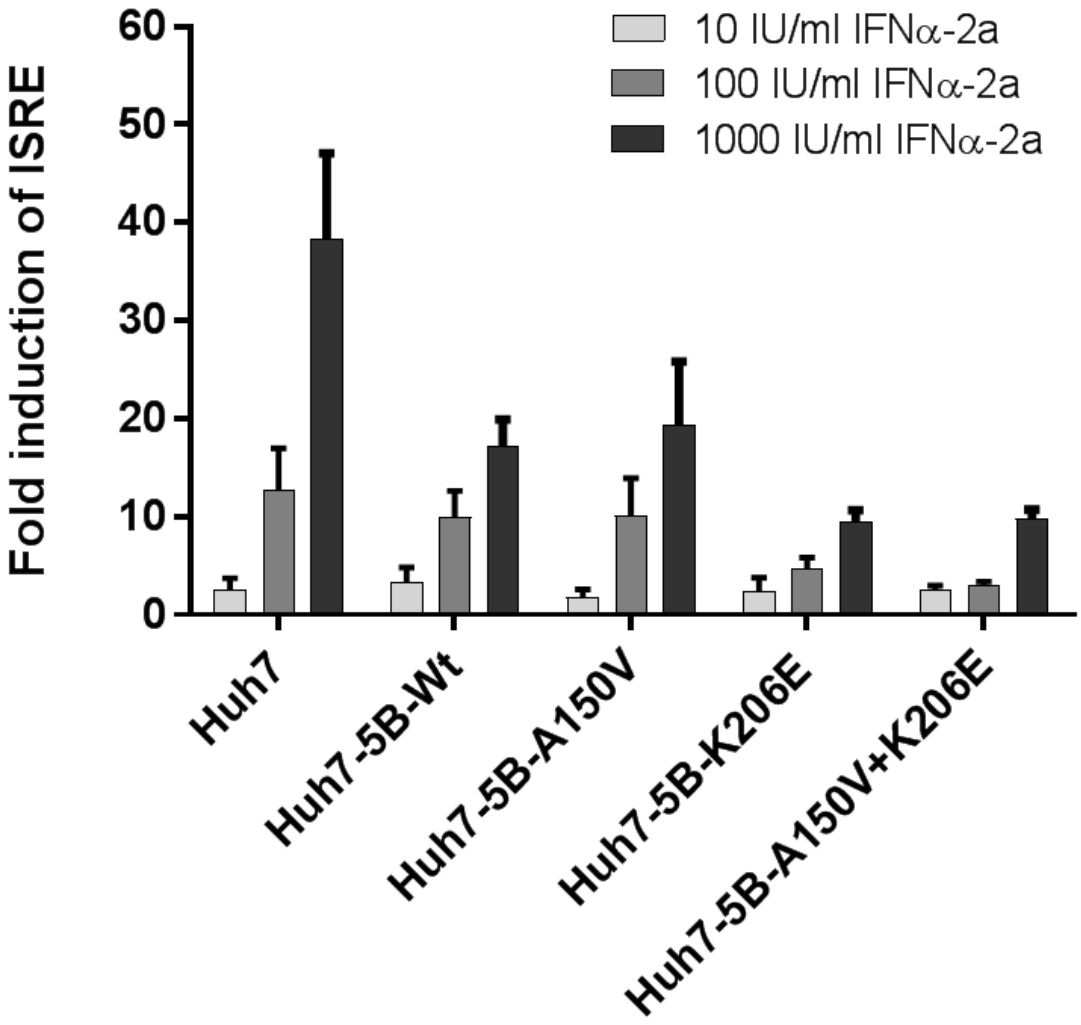

Fig 6.5 ISRE activity in NS5B Huh7 Cells
Huh-NS5B cells were transfected with the ISRE reporter plasmid and treated with a range of doses of IFNα-2A for 24hrs after which cells were lysed and luciferase activity quantified. Cells were co-transfected with a Nanoluc expression vector to account or transfection efficiency. Fold induction of ISRE was calculated from the no-IFN treated control. Data presented is form 2 independent experiments; graphs depict mean ±SEM. Statistical analysis was performed using GraphPad Prism 7.

We next assessed whether over-expression of Wt or NS5B bearing our mutations of interest had any impact on MxA induction in response to IFNα. We treated cells with 10 and 100 IU/ml of IFNα sampling MxA levels at 6 and 24 hrs post treatment. Comparable levels of MxA were detected in all cell lines after 6hrs and in the Huh7 and Huh7-5B-Wt cells after 24 hrs of IFN treatment (Fig 6.6A, B). However, MxA induction with 100 IU/ml of IFNα in cells expressing NS5B with A150V, K206E and

A150V+K206E mutations was found to be significantly reduced (p= 0.0083, 0.039 and 0.011 respectively), in cells treated for 24 hours, with the greatest reduction observed in the cells expressing the NS5B A150V mutation.

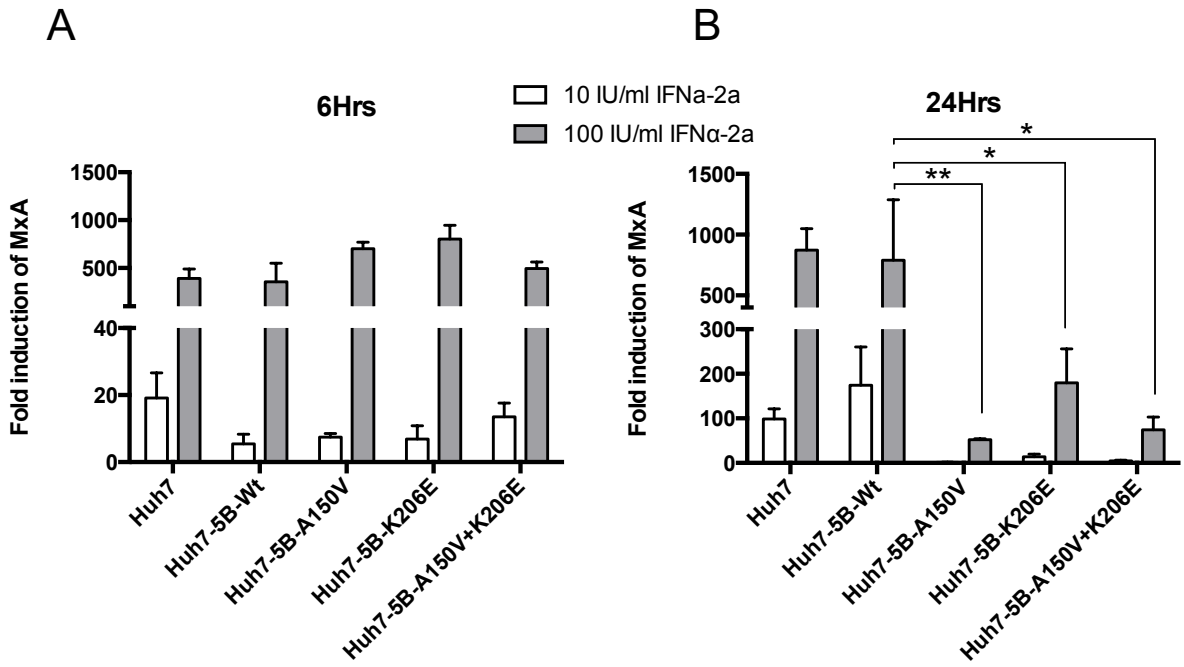

Fig 6.6 MxA mRNA levels in Huh7-NS5B cells
MxA mRNA expression was measured in Huh7 and Huh7-NS5B cells bearing indicated mutations in NS5B. Cells were treated with 10 and 100 IU/ml of IFNα-2A and MxA levels quantified at 6 (A) and 24 hrs (B) post-treatment by qPCR. Fold induction of MxA was calculated by comparison of treated values to that of the no-IFN control. Data is representative of 2 independent experiments. p<0.001 = ** p<0.05 = *. Statistical analysis was performed using Graphs depict mean ±SEM.

Taken together, these results indicate that the 'late response' to interferon is reduced in cells expressing the A150V variant NS5B protein and confirm data from cells expressing intact virus. NS5B expressing cells provide a more stable platform for dissecting the effect of the A150V mutation on the type I IFN pathway and will allow the site of interaction with the interferon-signalling pathway to be identified.

6.2 Huh7-NS5B cells with the A150V mutation have reduced basal levels of STAT-1 and STAT-2

Recent work has shown that prolonged infection of hepatocytes and Huh7.5 cell lines result in a considerable production of IFN-λs and IFN-ß, which continually stimulate hepatocyte cells to produce IRF9, STAT-1 and STAT-2 without tyrosine phosphorylation) (Sung *et al.*, 2015). We hypothesised that the impairment of MxA production in the Huh7-5B-A150V cells may be due to a dysregulation or reduction in basal levels of key signalling molecules such as STAT-1 or STAT-2.

To this end, expression levels of STAT-1 and STAT-2 were examined in both infected cells and cells expressing Wt and mutated versions of NS5B. Infected cells showed comparable expression levels of STAT-1 and STAT-2. Though a very slight reduction was observed in STAT-2 in cells infected with the DBN-A150V virus. A more noticeable reduction in total STAT-1 and STAT-2 levels were found in cells expressing the NS5B-A150V mutation compared to un-transfected Huh7 cells and cells expressing Wt NS5B(Fig 6.7). As an additional control for potential proteasomal degradation, cells were treated with a proteasome inhibitor to see if any reduction in STAT-1 or 2 could be rescued. A slight increase in STAT-1 and STAT-2 with the A150V can be seen with this treatment, however it does not appear to restore comparable expression levels to the Huh7 to Wt-NS5B control.

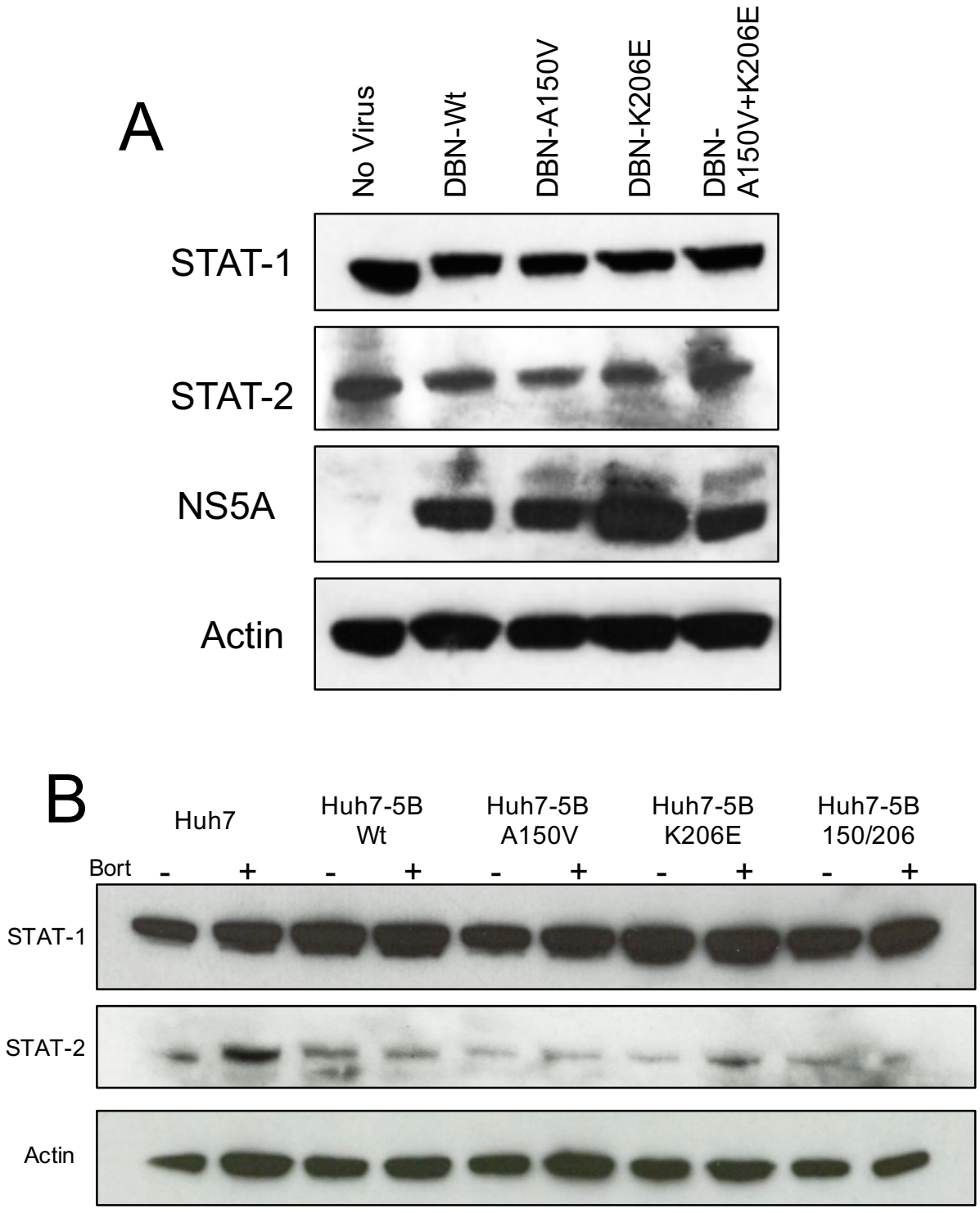

Fig 6.7 STAT-1 and STAT-2 Expression in DBN infection and Huh7-NS5B cells
(A) Huh7.5-SEC cells were infected with the DBN WT and mutated viruses at an MOI of 1 for 3 days after which cells were lysed for protein extracts. Expression of STAT-1, STAT-2 and NS5A were assessed by immunoblot. Actin was used as a loading control. (B) Expression of STAT-1 and STAT-2 in Huh7-NS5B cells. Cells were treated with the 10nM of the proteasomal inhibitor bortezamib for 16 hrs before immunoblotting of STAT1 and STAT2 was performed. Expression levels were compared to un-transfected Huh7 cells. The above blot is representative of 2 independent experiments.

6.3 Summary

Together, the data presented here implies that the A150V polymorphism in Genotype 3 HCV impairs interferon signal transduction. Viruses bearing the A150V mutation are able to more readily infect and propagate in cells pre-treated with IFN indicating that these viruses interfere with the action of ISGs downstream of classical signal transduction. The development of the NS5B expressing Huh7 cells provided a more stable platform to dissect the contribution of this mutation to MxA induction without the inherent variability of viral infection. Stimulation of these cells with IFN revealed that while MxA levels could be induced 6 hrs post treatment, presence of NS5B with A150V caused these levels to drop after 24hrs. Basal levels of STAT-1 and 2 were slightly reduced in NS5B-A150V expressing cells, which may contribute towards a reduced activation of U-ISGF3 ISGs as part of the 'late' IFN response. An exact mechanism as to how A150V can overcome the IFN response has not yet been defined and further work is underway to identify the site of action of the variant A150V containing polymerase

7 Discussion

The remarkable change in the treatment landscape for HCV brought about by the replacement of pegIFN/RBV with a regimen of highly effective antiviral drugs has resulted in the WHO declaring a target of HCV elimination by 2030. Yet to eradicate this virus potent antiviral therapy may not be sufficient. The biology of HCV, with its high mutation rate, gives the virus the ability to develop mutations to overcome antiviral drug treatment. While modern DAA therapy achieves high SVR rates, approaching 100% in some clinical trials, the genotype being treated remains one of the largest factors in determining optimal response to treatment as well as previous treatment with IFN therapy and stage of liver disease (EASL, 2017). In particular response rates to G3 HCV from patients with advanced liver disease are reduced in comparison to treatment of G1 or G2, in both clinical trial and real world setting (Cheung *et al.*, 2016; Foster *et al.*, 2015b). It was the aim of this work to determine if there was a virological cause for the reduced response rates observed in G3 virus from patients who did not respond to SOF based therapy. Using a novel assay we were able to determine the antiviral phenotype of G3 virus derived from patients who relapsed following SOF based therapy and we found that a subset of these patients had a reduced sensitivity to SOF. Subsequent sequencing analysis revealed a unique mutational pattern in the NS5B of patients who were insensitive to SOF. Introduction of these mutations into both a subgenomic and infectious viral system recapitulated the reduced sensitivity to SOF observed in capture fusion experiments.

7.1 Capture fusion assay as a system to phenotype patient virus

The HCV capture fusion assay is the only published method to assay the antiviral phenotype of patient derived virus (Cunningham *et al.*, 2014; Jones *et al.*, 2017). Limitations of the assay include the low replication levels observed in certain patient samples, the short duration that fused cells can be sustained for and the reliance on a sensitive RT-qPCR assay to detect viral replication. It was postulated that improving the rate of fusion between infected THP-1 and Huh7.5 cells would improve HCV RNA making detection of viral replication more robust.

Two attempts using different rationales were pursued to improve fusion between THP-1 and Huh7.5 cells. The first was using a biotin-streptavidin-biotin (BSB) bridge to improve cell-to-cell contract between two cells which was reported to improve PEG fusion (Li *et al.*, 2014). Despite several attempts this system did not improve rates of PEG fusion between THP-1 and Huh7.5 cells, though it is not known whether this was a failure in the biotin coating of the cells or in the establishment of the BSB-bridge between the cells. The second attempt at improving rates of PEG fusion was replacing the fusion method itself with a reportedly more efficient viral fusion protein based system by the expression of the acid-inducible fusogenic G-protein from Vesicular Stomatitis Virus (VSVG) (Gottesman *et al.*, 2010). While expression of VSVG was confirmed in the Huh7.5 cells exposure to the recommended acid buffer fusion did not result in detectable fusion events with THP-1 cells assessed by a FACS. A functional assay to assess whether 'VSVG fusion' could support viral replication further revealed that HCV RNA levels were significantly higher in cells fused by PEG compared to 'VSV-G fusion'. The lack of fusion events between Huh7.5-VSVG and THP-1 cells strongly suggests that the VSVG protein is unable to perform its fusogenic function in

these cells. While VSVG expression was shown by immunoblotting to be present in the Huh7.5-VSVG cells it is possible that the protein was not being expressed at a location where it could fuse cellular membranes. Additional work that could be performed involves expressing VSV-G on the THP-1 cells to assess whether that cell line might express VSVG in an arrangement more conducive to VSV-G fusion. Though as the THP-1 cells are critical for binding of patient derived virus in capture fusion, expression of VSV-G within the cell may affect this process. In conclusion our experiments suggest that PEG fusion remains the best method to fuse infected THP-1 and Huh7.5 cells in the capture fusion assay to propagate patient derived virus. Although more efficient means of fusion may exist they did not improve either fusion or HCV replication in this context and our attempts to improve fusion were not pursued further.

The recent identification of SEC14L2 as a key host factor for both HCV replicon and clinical isolate replication (Saeed *et al.*, 2015) led us to assess whether Huh7.5-SEC14L2 cells could either be an alternative to capture fusion or be incorporated in to the assay. In our hands we found direct infection of these cells to yield variable levels of replication of patient derived HCV and we were unable to replicate published work showing that these cells are permissive to HCV infection with a variety of different isolates. Viral RNA levels of samples tested tended to decrease over a period of 10 days particularly in G1 samples, indicating that RNA replication was either occurring at a very low level or not occurring at all. A small increase in HCV copy numbers was however observed with direct infection of G3 samples possibly indicating that these cells were more permissive to G3 infection. The viability of cells as an antiviral phenotyping assay was assessed both by a RT-qPCR assay and a HCV specific

SEAP reporter. While use of the HCV SEAP reporter system did distinguish between SEC14L2 expression producing a higher luminescent signal in the presence of SEC14L2, a robust dose response to SOF could not be established. However assessment of viral RNA levels by qPCR did reveal a dose response curve in SEC14L2 cells though only in two G3 samples with high viral loads. Direct comparison of capture fusion to infection of SEC14L2 cells did result in comparable IC_{50} values for SOF indicating that both systems can determine the sensitivity of matched clinical isolates at a similar level. It was noted however that the level of HCV RNA replication was lower with direct infection of Huh7.5-SEC14L2 cells compared to capture fusion in matched patient isolates. This may reflect the fusion process being a more efficient 'delivery' method of clinical virus into naïve Huh7.5 cells than direct infection with clinical virus. While use of the Huh7.5-SEC cells appears to be able to replicate patient virus from high-titre samples, its failure to replicate and establish dose response curves in all virus samples resulted in it being a less robust system on its own than capture fusion. Yet, the incorporation of Huh7.5-SEC14L2 cells into the capture fusion assay in the place of Huh7.5 cells significantly increased HCV RNA levels in all viral samples tested. Hence, while direct infection of these cells is not superior to capture fusion the use of these cells in capture fusion does enhance the assay.

While the identification of SEC14L2 is an important discovery in our understanding of critical host factors required by HCV to propagate, there may be more to be discovered. The beneficial effects of SEC14L2 are proposed to be protection of the virus against lipid peroxidation (Saeed *et al.*, 2015; Witteveldt *et al.*, 2016). For this protection to occur patient derived virus must still enter the cell and is therefore reliant on the natural HCV infection pathway. The fusion of infected THP-1s into Huh7.5 cells

introduces virus directly into the cytoplasm of Huh7.5 cells, where it can benefit from the positive influence of SEC14L2 on its replication without having to negotiate the HCV infection pathway. This in turn may explain why expression of SEC14L2 in Huh7.5 cells improved levels of HCV clinical isolates in capture fusion.

7.2 Identification of G3 relapse samples insensitive to SOF and RBV using the capture fusion model

A key aim of this work was to assess whether baseline viral samples from G3 patients who relapsed to SOF based had a phenotypic difference in drug sensitivity compared to those who achieved an SVR. We tested our hypothesis by determining the sensitivity of G3 clinical isolates to SOF and RBV by capture fusion. We identified a group of G3 relapse patients who had significantly reduced sensitivity to both SOF and RBV. The strength of our analysis came from all phenotyping experiments being performed in a blinded fashion to clinical outcome, so that our analysis was not influenced by prior knowledge of which patients relapsed and which achieved an SVR. Subsequent analysis of the viral sequencing data did not reveal any previously reported variants known affect either SOF or RBV sensitivity in drug insensitive samples, though some instances of the NS5A resistance variant were reported.

A central finding of these experiments was that not all patients who relapsed were insensitive to SOF and RBV as a minority of samples retained comparable sensitivity to both drugs to the SVR samples. This was of particular importance in our more extensive analysis of the NS5B sequences, which grouped the sequencing data by SOF and RBV phenotype as opposed to clinical outcome. Our analysis identified two mutational patterns in insensitive relapse patients. The first was only observed in one

sample and consisted of a multitude of changes across the NS5B that were seemingly unique to that patient. The second was a combination of two changes A150V and K206E that while observed in isolation in drug sensitive samples, the combination was only observed in insensitive relapse isolates. Phylogenetic analysis of the NS5B sequences found that samples with this particular motif formed a distinctive group. Analysis of the frequency of these mutations in the viral population in each sample revealed that both A150V and K206E dominated the quasispecies. Furthermore, these mutations continued to dominate in sequencing samples taken from patients post-relapse. This may indicate that these changes are important to the viral population in the face of antiviral treatment. It would have been of interest to this study to have tested post-relapse samples in capture fusion, which was unfortunately not possible due to insufficient viral loads post-relapse to robustly perform capture fusion experiments.

We went on to assess the prevalence of these mutations in a second independent cohort from the HCV BOSON trial. We demonstrated that the A150V mutation had a significant negative impact upon SVR rates in G3 patients, with V at this position having a higher association with relapse than SVR. In this cohort the both the K206E and combination mutation were present at a frequency too low to accurately determine its effect upon SVR.

7.3 Impact of identified NS5B mutations in HCV subgenomic and infectious assays

We utilised two models of HCV subgenomic replication and a newly described G3 infectious clone to assess the impact of NS5B mutations identified by sequence

analysis on sensitivity to SOF and RBV. HCV subgenomic replicons are well-described systems whereby the HCV replication complex can be analysed (Blight *et al.*, 2000; Blight & Norgard, 2006; Saeed *et al.*, 2013; Saeed *et al.*, 2012). In particular generation of stable cell lines expressing HCV replicons with a suitable reporter is a particularly robust system to determine sensitivity to antivirals. Drawbacks with this system are that transfection of replicon RNA by electroporation is an inefficient process coupled with stable colonies taking a substantial amount of time to grow through G418 selection. Also, the selection process itself can generate adaptive mutations throughout the genome that can affect replication efficiency. Our attempts at creating stable replicons resulted in only 3 out of the 6 NS5B mutations, K100R, G188D and K206E being created as stable lines. Antiviral sensitivity experiments performed on these replicon lines demonstrated that K100R and G188D mutations had a modest effect on SOF but more of an effect of RBV. The K206E mutation did reduce SOF sensitivity to a greater degree than either the K100R or G188D mutation indicating that in isolation this mutation can affect SOF sensitivity. Yet patients with only this mutation did not exhibit SOF insensitivity when assessed by capture fusion. Though it should be noted that a slight increase in IC_{50} values was observed from SOF sensitive patients with only the K206E mutation.

The stable replicon system while robust did not permit the study of all of the NS5B mutations of interest or the key A150V/K206E combination. An alternative approach was to use the S52 subgenomic replicons in a transient assay by preforming drug sensitivity experiments immediately after the cells have been electroporated. Transient subgenomic replicon assays using the G3 subgenomic replicon are well described and can also be enhanced by the use of the Huh-SEC14L2 cell line

(Witteveldt *et al.*, 2016). Use of the G3-subgenomic replicon in a transient assay allowed us to rapidly test the sensitivity of replicons bearing all our mutations to SOF and RBV. However a high degree of variability was observed with this system between experiments due to the variable transfection rates of electroporation. Nevertheless the reproducible pattern of response seen in the transient assay led us to conclude that the polymorphisms under investigation did modify the response to SOF.

Using this system we found that the combination of A150V and K206E had the greatest impact upon sensitivity to SOF and RBV sensitivity then any mutation assessed in isolation. Although the reduction in sensitivity was not as severe as the well described SOF resistance mutation S282T (Svarovskaia *et al.*, 2014). This was the first evidence that the presence of this combination of mutations has the ability to reduce sensitivity of HCV to the anti-viral effects of both SOF and RBV. In the single patient isolate with a rare set of multiple NS5B mutations, the two that had the greatest effect on SOF sensitivity were G188D and N244I. Though these mutations were not assessed in combination, their individual effects on SOF were likely the cause of the loss of SOF and RBV sensitivity observed in this patient isolate.

To confirm our findings we engineered the A150V and K206E mutations into the newly described DBN3a genotype 3 infectious clone, which allowed us to assess the effect of these mutations in the context of the entire viral life cycle (Ramirez *et al.*, 2016). Drug sensitivity experiments performed with these mutated viruses supported data obtained from the subgenomic replicon, that the combination of A150V and K206E caused the greatest reduction in sensitivity to both SOF and RBV. The ability of this system to produce high titre virus is based on 15-cell culture adaptive mutations

engineered throughout the HCV genome. While these mutations are not in regions close to either A150V or K206E they are artificial mutations that adapt the virus to replicate in cell culture not patients. However, this system is an improvement on subgenomic replicon assays as all stages of the viral life cycle are considered not just expression of non-structural proteins and the HCV replication complex.

Together with the data from the subgenomic replicon, these data indicate the combination of A150V and K206E mutations in the NS5B resulted in the loss of sensitivity to both SOF and RBV observed in clinical isolates with this mutation pattern. Variable fold shifts in SOF and RBV IC_{50} were observed between the infectious clone and subgenomic replicon, with the mutations appearing to exert more of an influence on drug sensitivity in the subgenomic replicon than the infectious virus. A cause for this discrepancy might be that the as the virus infects the cell it will be sensed by the host immune response through classical antiviral detection pathways, which may enhance the effect of SOF treatment. The subgenomic replicon is however introduced via electroporation, which in itself is quite an invasive process, and may not be detected so readily by the immune response. Importantly in both assays show that the greatest effect on SOF and RBV sensitivity is the combination of A150V and K206E.

The association of the A150V mutation to the IFNλ3 gene made in a recent genome wide association study led us to discover that infectious virus with this mutation had an almost 100 fold reduction in sensitivity to IFNα (Ansari *et al.*, 2017). The dramatic effect of A150V on the host IFN response led us to hypothesise that to achieve the maximum antiviral effect SOF requires an intact immune response. Our findings that in a cell line lacking an IFN response the IC_{50} of SOF in response to DBN-Wt viral

infection is reduced by approximately 10-fold support this hypothesis. Furthermore in these cells A150V had little effect on SOF sensitivity while viruses with the K206E mutation including the dual mutant still reduced sensitivity to SOF albeit to much less of an extent then observed in cells with an intact IFN response. K206E however was not found to have any impact on the IFN sensitivity suggesting that this mutation has a direct effect on the antiviral properties of SOF. The area in which this mutation is located is close to a domain previously reported to effect the RNA binding properties of the NS5B (Qin *et al.*, 2001). Whether this mutation can affect RNA binding of NS5B is unknown however additional work to characterise any potential of this mutation may explain how it exerts its effects on SOF sensitivity.

7.4 The effect of A150V on the host IFN response

Work to characterise the mechanism behind the substantial reduction in IFN sensitivity was undertaken to assess if virus with A150V could disrupt the IFN signal transduction pathway or evade the antiviral effects of ISG induction. In infected cells presence of A150V had a minimal impact in the ability of the cell to produce MxA in response to IFN treatment or on the activity of the ISRE. The mutation was found to have more of an impact on enabling the virus to resist the IFN induced anti-viral state evidenced by higher infection rates with A150V virus on cells pre-treated with IFN. A stable cell line was generated expressing the mutated NS5B to create a more robust system whereby the effect of the A150V mutation could be more reliably investigated. It was found that in cells expressing the A150V mutated NS5B a significant reduction in MxA was observed after treatment with IFN for 24hrs while comparable levels of induction were observed after 6hrs indicating ‘late response’ to IFN is reduced. Immunoblot analysis of STAT-1 and STAT-2 expression showed no real change in basal levels of these two

key signalling proteins in cells overexpressing NS5B with A150V. The reduction in signal was slight and it is likely that there may be other elements that may explain this effect that are as yet unknown. Additional work would need to be performed to fully characterise the effect the A150V mutation is having on the cellular IFN response. Experiments that may be informative would be performing an IFN gene expression array on both infected cells and NS5B expressing cells to assess if any expression of key genes involved in the IFN response are affected in any way by the A150V mutation.

7.5 Concluding remarks

This work has identified a novel set of NS5B mutations that reduce response to DAA based therapy in G3 patients. Characterisation of the effect of these mutations in two models of HCV replication consistently shows that the combination of both A150V and K206E have the greatest impact on sensitivity to SOF. Furthermore the observation that the A150V mutation could significantly reduce sensitivity to IFNα, led to the observation that SOF has a reduced potency in a cell line unable to generate an IFN response. This suggests that the way in which A150V exerts its effect on SOF sensitivity is through reducing the effectiveness of the host IFN response resulting in less immune mediated clearance of the virus from the cell. This however is not sufficient to allow the virus to evade the antiviral effects of SOF. There is a requirement for the K206E mutation, which exerts a direct effect on SOF sensitivity, reducing the effectiveness of the drug even further preventing total clearance of the virus from the cell. How the A150V mutation allows the virus to evade the host IFN response remains undefined. Yet this work may allude to a unique way in which G3 HCV is able to overcome DAA therapy.

References

Afdhal, N., Reddy, K. R., Nelson, D. R., Lawitz, E., Gordon, S. C., Schiff, E., Nahass, R., Ghalib, R., Gitlin, N., Herring, R., Lalezari, J., Younes, Z. H., Pockros, P. J., Di Bisceglie, A. M., Arora, S., Subramanian, G. M., Zhu, Y., Dvory-Sobol, H., Yang, J. C., Pang, P. S., Symonds, W. T., McHutchison, J. G., Muir, A. J., Sulkowski, M. & Kwo, P. (2014). Ledipasvir and sofosbuvir for previously treated HCV genotype 1 infection. *The New England journal of medicine* **370**, 1483-1493.

Alexopoulou, L., Holt, A. C., Medzhitov, R. & Flavell, R. A. (2001). Recognition of double-stranded RNA and activation of NF-kappa B by Toll-like receptor 3. *Nature* **413**, 732-738.

Aligeti, M., Roder, A. & Horner, S. M. (2015). Cooperation between the Hepatitis C Virus p7 and NS5B Proteins Enhances Virion Infectivity. *J Virol* **89**, 11523-11533.

Alter, H. J., Holland, P. V., Morrow, A. G., Purcell, R. H., Feinstone, S. M. & Moritsugu, Y. (1975). Clinical and serological analysis of transfusion-associated hepatitis. *Lancet* **2**, 838-841.

Ansari, M. A., Pedergnana, V., C, L. C. I., Magri, A., Von Delft, A., Bonsall, D., Chaturvedi, N., Bartha, I., Smith, D., Nicholson, G., McVean, G., Trebes, A., Piazza, P., Fellay, J., Cooke, G., Foster, G. R., Hudson, E., McLauchlan, J., Simmonds, P., Bowden, R., Klenerman, P., Barnes, E. & Spencer, C. C. (2017). Genome-to-genome analysis highlights the effect of the human innate and adaptive immune systems on the hepatitis C virus. *Nature genetics*.

Appel, N., Zayas, M., Miller, S., Krijnse-Locker, J., Schaller, T., Friebe, P., Kallis, S., Engel, U. & Bartenschlager, R. (2008). Essential role of domain III of nonstructural protein 5A for hepatitis C virus infectious particle assembly. *Plos Pathogens* **4**.

Appleby, T. C., Perry, J. K., Murakami, E., Barauskas, O., Feng, J., Cho, A., Fox, D., 3rd, Wetmore, D. R., McGrath, M. E., Ray, A. S., Sofia, M. J., Swaminathan, S. & Edwards, T. E. (2015). Viral replication. Structural basis for RNA replication by the hepatitis C virus polymerase. *Science* **347**, 771-775.

Ara, A. K. & Paul, J. P. (2015). New Direct-Acting Antiviral Therapies for Treatment of Chronic Hepatitis C Virus Infection. *Gastroenterol Hepatol (N Y)* **11**, 458-466.

Ascher, D. B., Wielens, J., Nero, T. L., Doughty, L., Morton, C. J. & Parker, M. W. (2014). Potent hepatitis C inhibitors bind directly to NS5A and reduce its affinity for RNA. In *Scientific reports*.

Asselah, T., Estrabaud, E., Bieche, I., Lapalus, M., De Muynck, S., Vidaud, M., Saadoun, D., Soumelis, V. & Marcellin, P. (2010). Hepatitis C: viral and host

factors associated with non-response to pegylated interferon plus ribavirin. *Liver Int* **30**, 1259-1269.

Bacon, B. R., Gordon, S. C., Lawitz, E., Marcellin, P., Vierling, J. M., Zeuzem, S., Poordad, F., Goodman, Z. D., Sings, H. L., Boparai, N., Burroughs, M., Brass, C. A., Albrecht, J. K. & Esteban, R. (2011). Boceprevir for previously treated chronic HCV genotype 1 infection. *The New England journal of medicine* **364**, 1207-1217.

Barba, G., Harper, F., Harada, T., Kohara, M., Goulinet, S., Matsuura, Y., Eder, G., Schaff, Z., Chapman, M. J., Miyamura, T. & Brechot, C. (1997). Hepatitis C virus core protein shows a cytoplasmic localization and associates to cellular lipid storage droplets. *Proc Natl Acad Sci U S A* **94**, 1200-1205.

Barritt, A. S. & Fried, M. W. (2012). Maximizing Opportunities and Avoiding Mistakes in Triple Therapy for Hepatitis C Virus. *Gastroenterology* **142**, 1314-1323 e1311.

Bartenschlager, R. (2002). Hepatitis C virus replicons: potential role for drug development. *Nature Reviews Drug Discovery* **1**, 911-916.

Bartenschlager, R., Ahlbornlaake, L., Mous, J. & Jacobsen, H. (1993). NONSTRUCTURAL PROTEIN-3 OF THE HEPATITIS-C VIRUS ENCODES A SERINE-TYPE PROTEINASE REQUIRED FOR CLEAVAGE AT THE NS3/4 AND NS4/5 JUNCTIONS. *Journal of Virology* **67**, 3835-3844.

Bartenschlager, R. & Lohmann, V. (2001). Novel cell culture systems for the hepatitis C virus. *Antiviral Res* **52**, 1-17.

Bartenschlager, R., Penin, F., Lohmann, V. & Andre, P. (2011). Assembly of infectious hepatitis C virus particles. *Trends Microbiol* **19**, 95-103.

Blight, K. J., Kolykhalov, A. A. & Rice, C. M. (2000). Efficient initiation of HCV RNA replication in cell culture. *Science* **290**, 1972-1974.

Blight, K. J., McKeating, J. A. & Rice, C. M. (2002). Highly permissive cell lines for subgenomic and genomic hepatitis C virus RNA replication. *J Virol* **76**, 13001-13014.

Blight, K. J. & Norgard, E. A. (2006). HCV Replicon Systems.

Bolen, C. R., Ding, S., Robek, M. D. & Kleinstein, S. H. (2014). Dynamic Expression Profiling of Type I and Type III Interferon-Stimulated Hepatocytes Reveals a Stable Hierarchy of Gene Expression. *Hepatology* **59**, 1262-1272.

Bougie, I. & Bisaillon, M. (2003). Initial binding of the broad spectrum antiviral nucleoside ribavirin to the hepatitis C virus RNA polymerase. *The Journal of biological chemistry* **278**, 52471-52478.

Boulant, S., Montserret, R., Hope, R. G., Ratinier, M., Targett-Adams, P., Lavergne, J.-P., Penin, F. & McLauchlan, J. (2006). Structural determinants

that target the hepatitis C virus core protein to lipid droplets. *Journal of Biological Chemistry* **281**, 22236-22247.

Boulestin, A., Sandres-Saune, K., Payen, J. L., Alric, L., Dubois, M., Pasquier, C., Vinel, J. P., Pascal, J. P., Puel, J. & Izopet, J. (2002). Genetic heterogeneity of the envelope 2 gene and eradication of hepatitis C virus after a second course of interferon-alpha. *Journal of Medical Virology* **68**, 221-228.

Bowen, D. G. & Walker, C. M. (2005). Mutational escape from CD8(+) T cell immunity: HCV evolution, from chimpanzees to man. *Journal of Experimental Medicine* **201**, 1709-1714.

Bradley, D. W., McCaustland, K. A., Cook, E. H., Schable, C. A., Ebert, J. W. & Maynard, J. E. (1985). Posttransfusion non-A, non-B hepatitis in chimpanzees. Physicochemical evidence that the tubule-forming agent is a small, enveloped virus. *Gastroenterology* **88**, 773-779.

Brillanti, S., Garson, J., Foli, M., Whitby, K., Deaville, R., Masci, C., Miglioli, M. & Barbara, L. (1994). A pilot study of combination therapy with ribavirin plus interferon alfa for interferon alfa-resistant chronic hepatitis C. *Gastroenterology* **107**, 812-817.

Carrere-Kremer, S., Montpellier-Pala, C., Cocquerel, L., Wychowski, C., Penin, F. & Dubuisson, J. (2002). Subcellular localization and topology of the p7 polypeptide of hepatitis C virus. *J Virol* **76**, 3720-3730.

Catanese, M. T. & Dorner, M. (2015). Advances in experimental systems to study hepatitis C virus in vitro and in vivo. *Virology* **479-480**, 221-233.

Chang, J., Guo, J. T., Jiang, D., Guo, H., Taylor, J. M. & Block, T. M. (2008). Liver-specific microRNA miR-122 enhances the replication of hepatitis C virus in nonhepatic cells. *J Virol* **82**, 8215-8223.

Chang, K. M., Rehermann, B., McHutchison, J. G., Pasquinelli, C., Southwood, S., Sette, A. & Chisari, F. V. (1997). Immunological significance of cytotoxic T lymphocyte epitope variants in patients chronically infected by the hepatitis C virus. *Journal of Clinical Investigation* **100**, 2376-2385.

Chayama, K., Suzuki, F., Tsubota, A., Kobayashi, M., Arase, Y., Saitoh, S., Suzuki, Y., Murashima, N., Ikeda, K., Takahashi, N., Kinoshita, M. & Kumada, H. (2000). Association of amino acid sequence in the PKR-eIF2 phosphorylation homology domain and response to interferon therapy. *Hepatology* **32**, 1138-1144.

Cheon, H., Borden, E. C. & Stark, G. R. (2014). Interferons and their stimulated genes in the tumor microenvironment. *Seminars in oncology* **41**, 156-173.

Cheon, H., Holvey-Bates, E. G., Schoggins, J. W., Forster, S., Hertzog, P., Imanaka, N., Rice, C. M., Jackson, M. W., Junk, D. J. & Stark, G. R. (2013).

IFNbeta-dependent increases in STAT1, STAT2, and IRF9 mediate resistance to viruses and DNA damage. *The EMBO journal* **32**, 2751-2763.

Cheon, H. & Stark, G. R. (2009). Unphosphorylated STAT1 prolongs the expression of interferon-induced immune regulatory genes. *Proc Natl Acad Sci U S A* **106**, 9373-9378.

Cheruvattath, R., Rosati, M. J., Gautam, M., Vargas, H. E., Rakela, J. & Balan, V. (2007). Pegylated interferon and ribavirin failures: Is retreatment an option? *Digestive Diseases and Sciences* **52**, 732-736.

Cheung, M. C., Walker, A. J., Hudson, B. E., Verma, S., McLauchlan, J., Mutimer, D. J., Brown, A., Gelson, W. T., MacDonald, D. C., Agarwal, K., Foster, G. R. & Irving, W. L. (2016). Outcomes after successful direct-acting antiviral therapy for patients with chronic hepatitis C and decompensated cirrhosis. *Journal of hepatology* **65**, 741-747.

Choo, Q. L., Kuo, G., Weiner, A. J., Overby, L. R., Bradley, D. W. & Houghton, M. (1989). Isolation of a cDNA clone derived from a blood-borne non-A, non-B viral hepatitis genome. *Science* **244**, 359-362.

Coquillard, G. & Patterson, B. K. (2009). Determination of Hepatitis C Virus-Infected, Monocyte Lineage Reservoirs in Individuals With or Without HIV Coinfection. *Journal of Infectious Diseases* **200**, 947-954.

Cristofari, G., Ivanyi-Nagy, R., Gabus, C., Boulant, S., Lavergne, J. P., Penin, F. & Darlix, J. L. (2004). The hepatitis C virus Core protein is a potent nucleic acid chaperone that directs dimerization of the viral(+) strand RNA in vitro. *Nucleic Acids Research* **32**, 2623-2631.

Cunningham, M. E., Javaid, A., Waters, J., Davidson-Wright, J., Wong, J. L., Jones, M. & Foster, G. R. (2014). Development and validation of a 'capture-fusion' model to study drug sensitivity of patient-derived hepatitis C. *Hepatology*.

Dao Thi, V. L., Granier, C., Zeisel, M. B., Guerin, M., Mancip, J., Granio, O., Penin, F., Lavillette, D., Bartenschlager, R., Baumert, T. F., Cosset, F. L. & Dreux, M. (2012). Characterization of hepatitis C virus particle subpopulations reveals multiple usage of the scavenger receptor BI for entry steps. *The Journal of biological chemistry* **287**, 31242-31257.

Davis, G. L., Esteban-Mur, R., Rustgi, V., Hoefs, J., Gordon, S. C., Trepo, C., Shiffman, M. L., Zeuzem, S., Craxi, A., Ling, M. H. & Albrecht, J. (1998). Interferon alfa-2b alone or in combination with ribavirin for the treatment of relapse of chronic hepatitis C. International Hepatitis Interventional Therapy Group. *The New England journal of medicine* **339**, 1493-1499.

Di Maio, V. C., Cento, V., Mirabelli, C., Artese, A., Costa, G., Alcaro, S., Perno, C. F. & Ceccherini-Silberstein, F. (2014). Hepatitis C Virus Genetic Variability and the Presence of NS5B Resistance-Associated Mutations as Natural

Polymorphisms in Selected Genotypes Could Affect the Response to NS5B Inhibitors. *Antimicrobial agents and chemotherapy* **58**, 2781-2797.

Donnelly, R. P. & Kotenko, S. V. (2010a). Interferon-Lambda: A New Addition to an Old Family. *Journal of Interferon and Cytokine Research* **30**, 555-564.

Donnelly, R. P. & Kotenko, S. V. (2010b). Interferon-lambda: a new addition to an old family. *Journal of interferon & cytokine research : the official journal of the International Society for Interferon and Cytokine Research* **30**, 555-564.

Donnelly, R. P., Sheikh, F., Kotenko, S. V. & Dickensheets, H. (2004). The expanded family of class II cytokines that share the IL-10 receptor-2 (IL-10R2) chain. *Journal of Leukocyte Biology* **76**, 314-321.

Dore, G. J., Lawitz, E., Hezode, C., Shafran, S. D., Ramji, A., Tatum, H. A., Taliani, G., Tran, A., Brunetto, M. R., Zaltron, S., Strasser, S. I., Weis, N., Ghesquiere, W., Lee, S. S., Larrey, D., Pol, S., Harley, H., George, J., Fung, S. K., de Ledinghen, V., Hagens, P., McPhee, F., Hernandez, D., Cohen, D., Cooney, E., Noviello, S. & Hughes, E. A. (2015). Daclatasvir plus peginterferon and ribavirin is noninferior to peginterferon and ribavirin alone, and reduces the duration of treatment for HCV genotype 2 or 3 infection. *Gastroenterology* **148**, 355-366.e351.

Dorner, M., Horwitz, J. a., Donovan, B. M., Labitt, R. N., Budell, W. C., Friling, T., Vogt, A., Catanese, M. T., Satoh, T., Kawai, T., Akira, S., Law, M., Rice, C. M. & Ploss, A. (2013). Completion of the entire hepatitis C virus life cycle in genetically humanized mice. *Nature* **501**, 237-241.

Ducoulombier, D., Roque-Afonso, A. M., Di Liberto, G., Penin, F., Kara, R., Richard, Y., Dussaix, E. & Feray, C. (2004). Frequent compartmentalization of hepatitis C virus variants in circulating B cells and monocytes. *Hepatology* **39**, 817-825.

EASL (2017). EASL Recommendations on Treatment of Hepatitis C 2016. *Journal of hepatology* **66**, 153-194.

Elaut, G., Henkens, T., Papeleu, P., Snykers, S., Vinken, M., Vanhaecke, T. & Rogiers, V. (2006). Molecular mechanisms underlying the dedifferentiation process of isolated hepatocytes and their cultures. *Current Drug Metabolism* **7**, 629-660.

Enomoto, N., Sakuma, I., Asahina, Y., Kurosaki, M., Murakami, T., Yamamoto, C., Ogura, Y., Izumi, N., Marumo, F. & Sato, C. (1996). Mutations in the nonstructural protein 5A gene and response to interferon in patients with chronic hepatitis C virus 1b infection. *New England Journal of Medicine* **334**, 77-81.

Erickson, A. L., Kimura, Y., Igarashi, S., Eichelberger, J., Houghton, M., Sidney, J., McKinney, D., Sette, A., Hughes, A. L. & Walker, C. M. (2001). The

outcome of hepatitis C virus infection is predicted by escape mutations in epitopes targeted by cytotoxic T lymphocytes. *Immunity* **15**, 883-895.

Evans, M. J., von Hahn, T., Tscherne, D. M., Syder, A. J., Panis, M., Wolk, B., Hatziioannou, T., McKeating, J. A., Bieniasz, P. D. & Rice, C. M. (2007). Claudin-1 is a hepatitis C virus co-receptor required for a late step in entry. *Nature* **446**, 801-805.

Eyre, N. S., Aloia, A. L., Joyce, M. A., Chulanetra, M., Tyrrell, D. L. & Beard, M. R. (2017). Sensitive luminescent reporter viruses reveal appreciable release of hepatitis C virus NS5A protein into the extracellular environment. *Virology* **507**, 20-31.

Farci, P., Shimoda, A., Wong, D., Cabezon, T., DeGioannis, D., Strazzera, A., Shimizu, Y., Shapiro, M., Alter, H. J. & Purcell, R. H. (1996). Prevention of hepatitis C virus infection in chimpanzees by hyperimmune serum against the hypervariable region 1 of the envelope 2 protein. *Proceedings of the National Academy of Sciences of the United States of America* **93**, 15394-15399.

Farquhar, M. J., Hu, K., Harris, H. J., Davis, C., Brimacombe, C. L., Fletcher, S. J., Baumert, T. F., Rappoport, J. Z., Balfe, P. & McKeating, J. A. (2012). Hepatitis C virus induces CD81 and claudin-1 endocytosis. *J Virol* **86**, 4305-4316.

Feigelstock, D. A., Mihalik, K. B. & Feinstone, S. M. (2011). Selection of hepatitis C virus resistant to ribavirin. *Virol J* **8**, 402.

Feinstone, S. M., Kapikian, A. Z., Purcell, R. H., Alter, H. J. & Holland, P. V. (1975). Transfusion-associated hepatitis not due to viral hepatitis type A or B. *The New England journal of medicine* **292**, 767-770.

Feld, J. J., Jacobson, I. M., Hezode, C., Asselah, T., Ruane, P. J., Gruener, N., Abergel, A., Mangia, A., Lai, C. L., Chan, H. L., Mazzotta, F., Moreno, C., Yoshida, E., Shafran, S. D., Towner, W. J., Tran, T. T., McNally, J., Osinusi, A., Svarovskaia, E., Zhu, Y., Brainard, D. M., McHutchison, J. G., Agarwal, K. & Zeuzem, S. (2015). Sofosbuvir and Velpatasvir for HCV Genotype 1, 2, 4, 5, and 6 Infection. *The New England journal of medicine* **373**, 2599-2607.

Feld, J. J., Nanda, S., Huang, Y., Chen, W. P., Cam, M., Pusek, S. N., Schweigler, L. M., Theodore, D., Zacks, S. L., Liang, T. J. & Fried, M. W. (2007). Hepatic gene expression during treatment with peginterferon and ribavirin: Identifying molecular pathways for treatment response. *Hepatology* **46**, 1548-1563.

Figlerowicz, M., Alejska, M. & Kurzynska-Kokorniak, A. (2003). Genetic variability: the key problem in the prevention and therapy of RNA-based virus infections. *Medicinal research reviews* **23**, 488-518.

Fischer, J., Bohm, S., Muller, T., Witt, H., Sarrazin, C., Susser, S., Migaud, P., Schott, E., Stewart, G., Brodzinski, A., Fulop, B., van Bommel, F., George, J. & Berg, T. (2013). Association of IFNL3 rs12979860 and rs8099917 with

Biochemical Predictors of Interferon Responsiveness in Chronic Hepatitis C Virus Infection. *PLoS One* **8**, e77530.

Foster, G. R., Afdhal, N., Roberts, S. K., Brau, N., Gane, E. J., Pianko, S., Lawitz, E., Thompson, A., Shiffman, M. L., Cooper, C., Towner, W. J., Conway, B., Ruane, P., Bourliere, M., Asselah, T., Berg, T., Zeuzem, S., Rosenberg, W., Agarwal, K., Stedman, C. A., Mo, H., Dvory-Sobol, H., Han, L., Wang, J., McNally, J., Osinusi, A., Brainard, D. M., McHutchison, J. G., Mazzotta, F., Tran, T. T., Gordon, S. C., Patel, K., Reau, N., Mangia, A. & Sulkowski, M. (2015a). Sofosbuvir and Velpatasvir for HCV Genotype 2 and 3 Infection. *The New England journal of medicine* **373**, 2608-2617.

Foster, G. R., Pianko, S., Brown, A., Forton, D., Nahass, R. G., George, J., Barnes, E., Brainard, D. M., Massetto, B., Lin, M., Han, B., McHutchison, J. G., Subramanian, G. M., Cooper, C. & Agarwal, K. (2015b). Efficacy of Sofosbuvir Plus Ribavirin With or Without Peginterferon-Alfa in Patients With Hepatitis C Virus Genotype 3 Infection and Treatment-Experienced Patients With Cirrhosis and Hepatitis C Virus Genotype 2 Infection. *Gastroenterology* **149**, 1462-1470.

Foy, E., Li, K., Sumpter, R., Loo, Y. M., Johnson, C. L., Wang, C. F., Fish, P. M., Yoneyama, M., Fujita, T., Lemon, S. M. & Gale, M. (2005). Control of antiviral defenses through hepatitis C virus disruption of retinoic acid-inducible gene-I signaling. *Proceedings of the National Academy of Sciences of the United States of America* **102**, 2986-2991.

Foy, E., Li, K., Wang, C. F., Sumpter, R., Ikeda, M., Lemon, S. M. & Gale, M. (2003). Regulation of interferon regulatory factor-3 by the hepatitis C virus serine protease. *Science* **300**, 1145-1148.

Francois, C., Duverlie, G., Rebouillat, D., Khorsi, H., Castelain, S., Blum, H. E., Gatignol, A., Wychowski, C., Moradpour, D. & Meurs, E. F. (2000). Expression of hepatitis C virus proteins interferes with the antiviral action of interferon independently of PKR-mediated control of protein synthesis. *J Virol* **74**, 5587-5596.

Francois-Newton, V., Almeida, G. M. d. F., Payelle-Brogard, B., Monneron, D., Pichard-Garcia, L., Piehler, J., Pellegrini, S. & Uze, G. (2011). USP18-Based Negative Feedback Control Is Induced by Type I and Type III Interferons and Specifically Inactivates Interferon alpha Response. *Plos One* **6**.

Fridell, R. A., Wang, C., Sun, J. H., O'Boyle, D. R., 2nd, Nower, P., Valera, L., Qiu, D., Roberts, S., Huang, X., Kienzle, B., Bifano, M., Nettles, R. E. & Gao, M. (2011). Genotypic and phenotypic analysis of variants resistant to hepatitis C virus nonstructural protein 5A replication complex inhibitor BMS-790052 in humans: in vitro and in vivo correlations. *Hepatology* **54**, 1924-1935.

Fried, M. W., Shiffman, M. L., Reddy, K. R., Smith, C., Marinos, G., Goncales, F. L., Haussinger, D., Diago, M., Carosi, G., Dhumeaux, D., Craxi, A., Lin, A.,

Hoffman, J. & Yu, J. (2002). Peginterferon alfa-2a plus ribavirin for chronic hepatitis C virus infection. *New England Journal of Medicine* **347**, 975-982.

Gallinari, P., Brennan, D., Nardi, C., Brunetti, M., Tomei, L., Steinkuhler, C. & De Francesco, R. (1998). Multiple enzymatic activities associated with recombinant NS3 protein of hepatitis C virus. *Journal of Virology* **72**, 6758-6769.

Gane, E. J., Stedman, C. A., Hyland, R. H., Ding, X., Svarovskaia, E., Symonds, W. T., Hindes, R. G. & Berrey, M. M. (2013). Nucleotide polymerase inhibitor sofosbuvir plus ribavirin for hepatitis C. *The New England journal of medicine* **368**, 34-44.

Gao, M. (2013). Antiviral activity and resistance of HCV NS5A replication complex inhibitors. *Current opinion in virology* **3**, 514-520.

Gao, M., Nettles, R. E., Belema, M., Snyder, L. B., Nguyen, V. N., Fridell, R. A., Serrano-Wu, M. H., Langley, D. R., Sun, J. H., O'Boyle, D. R., 2nd, Lemm, J. A., Wang, C., Knipe, J. O., Chien, C., Colonno, R. J., Grasela, D. M., Meanwell, N. A. & Hamann, L. G. (2010). Chemical genetics strategy identifies an HCV NS5A inhibitor with a potent clinical effect. *Nature* **465**, 96-100.

Gawlik, K. & Gallay, P. A. (2014). HCV core protein and virus assembly: what we know without structures. *Immunologic research* **60**, 1-10.

Germi, R., Crance, J. M., Garin, D., Guimet, J., Lortat-Jacob, H., Ruigrok, R. W., Zarski, J. P. & Drouet, E. (2002). Cellular glycosaminoglycans and low density lipoprotein receptor are involved in hepatitis C virus adsorption. *J Med Virol* **68**, 206-215.

Gerold, G., Bruening, J., Weigel, B. & Pietschmann, T. (2017). Protein Interactions during the Flavivirus and Hepacivirus Life Cycle. *Molecular & cellular proteomics : MCP* **16**, S75-s91.

Ghany, M. G., Strader, D. B., Thomas, D. L. & Seeff, L. B. (2009). Diagnosis, management, and treatment of hepatitis C: an update. *Hepatology* **49**, 1335-1374.

Gnadig, N. F., Beaucourt, S., Campagnola, G., Borderia, A. V., Sanz-Ramos, M., Gong, P., Blanc, H., Peersen, O. B. & Vignuzzi, M. (2012). Coxsackievirus

B3 mutator strains are attenuated in vivo. *Proc Natl Acad Sci U S A* **109**, E2294-2303.

Goffard, A., Callens, N., Bartosch, B., Wychowski, C., Cosset, F. L., Montpellier, C. & Dubuisson, J. (2005). Role of N-linked glycans in the functions of hepatitis C virus envelope glycoproteins. *Journal of Virology* **79**, 8400-8409.

Golestani, R., Pourfathollah, A. A. & Moazzeni, S. M. (2007). Cephalin as an efficient fusogen in hybridoma technology: can it replace poly ethylene glycol? *Hybridoma (2005)* **26**, 296-301.

Goonawardane, N., Gebhardt, A., Bartlett, C., Pichlmair, A. & Harris, M. (2017). Phosphorylation of serine 225 in hepatitis C virus NS5A regulates protein-protein interactions. *J Virol*.

Gosert, R., Egger, D., Lohmann, V., Bartenschlager, R., Blum, H. E., Bienz, K. & Moradpour, D. (2003). Identification of the hepatitis C virus RNA replication complex in Huh-7 cells harboring subgenomic replicons. *J Virol* **77**, 5487-5492.

Gottesman, A., Milazzo, J. & Lazebnik, Y. (2010). V-fusion: a convenient, nontoxic method for cell fusion. *BioTechniques* **49**, 747-750.

Gottwein, J. M., Jensen, T. B., Mathiesen, C. K., Meuleman, P., Serre, S. B., Lademann, J. B., Ghanem, L., Scheel, T. K., Leroux-Roels, G. & Bukh, J. (2011). Development and application of hepatitis C reporter viruses with genotype 1 to 7 core-nonstructural protein 2 (NS2) expressing fluorescent proteins or luciferase in modified JFH1 NS5A. *J Virol* **85**, 8913-8928.

Gower, E., Estes, C., Blach, S., Razavi-Shearer, K. & Razavi, H. (2014). Global epidemiology and genotype distribution of the hepatitis C virus infection. *Journal of hepatology* **61**, S45-57.

Grove, J., Huby, T., Stamataki, Z., Vanwolleghem, T., Meuleman, P., Farquhar, M., Schwarz, A., Moreau, M., Owen, J. S., Leroux-Roels, G., Balfe, P. & McKeating, J. A. (2007). Scavenger receptor BI and BII expression levels modulate hepatitis C virus infectivity. *J Virol* **81**, 3162-3169.

Gu, M. & Rice, C. M. (2010). Three conformational snapshots of the hepatitis C virus NS3 helicase reveal a ratchet translocation mechanism. *Proc Natl Acad Sci U S A* **107**, 521-528.

Hadziyannis, S. J., Sette, H., Morgan, T. R., Balan, V., Diago, M., Marcellin, P., Ramadori, G., Bodenheimer, H., Bernstein, D., Rizzetto, M., Zeuzem, S., Pockros, P. J., Lin, A., Ackrill, A. M. & Grp, P. I. S. (2004). Peginterferon-alpha 2a and ribavirin combination therapy in chronic hepatitis C - A

randomized study of treatment duration and ribavirin dose. *Annals of Internal Medicine* **140**, 346-355.

Hagedorn, C. H. (1999). Hepatitis C Virus RNA-Dependent RNA Polymerase (NS5B Polymerase). *Methods in molecular medicine* **19**, 365-372.

Hamming, O. J., Terczynska-Dyla, E., Vieyres, G., Dijkman, R., Jorgensen, S. E., Akhtar, H., Siupka, P., Pietschmann, T., Thiel, V. & Hartmann, R. (2013). Interferon lambda 4 signals via the IFN lambda receptor to regulate antiviral activity against HCV and coronaviruses. *Embo Journal* **32**, 3055-3065.

Harris, H. J., Davis, C., Mullins, J. G., Hu, K., Goodall, M., Farquhar, M. J., Mee, C. J., McCaffrey, K., Young, S., Drummer, H., Balfe, P. & McKeating, J. A. (2010). Claudin association with CD81 defines hepatitis C virus entry. *The Journal of biological chemistry* **285**, 21092-21102.

Harrison, S. C. (2008). Viral membrane fusion. *Nature structural & molecular biology* **15**, 690-698.

Hoffman, A. N., Bamba, R., Pollins, A. C. & Thayer, W. P. (2017). Analysis of polyethylene glycol (PEG) fusion in cultured neuroblastoma cells via flow cytometry: Techniques & optimization. *Journal of clinical neuroscience : official journal of the Neurosurgical Society of Australasia* **36**, 125-128.

Horner, S. M., Liu, H. M., Park, H. S., Briley, J. & Gale, M., Jr. (2011). Mitochondrial-associated endoplasmic reticulum membranes (MAM) form innate immune synapses and are targeted by hepatitis C virus. *Proc Natl Acad Sci U S A* **108**, 14590-14595.

Houghton, M. (2009). Discovery of the hepatitis C virus. *Liver Int* **29 Suppl 1**, 82-88.

Huang, H., Sun, F., Owen, D. M., Li, W., Chen, Y., Gale, M., Jr. & Ye, J. (2007). Hepatitis C virus production by human hepatocytes dependent on assembly and secretion of very low-density lipoproteins. *Proc Natl Acad Sci U S A* **104**, 5848-5853.

Hultgren, C., Milich, D. R., Weiland, O. & Sallberg, M. (1998). The antiviral compound ribavirin modulates the T helper (Th) 1/Th2 subset balance in hepatitis B and C virus-specific immune responses. *The Journal of general virology* **79 (Pt 10)**, 2381-2391.

Iro, M., Witteveldt, J., Angus, A. G., Woerz, I., Kaul, A., Bartenschlager, R. & Patel, A. H. (2009). A reporter cell line for rapid and sensitive evaluation of hepatitis C virus infectivity and replication. *Antiviral Res* **83**, 148-155.

Iyer, R., Coughlin, J., Padmanabhan, S., Korba, B. & Myong, S. (2010). Activation of Retinoic Acid Inducible Gene (RIG-I) by Nucleotide Analogs: A Potential Novel Mechanism for Antiviral Discovery. *Antiviral Res* **86**, A35.

Jackowiak, P., Kuls, K., Budzko, L., Mania, A. & Figlerowicz, M. (2014). Phylogeny and molecular evolution of the hepatitis C virus. *Infection, genetics and*

evolution : journal of molecular epidemiology and evolutionary genetics in infectious diseases **21c**, 67-82.

Jacobson, I. M., Ahmed, F., Russo, M. W., Lebovics, E., Dieterich, D. I., Esposito, S. P., Bach, N., Klion, F., Tobias, H., Antignano, L., Brown, R. S., Gabbaizadeh, D., Geders, J. & Levendoglu, H. (2004). Interferon alpha-2b and ribavirin for patients with chronic hepatitis C and normal ALT. *American Journal of Gastroenterology* **99**, 1700-1705.

Jacobson, I. M., Dore, G. J., Foster, G. R., Fried, M. W., Radu, M., Rafalsky, V. V., Moroz, L., Craxi, A., Peeters, M., Lenz, O., Ouwerkerk-Mahadevan, S., De La Rosa, G., Kalmeijer, R., Scott, J., Sinha, R. & Beumont-Mauviel, M. (2014). Simeprevir with pegylated interferon alfa 2a plus ribavirin in treatment-naive patients with chronic hepatitis C virus genotype 1 infection (QUEST-1): a phase 3, randomised, double-blind, placebo-controlled trial. *Lancet* **384**, 403-413.

Jacobson, I. M., Gordon, S. C., Kowdley, K. V., Yoshida, E. M., Rodriguez-Torres, M., Sulkowski, M. S., Shiffman, M. L., Lawitz, E., Everson, G., Bennett, M., Schiff, E., Al-Assi, M. T., Subramanian, G. M., An, D., Lin, M., McNally, J., Brainard, D., Symonds, W. T., McHutchison, J. G., Patel, K., Feld, J., Pianko, S. & Nelson, D. R. (2013). Sofosbuvir for hepatitis C genotype 2 or 3 in patients without treatment options. *The New England journal of medicine* **368**, 1867-1877.

Jacobson, I. M., McHutchison, J. G., Dusheiko, G., Di Bisceglie, A. M., Reddy, K. R., Bzowej, N. H., Marcellin, P., Muir, A. J., Ferenci, P., Flisiak, R., George, J., Rizzetto, M., Shouval, D., Sola, R., Terg, R. A., Yoshida, E. M., Adda, N., Bengtsson, L., Sankoh, A. J., Kieffer, T. L., George, S., Kauffman, R. S. & Zeuzem, S. (2011). Telaprevir for previously untreated chronic hepatitis C virus infection. *The New England journal of medicine* **364**, 2405-2416.

Jirasko, V., Montserret, R., Lee, J. Y., Gouttenoire, J., Moradpour, D., Penin, F. & Bartenschlager, R. (2010). Structural and functional studies of nonstructural protein 2 of the hepatitis C virus reveal its key role as organizer of virion assembly. *PLoS Pathog* **6**, e1001233.

Jones, C. T., Catanese, M. T., Law, L. M. J., Khetani, S. R., Syder, A. J., Ploss, A., Oh, T. S., Schoggins, J. W., MacDonald, M. R., Bhatia, S. N. & Rice, C. M. (2010). Real-time imaging of hepatitis C virus infection using a fluorescent cell-based reporter system. *Nat Biotechnol* **28**, 167-171.

Jones, M., Cunningham, M. E., Wing, P., DeSilva, S., Challa, R., Sheri, A., Padmanabhan, S., Iyer, R. P., Korba, B. E., Afdhal, N. & Foster, G. R. (2017). SB 9200, a novel agonist of innate immunity, shows potent antiviral activity against resistant HCV variants. *J Med Virol*.

Kalie, E., Jaitin, D. A., Podoplelova, Y., Piehler, J. & Schreiber, G. (2008). The Stability of the Ternary Interferon-Receptor Complex Rather than the Affinity to

the Individual Subunits Dictates Differential Biological Activities. *Journal of Biological Chemistry* **283**, 32925-32936.

Kanazawa, N., Kurosaki, M., Sakamoto, N., Enomoto, N., Itsui, Y., Yamashiro, T., Tanabe, Y., Maekawa, S., Nakagawa, M., Chen, C. H., Kakinuma, S., Oshima, S., Nakamura, T., Kato, T., Wakita, T. & Watanabe, M. (2004). Regulation of Hepatitis C Virus Replication by Interferon Regulatory Factor 1. *J Virol* **78**, 9713-9720.

Kato, T., Date, T., Miyamoto, M., Furusaka, A., Tokushige, K., Mizokami, M. & Wakita, T. (2003). Efficient replication of the genotype 2a hepatitis C virus subgenomic replicon. *Gastroenterology* **125**, 1808-1817.

Kearse, M., Moir, R., Wilson, A., Stones-Havas, S., Cheung, M., Sturrock, S., Buxton, S., Cooper, A., Markowitz, S., Duran, C., Thierer, T., Ashton, B., Meintjes, P. & Drummond, A. (2012). Geneious Basic: an integrated and extendable desktop software platform for the organization and analysis of sequence data. *Bioinformatics (Oxford, England)* **28**, 1647-1649.

Kelly, L., Badhan, A., Roberts, G. C., Mbisa, J. L. & Harris, M. (2017). Manipulation of both virus- and cell-specific factors is required for robust transient replication of a hepatitis C virus genotype 3a sub-genomic replicon. In *The Journal of general virology*, pp. 2495-2506.

Kim, A. Y., Kuntzen, T., Timm, J., Nolan, B. E., Baca, M. A., Reyor, L. L., Berical, A. C., Feller, A. J., Johnson, K. L., Zur Wiesch, J. S., Robbins, G. K., Chung, R. T., Walker, B. D., Carrington, M., Allen, T. M. & Lauer, G. M. (2011). Spontaneous Control of HCV Is Associated With Expression of HLA-B*57 and Preservation of Targeted Epitopes. *Gastroenterology* **140**, 686-U434.

Kim, C. W. & Chang, K. M. (2013). Hepatitis C virus: virology and life cycle. *Clinical and molecular hepatology* **19**, 17-25.

Kim, J. L., Morgenstern, K. A., Lin, C., Fox, T., Dwyer, M. D., Landro, J. A., Chambers, S. P., Markland, W., Lepre, C. A., Omalley, E. T., Harbeson, S. L., Rice, C. M., Murcko, M. A., Caron, P. R. & Thomson, J. A. (1996). Crystal structure of the hepatitis C virus NS3 protease domain complexed with a synthetic NS4A cofactor peptide. *Cell* **87**, 343-355.

Kim, S., Date, T., Yokokawa, H., Kono, T., Aizaki, H., Maurel, P., Gondeau, C. & Wakita, T. (2014). Development of Hepatitis C Virus Genotype 3a Cell Culture System. *Hepatology*.

Kolykhalov, A. A., Feinstone, S. M. & Rice, C. M. (1996). Identification of a highly conserved sequence element at the 3' terminus of hepatitis C virus genome RNA. *J Virol* **70**, 3363-3371.

Kowdley, K. V., Lawitz, E., Poordad, F., Cohen, D. E., Nelson, D. R., Zeuzem, S., Everson, G. T., Kwo, P., Foster, G. R., Sulkowski, M. S., Xie, W., Pilot-Matias, T., Liossis, G., Larsen, L., Khatri, A., Podsadecki, T. & Bernstein,

B. (2014). Phase 2b trial of interferon-free therapy for hepatitis C virus genotype 1. *The New England journal of medicine* **370**, 222-232.

Kumar, S., Stecher, G. & Tamura, K. (2016). MEGA7: Molecular Evolutionary Genetics Analysis Version 7.0 for Bigger Datasets. *Molecular biology and evolution* **33**, 1870-1874.

Kumthip, K., Chusri, P., Jilg, N., Zhao, L., Fusco, D. N., Zhao, H., Goto, K., Cheng, D., Schaefer, E. A., Zhang, L., Pantip, C., Thongsawat, S., O'Brien, A., Peng, L. F., Maneekarn, N., Chung, R. T. & Lin, W. (2012). Hepatitis C virus NS5A disrupts STAT1 phosphorylation and suppresses type I interferon signaling. *J Virol* **86**, 8581-8591.

Lambert, S. M., Langley, D. R., Garnett, J. A., Angell, R., Hedgethorne, K., Meanwell, N. A. & Matthews, S. J. (2014). The crystal structure of NS5A domain 1 from genotype 1a reveals new clues to the mechanism of action for dimeric HCV inhibitors. *Protein Science* **23**, 723-734.

Lauck, M., Alvarado-Mora, M. V., Becker, E. A., Bhattacharya, D., Striker, R., Hughes, A. L., Carrilho, F. J., O'Connor, D. H. & Pinho, J. R. R. (2012). Analysis of Hepatitis C Virus Intrahost Diversity across the Coding Region by Ultradeep Pyrosequencing. *J Virol* **86**, 3952-3960.

Lawitz, E., Mangia, A., Wyles, D., Rodriguez-Torres, M., Hassanein, T., Gordon, S. C., Schultz, M., Davis, M. N., Kayali, Z., Reddy, K. R., Jacobson, I. M., Kowdley, K. V., Nyberg, L., Subramanian, G. M., Hyland, R. H., Arterburn, S., Jiang, D., McNally, J., Brainard, D., Symonds, W. T., McHutchison, J. G., Sheikh, A. M., Younossi, Z. & Gane, E. J. (2013). Sofosbuvir for previously untreated chronic hepatitis C infection. *The New England journal of medicine* **368**, 1878-1887.

Lawitz, E., Poordad, F., Brainard, D. M., Hyland, R. H., An, D., Dvory-Sobol, H., Symonds, W. T., McHutchison, J. G. & Membreno, F. E. (2015). Sofosbuvir with peginterferon-ribavirin for 12 weeks in previously treated patients with hepatitis C genotype 2 or 3 and cirrhosis. *Hepatology* **61**, 769-775.

Lee, S. S., Bain, V. G., Peltekian, K., Krajden, M., Yoshida, E. M., Deschenes, M., Heathcote, J., Bailey, R. J., Simonyi, S. & Sherman, M. (2006). Treating chronic hepatitis C with pegylated interferon alfa-2a (40 KD) and ribavirin in clinical practice. *Alimentary pharmacology & therapeutics* **23**, 397-408.

Lentz, B. R. & Lee, J. K. (1999). Poly(ethylene glycol) (PEG)-mediated fusion between pure lipid bilayers: a mechanism in common with viral fusion and secretory vesicle release? *Molecular membrane biology* **16**, 279-296.

Leroy, V., Angus, P., Bronowicki, J. P., Dore, G. J., Hezode, C., Pianko, S., Pol, S., Stuart, K., Tse, E., McPhee, F., Bhore, R., Jimenez-Exposito, M. J. & Thompson, A. J. (2016). Daclatasvir, sofosbuvir, and ribavirin for hepatitis C

virus genotype 3 and advanced liver disease: A randomized phase III study (ALLY-3+). *Hepatology* **63**, 1430-1441.

Li, J., Yu, X., Wagner, T. E. & Wei, Y. (2014). A biotin-streptavidin-biotin bridge dramatically enhances cell fusion. In *Oncol Lett*, pp. 198-202.

Li, K., Foy, E., Ferreon, J. C., Nakamura, M., Ferreon, A. C. M., Ikeda, M., Ray, S. C., Gale, M. & Lemon, S. M. (2005). Immune evasion by hepatitis C virus NS3/4A protease-mediated cleavage of the Toll-like receptor 3 adaptor protein TRIF. *Proceedings of the National Academy of Sciences of the United States of America* **102**, 2992-2997.

Liang, T. J., Rehermann, B., Seeff, L. B. & Hoofnagle, J. H. (2000). Pathogenesis, Natural History, Treatment, and Prevention of Hepatitis C. *Annals of Internal Medicine* **132**, 296-305.

Lindenbach, B. D., Murray, C. L., Thiel, H. J. & Rice, C. M. (2013). In *Fields Virology*, Knipe, D. M. & Howley, P. M. edn, pp. 712–746: Lippincott Williams & Wilkins.

Lindenbach, B. D. & Rice, C. M. (2013). The ins and outs of hepatitis C virus entry and assembly. *Nat Rev Micro* **11**, 688-700.

Liu, W. L., Su, W. C., Cheng, C. W., Hwang, L. H., Wang, C. C., Chen, H. L., Chen, D. S. & Lai, M. Y. (2007). Ribavirin up-regulates the activity of double-stranded RNA-activated protein kinase and enhances the action of interferon-alpha against hepatitis C virus. *The Journal of infectious diseases* **196**, 425-434.

Lohmann, V., Hoffmann, S., Herian, U., Penin, F. & Bartenschlager, R. (2003). Viral and cellular determinants of hepatitis C virus RNA replication in cell culture. *J Virol* **77**, 3007-3019.

Lohmann, V., Korner, F., Dobierzewska, A. & Bartenschlager, R. (2001). Mutations in hepatitis C virus RNAs conferring cell culture adaptation. *J Virol* **75**, 1437-1449.

Lohmann, V., Korner, F., Koch, J., Herian, U., Theilmann, L. & Bartenschlager, R. (1999). Replication of subgenomic hepatitis C virus RNAs in a hepatoma cell line. *Science* **285**, 110-113.

Lontok, E., Harrington, P., Howe, A., Kieffer, T., Lennerstrand, J., Lenz, O., McPhee, F., Mo, H., Parkin, N., Pilot-Matias, T. & Miller, V. (2015). Hepatitis C virus drug resistance-associated substitutions: State of the art summary. *Hepatology* **62**, 1623-1632.

Love, R. A., Brodsky, O., Hickey, M. J., Wells, P. A. & Cronin, C. N. (2009). Crystal Structure of a Novel Dimeric Form of NS5A Domain I Protein from Hepatitis C Virus. *Journal of Virology* **83**, 4395-4403.

Lovy, A., Molina, A. J., Cerqueira, F. M., Trudeau, K. & Shirihai, O. S. (2012). A faster, high resolution, mtPA-GFP-based mitochondrial fusion assay acquiring

kinetic data of multiple cells in parallel using confocal microscopy. *Journal of visualized experiments : JoVE*, e3991.

Lundin, M., Lindstrom, H., Gronwall, C. & Persson, M. A. A. (2006). Dual topology of the processed hepatitis C virus protein NS4B is influenced by the NS5A protein. *Journal of General Virology* **87**, 3263-3272.

Lupberger, J., Zeisel, M. B., Xiao, F., Thumann, C., Fofana, I., Zona, L., Davis, C., Mee, C. J., Turek, M., Gorke, S., Royer, C., Fischer, B., Zahid, M. N., Lavillette, D., Fresquet, J., Cosset, F. L., Rothenberg, S. M., Pietschmann, T., Patel, A. H., Pessaux, P., Doffoel, M., Raffelsberger, W., Poch, O., McKeating, J. A., Brino, L. & Baumert, T. F. (2011). EGFR and EphA2 are host factors for hepatitis C virus entry and possible targets for antiviral therapy. *Nat Med* **17**, 589-595.

Lutchman, G., Danehower, S., Song, B. C., Liang, T. J., Hoofnagle, J. H., Thomson, M. & Ghany, M. G. (2007). Mutation Rate of the Hepatitis C Virus NS5B in Patients Undergoing Treatment With Ribavirin Monotherapy. *Gastroenterology* **132**, 1757-1766.

Maag, D., Castro, C., Hong, Z. & Cameron, C. E. (2001). Hepatitis C virus RNA-dependent RNA polymerase (NS5B) as a mediator of the antiviral activity of ribavirin. *The Journal of biological chemistry* **276**, 46094-46098.

Magiorkinis, G., Magiorkinis, E., Paraskevis, D., Ho, S. Y., Shapiro, B., Pybus, O. G., Allain, J. P. & Hatzakis, A. (2009). The global spread of hepatitis C virus 1a and 1b: a phylodynamic and phylogeographic analysis. *PLoS medicine* **6**, e1000198.

Mahlakoiv, T., Ritz, D., Mordstein, M., DeDiego, M. L., Enjuanes, L., Mueller, M. A., Drosten, C. & Staeheli, P. (2012). Combined action of type I and type III interferon restricts initial replication of severe acute respiratory syndrome coronavirus in the lung but fails to inhibit systemic virus spread. *Journal of General Virology* **93**, 2601-2605.

Malinoski, F. & Stollar, V. (1981). Inhibitors of IMP dehydrogenase prevent sindbis virus replication and reduce GTP levels in Aedes albopictus cells. *Virology* **110**, 281-289.

Manns, M., Marcellin, P., Poordad, F., de Araujo, E. S., Buti, M., Horsmans, Y., Janczewska, E., Villamil, F., Scott, J., Peeters, M., Lenz, O., Ouwerkerk-Mahadevan, S., De La Rosa, G., Kalmeijer, R., Sinha, R. & Beumont-Mauviel, M. (2014). Simeprevir with pegylated interferon alfa 2a or 2b plus ribavirin in treatment-naive patients with chronic hepatitis C virus genotype 1 infection (QUEST-2): a randomised, double-blind, placebo-controlled phase 3 trial. *Lancet* **384**, 414-426.

Manns, M. P., McHutchison, J. G., Gordon, S. C., Rustgi, V. K., Shiffman, M., Reindollar, R., Goodman, Z. D., Koury, K., Ling, M. H., Albrecht, J. K. & Int Hepatitis Interventional, T. (2001). Peginterferon alfa-2b plus ribavirin

compared with interferon alfa-2b plus ribavirin for initial treatment of chronic hepatitis C: a randomised trial. *Lancet* **358**, 958-965.

Marino, R., Deibis, L., De Sanctis, J. B., Bianco, N. E. & Toro, F. (2005). Interaction of immune complexes isolated from hepatitis C virus-infected individuals with human cell lines. *Medical microbiology and immunology* **194**, 73-80.

Markland, W., McQuaid, T. J., Jain, J. & Kwong, A. D. (2000). Broad-spectrum antiviral activity of the IMP dehydrogenase inhibitor VX-497: a comparison with ribavirin and demonstration of antiviral additivity with alpha interferon. *Antimicrobial agents and chemotherapy* **44**, 859-866.

Marks, K. M. & Jacobson, I. M. (2012). The first wave: HCV NS3 protease inhibitors telaprevir and boceprevir. *Antiviral therapy* **17**, 1119-1131.

Martell, M., Esteban, J. I., Quer, J., Genescà, J., Weiner, A., Esteban, R., Guardia, J. & Gómez, J. (1992). Hepatitis C virus (HCV) circulates as a population of different but closely related genomes: quasispecies nature of HCV genome distribution. *J Virol* **66**, 3225-3229.

McHutchison, J. G., Gordon, S. C., Schiff, E. R., Shiffman, M. L., Lee, W. M., Rustgi, V. K., Goodman, Z. D., Ling, M. H., Cort, S. & Albrecht, J. K. (1998). Interferon alfa-2b alone or in combination with ribavirin as initial treatment for chronic hepatitis C. Hepatitis Interventional Therapy Group. *The New England journal of medicine* **339**, 1485-1492.

McLauchlan, J. (2000). Properties of the hepatitis C virus core protein: a structural protein that modulates cellular processes. *Journal of Viral Hepatitis* **7**, 2-14.

Mellor, J., Haydon, G., Blair, C., Livingstone, W. & Simmonds, P. (1998). Low level or absent in vivo replication of hepatitis C virus and hepatitis G virus GB virus C in peripheral blood mononuclear cells. *Journal of General Virology* **79**, 705-714.

Messina, J. P., Humphreys, I., Flaxman, A., Brown, A., Cooke, G. S., Pybus, O. G. & Barnes, E. (2015). Global distribution and prevalence of hepatitis C virus genotypes. *Hepatology* **61**, 77-87.

Meuleman, P., Catanese, M. T., Verhoye, L., Desombere, I., Farhoudi, A., Jones, C. T., Sheahan, T., Grzyb, K., Cortese, R., Rice, C. M., Leroux-Roels, G. & Nicosia, A. (2012). A human monoclonal antibody targeting SR-BI precludes hepatitis C virus infection and viral spread in vitro and in vivo. *Hepatology* **55**, 364-372.

Meylan, E., Curran, J., Hofmann, K., Moradpour, D., Binder, M., Bartenschlager, R. & Tschopp, R. (2005). Cardif is an adaptor protein in the RIG-I antiviral pathway and is targeted by hepatitis C virus. *Nature* **437**, 1167-1172.

Middleton, T., He, Y., Pilot-Matias, T., Tripathi, R., Lim, B. H., Roth, A., Chen, C. M., Koev, G., Ng, T. I., Krishnan, P., Pithawalla, R., Mondal, R., Dekhtyar, T., Lu, L., Mo, H., Kati, W. M. & Molla, A. (2007). A replicon-based shuttle

vector system for assessing the phenotype of HCV NS5B polymerase genes isolated from patient populations. *Journal of virological methods* **145**, 137-145.

Mihalik, K. B. & Feigelstock, D. A. (2013). Sensitivity of a Ribavirin Resistant Mutant of Hepatitis C Virus to Other Antiviral Drugs. *Plos One* **8**.

Miller, J. P., Kigwana, L. J., Streeter, D. G., Robins, R. K., Simon, L. N. & Roboz, J. (1977). The relationship between the metabolism of ribavirin and its proposed mechanism of action. *Annals of the New York Academy of Sciences* **284**, 211-229.

Miyanari, Y., Atsuzawa, K., Usuda, N., Watashi, K., Hishiki, T., Zayas, M., Bartenschlager, R., Wakita, T., Hijikata, M. & Shimotohno, K. (2007). The lipid droplet is an important organelle for hepatitis C virus production. *Nat Cell Biol* **9**, 1089-U1074.

Miyanari, Y., Hijikata, M., Yamaji, M., Hosaka, M., Takahashi, H. & Shimotohno, K. (2003). Hepatitis C virus non-structural proteins in the probable membranous compartment function in viral genome replication. *The Journal of biological chemistry* **278**, 50301-50308.

Monazahian, M., Bohme, I., Bonk, S., Koch, A., Scholz, C., Grethe, S. & Thomssen, R. (1999). Low density lipoprotein receptor as a candidate receptor for hepatitis C virus. *J Med Virol* **57**, 223-229.

Moradpour, D. & Penin, F. (2013). Hepatitis C virus proteins: from structure to function. *Curr Top Microbiol Immunol* **369**, 113-142.

Mukhopadhyay, S., Kuhn, R. J. & Rossmann, M. G. (2005). A structural perspective of the flavivirus life cycle. *Nat Rev Microbiol* **3**, 13-22.

Murayama, A., Date, T., Morikawa, K., Akazawa, D., Miyamoto, M., Kaga, M., Ishii, K., Suzuki, T., Kato, T., Mizokami, M. & Wakita, T. (2007). The NS3 helicase and NS5B-to-3'X regions are important for efficient hepatitis C virus strain JFH-1 replication in Huh7 cells. *J Virol* **81**, 8030-8040.

Murray, C. L., Jones, C. T. & Rice, C. M. (2008). Architects of assembly: roles of Flaviviridae non-structural proteins in virion morphogenesis. *Nat Rev Microbiol* **6**, 699-708.

Nelson, D. R., Cooper, J. N., Lalezari, J. P., Lawitz, E., Pockros, P. J., Gitlin, N., Freilich, B. F., Younes, Z. H., Harlan, W., Ghalib, R., Oguchi, G., Thuluvath, P. J., Ortiz-Lasanta, G., Rabinovitz, M., Bernstein, D., Bennett, M., Hawkins, T., Ravendhran, N., Sheikh, A. M., Varunok, P., Kowdley, K. V., Hennicken, D., McPhee, F., Rana, K. & Hughes, E. A. (2015). All-oral 12-week treatment with daclatasvir plus sofosbuvir in patients with hepatitis C virus genotype 3 infection: ALLY-3 phase III study. *Hepatology* **61**, 1127-1135.

Nielsen, S. U., Bassendine, M. F., Burt, A. D., Bevitt, D. J. & Toms, G. L. (2004). Characterization of the genome and structural proteins of hepatitis C virus

resolved from infected human liver. *The Journal of general virology* **85**, 1497-1507.

Ning, Q., Brown, D., Parodo, J., Cattral, M., Gorczynski, R., Cole, E., Fung, L., Ding, J. W., Liu, M. F., Rotstein, O., Phillips, M. J. & Levy, G. (1998). Ribavirin inhibits viral-induced macrophage production of TNF, IL-1, the procoagulant fgl2 prothrombinase and preserves Th1 cytokine production but inhibits Th2 cytokine response. *J Immunol* **160**, 3487-3493.

Okada, Y. (1993). Sendai virus-induced cell fusion. *Methods Enzymol* **221**, 18-41.

Ortega-Prieto, A. M. & Dorner, M. (2016). The expanding toolbox for hepatitis C virus research. *J Viral Hepat* **23**, 320-329.

Paul, D., Romero-Brey, I., Gouttenoire, J., Stoitsova, S., Krijnse-Locker, J., Moradpour, D. & Bartenschlager, R. (2011). NS4B self-interaction through conserved C-terminal elements is required for the establishment of functional hepatitis C virus replication complexes. *J Virol* **85**, 6963-6976.

Pawlotsky, J.-M. (2013). NS5A inhibitors in the treatment of hepatitis C. *Journal of hepatology* **59**, 375-382.

Pawlotsky, J. M., Dahari, H., Neumann, A. U., Hezode, C., Germanidis, G., Lonjon, I., Castera, L. & Dhumeaux, D. (2004). Antiviral action of ribavirin in chronic hepatitis C. *Gastroenterology* **126**, 703-714.

Pawlotsky, J. M., Germanidis, G., Neumann, A. U., Pellerin, M., Frainais, P. O. & Dhumeaux, D. (1998a). Interferon resistance of hepatitis C virus genotype 1b: Relationship to nonstructural 5A gene quasispecies mutations. *Journal of Virology* **72**, 2795-2805.

Pawlotsky, J. M., Pellerin, M., Bouvier, M., Roudot-Thoraval, F., Germanidis, G., Bastie, A., Darthuy, F., Remire, J., Soussy, C. J. & Dhumeaux, D. (1998b). Genetic complexity of the hypervariable region 1 (HVR1) of hepatitis C virus (HCV): Influence on the characteristics of the infection and responses to interferon alfa therapy in patients with chronic hepatitis C. *Journal of Medical Virology* **54**, 256-264.

Petracca, R., Falugi, F., Galli, G., Norais, N., Rosa, D., Campagnoli, S., Burgio, V., Di Stasio, E., Giardina, B., Houghton, M., Abrignani, S. & Grandi, G.

(2000). Structure-function analysis of hepatitis C virus envelope-CD81 binding. *J Virol* **74**, 4824-4830.

Pfeiffer, J. K. & Kirkegaard, K. (2005a). Ribavirin resistance in hepatitis C virus replicon-containing cell lines conferred by changes in the cell line or mutations in the replicon RNA. *J Virol* **79**, 2346-2355.

Pfeiffer, J. K. & Kirkegaard, K. (2005b). Ribavirin Resistance in Hepatitis C Virus Replicon-Containing Cell Lines Conferred by Changes in the Cell Line or Mutations in the Replicon RNA.

Pham, T. N. Q., King, D., Macparland, S. A., McGrath, J. S., Reddy, S. B., Bursey, F. R. & Michalak, T. I. (2008). Hepatitis C virus replicates in the same immune cell subsets in chronic hepatitis C and occult infection. *Gastroenterology* **134**, 812-822.

Pietschmann, T., Zayas, M., Meuleman, P., Long, G., Appel, N., Koutsoudakis, G., Kallis, S., Leroux-Roels, G., Lohmann, V. & Bartenschlager, R. (2009). Production of infectious genotype 1b virus particles in cell culture and impairment by replication enhancing mutations. *PLoS Pathog* **5**, e1000475.

Pileri, P., Uematsu, Y., Campagnoli, S., Galli, G., Falugi, F., Petracca, R., Weiner, A. J., Houghton, M., Rosa, D., Grandi, G. & Abrignani, S. (1998). Binding of hepatitis C virus to CD81. *Science* **282**, 938-941.

Ploss, A., Evans, M. J., Gaysinskaya, V. A., Panis, M., You, H., de Jong, Y. P. & Rice, C. M. (2009). Human occludin is a hepatitis C virus entry factor required for infection of mouse cells. *Nature* **457**, 882-886.

Poch, O., Sauvaget, I., Delarue, M. & Tordo, N. (1989). Identification of four conserved motifs among the RNA-dependent polymerase encoding elements. *The EMBO journal* **8**, 3867-3874.

Podbilewicz, B. (2014). Virus and cell fusion mechanisms. *Annual review of cell and developmental biology* **30**, 111-139.

Poenisch, M., Metz, P., Blankenburg, H., Ruggieri, A., Lee, J. Y., Rupp, D., Rebhan, I., Diederich, K., Kaderali, L., Domingues, F. S., Albrecht, M., Lohmann, V., Erfle, H. & Bartenschlager, R. (2015). Identification of HNRNPK as regulator of hepatitis C virus particle production. *PLoS Pathog* **11**, e1004573.

Polyak, S. J., McArdle, S., Liu, S. L., Sullivan, D. G., Chung, M. J., Hofgartner, W. T., Carithers, R. L., McMahon, B. J., Mullins, J. I., Corey, L. & Gretch, D. R. (1998). Evolution of hepatitis C virus quasispecies in hypervariable region 1 and the putative interferon sensitivity-determining region during interferon therapy and natural infection. *Journal of Virology* **72**, 4288-4296.

Poordad, F., McCone, J., Jr., Bacon, B. R., Bruno, S., Manns, M. P., Sulkowski, M. S., Jacobson, I. M., Reddy, K. R., Goodman, Z. D., Boparai, N., DiNubile, M. J., Sniukiene, V., Brass, C. A., Albrecht, J. K. & Bronowicki, J. P. (2011).

Boceprevir for untreated chronic HCV genotype 1 infection. *The New England journal of medicine* **364**, 1195-1206.

Poordad, F., Schiff, E. R., Vierling, J. M., Landis, C., Fontana, R. J., Yang, R., McPhee, F., Hughes, E. A., Noviello, S. & Swenson, E. S. (2016). Daclatasvir with sofosbuvir and ribavirin for hepatitis C virus infection with advanced cirrhosis or post-liver transplantation recurrence. *Hepatology* **63**, 1493-1505.

Powdrill, M. H., Tchesnokov, E. P., Kozak, R. A., Russell, R. S., Martin, R., Svarovskaia, E. S., Mo, H., Kouyos, R. D. & Gotte, M. (2011). Contribution of a mutational bias in hepatitis C virus replication to the genetic barrier in the development of drug resistance. *Proc Natl Acad Sci U S A* **108**, 20509-20513.

Poynard, T., Marcellin, P., Lee, S. S., Niederau, C., Minuk, G. S., Ideo, G., Bain, V., Heathcote, J., Zeuzem, S., Trepo, C. & Albrecht, J. (1998). Randomised trial of interferon alpha2b plus ribavirin for 48 weeks or for 24 weeks versus interferon alpha2b plus placebo for 48 weeks for treatment of chronic infection with hepatitis C virus. International Hepatitis Interventional Therapy Group (IHIT). *Lancet* **352**, 1426-1432.

Pybus, O. G., Cochrane, A., Holmes, E. C. & Simmonds, P. (2005). The hepatitis C virus epidemic among injecting drug users. *Infection, genetics and evolution : journal of molecular epidemiology and evolutionary genetics in infectious diseases* **5**, 131-139.

Qashqari, H., Al-Mars, A., Chaudhary, A., Abuzenadah, A., Damanhouri, G., Alqahtani, M., Mahmoud, M., El Sayed Zaki, M., Fatima, K. & Qadri, I. (2013). Understanding the molecular mechanism(s) of hepatitis C virus (HCV) induced interferon resistance. *Infection, genetics and evolution : journal of molecular epidemiology and evolutionary genetics in infectious diseases* **19**, 113-119.

Qin, W., Yamashita, T., Shirota, Y., Lin, Y., Wei, W. & Murakami, S. (2001). Mutational analysis of the structure and functions of hepatitis C virus RNA-dependent RNA polymerase. *Hepatology* **33**, 728-737.

Rahman, F., Heller, T., Sobao, Y., Mizukoshi, E., Nascimbeni, M., Alter, H., Herrine, S., Hoofnagle, J., Liang, T. J. & Rehermann, B. (2004). Effects of antiviral therapy on the cellular immune response in acute hepatitis C. *Hepatology* **40**, 87-97.

Ramirez, S., Mikkelsen, L. S., Gottwein, J. M. & Bukh, J. (2016). Robust HCV Genotype 3a Infectious Cell Culture System Permits Identification of Escape Variants With Resistance to Sofosbuvir. *Gastroenterology* **151**, 973-985.e972.

Razavi, H. (2017). Hepatitis C virus prevalence and level of intervention required to achieve the WHO targets for elimination in the European Union by 2030: a modelling study. *The lancet Gastroenterology & hepatology* **2**, 325-336.

Reiss, S., Harak, C., Romero-Brey, I., Radujkovic, D., Klein, R., Ruggieri, A., Rebhan, I., Bartenschlager, R. & Lohmann, V. (2013). The Lipid Kinase

Phosphatidylinositol-4 Kinase III Alpha Regulates the Phosphorylation Status of Hepatitis C Virus NS5A. *Plos Pathogens* **9**.

Reiss, S., Rebhan, I., Backes, P., Romero-Brey, I., Erfle, H., Matula, P., Kaderali, L., Poenisch, M., Blankenburg, H., Hiet, M. S., Longerich, T., Diehl, S., Ramirez, F., Balla, T., Rohr, K., Kaul, A., Buhler, S., Pepperkok, R., Lengauer, T., Albrecht, M., Eils, R., Schirmacher, P., Lohmann, V. & Bartenschlager, R. (2011). Recruitment and activation of a lipid kinase by hepatitis C virus NS5A is essential for integrity of the membranous replication compartment. *Cell host & microbe* **9**, 32-45.

Roberts, A. P., Lewis, A. P. & Jopling, C. L. (2011). miR-122 activates hepatitis C virus translation by a specialized mechanism requiring particular RNA components. *Nucleic Acids Res* **39**, 7716-7729.

Roelandt, P., Obeid, S., Paeshuyse, J., Vanhove, J., Van Lommel, A., Nahmias, Y., Nevens, F., Neyts, J. & Verfaillie, C. M. (2012). Human pluripotent stem cell-derived hepatocytes support complete replication of hepatitis C virus. *Journal of hepatology* **57**, 246-251.

Romero-Gomez, M. (2006). Insulin resistance and hepatitis C. *World Journal of Gastroenterology* **12**, 7075-7080.

Ross-Thriepland, D. & Harris, M. (2015). Hepatitis C virus NS5A: enigmatic but still promiscuous 10 years on! *The Journal of general virology* **96**, 727-738.

Sa-ngiamsuntorn, K., Wongkajornsilp, A., Phanthong, P., Borwornpinyo, S., Kitiyanant, N., Chantratita, W. & Hongeng, S. (2016a). A robust model of natural hepatitis C infection using hepatocyte-like cells derived from human induced pluripotent stem cells as a long-term host. *Virology Journal* **13**, 59.

Sa-Ngiamsuntorn, K., Wongkajornsilp, A., Phanthong, P., Borwornpinyo, S., Kitiyanant, N., Chantratita, W. & Hongeng, S. (2016b). A robust model of natural hepatitis C infection using hepatocyte-like cells derived from human induced pluripotent stem cells as a long-term host. *Virol J* **13**, 59.

Saeed, M., Andreo, U., Chung, H.-Y., Espiritu, C., Branch, A. D., Silva, J. M. & Rice, C. M. (2015). SEC14L2 enables pan-genotype HCV replication in cell culture. *Nature* **524**, 471-475.

Saeed, M., Gondeau, C., Hmwe, S., Yokokawa, H., Date, T., Suzuki, T., Kato, T., Maurel, P. & Wakita, T. (2013). Replication of Hepatitis C Virus Genotype 3a in Cultured Cells. *Gastroenterology* **144**, 56-U137.

Saeed, M., Scheel, T. K. H., Gottwein, J. M., Marukian, S., Dustin, L. B., Bukh, J. & Rice, C. M. (2012). Efficient Replication of Genotype 3a and 4a Hepatitis C

Virus Replicons in Human Hepatoma Cells. In *Antimicrobial agents and chemotherapy*, pp. 5365-5373.

Saito, T., Owen, D. M., Jiang, F., Marcotrigiano, J. & Gale, M. (2008). Innate immunity induced by composition-dependent RIG-I recognition of Hepatitis C virus RNA. *Nature* **454**, 523-527.

Santolini, E., Migliaccio, G. & Lamonica, N. (1994). BIOSYNTHESIS AND BIOCHEMICAL-PROPERTIES OF THE HEPATITIS-C VIRUS CORE PROTEIN. *Journal of Virology* **68**, 3631-3641.

Scarselli, E., Ansuini, H., Cerino, R., Roccasecca, R. M., Acali, S., Filocamo, G., Traboni, C., Nicosia, A., Cortese, R. & Vitelli, A. (2002). The human scavenger receptor class B type I is a novel candidate receptor for the hepatitis C virus. *The EMBO journal* **21**, 5017-5025.

Scheel, T. K. H. & Rice, C. M. (2013). Understanding the hepatitis C virus life cycle paves the way for highly effective therapies. *Nature Medicine* **19**, 837-849.

Schneiderman, S., Farber, J. L. & Baserga, R. (1979). A simple method for decreasing the toxicity of polyethylene glycol in mammalian cell hybridization. *Somatic cell genetics* **5**, 263-269.

Schregel, V., Jacobi, S., Penin, F. & Tautz, N. (2009). Hepatitis C virus NS2 is a protease stimulated by cofactor domains in NS3. *Proc Natl Acad Sci U S A* **106**, 5342-5347.

Schwartz, R. E., Trehan, K., Andrus, L., Sheahan, T. P., Ploss, A., Duncan, S. A., Rice, C. M. & Bhatia, S. N. (2012). Modeling hepatitis C virus infection using human induced pluripotent stem cells. *Proc Natl Acad Sci U S A* **109**, 2544-2548.

Sharma, N. R., Mateu, G., Dreux, M., Grakoui, A., Cosset, F. L. & Melikyan, G. B. (2011). Hepatitis C virus is primed by CD81 protein for low pH-dependent fusion. *The Journal of biological chemistry* **286**, 30361-30376.

Shiffman, M. L., Di Bisceglie, A. M., Lindsay, K. L., Morishima, C., Wright, E. C., Everson, G. T., Lok, A. S., Morgan, T. R., Bonkovsky, H. L., Lee, W. M., Dienstag, J. L., Ghany, M. G., Goodman, Z. D., Everhart, J. E. & Grp, H.-C. T. (2004). Peginterferon alfa-2a and ribavirin in patients with chronic hepatitis C who have failed prior treatment. *Gastroenterology* **126**, 1015-1023.

Shimakami, T., Hijikata, M., Luo, H., Ma, Y. Y., Kaneko, S., Shimotohno, K. & Murakami, S. (2004). Effect of interaction between hepatitis C virus NS5A and NS5B on hepatitis C virus RNA replication with the hepatitis C virus replicon. *J Virol* **78**, 2738-2748.

Shirota, Y., Luo, H., Qin, W., Kaneko, S., Yamashita, T., Kobayashi, K. & Murakami, S. (2002). Hepatitis C virus (HCV) NS5A binds RNA-dependent

RNA polymerase (RdRP) NS5B and modulates RNA-dependent RNA polymerase activity. *The Journal of biological chemistry* **277**, 11149-11155.

Simister, P., Schmitt, M., Geitmann, M., Wicht, O., Danielson, U. H., Klein, R., Bressanelli, S. & Lohmann, V. (2009). Structural and functional analysis of hepatitis C virus strain JFH1 polymerase. *J Virol* **83**, 11926-11939.

Sofia, M. J., Bao, D., Chang, W., Du, J., Nagarathnam, D., Rachakonda, S., Reddy, P. G., Ross, B. S., Wang, P., Zhang, H. R., Bansal, S., Espiritu, C., Keilman, M., Lam, A. M., Steuer, H. M., Niu, C., Otto, M. J. & Furman, P. A. (2010). Discovery of a beta-d-2'-deoxy-2'-alpha-fluoro-2'-beta-C-methyluridine nucleotide prodrug (PSI-7977) for the treatment of hepatitis C virus. *Journal of medicinal chemistry* **53**, 7202-7218.

Sommereyns, C., Paul, S., Staeheli, P. & Michiels, T. (2008). IFN-lambda (IFN-lambda) is expressed in a tissue-dependent fashion and primarily acts on epithelial cells in vivo. *Plos Pathogens* **4**.

Sourisseau, M., Michta, M. L., Zony, C., Israelow, B., Hopcraft, S. E., Narbus, C. M., Parra Martin, A. & Evans, M. J. (2013). Temporal analysis of hepatitis C virus cell entry with occludin directed blocking antibodies. *PLoS Pathog* **9**, e1003244.

Streeter, D. G., Witkowski, J. T., Khare, G. P., Sidwell, R. W., Bauer, R. J., Robins, R. K. & Simon, L. N. (1973). Mechanism of action of 1- -D-ribofuranosyl-1,2,4-triazole-3-carboxamide (Virazole), a new broad-spectrum antiviral agent. *Proc Natl Acad Sci U S A* **70**, 1174-1178.

Su, W.-C., Liu, W.-L., Cheng, C.-W., Chou, Y.-B., Hung, K.-H., Huang, W.-H., Wu, C.-L., Li, Y.-T., Shiau, A.-L. & Lai, M.-Y. (2009). Ribavirin enhances interferon signaling via stimulation of mTOR and p53 activities. *FEBS Letters* **583**, 2793-2798.

Sulkowski, M. S., Gardiner, D. F., Rodriguez-Torres, M., Reddy, K. R., Hassanein, T., Jacobson, I., Lawitz, E., Lok, A. S., Hinestrosa, F., Thuluvath, P. J., Schwartz, H., Nelson, D. R., Everson, G. T., Eley, T., Wind-Rotolo, M., Huang, S. P., Gao, M., Hernandez, D., McPhee, F., Sherman, D., Hindes, R., Symonds, W., Pasquinelli, C. & Grasela, D. M. (2014). Daclatasvir plus sofosbuvir for previously treated or untreated chronic HCV infection. *The New England journal of medicine* **370**, 211-221.

Sumpter, R., Jr., Loo, Y. M., Foy, E., Li, K., Yoneyama, M., Fujita, T., Lemon, S. M. & Gale, M., Jr. (2005). Regulating intracellular antiviral defense and permissiveness to hepatitis C virus RNA replication through a cellular RNA helicase, RIG-I. *J Virol* **79**, 2689-2699.

Sung, P. S., Cheon, H., Cho, C. H., Hong, S. H., Park, D. Y., Seo, H. I., Park, S. H., Yoon, S. K., Stark, G. R. & Shin, E. C. (2015). Roles of unphosphorylated

ISGF3 in HCV infection and interferon responsiveness. *Proc Natl Acad Sci U S A* **112**, 10443-10448.

Svarovskaia, E. S., Dvory-Sobol, H., Parkin, N., Hebner, C., Gontcharova, V., Martin, R., Ouyang, W., Han, B., Xu, S., Ku, K., Chiu, S., Gane, E., Jacobson, I. M., Nelson, D. R., Lawitz, E., Wyles, D. L., Bekele, N., Brainard, D., Symonds, W. T., McHutchison, J. G., Miller, M. D. & Mo, H. (2014). Infrequent development of resistance in genotype 1-6 hepatitis C virus-infected subjects treated with sofosbuvir in phase 2 and 3 clinical trials. *Clinical infectious diseases : an official publication of the Infectious Diseases Society of America* **59**, 1666-1674.

Taliani, G., Gemignani, G., Ferrari, C., Aceti, A., Bartolozzi, D., Blanc, P. L., Capanni, M., Esperti, F., Forte, P., Guadagnino, V., Mari, T., Marino, N., Milani, S., Pasquazzi, C., Rosina, F., Tacconi, D., Toti, M., Zignego, A. L., Messerini, L., Stroffolini, T. & Nonresponder Retreatment, G. (2006). Pegylated interferon alfa-2b plus ribavirin in the retreatment of interferon-ribavirin nonresponder patients. *Gastroenterology* **130**, 1098-1106.

Tam, R. C., Pai, B., Bard, J., Lim, C., Averett, D. R., Phan, U. T. & Milovanovic, T. (1999). Ribavirin polarizes human T cell responses towards a Type 1 cytokine profile. *Journal of hepatology* **30**, 376-382.

Targett-Adams, P., Hope, G., Boulant, S. & McLauchlan, J. (2008). Maturation of hepatitis C virus core protein by signal peptide peptidase is required for virus production. *Journal of Biological Chemistry* **283**, 16850-16859.

Targett-Adams, P. & McLauchlan, J. (2005). Development and characterization of a transient-replication assay for the genotype 2a hepatitis C virus subgenomic replicon. *The Journal of general virology* **86**, 3075-3080.

Tellinghuisen, T. L., Evans, M. J., von Hahn, T., You, S. & Rice, C. M. (2007). Studying hepatitis C virus: Making the best of a bad virus. *Journal of Virology* **81**, 8853-8867.

Tellinghuisen, T. L., Foss, K. L., Treadaway, J. C. & Rice, C. M. (2008). Identification of residues required for RNA replication in domains II and III of the hepatitis C virus NS5A protein. *Journal of Virology* **82**, 1073-1083.

Tellinghuisen, T. L., Marcotrigiano, J., Gorbalenya, A. E. & Rice, C. M. (2004). The NS5A protein of hepatitis C virus is a zinc metalloprotein. *Journal of Biological Chemistry* **279**, 48576-48587.

Thiagarajan, P. & Ryder, S. D. (2015). The hepatitis C revolution part 1: antiviral treatment options. *Curr Opin Infect Dis* **28**, 563-571.

Thomas, E., Ghany, M. G. & Liang, T. J. (2013). The application and mechanism of action of ribavirin in therapy of hepatitis C. *Antiviral chemistry & chemotherapy* **23**, 1-12.

Thompson, A., Roberts, S., Cheng, W., Angus, P., Visvanathan, K., Iyer, R. & Barclay, M. (2015). LP40 : SB 9200, A novel immunomodulator for patients

with viral hepatitis: Phase 1 mad study in patients with hepatitis c virus (HCV) infection. *Journal of hepatology* **62**.

Thomson, E., Ip, C. L., Badhan, A., Christiansen, M. T., Adamson, W., Ansari, M. A., Bibby, D., Breuer, J., Brown, A., Bowden, R., Bryant, J., Bonsall, D., Da Silva Filipe, A., Hinds, C., Hudson, E., Klenerman, P., Lythgow, K., Mbisa, J. L., McLauchlan, J., Myers, R., Piazza, P., Roy, S., Trebes, A., Sreenu, V. B., Witteveldt, J., Barnes, E. & Simmonds, P. (2016). Comparison of Next-Generation Sequencing Technologies for Comprehensive Assessment of Full-Length Hepatitis C Viral Genomes. *J Clin Microbiol* **54**, 2470-2484.

Tillmann, H. L., Thompson, A. J., Patel, K., Wiese, M., Tenckhoff, H., Nischalke, H. D., Lokhnygina, Y., Kullig, U., Gobel, U., Capka, E., Wiegand, J., Schiefke, I., Guthoff, W., Grungreiff, K., Konig, I., Spengler, U., McCarthy, J., Shianna, K. V., Goldstein, D. B., McHutchison, J. G., Timm, J. & Nattermann, J. (2010). A polymorphism near IL28B is associated with spontaneous clearance of acute hepatitis C virus and jaundice. *Gastroenterology* **139**, 1586-1592, 1592.e1581.

Tokumoto, Y., Hiasa, Y., Uesugi, K., Watanabe, T., Mashiba, T., Abe, M., Kumagi, T., Ikeda, Y., Matsuura, B. & Onji, M. (2012). Ribavirin regulates hepatitis C virus replication through enhancing interferon-stimulated genes and interleukin 8. *The Journal of infectious diseases* **205**, 1121-1130.

Tsai, S. L., Chen, Y. M., Chen, M. H., Huang, C. Y., Sheen, I. S., Yeh, C. T., Huang, J. H., Kuo, G. C. & Liaw, Y. F. (1998). Hepatitis c virus variants circumventing cytotoxic T lymphocyte activity as a mechanism of chronicity. *Gastroenterology* **115**, 954-966.

Vieyres, G., Thomas, X., Descamps, V., Duverlie, G., Patel, A. H. & Dubuisson, J. (2010). Characterization of the envelope glycoproteins associated with infectious hepatitis C virus. *J Virol* **84**, 10159-10168.

Vignuzzi, M., Wendt, E. & Andino, R. (2008). Engineering attenuated virus vaccines by controlling replication fidelity. *Nature Medicine* **14**, 154-161.

Waheed, Y., Saeed, U., Anjum, S., Afzal, M. S. & Ashraf, M. (2012). Development of Global Consensus Sequence and Analysis of Highly Conserved Domains of the HCV NS5B Protein. *Hepat Mon* **12**.

Wakita, T., Pietschmann, T., Kato, T., Date, T., Miyamoto, M., Zhao, Z., Murthy, K., Habermann, A., Kräusslich, H. G., Mizokami, M., Bartenschlager, R. &

Liang, T. J. (2005). Production of infectious hepatitis C virus in tissue culture from a cloned viral genome. *Nat Med* **11**, 791-796.

Wang, C., Sarnow, P. & Siddiqui, A. (1993). Translation of human hepatitis C virus RNA in cultured cells is mediated by an internal ribosome-binding mechanism. *J Virol* **67**, 3338-3344.

Wang, C., Valera, L., Jia, L., Kirk, M. J., Gao, M. & Fridell, R. A. (2013). In Vitro Activity of Daclatasvir on Hepatitis C Virus Genotype 3 NS5A. *Antimicrobial agents and chemotherapy* **57**, 611-613.

Welzel, T. M., Dultz, G. & Zeuzem, S. (2014). Interferon-free antiviral combination therapies without nucleosidic polymerase inhibitors. *Journal of hepatology* **61**, S98-s107.

Wilby, K. J., Partovi, N., Ford, J. A. E., Greanya, E. D. & Yoshida, E. M. (2012). Review of boceprevir and telaprevir for the treatment of chronic hepatitis C. In *Can J Gastroenterol*, pp. 205-210.

Witteveldt, J., Martin-Gans, M. & Simmonds, P. (2016). Enhancement of the Replication of Hepatitis C Virus Replicons of Genotypes 1 to 4 by Manipulation of CpG and UpA Dinucleotide Frequencies and Use of Cell Lines Expressing SECL14L2 for Antiviral Resistance Testing. *Antimicrobial agents and chemotherapy* **60**, 2981-2992.

World Health Organization (2015). WHO | Hepatitis C Fact Sheet No164. *WHO*.

Wozniak, A. L., Griffin, S., Rowlands, D., Harris, M., Yi, M., Lemon, S. M. & Weinman, S. A. (2010). Intracellular proton conductance of the hepatitis C virus p7 protein and its contribution to infectious virus production. *PLoS Pathog* **6**, e1001087.

Wu, X., Lee, E. M., Hammack, C., Robotham, J. M., Basu, M., Lang, J., Brinton, M. A. & Tang, H. (2014). Cell death-inducing DFFA-like effector b is required for hepatitis C virus entry into hepatocytes. *J Virol* **88**, 8433-8444.

Yamauchi, S., Takeuchi, K., Chihara, K., Honjoh, C., Kato, Y., Yoshiki, H., Hotta, H. & Sada, K. (2016). STAT1 is essential for the inhibition of hepatitis C virus

replication by interferon-lambda but not by interferon-alpha. *Scientific reports* **6**, 38336.

Yang, F., Robotham, J. M., Nelson, H. B., Irsigler, A., Kenworthy, R. & Tang, H. (2008). Cyclophilin A is an essential cofactor for hepatitis C virus infection and the principal mediator of cyclosporine resistance in vitro. *J Virol* **82**, 5269-5278.

Yoshimura, A., Naka, T. & Kubo, M. (2007). SOCS proteins, cytokine signalling and immune regulation. *Nature Reviews Immunology* **7**, 454-465.

Yu, K. L., Jang, S. I. & You, J. C. (2009). Identification of in vivo interaction between Hepatitis C Virus core protein and 5 ' and 3 ' UTR RNA. *Virus research* **145**, 285-292.

Zahid, M. N., Turek, M., Xiao, F., Thi, V. L., Guerin, M., Fofana, I., Bachellier, P., Thompson, J., Delang, L., Neyts, J., Bankwitz, D., Pietschmann, T., Dreux, M., Cosset, F. L., Grunert, F., Baumert, T. F. & Zeisel, M. B. (2013). The postbinding activity of scavenger receptor class B type I mediates initiation of hepatitis C virus infection and viral dissemination. *Hepatology* **57**, 492-504.

Zeng, J., Wang, H., Xie, X., Li, C., Zhou, G., Yang, D. & Yu, L. (2014). Ribavirin-Resistant Variants of Foot-and-Mouth Disease Virus: the Effect of Restricted Quasispecies Diversity on Viral Virulence. In *J Virol*, pp. 4008-4020.

Zeuzem, S., Andreone, P., Pol, S., Lawitz, E., Diago, M., Roberts, S., Focaccia, R., Younossi, Z., Foster, G. R., Horban, A., Ferenci, P., Nevens, F., Mullhaupt, B., Pockros, P., Terg, R., Shouval, D., van Hoek, B., Weiland, O., Van Heeswijk, R., De Meyer, S., Luo, D., Boogaerts, G., Polo, R., Picchio, G. & Beumont, M. (2011). Telaprevir for retreatment of HCV infection. *The New England journal of medicine* **364**, 2417-2428.

Zeuzem, S., Dusheiko, G. M., Salupere, R., Mangia, A., Flisiak, R., Hyland, R. H., Illeperuma, A., Svarovskaia, E., Brainard, D. M., Symonds, W. T., Subramanian, G. M., McHutchison, J. G., Weiland, O., Reesink, H. W., Ferenci, P., Hezode, C. & Esteban, R. (2014a). Sofosbuvir and Ribavirin in HCV Genotypes 2 and 3. *The New England journal of medicine*.

Zeuzem, S., Dusheiko, G. M., Salupere, R., Mangia, A., Flisiak, R., Hyland, R. H., Illeperuma, A., Svarovskaia, E., Brainard, D. M., Symonds, W. T., Subramanian, G. M., McHutchison, J. G., Weiland, O., Reesink, H. W., Ferenci, P., Hezode, C. & Esteban, R. (2014b). Sofosbuvir and ribavirin in HCV genotypes 2 and 3. *The New England journal of medicine* **370**, 1993-2001.

8 Appendix: NS5B sequences from HCV Patients

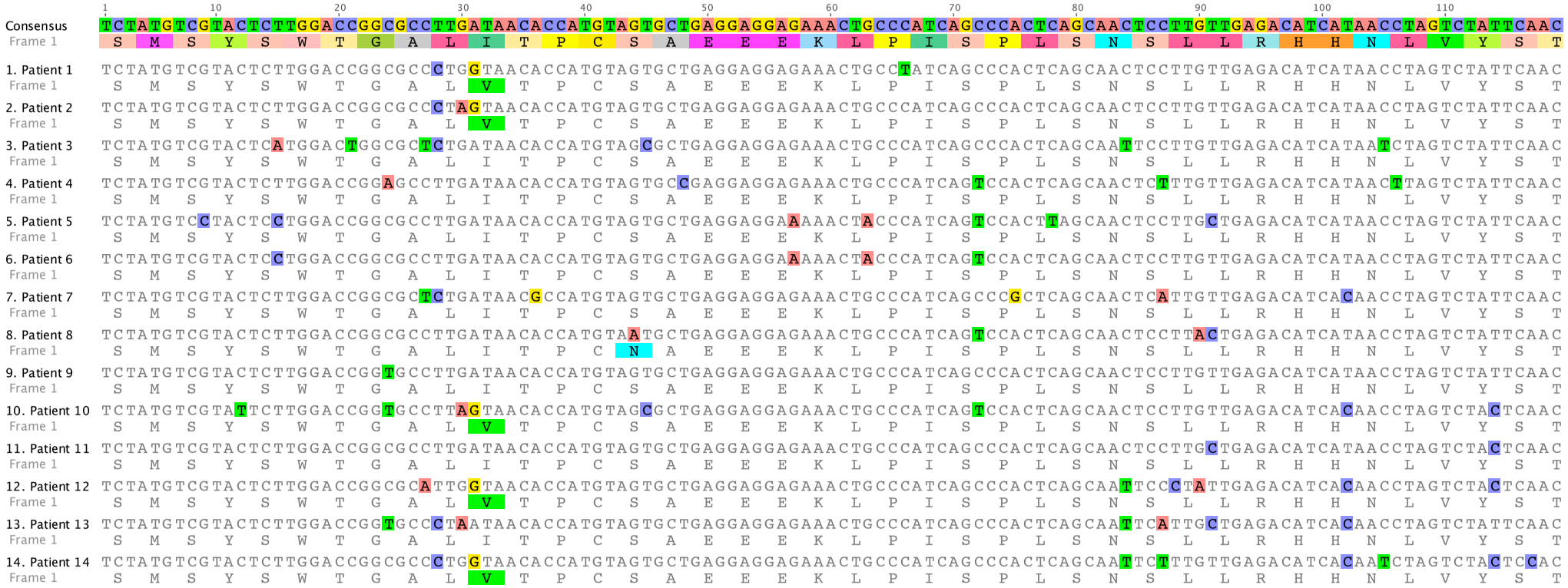
Consensus
Frame 1
1. Patient 1
2. Patient 2
3. Patient 3
4. Patient 4
5. Patient 5
6. Patient 6
7. Patient 7
8. Patient 8
9. Patient 9
10. Patient 10
11. Patient 11
12. Patient 12
13. Patient 13
14. Patient 14

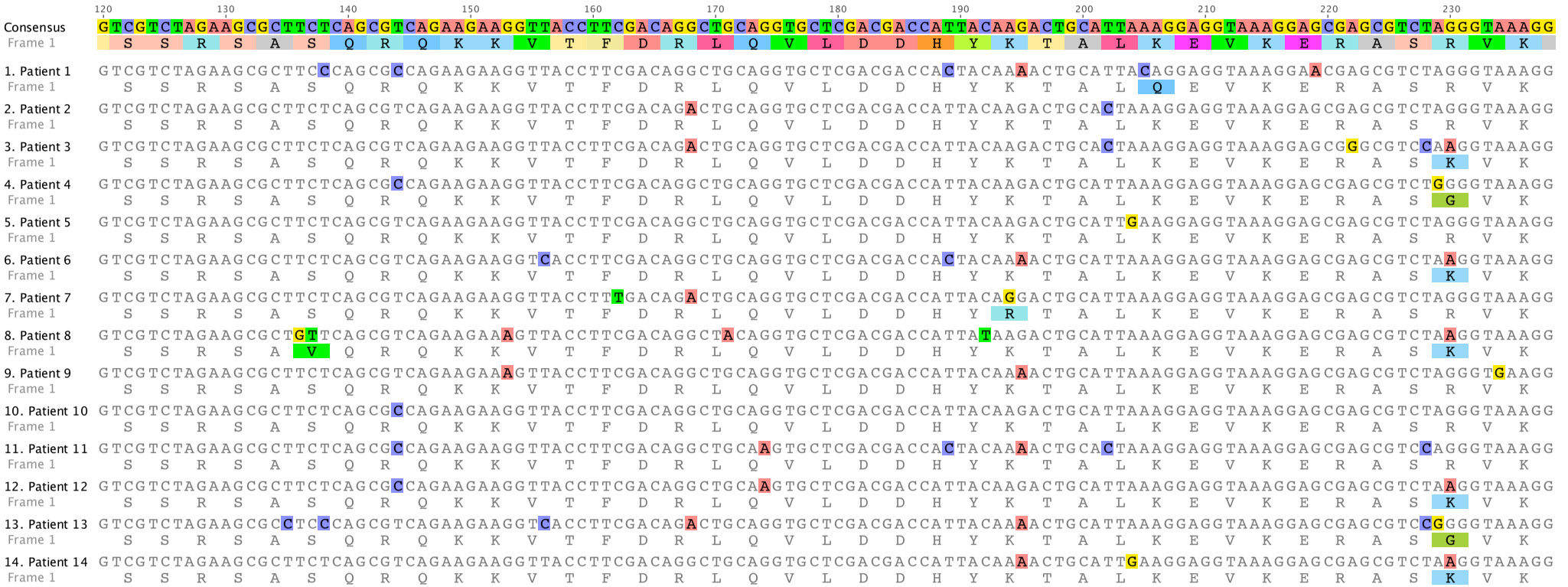
120 130 140 150 160 170 180 190 200 210 220 230
Consensus
GTCGTCTAGAAGCGCTTCTCAGCGTCAGAAGAAGGTTACCTTCGACAGGCTGCAGGTGCTCGACGACCATTACAAGACTGCATTAAAGGAGGTAAAGGAGCGAGCGTCTAGGGTAAAGG
Frame 1
S S R S A S Q R Q K K V T F D R L Q V L D D H Y K T A L K E V K E R A S R V K
1. Patient 1
GTCGTCTAGAAGCGCTTCCCAGCGCCAGAAGAAGGTTACCTTCGACAGGCTGCAGGTGCTCGACGACCACTACAAAACTGCATTACAGGAGGTAAAGGAACGAGCGTCTAGGGTAAAGG
Frame 1
S S R S A S Q R Q K K V T F D R L Q V L D D H Y K T A L Q E V K E R A S R V K
2. Patient 2
GTCGTCTAGAAGCGCTTCTCAGCGTCAGAAGAAGGTTACCTTCGACAGACTGCAGGTGCTCGACGACCATTACAAGACTGCACTAAAGGAGGTAAAGGAGCGAGCGTCTAGGGTAAAGG
Frame 1
S S R S A S Q R Q K K V T F D R L Q V L D D H Y K T A L K E V K E R A S R V K
3. Patient 3
GTCGTCTAGAAGCGCTTCTCAGCGTCAGAAGAAGGTTACCTTCGACAGACTGCAGGTGCTCGACGACCATTACAAGACTGCACTAAAGGAGGTAAAGGAGCGGGCGTCCAAGGTAAAGG
Frame 1
S S R S A S Q R Q K K V T F D R L Q V L D D H Y K T A L K E V K E R A S K V K
4. Patient 4
GTCGTCTAGAAGCGCTTCTCAGCGCCAGAAGAAGGTTACCTTCGACAGGCTGCAGGTGCTCGACGACCATTACAAGACTGCATTAAAGGAGGTAAAGGAGCGAGCGTCTGGGGTAAAGG
Frame 1
S S R S A S Q R Q K K V T F D R L Q V L D D H Y K T A L K E V K E R A S G V K
5. Patient 5
GTCGTCTAGAAGCGCTTCTCAGCGTCAGAAGAAGGTTACCTTCGACAGGCTGCAGGTGCTCGACGACCATTACAAGACTGCATTGAAGGAGGTAAAGGAGCGAGCGTCTAGGGTAAAGG
Frame 1
S S R S A S Q R Q K K V T F D R L Q V L D D H Y K T A L K E V K E R A S R V K
6. Patient 6
GTCGTCTAGAAGCGCTTCTCAGCGTCAGAAGAAGGTCACCTTCGACAGGCTGCAGGTGCTCGACGACCACTACAAAACTGCATTAAAGGAGGTAAAGGAGCGAGCGTCTAAGGTAAAGG
Frame 1
S S R S A S Q R Q K K V T F D R L Q V L D D H Y K T A L K E V K E R A S K V K
7. Patient 7
GTCGTCTAGAAGCGCTTCTCAGCGTCAGAAGAAGGTTACCTTTGACAGACTGCAGGTGCTCGACGACCATTACAGGACTGCATTAAAGGAGGTAAAGGAGCGAGCGTCTAGGGTAAAGG
Frame 1
S S R S A S Q R Q K K V T F D R L Q V L D D H Y R T A L K E V K E R A S R V K
8. Patient 8
GTCGTCTAGAAGCGCTGTTCAGCGTCAGAAGAAAGTTACCTTCGACAGGCTACAGGTGCTCGACGACCATTATAAGACTGCATTAAAGGAGGTAAAGGAGCGAGCGTCTAAGGTAAAGG
Frame 1
S S R S A V Q R Q K K V T F D R L Q V L D D H Y K T A L K E V K E R A S K V K
9. Patient 9
GTCGTCTAGAAGCGCTTCTCAGCGTCAGAAGAAAGTTACCTTCGACAGGCTGCAGGTGCTCGACGACCATTACAAAACTGCATTAAAGGAGGTAAAGGAGCGAGCGTCTAGGGTGAAGG
Frame 1
S S R S A S Q R Q K K V T F D R L Q V L D D H Y K T A L K E V K E R A S R V K
10. Patient 10
GTCGTCTAGAAGCGCTTCTCAGCGCCAGAAGAAGGTTACCTTCGACAGGCTGCAGGTGCTCGACGACCATTACAAGACTGCATTAAAGGAGGTAAAGGAGCGAGCGTCTAGGGTAAAGG
Frame 1
S S R S A S Q R Q K K V T F D R L Q V L D D H Y K T A L K E V K E R A S R V K
11. Patient 11
GTCGTCTAGAAGCGCTTCTCAGCGCCAGAAGAAGGTTACCTTCGACAGGCTGCAAGTGCTCGACGACCACTACAAAACTGCACTAAAGGAGGTAAAGGAGCGAGCGTCCAGGGTAAAGG
Frame 1
S S R S A S Q R Q K K V T F D R L Q V L D D H Y K T A L K E V K E R A S R V K
12. Patient 12
GTCGTCTAGAAGCGCTTCTCAGCGCCAGAAGAAGGTTACCTTCGACAGGCTGCAAGTGCTCGACGACCATTACAAGACTGCATTAAAGGAGGTAAAGGAGCGAGCGTCTAAGGTAAAGG
Frame 1
S S R S A S Q R Q K K V T F D R L Q V L D D H Y K T A L K E V K E R A S K V K
13. Patient 13
GTCGTCTAGAAGCGCCTCCCAGCGTCAGAAGAAGGTCACCTTCGACAGACTGCAGGTGCTCGACGACCATTACAAAACTGCATTAAAGGAGGTAAAGGAGCGAGCGTCCGGGGTAAAGG
Frame 1
S S R S A S Q R Q K K V T F D R L Q V L D D H Y K T A L K E V K E R A S G V K
14. Patient 14
GTCGTCTAGAAGCGCTTCTCAGCGTCAGAAGAAGGTTACCTTCGACAGGCTGCAGGTGCTCGACGACCATTACAAAACTGCATTGAAGGAGGTAAAGGAGCGAGCGTCTAAGGTAAAGG
Frame 1
S S R S A S Q R Q K K V T F D R L Q V L D D H Y K T A L K E V K E R A S K V K

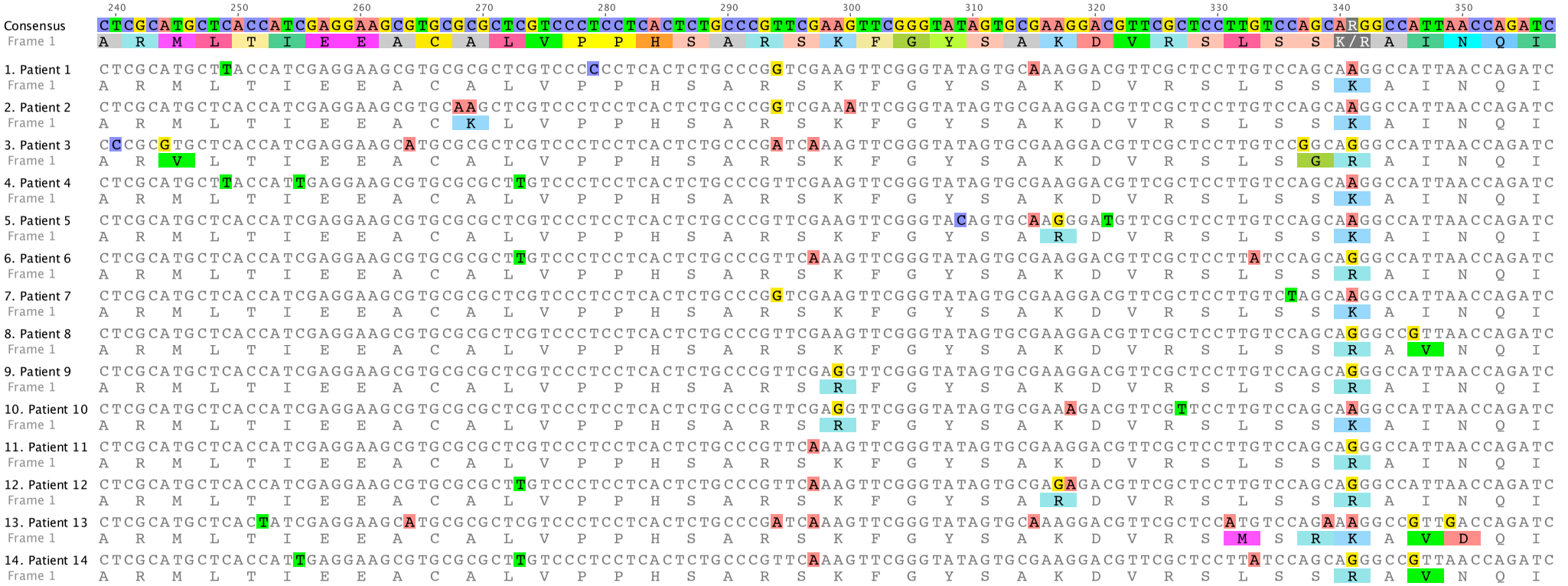
240 250 260 270 280 290 300 310 320 330 340 350
Consensus
CTCGCATGCTCACCATCGAGGAAGCGTGCGCGCTCGTCCCTCCTCACTCTGCCCGTTCGAAGTTCGGGTATAGTGCGAAGGACGTTCGCTCCTTGTCCAGCARGGCCATTAACCAGATC
Frame 1
A R M L T I E E A C A L V P P H S A R S K F G Y S A K D V R S L S S K/R A I N Q I
1. Patient 1
CTCGCATGCTTACCATCGAGGAAGCGTGCGCGCTCGTCCCCCCTCACTCTGCCCGGTCGAAGTTCGGGTATAGTGCAAAGGACGTTCGCTCCTTGTCCAGCAAGGCCATTAACCAGATC
Frame 1
A R M L T I E E A C A L V P P H S A R S K F G Y S A K D V R S L S S K A I N Q I
2. Patient 2
CTCGCATGCTCACCATCGAGGAAGCGTGCAAGCTCGTCCCTCCTCACTCTGCCCGGTCGAAATTCGGGTATAGTGCGAAGGACGTTCGCTCCTTGTCCAGCAAGGCCATTAACCAGATC
Frame 1
A R M L T I E E A C K L V P P H S A R S K F G Y S A K D V R S L S S K A I N Q I
3. Patient 3
CCCGCGTGCTCACCATCGAGGAAGCATGCGCGCTCGTCCCTCCTCACTCTGCCCGATCAAAGTTCGGGTATAGTGCGAAGGACGTTCGCTCCTTGTCCGGCAGGGCCATTAACCAGATC
Frame 1
A R V L T I E E A C A L V P P H S A R S K F G Y S A K D V R S L S G R A I N Q I
4. Patient 4
CTCGCATGCTTACCATTGAGGAAGCGTGCGCGCTTGTCCCTCCTCACTCTGCCCGTTCGAAGTTCGGGTATAGTGCGAAGGACGTTCGCTCCTTGTCCAGCAAGGCCATTAACCAGATC
Frame 1
A R M L T I E E A C A L V P P H S A R S K F G Y S A K D V R S L S S K A I N Q I
5. Patient 5
CTCGCATGCTCACCATCGAGGAAGCGTGCGCGCTCGTCCCTCCTCACTCTGCCCGTTCGAAGTTCGGGTACAGTGCAAGGGATGTTCGCTCCTTGTCCAGCAAGGCCATTAACCAGATC
Frame 1
A R M L T I E E A C A L V P P H S A R S K F G Y S A R D V R S L S S K A I N Q I
6. Patient 6
CTCGCATGCTCACCATCGAGGAAGCGTGCGCGCTTGTCCCTCCTCACTCTGCCCGTTCAAAGTTCGGGTATAGTGCGAAGGACGTTCGCTCCTTATCCAGCAGGGCCATTAACCAGATC
Frame 1
A R M L T I E E A C A L V P P H S A R S K F G Y S A K D V R S L S S R A I N Q I
7. Patient 7
CTCGCATGCTCACCATCGAGGAAGCGTGCGCGCTCGTCCCTCCTCACTCTGCCCGGTCGAAGTTCGGGTATAGTGCGAAGGACGTTCGCTCCTTGTCTAGCAAGGCCATTAACCAGATC
Frame 1
A R M L T I E E A C A L V P P H S A R S K F G Y S A K D V R S L S S K A I N Q I
8. Patient 8
CTCGCATGCTCACCATCGAGGAAGCGTGCGCGCTCGTCCCTCCTCACTCTGCCCGTTCGAAGTTCGGGTATAGTGCGAAGGACGTTCGCTCCTTGTCCAGCAGGGCCGTTAACCAGATC
Frame 1
A R M L T I E E A C A L V P P H S A R S K F G Y S A K D V R S L S S R A V N Q I
9. Patient 9
CTCGCATGCTCACCATCGAGGAAGCGTGCGCGCTCGTCCCTCCTCACTCTGCCCGTTCGAGGTTCGGGTATAGTGCGAAGGACGTTCGCTCCTTGTCCAGCAGGGCCATTAACCAGATC
Frame 1
A R M L T I E E A C A L V P P H S A R S R F G Y S A K D V R S L S S R A I N Q I
10. Patient 10
CTCGCATGCTCACCATCGAGGAAGCGTGCGCGCTCGTCCCTCCTCACTCTGCCCGTTCGAGGTTCGGGTATAGTGCGAAAGACGTTCGTTCCTTGTCCAGCAAGGCCATTAACCAGATC
Frame 1
A R M L T I E E A C A L V P P H S A R S R F G Y S A K D V R S L S S K A I N Q I
11. Patient 11
CTCGCATGCTCACCATCGAGGAAGCGTGCGCGCTCGTCCCTCCTCACTCTGCCCGTTCAAAGTTCGGGTATAGTGCGAAGGACGTTCGCTCCTTGTCCAGCAGGGCCATTAACCAGATC
Frame 1
A R M L T I E E A C A L V P P H S A R S K F G Y S A K D V R S L S S R A I N Q I
12. Patient 12
CTCGCATGCTCACCATCGAGGAAGCGTGCGCGCTTGTCCCTCCTCACTCTGCCCGTTCAAAGTTCGGGTATAGTGCGAGAGACGTTCGCTCCTTGTCCAGCAGGGCCATTAACCAGATC
Frame 1
A R M L T I E E A C A L V P P H S A R S K F G Y S A R D V R S L S S R A I N Q I
13. Patient 13
CTCGCATGCTCACTATCGAGGAAGCATGCGCGCTCGTCCCTCCTCACTCTGCCCGATCAAAGTTCGGGTATAGTGCAAAGGACGTTCGCTCCATGTCCAGAAAGGCCGTTGACCAGATC
Frame 1
A R M L T I E E A C A L V P P H S A R S K F G Y S A K D V R S M S R K A V D Q I
14. Patient 14
CTCGCATGCTCACCATTGAGGAAGCGTGCGCGCTTGTCCCTCCTCACTCTGCCCGTTCAAAGTTCGGGTATAGTGCGAAGGACGTTCGCTCCTTATCCAGCAGGGCCGTTAACCAGATC
Frame 1
A R M L T I E E A C A L V P P H S A R S K F G Y S A K D V R S L S S R A V N Q I

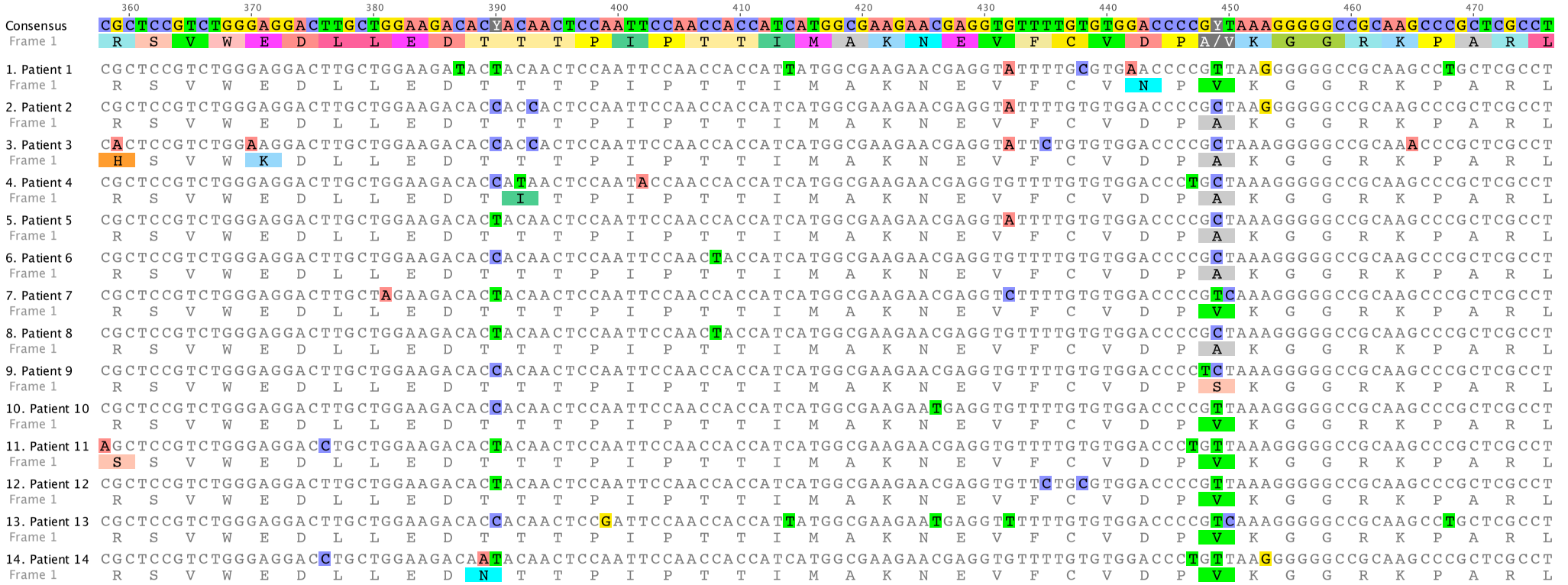
360 370 380 390 400 410 420 430 440 450 460 470
Consensus
CGCTCCGTCTGGGAGGACTTGCTGGAAGACACYACAACTCCAATTCCAACCACCATCATGGCGAAGAACGAGGTGTTTTGTGTGGACCCCGYTAAAGGGGGCCGCAAGCCCGCTCGCCT
Frame 1
R S V W E D L L E D T T T P I P T T I M A K N E V F C V D P A/V K G G R K P A R L
1. Patient 1
CGCTCCGTCTGGGAGGACTTGCTGGAAGATACTACAACTCCAATTCCAACCACCATTATGGCGAAGAACGAGGTATTTTGCGTGAACCCCGTTAAGGGGGGCCGCAAGCCTGCTCGCCT
Frame 1
R S V W E D L L E D T T T P I P T T I M A K N E V F C V N P V K G G R K P A R L
2. Patient 2
CGCTCCGTCTGGGAGGACTTGCTGGAAGACACCACCACTCCAATTCCAACCACCATCATGGCGAAGAACGAGGTATTTTGTGTGGACCCCGCTAAGGGGGGCCGCAAGCCCGCTCGCCT
Frame 1
R S V W E D L L E D T T T P I P T T I M A K N E V F C V D P A K G G R K P A R L
3. Patient 3
CACTCCGTCTGGAAGGACTTGCTGGAAGACACCACCACTCCAATTCCAACCACCATCATGGCGAAGAACGAGGTATTCTGTGTGGACCCCGCTAAAGGGGGCCGCAAACCCGCTCGCCT
Frame 1
H S V W K D L L E D T T T P I P T T I M A K N E V F C V D P A K G G R K P A R L
4. Patient 4
CGCTCCGTCTGGGAGGACTTGCTGGAAGACACCATAACTCCAATACCAACCACCATCATGGCGAAGAACGAGGTGTTTTGTGTGGACCCTGCTAAAGGGGGCCGCAAGCCCGCTCGCCT
Frame 1
R S V W E D L L E D T I T P I P T T I M A K N E V F C V D P A K G G R K P A R L
5. Patient 5
CGCTCCGTCTGGGAGGACTTGCTGGAAGACACTACAACTCCAATTCCAACCACCATCATGGCGAAGAACGAGGTATTTTGTGTGGACCCCGCTAAAGGGGGCCGCAAGCCCGCTCGCCT
Frame 1
R S V W E D L L E D T T T P I P T T I M A K N E V F C V D P A K G G R K P A R L
6. Patient 6
CGCTCCGTCTGGGAGGACTTGCTGGAAGACACCACAACTCCAATTCCAACTACCATCATGGCGAAGAACGAGGTGTTTTGTGTGGACCCCGCTAAAGGGGGCCGCAAGCCCGCTCGCCT
Frame 1
R S V W E D L L E D T T T P I P T T I M A K N E V F C V D P A K G G R K P A R L
7. Patient 7
CGCTCCGTCTGGGAGGACTTGCTAGAAGACACTACAACTCCAATTCCAACCACCATCATGGCGAAGAACGAGGTCTTTTGTGTGGACCCCGTCAAAGGGGGCCGCAAGCCCGCTCGCCT
Frame 1
R S V W E D L L E D T T T P I P T T I M A K N E V F C V D P V K G G R K P A R L
8. Patient 8
CGCTCCGTCTGGGAGGACTTGCTGGAAGACACTACAACTCCAATTCCAACTACCATCATGGCGAAGAACGAGGTGTTTTGTGTGGACCCCGCTAAAGGGGGCCGCAAGCCCGCTCGCCT
Frame 1
R S V W E D L L E D T T T P I P T T I M A K N E V F C V D P A K G G R K P A R L
9. Patient 9
CGCTCCGTCTGGGAGGACTTGCTGGAAGACACCACAACTCCAATTCCAACCACCATCATGGCGAAGAACGAGGTGTTTTGTGTGGACCCCTCTAAAGGGGGCCGCAAGCCCGCTCGCCT
Frame 1
R S V W E D L L E D T T T P I P T T I M A K N E V F C V D P S K G G R K P A R L
10. Patient 10
CGCTCCGTCTGGGAGGACTTGCTGGAAGACACCACAACTCCAATTCCAACCACCATCATGGCGAAGAATGAGGTGTTTTGTGTGGACCCCGTTAAAGGGGGCCGCAAGCCCGCTCGCCT
Frame 1
R S V W E D L L E D T T T P I P T T I M A K N E V F C V D P V K G G R K P A R L
11. Patient 11
AGCTCCGTCTGGGAGGACCTGCTGGAAGACACTACAACTCCAATTCCAACCACCATCATGGCGAAGAACGAGGTGTTTTGTGTGGACCCTGTTAAAGGGGGCCGCAAGCCCGCTCGCCT
Frame 1
S S V W E D L L E D T T T P I P T T I M A K N E V F C V D P V K G G R K P A R L
12. Patient 12
CGCTCCGTCTGGGAGGACTTGCTGGAAGACACTACAACTCCAATTCCAACCACCATCATGGCGAAGAACGAGGTGTTCTGCGTGGACCCCGTTAAAGGGGGCCGCAAGCCCGCTCGCCT
Frame 1
R S V W E D L L E D T T T P I P T T I M A K N E V F C V D P V K G G R K P A R L
13. Patient 13
CGCTCCGTCTGGGAGGACTTGCTGGAAGACACCACAACTCCGATTCCAACCACCATTATGGCGAAGAATGAGGTTTTTTGTGTGGACCCCGTTCAAAGGGGGCCGCAAGCCTGCTCGCCT
Frame 1
R S V W E D L L E D T T T P I P T T I M A K N E V F C V D P V K G G R K P A R L
14. Patient 14
CGCTCCGTCTGGGAGGACCTGCTGGAAGACAATACAACTCCAATTCCAACCACCATCATGGCGAAGAACGAGGTGTTTTGTGTGGACCCTGTTAAGGGGGGCCGCAAGCCCGCTCGCCT
Frame 1
R S V W E D L L E D N T T P I P T T I M A K N E V F C V D P V K G G R K P A R L

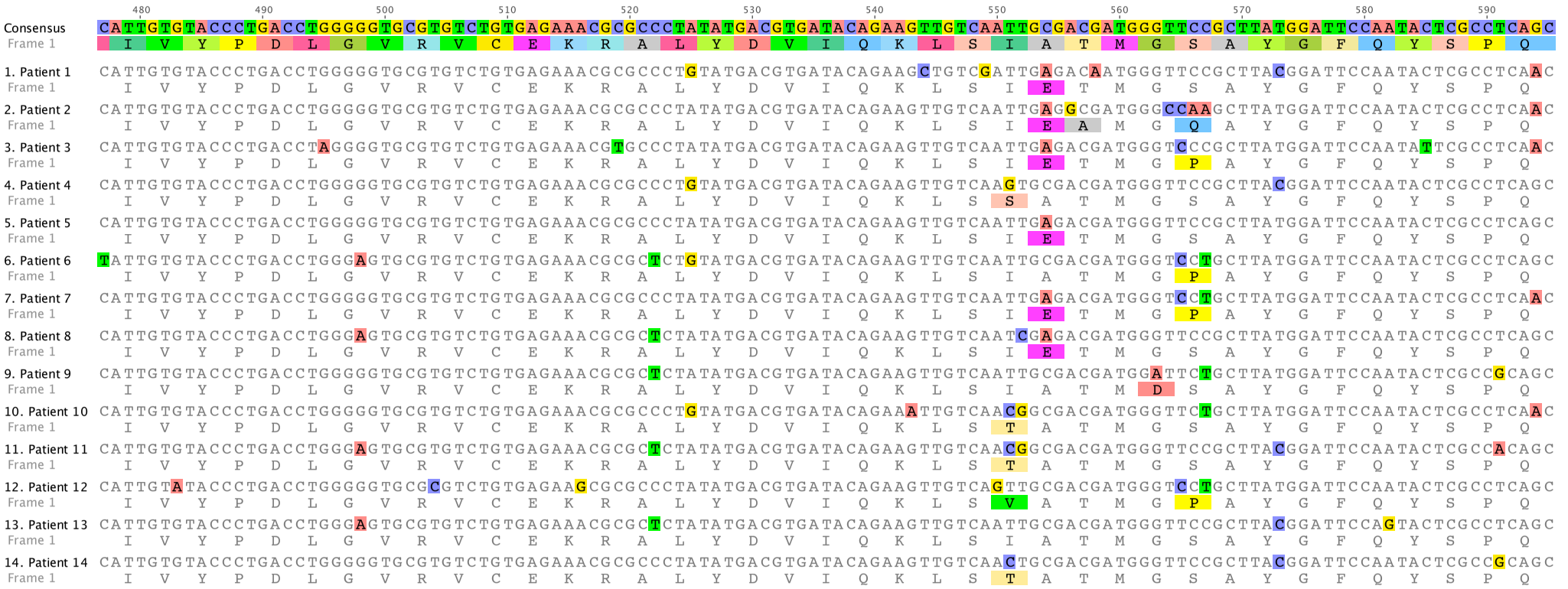
480 490 500 510 520 530 540 550 560 570 580 590
Consensus
CATTGTGTACCCTGACCTGGGGGTGCGTGTCTGTGAGAAACGCGCCCTATATGACGTGATACAGAAGTTGTCAATTGCGACGATGGGTTCCGCTTATGGATTCCAATACTCGCCTCAGC
Frame 1
I V Y P D L G V R V C E K R A L Y D V I Q K L S I A T M G S A Y G F Q Y S P Q
1. Patient 1
CATTGTGTACCCTGACCTGGGGGTGCGTGTCTGTGAGAAACGCGCCCTGTATGACGTGATACAGAAGCTGTCGATTGAGACAATGGGTTCCGCTTACGGATTCCAATACTCGCCTCAAC
Frame 1
I V Y P D L G V R V C E K R A L Y D V I Q K L S I E T M G S A Y G F Q Y S P Q
2. Patient 2
CATTGTGTACCCTGACCTGGGGGTGCGTGTCTGTGAGAAACGCGCCCTATATGACGTGATACAGAAGTTGTCAATTGAGGCGATGGGCCAAGCTTATGGATTCCAATACTCGCCTCAAC
Frame 1
I V Y P D L G V R V C E K R A L Y D V I Q K L S I E A M G Q A Y G F Q Y S P Q
3. Patient 3
CATTGTGTACCCTGACCTAGGGGTGCGTGTCTGTGAGAAACGTGCCCTATATGACGTGATACAGAAGTTGTCAATTGAGACGATGGGTCCCGCTTATGGATTCCAATATTCGCCTCAAC
Frame 1
I V Y P D L G V R V C E K R A L Y D V I Q K L S I E T M G P A Y G F Q Y S P Q
4. Patient 4
CATTGTGTACCCTGACCTGGGGGTGCGTGTCTGTGAGAAACGCGCCCTGTATGACGTGATACAGAAGTTGTCAAGTGCGACGATGGGTTCCGCTTACGGATTCCAATACTCGCCTCAGC
Frame 1
I V Y P D L G V R V C E K R A L Y D V I Q K L S S A T M G S A Y G F Q Y S P Q
5. Patient 5
CATTGTGTACCCTGACCTGGGGGTGCGTGTCTGTGAGAAACGCGCCCTATATGACGTGATACAGAAGTTGTCAATTGAGACGATGGGTTCCGCTTATGGATTCCAATACTCGCCTCAGC
Frame 1
I V Y P D L G V R V C E K R A L Y D V I Q K L S I E T M G S A Y G F Q Y S P Q
6. Patient 6
TATTGTGTACCCTGACCTGGGAGTGCGTGTCTGTGAGAAACGCGCTCTGTATGACGTGATACAGAAGTTGTCAATTGCGACGATGGGTCCTGCTTATGGATTCCAATACTCGCCTCAGC
Frame 1
I V Y P D L G V R V C E K R A L Y D V I Q K L S I A T M G P A Y G F Q Y S P Q
7. Patient 7
CATTGTGTACCCTGACCTGGGGGTGCGTGTCTGTGAGAAACGCGCCCTATATGACGTGATACAGAAGTTGTCAATTGAGACGATGGGTCCTGCTTATGGATTCCAATACTCGCCTCAAC
Frame 1
I V Y P D L G V R V C E K R A L Y D V I Q K L S I E T M G P A Y G F Q Y S P Q
8. Patient 8
CATTGTGTACCCTGACCTGGGAGTGCGTGTCTGTGAGAAACGCGCTCTATATGACGTGATACAGAAGTTGTCAATCGAGACGATGGGTTCCGCTTATGGATTCCAATACTCGCCTCAGC
Frame 1
I V Y P D L G V R V C E K R A L Y D V I Q K L S I E T M G S A Y G F Q Y S P Q
9. Patient 9
CATTGTGTACCCTGACCTGGGGGTGCGTGTCTGTGAGAAACGCGCTCTATATGACGTGATACAGAAGTTGTCAATTGCGACGATGGATTCTTGCTTATGGATTCCAATACTCGCCGCAGC
Frame 1
I V Y P D L G V R V C E K R A L Y D V I Q K L S I A T M D S A Y G F Q Y S P Q
10. Patient 10
CATTGTGTACCCTGACCTGGGGGTGCGTGTCTGTGAGAAACGCGCCCTGTATGACGTGATACAGAAATTGTCAACGGCGACGATGGGTTCTTGCTTATGGATTCCAATACTCGCCTCAAC
Frame 1
I V Y P D L G V R V C E K R A L Y D V I Q K L S T A T M G S A Y G F Q Y S P Q
11. Patient 11
CATTGTGTACCCTGACCTGGGAGTGCGTGTCTGTGAGAAACGCGCTCTATATGACGTGATACAGAAGTTGTCAACGGCGACGATGGGTTCCGCTTACGGATTCCAATACTCGCCACAGC
Frame 1
I V Y P D L G V R V C E K R A L Y D V I Q K L S T A T M G S A Y G F Q Y S P Q
12. Patient 12
CATTGTATACCCTGACCTGGGGGTGCGCGTCTGTGAGAAGCGCGCCCTATATGACGTGATACAGAAGTTGTCAGTTGCGACGATGGGTCCTGCTTATGGATTCCAATACTCGCCTCAGC
Frame 1
I V Y P D L G V R V C E K R A L Y D V I Q K L S V A T M G P A Y G F Q Y S P Q
13. Patient 13
CATTGTGTACCCTGACCTGGGAGTGCGTGTCTGTGAGAAACGCGCTCTATATGACGTGATACAGAAGTTGTCAATTGCGACGATGGGTTCCGCTTACGGATTCCAGTACTCGCCTCAGC
Frame 1
I V Y P D L G V R V C E K R A L Y D V I Q K L S I A T M G S A Y G F Q Y S P Q
14. Patient 14
CATTGTGTACCCTGACCTGGGGGTGCGTGTCTGTGAGAAACGCGCCCTATATGACGTGATACAGAAGTTGTCAACTGCGACGATGGGTTCCGCTTACGGATTCCAATACTCGCCGCAGC
Frame 1
I V Y P D L G V R V C E K R A L Y D V I Q K L S T A T M G S A Y G F Q Y S P Q

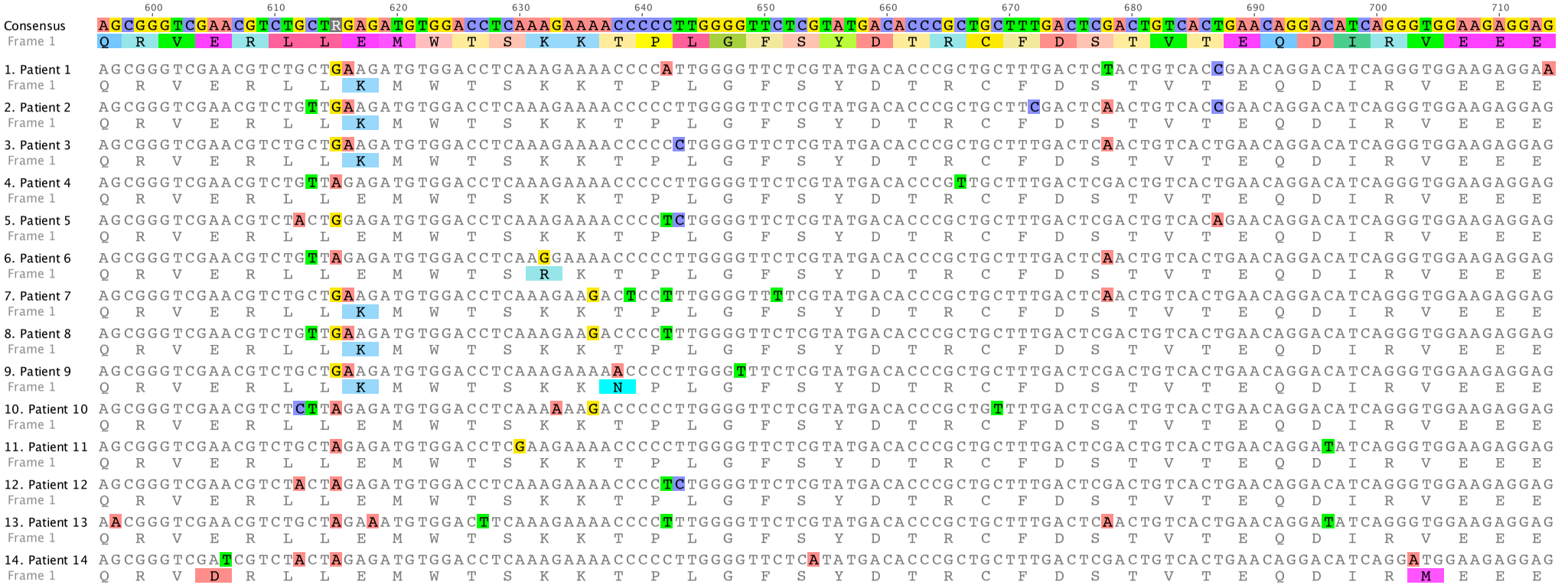
600 610 620 630 640 650 660 670 680 690 700 710
Consensus AGCGGGTCGAACGTCTGCTRGAGATGTGGACCTCAAAGAAAACCCCCTTGGGGTTCTCGTATGACACCCGCTGCTTTGACTCGACTGTCACTGAACAGGACATCAGGGTGGAAGAGGAG
Frame 1 Q R V E R L L E M W T S K K T P L G F S Y D T R C F D S T V T E Q D I R V E E E
1. Patient 1 AGCGGGTCGAACGTCTGCTGAAGATGTGGACCTCAAAGAAAACCCCATTGGGGTTCTCGTATGACACCCGCTGCTTTGACTCTACTGTCACCGAACAGGACATCAGGGTGGAAGAGGAA
Frame 1 Q R V E R L L K M W T S K K T P L G F S Y D T R C F D S T V T E Q D I R V E E E
2. Patient 2 AGCGGGTCGAACGTCTGTTGAAGATGTGGACCTCAAAGAAAACCCCCTTGGGGTTCTCGTATGACACCCGCTGCTTCGACTCAACTGTCACCGAACAGGACATCAGGGTGGAAGAGGAG
Frame 1 Q R V E R L L K M W T S K K T P L G F S Y D T R C F D S T V T E Q D I R V E E E
3. Patient 3 AGCGGGTCGAACGTCTGCTGAAGATGTGGACCTCAAAGAAAACCCCCCTGGGGTTCTCGTATGACACCCGCTGCTTTGACTCAACTGTCACTGAACAGGACATCAGGGTGGAAGAGGAG
Frame 1 Q R V E R L L K M W T S K K T P L G F S Y D T R C F D S T V T E Q D I R V E E E
4. Patient 4 AGCGGGTCGAACGTCTGTTAGAGATGTGGACCTCAAAGAAAACCCCCTTGGGGTTCTCGTATGACACCCGTTGCTTTGACTCGACTGTCACTGAACAGGACATCAGGGTGGAAGAGGAG
Frame 1 Q R V E R L L E M W T S K K T P L G F S Y D T R C F D S T V T E Q D I R V E E E
5. Patient 5 AGCGGGTCGAACGTCTACTGGAGATGTGGACCTCAAAGAAAACCCCTTCTGGGGTTCTCGTATGACACCCGCTGCTTTGACTCGACTGTCACAGAACAGGACATCAGGGTGGAAGAGGAG
Frame 1 Q R V E R L L E M W T S K K T P L G F S Y D T R C F D S T V T E Q D I R V E E E
6. Patient 6 AGCGGGTCGAACGTCTGTTAGAGATGTGGACCTCAAGGAAAACCCCCTTGGGGTTCTCGTATGACACCCGCTGCTTTGACTCAACTGTCACTGAACAGGACATCAGGGTGGAAGAGGAG
Frame 1 Q R V E R L L E M W T S R K T P L G F S Y D T R C F D S T V T E Q D I R V E E E
7. Patient 7 AGCGGGTCGAACGTCTGCTGAAGATGTGGACCTCAAAGAAGACTCCTTTGGGGTTTTCGTATGACACCCGCTGCTTTGACTCAACTGTCACTGAACAGGACATCAGGGTGGAAGAGGAG
Frame 1 Q R V E R L L K M W T S K K T P L G F S Y D T R C F D S T V T E Q D I R V E E E
8. Patient 8 AGCGGGTCGAACGTCTGTTGAAGATGTGGACCTCAAAGAAGACCCCTTTGGGGTTCTCGTATGACACCCGCTGCTTTGACTCGACTGTCACTGAACAGGACATCAGGGTGGAAGAGGAG
Frame 1 Q R V E R L L K M W T S K K T P L G F S Y D T R C F D S T V T E Q D I R V E E E
9. Patient 9 AGCGGGTCGAACGTCTGCTGAAGATGTGGACCTCAAAGAAAAACCCCCTTGGGTTTCTCGTATGACACCCGCTGCTTTGACTCGACTGTCACTGAACAGGACATCAGGGTGGAAGAGGAG
Frame 1 Q R V E R L L K M W T S K K N P L G F S Y D T R C F D S T V T E Q D I R V E E E
10. Patient 10 AGCGGGTCGAACGTCTCTTAGAGATGTGGACCTCAAAAAAGACCCCCTTGGGGTTCTCGTATGACACCCGCTGTTTTGACTCGACTGTCACTGAACAGGACATCAGGGTGGAAGAGGAG
Frame 1 Q R V E R L L E M W T S K K T P L G F S Y D T R C F D S T V T E Q D I R V E E E
11. Patient 11 AGCGGGTCGAACGTCTGCTAGAGATGTGGACCTCGAAGAAAACCCCCTTGGGGTTCTCGTATGACACCCGCTGCTTTGACTCGACTGTCACTGAACAGGATATCAGGGTGGAAGAGGAG
Frame 1 Q R V E R L L E M W T S K K T P L G F S Y D T R C F D S T V T E Q D I R V E E E
12. Patient 12 AGCGGGTCGAACGTCTACTAGAGATGTGGACCTCAAAGAAAACCCCTTCTGGGGTTCTCGTATGACACCCGCTGCTTTGACTCGACTGTCACTGAACAGGACATCAGGGTGGAAGAGGAG
Frame 1 Q R V E R L L E M W T S K K T P L G F S Y D T R C F D S T V T E Q D I R V E E E
13. Patient 13 AACGGGTCGAACGTCTGCTAGAAATGTGGACTTCAAAGAAAACCCCTTTGGGGTTCTCGTATGACACCCGCTGCTTTGACTCAACTGTCACTGAACAGGATATCAGGGTGGAAGAGGAG
Frame 1 Q R V E R L L E M W T S K K T P L G F S Y D T R C F D S T V T E Q D I R V E E E
14. Patient 14 AGCGGGTCGATCGTCTACTAGAGATGTGGACCTCAAAGAAAACCCCCTTGGGGTTCTCATATGACACCCGCTGCTTTGACTCGACTGTCACTGAACAGGACATCAGGATGGAAGAGGAG
Frame 1 Q R V D R L L E M W T S K K T P L G F S Y D T R C F D S T V T E Q D I R M E E E

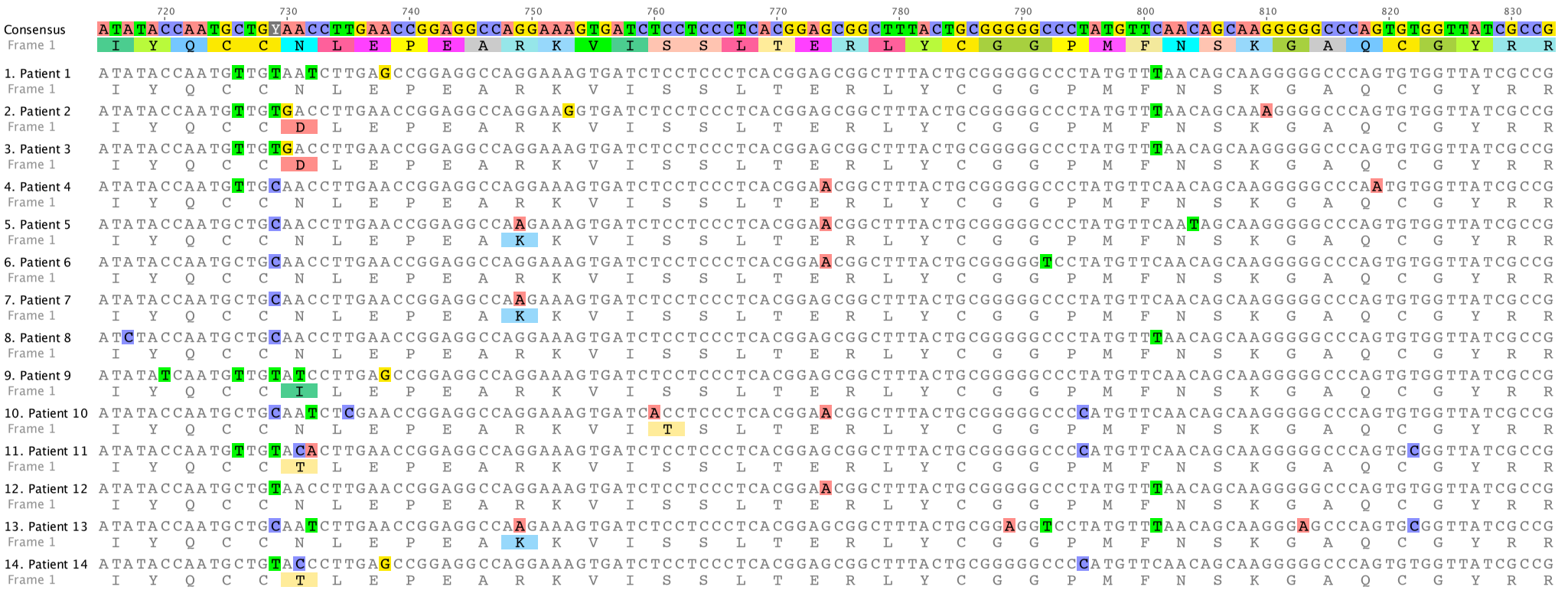
720 730 740 750 760 770 780 790 800 810 820 830
Consensus
ATATACCAATGCTGYAACCTTGAACCGGAGGCCAGGAAAGTGATCTCCTCCCTCACGGAGCGGCTTTACTGCGGGGGCCCTATGTTCAACAGCAAGGGGGCCCAGTGTGGTTATCGCCG
Frame 1
I Y Q C C N L E P E A R K V I S S L T E R L Y C G G P M F N S K G A Q C G Y R R
1. Patient 1
ATATACCAATGTTGTAATCTTGAGCCGGAGGCCAGGAAAGTGATCTCCTCCCTCACGGAGCGGCTTTACTGCGGGGGCCCTATGTTTAACAGCAAGGGGGCCCAGTGTGGTTATCGCCG
Frame 1
I Y Q C C N L E P E A R K V I S S L T E R L Y C G G P M F N S K G A Q C G Y R R
2. Patient 2
ATATACCAATGTTGTGACCTTGAACCGGAGGCCAGGAAGGTGATCTCCTCCCTCACGGAGCGGCTTTACTGCGGGGGCCCTATGTTTAACAGCAAAGGGGGCCCAGTGTGGTTATCGCCG
Frame 1
I Y Q C C D L E P E A R K V I S S L T E R L Y C G G P M F N S K G A Q C G Y R R
3. Patient 3
ATATACCAATGTTGTGACCTTGAACCGGAGGCCAGGAAAGTGATCTCCTCCCTCACGGAGCGGCTTTACTGCGGGGGCCCTATGTTTAACAGCAAGGGGGCCCAGTGTGGTTATCGCCG
Frame 1
I Y Q C C D L E P E A R K V I S S L T E R L Y C G G P M F N S K G A Q C G Y R R
4. Patient 4
ATATACCAATGTTGCAACCTTGAACCGGAGGCCAGGAAAGTGATCTCCTCCCTCACGGAACGGCTTTACTGCGGGGGCCCTATGTTCAACAGCAAGGGGGCCCAATGTGGTTATCGCCG
Frame 1
I Y Q C C N L E P E A R K V I S S L T E R L Y C G G P M F N S K G A Q C G Y R R
5. Patient 5
ATATACCAATGCTGCAACCTTGAACCGGAGGCCAAGAAAGTGATCTCCTCCCTCACGGAACGGCTTTACTGCGGGGGCCCTATGTTCAATAGCAAGGGGGCCCAGTGTGGTTATCGCCG
Frame 1
I Y Q C C N L E P E A K K V I S S L T E R L Y C G G P M F N S K G A Q C G Y R R
6. Patient 6
ATATACCAATGCTGCAACCTTGAACCGGAGGCCAGGAAAGTGATCTCCTCCCTCACGGAACGGCTTTACTGCGGGGGTCCTATGTTCAACAGCAAGGGGGCCCAGTGTGGTTATCGCCG
Frame 1
I Y Q C C N L E P E A R K V I S S L T E R L Y C G G P M F N S K G A Q C G Y R R
7. Patient 7
ATATACCAATGCTGCAACCTTGAACCGGAGGCCAAGAAAGTGATCTCCTCCCTCACGGAGCGGCTTTACTGCGGGGGCCCTATGTTCAACAGCAAGGGGGCCCAGTGTGGTTATCGCCG
Frame 1
I Y Q C C N L E P E A K K V I S S L T E R L Y C G G P M F N S K G A Q C G Y R R
8. Patient 8
ATCTACCAATGCTGCAACCTTGAACCGGAGGCCAGGAAAGTGATCTCCTCCCTCACGGAGCGGCTTTACTGCGGGGGCCCTATGTTTAACAGCAAGGGGGCCCAGTGTGGTTATCGCCG
Frame 1
I Y Q C C N L E P E A R K V I S S L T E R L Y C G G P M F N S K G A Q C G Y R R
9. Patient 9
ATATATCAATGTTGTATCCTTGAGCCGGAGGCCAGGAAAGTGATCTCCTCCCTCACGGAGCGGCTTTACTGCGGGGGCCCTATGTTCAACAGCAAGGGGGCCCAGTGTGGTTATCGCCG
Frame 1
I Y Q C C I L E P E A R K V I S S L T E R L Y C G G P M F N S K G A Q C G Y R R
10. Patient 10
ATATACCAATGCTGCAATCTCGAACCGGAGGCCAGGAAAGTGATCACCTCCCTCACGGAACGGCTTTACTGCGGGGGCCCCATGTTCAACAGCAAGGGGGCCCAGTGTGGTTATCGCCG
Frame 1
I Y Q C C N L E P E A R K V I T S L T E R L Y C G G P M F N S K G A Q C G Y R R
11. Patient 11
ATATACCAATGTTGTACACTTGAACCGGAGGCCAGGAAAGTGATCTCCTCCCTCACGGAGCGGCTTTACTGCGGGGGCCCCATGTTCAACAGCAAGGGGGCCCAGTGCGGTTATCGCCG
Frame 1
I Y Q C C T L E P E A R K V I S S L T E R L Y C G G P M F N S K G A Q C G Y R R
12. Patient 12
ATATACCAATGCTGTAACCTTGAACCGGAGGCCAGGAAAGTGATCTCCTCCCTCACGGAACGGCTTTACTGCGGGGGCCCTATGTTTAACAGCAAGGGGGCCCAGTGTGGTTATCGCCG
Frame 1
I Y Q C C N L E P E A R K V I S S L T E R L Y C G G P M F N S K G A Q C G Y R R
13. Patient 13
ATATACCAATGCTGCAATCTTGAACCGGAGGCCAAGAAAGTGATCTCCTCCCTCACGGAGCGGCTTTACTGCGGAGGTCCTATGTTTAACAGCAAGGGAGCCCAGTGCGGTTATCGCCG
Frame 1
I Y Q C C N L E P E A K K V I S S L T E R L Y C G G P M F N S K G A Q C G Y R R
14. Patient 14
ATATACCAATGCTGTACCCTTGAGCCGGAGGCCAGGAAAGTGATCTCCTCCCTCACGGAGCGGCTTTACTGCGGGGGCCCCATGTTCAACAGCAAGGGGGCCCAGTGTGGTTATCGCCG
Frame 1
I Y Q C C T L E P E A R K V I S S L T E R L Y C G G P M F N S K G A Q C G Y R R

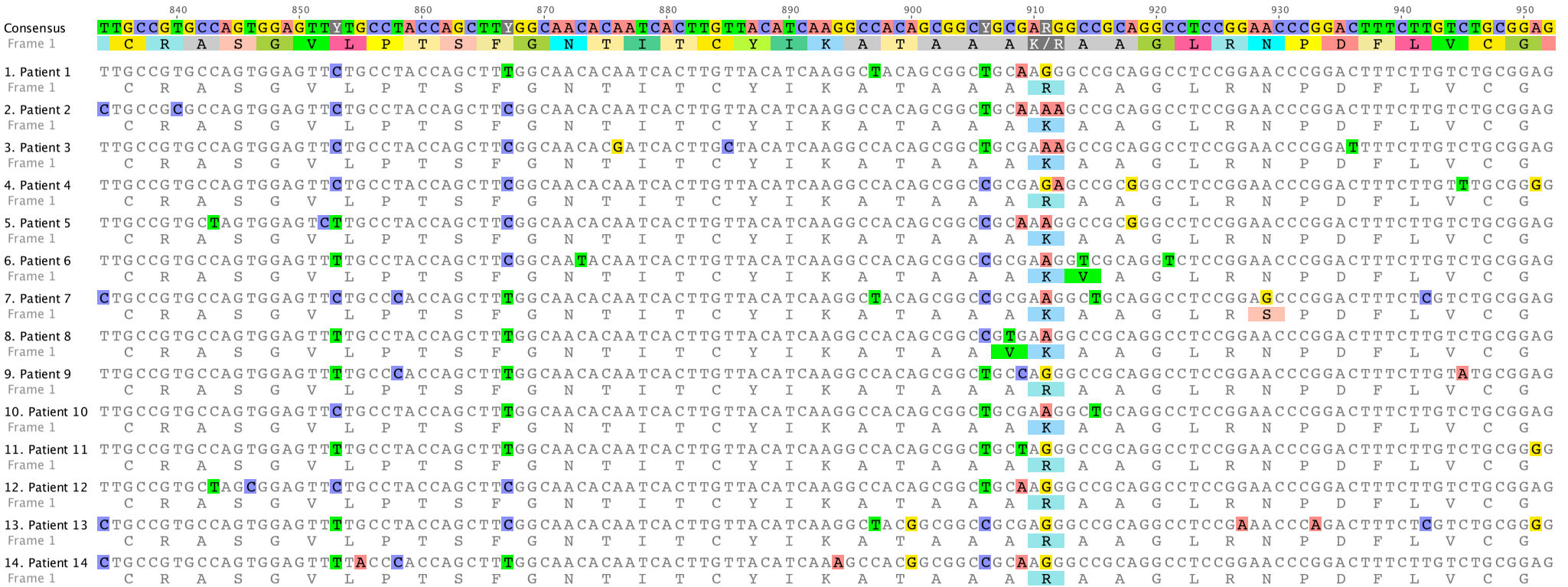
840 850 860 870 880 890 900 910 920 930 940 950
Consensus
TTGCCGTGCCAGTGGAGTTYTGCCTACCAGCTTYGGCAACACAATCACTTGTTACATCAAGGCCACAGCGGCYGCGARGGCCGCAGGCCTCCGGAACCCGGACTTTCTTGTCTGCGGAG
Frame 1
C R A S G V L P T S F G N T I T C Y I K A T A A A K/R A A G L R N P D F L V C G
1. Patient 1
TTGCCGTGCCAGTGGAGTTCTGCCTACCAGCTTTGGCAACACAATCACTTGTTACATCAAGGCTACAGCGGCTGCAAGGGCCGCAGGCCTCCGGAACCCGGACTTTCTTGTCTGCGGAG
Frame 1
C R A S G V L P T S F G N T I T C Y I K A T A A A R A A G L R N P D F L V C G
2. Patient 2
CTGCCGCGCCAGTGGAGTTCTGCCTACCAGCTTCGGCAACACAATCACTTGTTACATCAAGGCCACAGCGGCTGCAAAAGCCGCAGGCCTCCGGAACCCGGACTTTCTTGTCTGCGGAG
Frame 1
C R A S G V L P T S F G N T I T C Y I K A T A A A K A A G L R N P D F L V C G
3. Patient 3
TTGCCGTGCCAGTGGAGTTCTGCCTACCAGCTTCGGCAACACGATCACTTGCTACATCAAGGCCACAGCGGCTGCGAAAGCCGCAGGCCTCCGGAACCCGGATTTTCTTGTCTGCGGAG
Frame 1
C R A S G V L P T S F G N T I T C Y I K A T A A A K A A G L R N P D F L V C G
4. Patient 4
TTGCCGTGCCAGTGGAGTTCTGCCTACCAGCTTCGGCAACACAATCACTTGTTACATCAAGGCCACAGCGGCCGCGAGGAGCCGCGGGCCTCCGGAACCCGGACTTTCTTGTTTGCGGGG
Frame 1
C R A S G V L P T S F G N T I T C Y I K A T A A A R A A G L R N P D F L V C G
5. Patient 5
TTGCCGTGCTAGTGGAGTCTTGCCTACCAGCTTCGGCAACACAATCACTTGTTACATCAAGGCCACAGCGGCCGCAAAGGCCGCGGGCCTCCGGAACCCGGACTTTCTTGTCTGCGGAG
Frame 1
C R A S G V L P T S F G N T I T C Y I K A T A A A K A A G L R N P D F L V C G
6. Patient 6
TTGCCGTGCCAGTGGAGTTTTGCCTACCAGCTTCGGCAATACAATCACTTGTTACATCAAGGCCACAGCGGCCGCGAAGGTCGCAGGTCTCCGGAACCCGGACTTTCTTGTCTGCGGAG
Frame 1
C R A S G V L P T S F G N T I T C Y I K A T A A A K V A G L R N P D F L V C G
7. Patient 7
CTGCCGTGCCAGTGGAGTTCTGCCCACCAGCTTTGGCAACACAATCACTTGTTACATCAAGGCTACAGCGGCCGCGAAGGCTGCAGGCCTCCGGAGCCCGGACTTTCTCGTCTGCGGAG
Frame 1
C R A S G V L P T S F G N T I T C Y I K A T A A A K A A G L R S P D F L V C G
8. Patient 8
TTGCCGTGCCAGTGGAGTTTTGCCTACCAGCTTTGGCAACACAATCACTTGTTACATCAAGGCCACAGCGGCCGTGAAGGCCGCAGGCCTCCGGAACCCGGACTTTCTTGTCTGCGGAG
Frame 1
C R A S G V L P T S F G N T I T C Y I K A T A A V K A A G L R N P D F L V C G
9. Patient 9
TTGCCGTGCCAGTGGAGTTTTGCCCACCAGCTTTGGCAACACAATCACTTGTTACATCAAGGCCACAGCGGCTGCCAGGGCCGCAGGCCTCCGGAACCCGGACTTTCTTGTATGCGGAG
Frame 1
C R A S G V L P T S F G N T I T C Y I K A T A A A R A A G L R N P D F L V C G
10. Patient 10
TTGCCGTGCCAGTGGAGTTCTGCCTACCAGCTTTGGCAACACAATCACTTGTTACATCAAGGCCACAGCGGCTGCGAAGGCTGCAGGCCTCCGGAACCCGGACTTTCTTGTCTGCGGAG
Frame 1
C R A S G V L P T S F G N T I T C Y I K A T A A A K A A G L R N P D F L V C G
11. Patient 11
TTGCCGTGCCAGTGGAGTTTTGCCTACCAGCTTTGGCAACACAATCACTTGTTACATCAAGGCCACAGCGGCTGCTAGGGCCGCAGGCCTCCGGAACCCGGACTTTCTTGTCTGCGGGG
Frame 1
C R A S G V L P T S F G N T I T C Y I K A T A A A R A A G L R N P D F L V C G
12. Patient 12
TTGCCGTGCTAGCGGAGTTCTGCCTACCAGCTTCGGCAACACAATCACTTGTTACATCAAGGCCACAGCGGCTGCAAGGGCCGCAGGCCTCCGGAACCCGGACTTTCTTGTCTGCGGAG
Frame 1
C R A S G V L P T S F G N T I T C Y I K A T A A A R A A G L R N P D F L V C G
13. Patient 13
CTGCCGTGCCAGTGGAGTTTTGCCTACCAGCTTCGGCAACACAATCACTTGTTACATCAAGGCTACGGCGGCCGCGAGGGCCGCAGGCCTCCGAAACCCAGACTTTCTCGTCTGCGGGG
Frame 1
C R A S G V L P T S F G N T I T C Y I K A T A A A R A A G L R N P D F L V C G
14. Patient 14
CTGCCGTGCCAGTGGAGTTTTACCCACCAGCTTTGGCAACACAATCACTTGTTACATCAAAGCCACGGCGGCCGCAAGGGCCGCAGGCCTCCGGAACCCGGACTTTCTTGTCTGCGGAG
Frame 1
C R A S G V L P T S F G N T I T C Y I K A T A A A R A A G L R N P D F L V C G

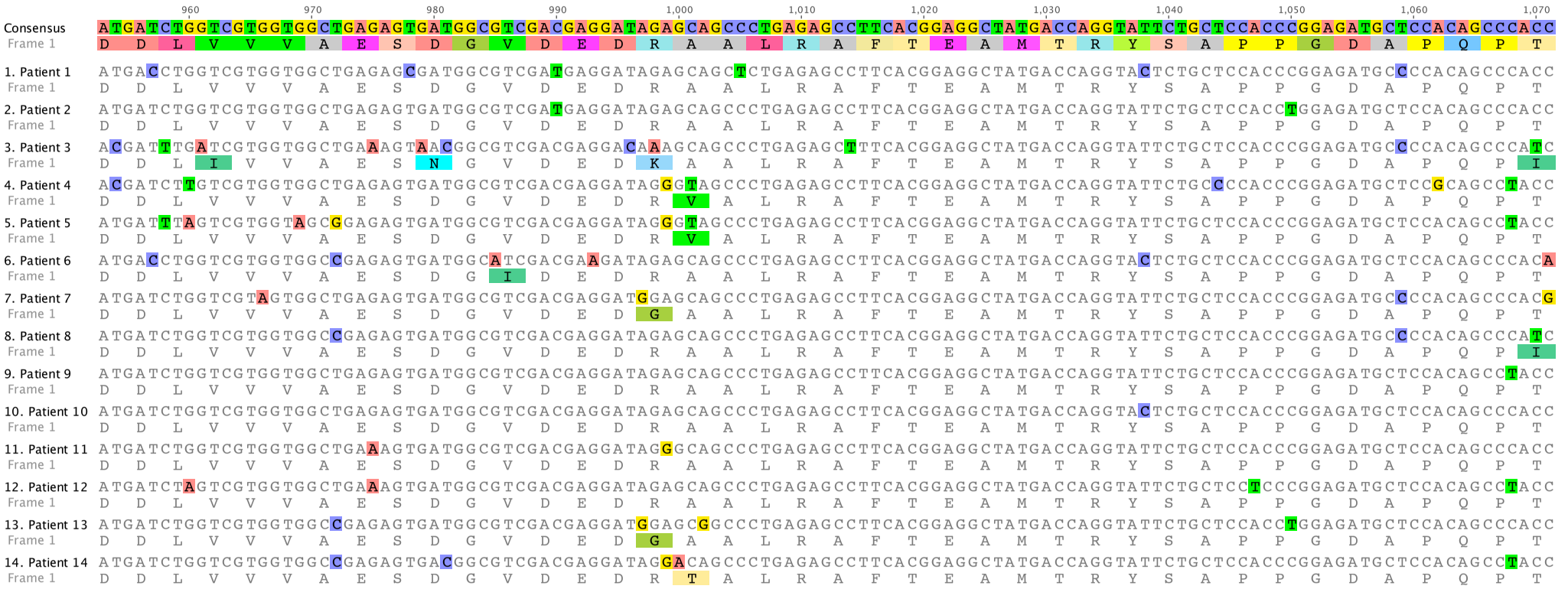
960 970 980 990 1,000 1,010 1,020 1,030 1,040 1,050 1,060 1,070
Consensus
ATGATCTGGTCGTGGTGGCTGAGAGTGATGGCGTCGACGAGGATAGAGCAGCCCTGAGAGCCTTCACGGAGGCTATGACCAGGTATTCTGCTCCACCCGGAGATGCTCCACAGCCCACC
Frame 1
D D L V V V A E S D G V D E D R A A L R A F T E A M T R Y S A P P G D A P Q P T
1. Patient 1
ATGACCTGGTCGTGGTGGCTGAGAGCGATGGCGTCGATGAGGATAGAGCAGCTCTGAGAGCCTTCACGGAGGCTATGACCAGGTACTCTGCTCCACCCGGAGATGCCCCACAGCCCACC
Frame 1
D D L V V V A E S D G V D E D R A A L R A F T E A M T R Y S A P P G D A P Q P T
2. Patient 2
ATGATCTGGTCGTGGTGGCTGAGAGTGATGGCGTCGATGAGGATAGAGCAGCCCTGAGAGCCTTCACGGAGGCTATGACCAGGTATTCTGCTCCACCTGGAGATGCTCCACAGCCCACC
Frame 1
D D L V V V A E S D G V D E D R A A L R A F T E A M T R Y S A P P G D A P Q P T
3. Patient 3
ACGATTTGATCGTGGTGGCTGAAAGTAACGGCGTCGACGAGGACAAAGCAGCCCTGAGAGCTTTCACGGAGGCTATGACCAGGTATTCTGCTCCACCCGGAGATGCCCCACAGCCCATC
Frame 1
D D L I V V A E S N G V D E D K A A L R A F T E A M T R Y S A P P G D A P Q P I
4. Patient 4
ACGATCTTGTCGTGGTGGCTGAGAGTGATGGCGTCGACGAGGATAGGGTAGCCCTGAGAGCCTTCACGGAGGCTATGACCAGGTATTCTGCCCACCCGGAGATGCTCCGCAGCCTACC
Frame 1
D D L V V V A E S D G V D E D R V A L R A F T E A M T R Y S A P P G D A P Q P T
5. Patient 5
ATGATTTAGTCGTGGTAGCGGAGAGTGATGGCGTCGACGAGGATAGGGTAGCCCTGAGAGCCTTCACGGAGGCTATGACCAGGTATTCTGCTCCACCCGGAGATGCTCCACAGCCTACC
Frame 1
D D L V V V A E S D G V D E D R V A L R A F T E A M T R Y S A P P G D A P Q P T
6. Patient 6
ATGACCTGGTCGTGGTGGCCGAGAGTGATGGCATCGACGAAGATAGAGCAGCCCTGAGAGCCTTCACGGAGGCTATGACCAGGTACTCTGCTCCACCCGGAGATGCTCCACAGCCCACA
Frame 1
D D L V V V A E S D G I D E D R A A L R A F T E A M T R Y S A P P G D A P Q P T
7. Patient 7
ATGATCTGGTCGTAGTGGCTGAGAGTGATGGCGTCGACGAGGATGGAGCAGCCCTGAGAGCCTTCACGGAGGCTATGACCAGGTATTCTGCTCCACCCGGAGATGCCCCACAGCCCACG
Frame 1
D D L V V V A E S D G V D E D G A A L R A F T E A M T R Y S A P P G D A P Q P T
8. Patient 8
ATGATCTGGTCGTGGTGGCCGAGAGTGATGGCGTCGACGAGGATAGAGCAGCCCTGAGAGCCTTCACGGAGGCTATGACCAGGTATTCTGCTCCACCCGGAGATGCCCCACAGCCCATC
Frame 1
D D L V V V A E S D G V D E D R A A L R A F T E A M T R Y S A P P G D A P Q P I
9. Patient 9
ATGATCTGGTCGTGGTGGCTGAGAGTGATGGCGTCGACGAGGATAGAGCAGCCCTGAGAGCCTTCACGGAGGCTATGACCAGGTATTCTGCTCCACCCGGAGATGCTCCACAGCCTACC
Frame 1
D D L V V V A E S D G V D E D R A A L R A F T E A M T R Y S A P P G D A P Q P T
10. Patient 10
ATGATCTGGTCGTGGTGGCTGAGAGTGATGGCGTCGACGAGGATAGAGCAGCCCTGAGAGCCTTCACGGAGGCTATGACCAGGTACTCTGCTCCACCCGGAGATGCTCCACAGCCCACC
Frame 1
D D L V V V A E S D G V D E D R A A L R A F T E A M T R Y S A P P G D A P Q P T
11. Patient 11
ATGATCTGGTCGTGGTGGCTGAAAGTGATGGCGTCGACGAGGATAGGGCAGCCCTGAGAGCCTTCACGGAGGCTATGACCAGGTATTCTGCTCCACCCGGAGATGCTCCACAGCCCACC
Frame 1
D D L V V V A E S D G V D E D R A A L R A F T E A M T R Y S A P P G D A P Q P T
12. Patient 12
ATGATCTAGTCGTGGTGGCTGAAAGTGATGGCGTCGACGAGGATAGAGCAGCCCTGAGAGCCTTCACGGAGGCTATGACCAGGTATTCTGCTCCTCCCGGAGATGCTCCACAGCCTACC
Frame 1
D D L V V V A E S D G V D E D R A A L R A F T E A M T R Y S A P P G D A P Q P T
13. Patient 13
ATGATCTGGTCGTGGTGGCCGAGAGTGATGGCGTCGACGAGGATGGAGCGGCCCTGAGAGCCTTCACGGAGGCTATGACCAGGTATTCTGCTCCACCTGGAGATGCTCCACAGCCCACC
Frame 1
D D L V V V A E S D G V D E D G A A L R A F T E A M T R Y S A P P G D A P Q P T
14. Patient 14
ATGATCTGGTCGTGGTGGCCGAGAGTGACGGCGTCGACGAGGATAGGACAGCCCTGAGAGCCTTCACGGAGGCTATGACCAGGTATTCTGCTCCACCCGGAGATGCTCCACAGCCTACC
Frame 1
D D L V V V A E S D G V D E D R T A L R A F T E A M T R Y S A P P G D A P Q P T

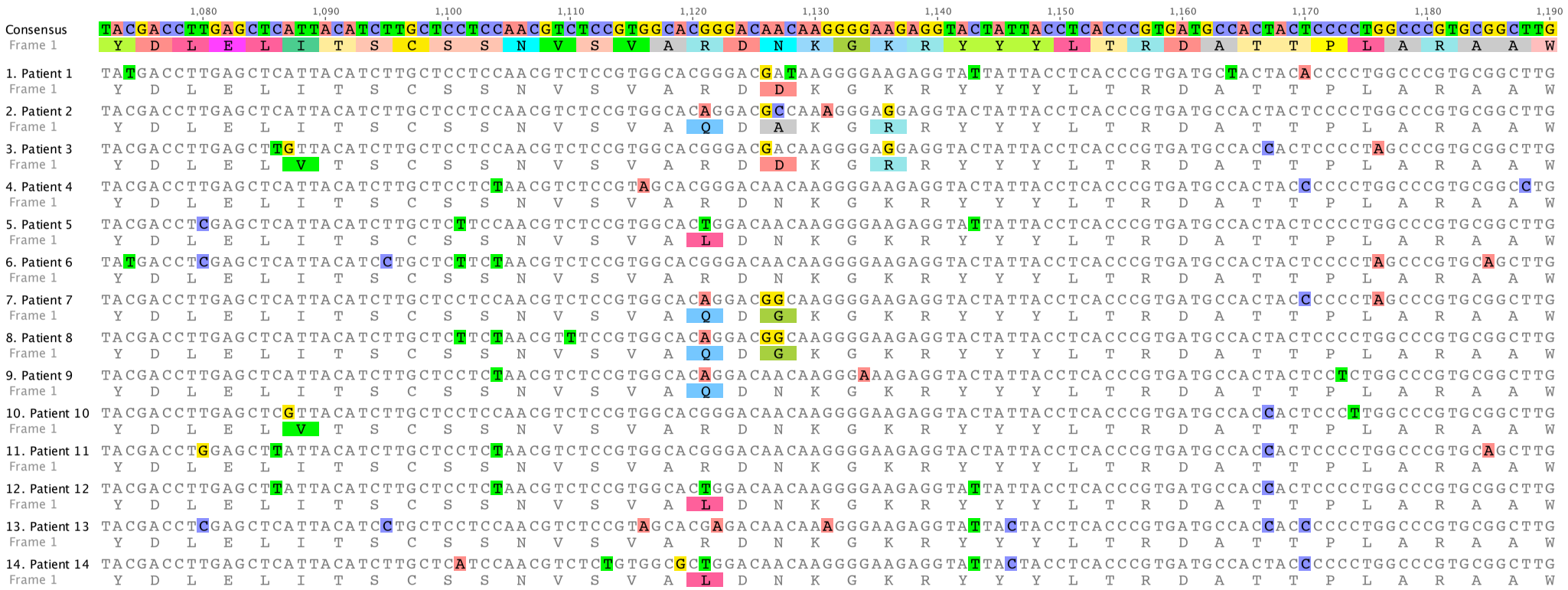
1,080
1,090
1,100
1,110
1,120
1,130
1,140
1,150
1,160
1,170
1,180
1,190
Consensus
TACGACCTTGAGCTCATTACATCTTGCTCCTCCAACGTCTCCGTGGCACGGGACAACAAGGGGAAGAGGTACTATTACCTCACCCGTGATGCCACTACTCCCCTGGCCCGTGCGGCTTG
Frame 1
Y D L E L I T S C S S N V S V A R D N K G K R Y Y Y L T R D A T T P L A R A A W
1. Patient 1
TATGACCTTGAGCTCATTACATCTTGCTCCTCCAACGTCTCCGTGGCACGGGACGATAAGGGGAAGAGGTATTATTACCTCACCCGTGATGCTACTACACCCCTGGCCCGTGCGGCTTG
Frame 1
Y D L E L I T S C S S N V S V A R D D K G K R Y Y Y L T R D A T T P L A R A A W
2. Patient 2
TACGACCTTGAGCTCATTACATCTTGCTCCTCCAACGTCTCCGTGGCACAGGACGCCAAAGGGAGGAGGTACTATTACCTCACCCGTGATGCCACTACTCCCCTGGCCCGTGCGGCTTG
Frame 1
Y D L E L I T S C S S N V S V A Q D A K G R R Y Y Y L T R D A T T P L A R A A W
3. Patient 3
TACGACCTTGAGCTTGTTACATCTTGCTCCTCCAACGTCTCCGTGGCACGGGACGACAAGGGGAGGAGGTACTATTACCTCACCCGTGATGCCACCACTCCCCTAGCCCGTGCGGCTTG
Frame 1
Y D L E L V T S C S S N V S V A R D D K G R R Y Y Y L T R D A T T P L A R A A W
4. Patient 4
TACGACCTTGAGCTCATTACATCTTGCTCCTCTAACGTCTCCGTAGCACGGGACAACAAGGGGAAGAGGTACTATTACCTCACCCGTGATGCCACTACCCCCCTGGCCCGTGCGGCCTG
Frame 1
Y D L E L I T S C S S N V S V A R D N K G K R Y Y Y L T R D A T T P L A R A A W
5. Patient 5
TACGACCTCGAGCTCATTACATCTTGCTCTTCCAACGTCTCCGTGGCACTGGACAACAAGGGGAAGAGGTATTATTACCTCACCCGTGATGCCACTACTCCCCTGGCCCGTGCGGCTTG
Frame 1
Y D L E L I T S C S S N V S V A L D N K G K R Y Y Y L T R D A T T P L A R A A W
6. Patient 6
TATGACCTCGAGCTCATTACATCCTGCTCTTCTAACGTCTCCGTGGCACGGGACAACAAGGGGAAGAGGTACTATTACCTCACCCGTGATGCCACTACTCCCCTAGCCCGTGCAGCTTG
Frame 1
Y D L E L I T S C S S N V S V A R D N K G K R Y Y Y L T R D A T T P L A R A A W
7. Patient 7
TACGACCTTGAGCTCATTACATCTTGCTCCTCCAACGTCTCCGTGGCACAGGACGGCAAGGGGAAGAGGTACTATTACCTCACCCGTGATGCCACTACCCCCCTAGCCCGTGCGGCTTG
Frame 1
Y D L E L I T S C S S N V S V A Q D G K G K R Y Y Y L T R D A T T P L A R A A W
8. Patient 8
TACGACCTTGAGCTCATTACATCTTGCTCTTCTAACGTTTCCGTGGCACAGGACGGCAAGGGGAAGAGGTACTATTACCTCACCCGTGATGCCACTACTCCCCTGGCCCGTGCGGCTTG
Frame 1
Y D L E L I T S C S S N V S V A Q D G K G K R Y Y Y L T R D A T T P L A R A A W
9. Patient 9
TACGACCTTGAGCTCATTACATCTTGCTCCTCTAACGTCTCCGTGGCACAGGACAACAAGGGAAAGAGGTACTATTACCTCACCCGTGATGCCACTACTCCTCTGGCCCGTGCGGCTTG
Frame 1
Y D L E L I T S C S S N V S V A Q D N K G K R Y Y Y L T R D A T T P L A R A A W
10. Patient 10
TACGACCTTGAGCTCGTTACATCTTGCTCCTCCAACGTCTCCGTGGCACGGGACAACAAGGGGAAGAGGTACTATTACCTCACCCGTGATGCCACCACTCCCTTGGCCCGTGCGGCTTG
Frame 1
Y D L E L V T S C S S N V S V A R D N K G K R Y Y Y L T R D A T T P L A R A A W
11. Patient 11
TACGACCTGGAGCTTATTACATCTTGCTCCTCTAACGTCTCCGTGGCACGGGACAACAAGGGGAAGAGGTACTATTACCTCACCCGTGATGCCACCACTCCCCTGGCCCGTGCAGCTTG
Frame 1
Y D L E L I T S C S S N V S V A R D N K G K R Y Y Y L T R D A T T P L A R A A W
12. Patient 12
TACGACCTTGAGCTTATTACATCTTGCTCCTCTAACGTCTCCGTGGCACTGGACAACAAGGGGAAGAGGTATTATTACCTCACCCGTGATGCCACCACTCCCCTGGCCCGTGCGGCTTG
Frame 1
Y D L E L I T S C S S N V S V A L D N K G K R Y Y Y L T R D A T T P L A R A A W
13. Patient 13
TACGACCTCGAGCTCATTACATCCTGCTCCTCCAACGTCTCCGTAGCACGAGACAACAAAGGGAAGAGGTATTACTACCTCACCCGTGATGCCACCACACCCCCTGGCCCGTGCGGCTTG
Frame 1
Y D L E L I T S C S S N V S V A R D N K G K R Y Y Y L T R D A T T P L A R A A W
14. Patient 14
TACGACCTTGAGCTCATTACATCTTGCTCATCCAACGTCTCTGTGGCGCTGGACAACAAGGGGAAGAGGTATTACTACCTCACCCGTGATGCCACTACCCCCCTGGCCCGTGCGGCTTG
Frame 1
Y D L E L I T S C S S N V S V A L D N K G K R Y Y Y L T R D A T T P L A R A A W

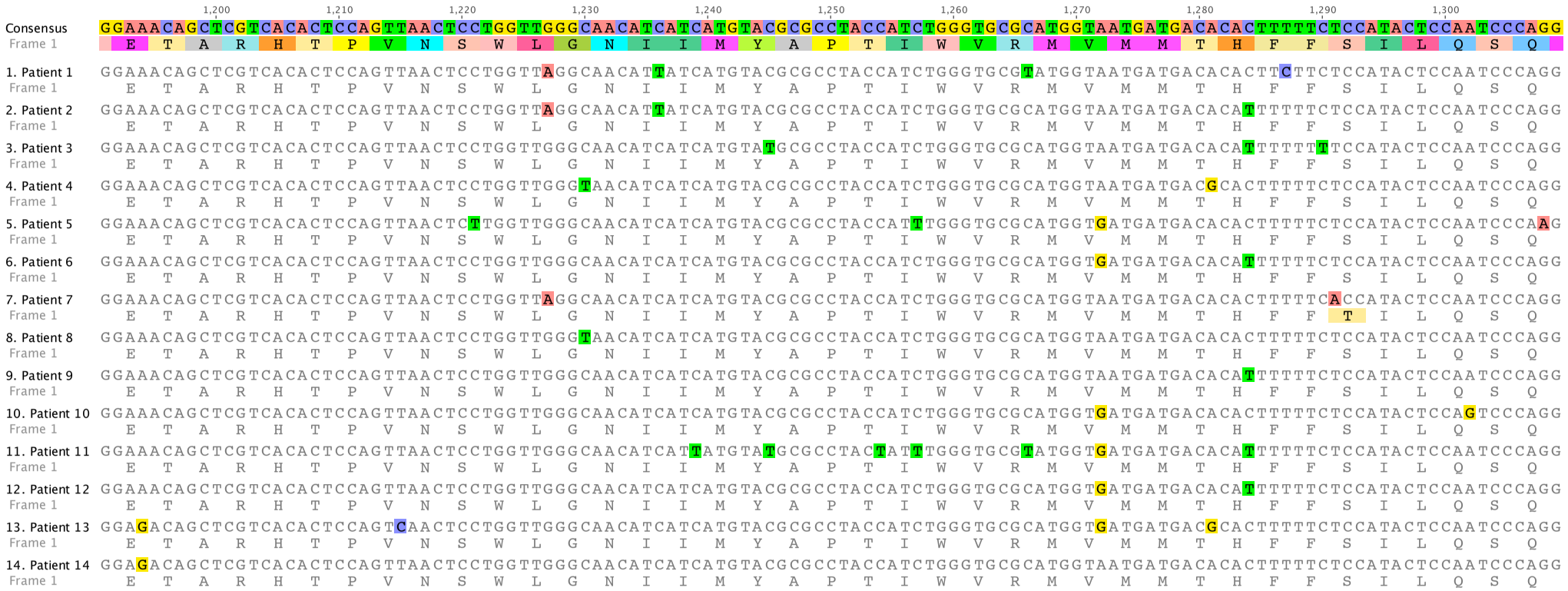
1,200
1,210
1,220
1,230
1,240
1,250
1,260
1,270
1,280
1,290
1,300
Consensus
GGAAACAGCTCGTCACACTCCAGTTAACTCCTGGTTGGGCAACATCATCATGTACGCGCCTACCATCTGGGTGCGCATGGTAATGATGACACACTTTTTCTCCATACTCCAATCCCAGG
Frame 1
E T A R H T P V N S W L G N I I M Y A P T I W V R M V M M T H F F S I L Q S Q
1. Patient 1
GGAAACAGCTCGTCACACTCCAGTTAACTCCTGGTTAGGCAACATTATCATGTACGCGCCTACCATCTGGGTGCGTATGGTAATGATGACACACTTCTTCTCCATACTCCAATCCCAGG
Frame 1
E T A R H T P V N S W L G N I I M Y A P T I W V R M V M M T H F F S I L Q S Q
2. Patient 2
GGAAACAGCTCGTCACACTCCAGTTAACTCCTGGTTAGGCAACATTATCATGTACGCGCCTACCATCTGGGTGCGCATGGTAATGATGACACATTTTTTCTCCATACTCCAATCCCAGG
Frame 1
E T A R H T P V N S W L G N I I M Y A P T I W V R M V M M T H F F S I L Q S Q
3. Patient 3
GGAAACAGCTCGTCACACTCCAGTTAACTCCTGGTTGGGCAACATCATCATGTATGCGCCTACCATCTGGGTGCGCATGGTAATGATGACACATTTTTTTTCCATACTCCAATCCCAGG
Frame 1
E T A R H T P V N S W L G N I I M Y A P T I W V R M V M M T H F F S I L Q S Q
4. Patient 4
GGAAACAGCTCGTCACACTCCAGTTAACTCCTGGTTGGGTAACATCATCATGTACGCGCCTACCATCTGGGTGCGCATGGTAATGATGACGCACTTTTTCTCCATACTCCAATCCCAGG
Frame 1
E T A R H T P V N S W L G N I I M Y A P T I W V R M V M M T H F F S I L Q S Q
5. Patient 5
GGAAACAGCTCGTCACACTCCAGTTAACTCTTGGTTGGGCAACATCATCATGTACGCGCCTACCATTTGGGTGCGCATGGTGATGATGACACACTTTTTCTCCATACTCCAATCCCAAG
Frame 1
E T A R H T P V N S W L G N I I M Y A P T I W V R M V M M T H F F S I L Q S Q
6. Patient 6
GGAAACAGCTCGTCACACTCCAGTTAACTCCTGGTTGGGCAACATCATCATGTACGCGCCTACCATCTGGGTGCGCATGGTGATGATGACACATTTTTTCTCCATACTCCAATCCCAGG
Frame 1
E T A R H T P V N S W L G N I I M Y A P T I W V R M V M M T H F F S I L Q S Q
7. Patient 7
GGAAACAGCTCGTCACACTCCAGTTAACTCCTGGTTAGGCAACATCATCATGTACGCGCCTACCATCTGGGTGCGCATGGTAATGATGACACACTTTTTCACCATACTCCAATCCCAGG
Frame 1
E T A R H T P V N S W L G N I I M Y A P T I W V R M V M M T H F F T I L Q S Q
8. Patient 8
GGAAACAGCTCGTCACACTCCAGTTAACTCCTGGTTGGGTAACATCATCATGTACGCGCCTACCATCTGGGTGCGCATGGTAATGATGACACACTTTTTCTCCATACTCCAATCCCAGG
Frame 1
E T A R H T P V N S W L G N I I M Y A P T I W V R M V M M T H F F S I L Q S Q
9. Patient 9
GGAAACAGCTCGTCACACTCCAGTTAACTCCTGGTTGGGCAACATCATCATGTACGCGCCTACCATCTGGGTGCGCATGGTAATGATGACACATTTTTTCTCCATACTCCAATCCCAGG
Frame 1
E T A R H T P V N S W L G N I I M Y A P T I W V R M V M M T H F F S I L Q S Q
10. Patient 10
GGAAACAGCTCGTCACACTCCAGTTAACTCCTGGTTGGGCAACATCATCATGTACGCGCCTACCATCTGGGTGCGCATGGTGATGATGACACACTTTTTCTCCATACTCCAGTCCCAGG
Frame 1
E T A R H T P V N S W L G N I I M Y A P T I W V R M V M M T H F F S I L Q S Q
11. Patient 11
GGAAACAGCTCGTCACACTCCAGTTAACTCCTGGTTGGGCAACATCATTATGTATGCGCCTACTATTTGGGTGCGTATGGTGATGATGACACATTTTTTCTCCATACTCCAATCCCAGG
Frame 1
E T A R H T P V N S W L G N I I M Y A P T I W V R M V M M T H F F S I L Q S Q
12. Patient 12
GGAAACAGCTCGTCACACTCCAGTTAACTCCTGGTTGGGCAACATCATCATGTACGCGCCTACCATCTGGGTGCGCATGGTGATGATGACACATTTTTTCTCCATACTCCAATCCCAGG
Frame 1
E T A R H T P V N S W L G N I I M Y A P T I W V R M V M M T H F F S I L Q S Q
13. Patient 13
GGAGACAGCTCGTCACACTCCAGTCAACTCCTGGTTGGGCAACATCATCATGTACGCGCCTACCATCTGGGTGCGCATGGTGATGATGACGCACTTTTTCTCCATACTCCAATCCCAGG
Frame 1
E T A R H T P V N S W L G N I I M Y A P T I W V R M V M M T H F F S I L Q S Q
14. Patient 14
GGAGACAGCTCGTCACACTCCAGTTAACTCCTGGTTGGGCAACATCATCATGTACGCGCCTACCATCTGGGTGCGCATGGTAATGATGACACACTTTTTCTCCATACTCCAATCCCAGG
Frame 1
E T A R H T P V N S W L G N I I M Y A P T I W V R M V M M T H F F S I L Q S Q

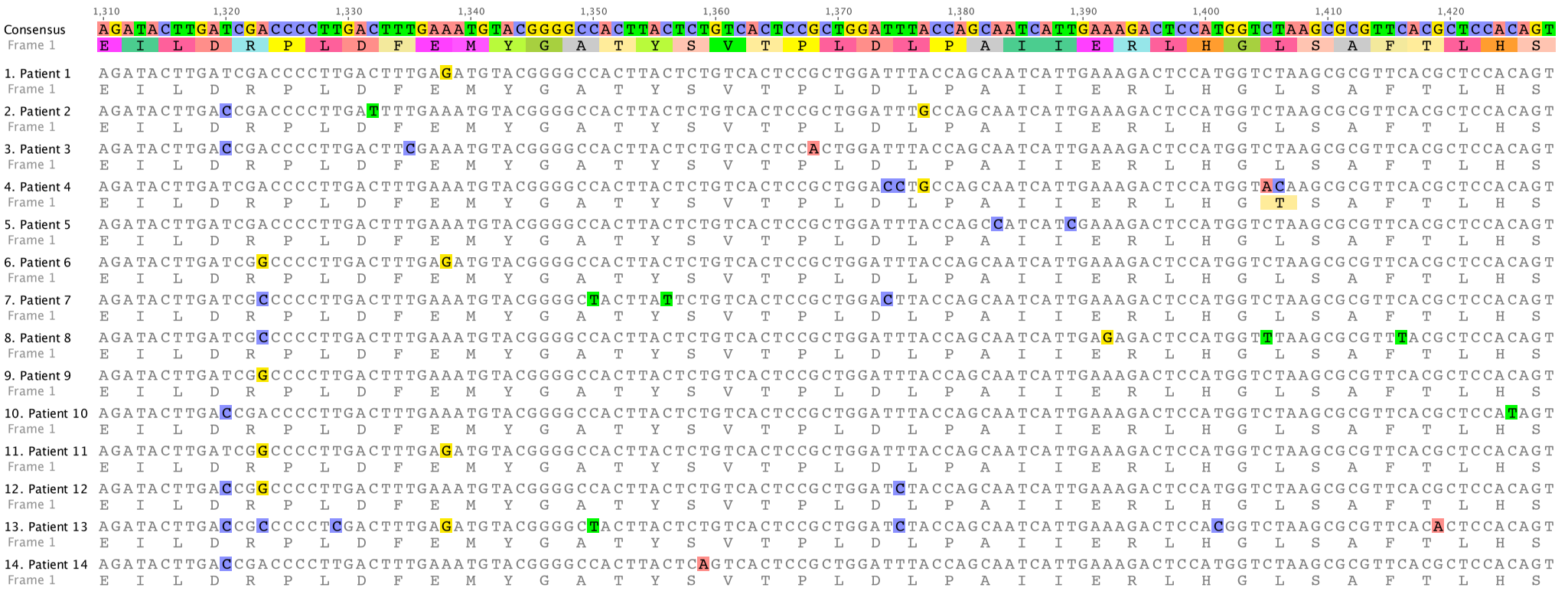
1,310 1,320 1,330 1,340 1,350 1,360 1,370 1,380 1,390 1,400 1,410 1,420
Consensus
AGATACTTGATCGACCCCTTGACTTTGAAATGTACGGGGCCACTTACTCTGTCACTCCGCTGGATTTACCAGCAATCATTGAAAGACTCCATGGTCTAAGCGCGTTCACGCTCCACAGT
Frame 1
E I L D R P L D F E M Y G A T Y S V T P L D L P A I I E R L H G L S A F T L H S
1. Patient 1
AGATACTTGATCGACCCCTTGACTTTGAGATGTACGGGGCCACTTACTCTGTCACTCCGCTGGATTTACCAGCAATCATTGAAAGACTCCATGGTCTAAGCGCGTTCACGCTCCACAGT
Frame 1
E I L D R P L D F E M Y G A T Y S V T P L D L P A I I E R L H G L S A F T L H S
2. Patient 2
AGATACTTGACCGACCCCTTGATTTTGAAATGTACGGGGCCACTTACTCTGTCACTCCGCTGGATTTGCCAGCAATCATTGAAAGACTCCATGGTCTAAGCGCGTTCACGCTCCACAGT
Frame 1
E I L D R P L D F E M Y G A T Y S V T P L D L P A I I E R L H G L S A F T L H S
3. Patient 3
AGATACTTGACCGACCCCTTGACTTCGAAATGTACGGGGCCACTTACTCTGTCACTCCACTGGATTTACCAGCAATCATTGAAAGACTCCATGGTCTAAGCGCGTTCACGCTCCACAGT
Frame 1
E I L D R P L D F E M Y G A T Y S V T P L D L P A I I E R L H G L S A F T L H S
4. Patient 4
AGATACTTGATCGACCCCTTGACTTTGAAATGTACGGGGCCACTTACTCTGTCACTCCGCTGGACCTGCCAGCAATCATTGAAAGACTCCATGGTACAAGCGCGTTCACGCTCCACAGT
Frame 1
E I L D R P L D F E M Y G A T Y S V T P L D L P A I I E R L H G T S A F T L H S
5. Patient 5
AGATACTTGATCGACCCCTTGACTTTGAAATGTACGGGGCCACTTACTCTGTCACTCCGCTGGATTTACCAGCCATCATCGAAAGACTCCATGGTCTAAGCGCGTTCACGCTCCACAGT
Frame 1
E I L D R P L D F E M Y G A T Y S V T P L D L P A I I E R L H G L S A F T L H S
6. Patient 6
AGATACTTGATCGGCCCCTTGACTTTGAGATGTACGGGGCCACTTACTCTGTCACTCCGCTGGATTTACCAGCAATCATTGAAAGACTCCATGGTCTAAGCGCGTTCACGCTCCACAGT
Frame 1
E I L D R P L D F E M Y G A T Y S V T P L D L P A I I E R L H G L S A F T L H S
7. Patient 7
AGATACTTGATCGCCCCCTTGACTTTGAAATGTACGGGGCTACTTATTCTGTCACTCCGCTGGACTTACCAGCAATCATTGAAAGACTCCATGGTCTAAGCGCGTTCACGCTCCACAGT
Frame 1
E I L D R P L D F E M Y G A T Y S V T P L D L P A I I E R L H G L S A F T L H S
8. Patient 8
AGATACTTGATCGCCCCCTTGACTTTGAAATGTACGGGGCCACTTACTCTGTCACTCCGCTGGATTTACCAGCAATCATTGAGAGACTCCATGGTTTAAGCGCGTTTACGCTCCACAGT
Frame 1
E I L D R P L D F E M Y G A T Y S V T P L D L P A I I E R L H G L S A F T L H S
9. Patient 9
AGATACTTGATCGGCCCCTTGACTTTGAAATGTACGGGGCCACTTACTCTGTCACTCCGCTGGATTTACCAGCAATCATTGAAAGACTCCATGGTCTAAGCGCGTTCACGCTCCACAGT
Frame 1
E I L D R P L D F E M Y G A T Y S V T P L D L P A I I E R L H G L S A F T L H S
10. Patient 10
AGATACTTGACCGACCCCTTGACTTTGAAATGTACGGGGCCACTTACTCTGTCACTCCGCTGGATTTACCAGCAATCATTGAAAGACTCCATGGTCTAAGCGCGTTCACGCTCCATAGT
Frame 1
E I L D R P L D F E M Y G A T Y S V T P L D L P A I I E R L H G L S A F T L H S
11. Patient 11
AGATACTTGATCGGCCCCTTGACTTTGAGATGTACGGGGCCACTTACTCTGTCACTCCGCTGGATTTACCAGCAATCATTGAAAGACTCCATGGTCTAAGCGCGTTCACGCTCCACAGT
Frame 1
E I L D R P L D F E M Y G A T Y S V T P L D L P A I I E R L H G L S A F T L H S
12. Patient 12
AGATACTTGACCGGCCCCTTGACTTTGAAATGTACGGGGCCACTTACTCTGTCACTCCGCTGGATCTACCAGCAATCATTGAAAGACTCCATGGTCTAAGCGCGTTCACGCTCCACAGT
Frame 1
E I L D R P L D F E M Y G A T Y S V T P L D L P A I I E R L H G L S A F T L H S
13. Patient 13
AGATACTTGACCGCCCCCTCGACTTTGAGATGTACGGGGCTACTTACTCTGTCACTCCGCTGGATCTACCAGCAATCATTGAAAGACTCCACGGTCTAAGCGCGTTCACACTCCACAGT
Frame 1
E I L D R P L D F E M Y G A T Y S V T P L D L P A I I E R L H G L S A F T L H S
14. Patient 14
AGATACTTGACCGACCCCTTGACTTTGAAATGTACGGGGCCACTTACTCAGTCACTCCGCTGGATTTACCAGCAATCATTGAAAGACTCCATGGTCTAAGCGCGTTCACGCTCCACAGT
Frame 1
E I L D R P L D F E M Y G A T Y S V T P L D L P A I I E R L H G L S A F T L H S

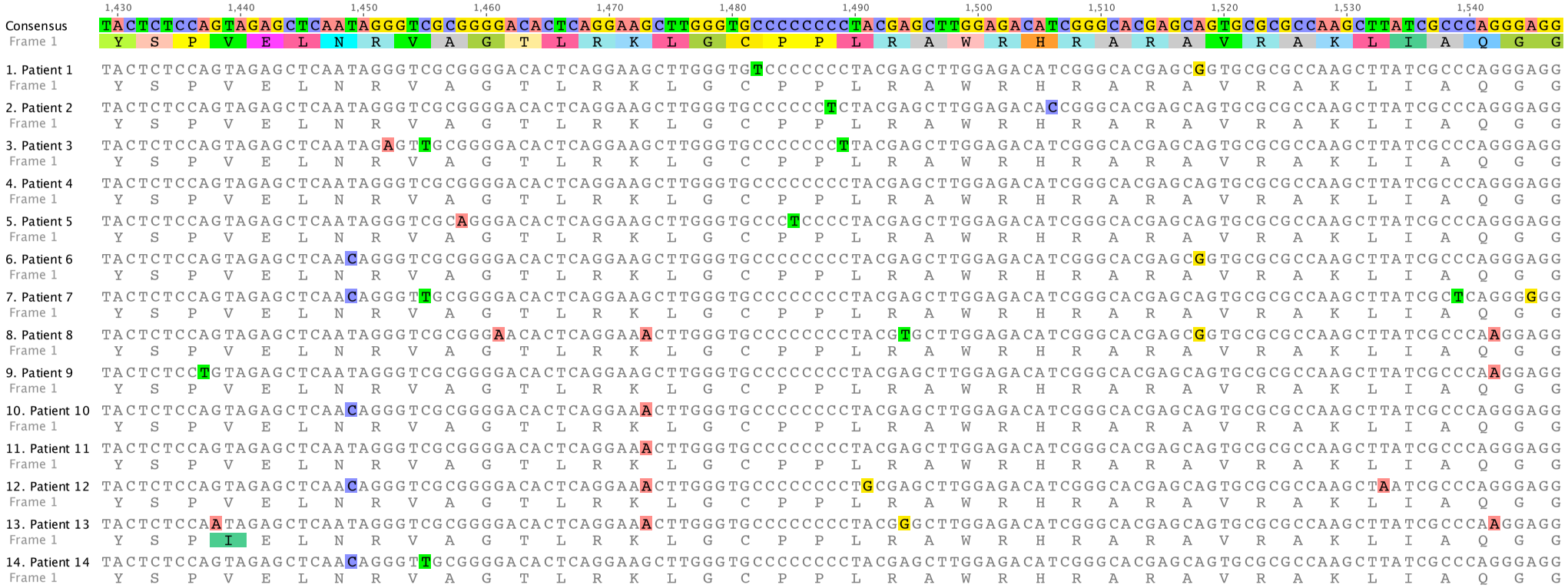
1,430
1,440
1,450
1,460
1,470
1,480
1,490
1,500
1,510
1,520
1,530
1,540
Consensus
Frame 1
1. Patient 1
2. Patient 2
3. Patient 3
4. Patient 4
5. Patient 5
6. Patient 6
7. Patient 7
8. Patient 8
9. Patient 9
10. Patient 10
11. Patient 11
12. Patient 12
13. Patient 13
14. Patient 14

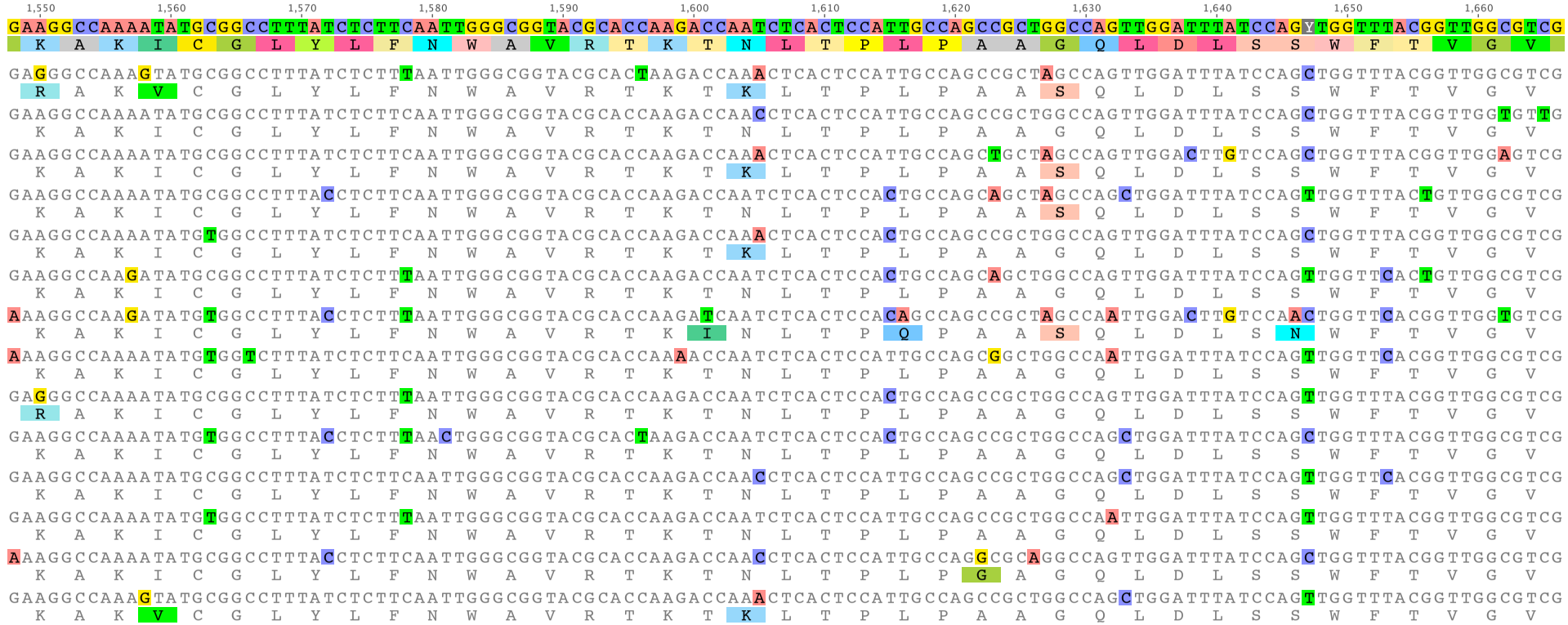
1,550
1,560
1,570
1,580
1,590
1,600
1,610
1,620
1,630
1,640
1,650
1,660
Consensus
GAAGGCCAAAATATGCGGCCTTTATCTCTTCAATTGGGCGGTACGCACCAAGACCAATCTCACTCCATTGCCAGCCGCTGGCCAGTTGGATTTATCCAGYTGGTTTACGGTTGGCGTCG
Frame 1
K A K I C G L Y L F N W A V R T K T N L T P L P A A G Q L D L S S W F T V G V
1. Patient 1
GAGGGCCAAAGTATGCGGCCTTTATCTCTTTAATTGGGCGGTACGCACTAAGACCAAACTCACTCCATTGCCAGCCGCTAGCCAGTTGGATTTATCCAGCTGGTTTACGGTTGGCGTCG
Frame 1
R A K V C G L Y L F N W A V R T K T K L T P L P A A S Q L D L S S W F T V G V
2. Patient 2
GAAGGCCAAAATATGCGGCCTTTATCTCTTCAATTGGGCGGTACGCACCAAGACCAACCTCACTCCATTGCCAGCCGCTGGCCAGTTGGATTTATCCAGCTGGTTTACGGTTGGTGTTG
Frame 1
K A K I C G L Y L F N W A V R T K T N L T P L P A A G Q L D L S S W F T V G V
3. Patient 3
GAAGGCCAAAATATGCGGCCTTTATCTCTTCAATTGGGCGGTACGCACCAAGACCAAACTCACTCCATTGCCAGCTGCTAGCCAGTTGGACTTGTCCAGCTGGTTTACGGTTGGAGTCG
Frame 1
K A K I C G L Y L F N W A V R T K T K L T P L P A A S Q L D L S S W F T V G V
4. Patient 4
GAAGGCCAAAATATGCGGCCTTTACCTCTTCAATTGGGCGGTACGCACCAAGACCAATCTCACTCCACTGCCAGCAGCTAGCCAGCTGGATTTATCCAGTTGGTTTACTGTTGGCGTCG
Frame 1
K A K I C G L Y L F N W A V R T K T N L T P L P A A S Q L D L S S W F T V G V
5. Patient 5
GAAGGCCAAAATATGTGGCCTTTATCTCTTCAATTGGGCGGTACGCACCAAGACCAAACTCACTCCACTGCCAGCCGCTGGCCAGTTGGATTTATCCAGCTGGTTTACGGTTGGCGTCG
Frame 1
K A K I C G L Y L F N W A V R T K T K L T P L P A A G Q L D L S S W F T V G V
6. Patient 6
GAAGGCCAAGATATGCGGCCTTTATCTCTTTAATTGGGCGGTACGCACCAAGACCAATCTCACTCCACTGCCAGCAGCTGGCCAGTTGGATTTATCCAGTTGGTTCACTGTTGGCGTCG
Frame 1
K A K I C G L Y L F N W A V R T K T N L T P L P A A G Q L D L S S W F T V G V
7. Patient 7
AAAGGCCAAGATATGTGGCCTTTACCTCTTTAATTGGGCGGTACGCACCAAGATCAATCTCACTCCACAGCCAGCCGCTAGCCAATTGGACTTGTCCAACTGGTTCACGGTTGGTGTCG
Frame 1
K A K I C G L Y L F N W A V R T K I N L T P Q P A A S Q L D L S N W F T V G V
8. Patient 8
AAAGGCCAAAATATGTGGTCTTTATCTCTTCAATTGGGCGGTACGCACCAAAACCAATCTCACTCCATTGCCAGCGGCTGGCCAATTGGATTTATCCAGTTGGTTCACGGTTGGCGTCG
Frame 1
K A K I C G L Y L F N W A V R T K T N L T P L P A A G Q L D L S S W F T V G V
9. Patient 9
GAGGGCCAAAATATGCGGCCTTTATCTCTTTAATTGGGCGGTACGCACCAAGACCAATCTCACTCCACTGCCAGCCGCTGGCCAGTTGGATTTATCCAGTTGGTTTACGGTTGGCGTCG
Frame 1
R A K I C G L Y L F N W A V R T K T N L T P L P A A G Q L D L S S W F T V G V
10. Patient 10
GAAGGCCAAAATATGTGGCCTTTACCTCTTTAACTGGGCGGTACGCACTAAGACCAATCTCACTCCACTGCCAGCCGCTGGCCAGCTGGATTTATCCAGCTGGTTTACGGTTGGCGTCG
Frame 1
K A K I C G L Y L F N W A V R T K T N L T P L P A A G Q L D L S S W F T V G V
11. Patient 11
GAAGGCCAAAATATGCGGCCTTTATCTCTTCAATTGGGCGGTACGCACCAAGACCAACCTCACTCCATTGCCAGCCGCTGGCCAGCTGGATTTATCCAGTTGGTTCACGGTTGGCGTCG
Frame 1
K A K I C G L Y L F N W A V R T K T N L T P L P A A G Q L D L S S W F T V G V
12. Patient 12
GAAGGCCAAAATATGTGGCCTTTATCTCTTTAATTGGGCGGTACGCACCAAGACCAATCTCACTCCATTGCCAGCCGCTGGCCAATTGGATTTATCCAGTTGGTTTACGGTTGGCGTCG
Frame 1
K A K I C G L Y L F N W A V R T K T N L T P L P A A G Q L D L S S W F T V G V
13. Patient 13
AAAGGCCAAAATATGCGGCCTTTACCTCTTCAATTGGGCGGTACGCACCAAGACCAACCTCACTCCATTGCCAGGCGCCAGGCCAGTTGGATTTATCCAGCTGGTTTACGGTTGGCGTCG
Frame 1
K A K I C G L Y L F N W A V R T K T N L T P L P G A G Q L D L S S W F T V G V
14. Patient 14
GAAGGCCAAAGGTATGCGGCCTTTATCTCTTCAATTGGGCGGTACGCACCAAGACCAAACTCACTCCATTGCCAGCCGCTGGCCAGCTGGATTTATCCAGTTGGTTTACGGTTGGCGTCG
Frame 1
K A K V C G L Y L F N W A V R T K T K L T P L P A A G Q L D L S S W F T V G V

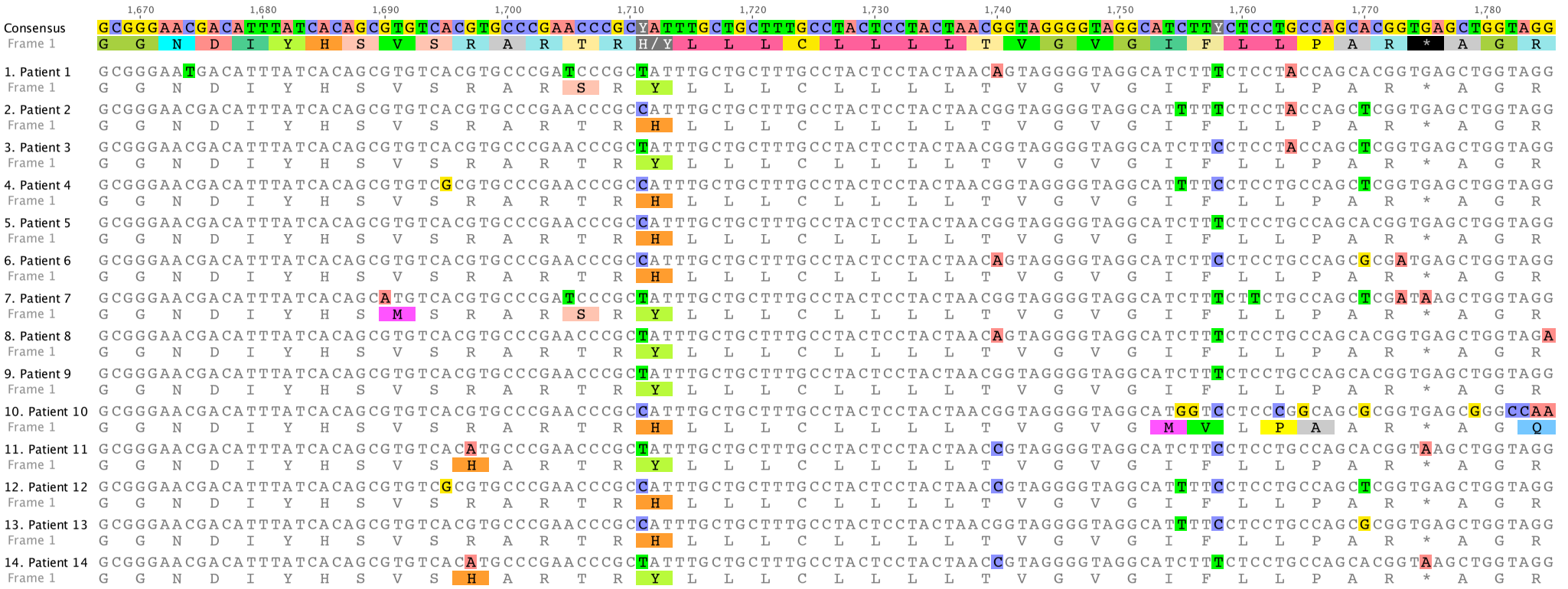
1,670
1,680
1,690
1,700
1,710
1,720
1,730
1,740
1,750
1,760
1,770
1,780
Consensus
GCGGGAACGACATTTATCACAGCGTGTCACGTGCCCGAACCCGCYATTTGCTGCTTTGCCTACTCCTACTAACGGTAGGGGTAGGCATCTTYCTCCTGCCAGCACGGTGAGCTGGTAGG
Frame 1
G G N D I Y H S V S R A R T R H/Y L L L C L L L L T V G V G I F L L P A R * A G R
1. Patient 1
GCGGGAATGACATTTATCACAGCGTGTCACGTGCCCGATCCCGCTATTTGCTGCTTTGCCTACTCCTACTAACAGTAGGGGTAGGCATCTTTCTCCTACCAGCACGGTGAGCTGGTAGG
Frame 1
G G N D I Y H S V S R A R S R Y L L L C L L L L T V G V G I F L L P A R * A G R
2. Patient 2
GCGGGAACGACATTTATCACAGCGTGTCACGTGCCCGAACCCGCCATTTGCTGCTTTGCCTACTCCTACTAACGGTAGGGGTAGGCATTTTTCTCCTACCAGCTCGGTGAGCTGGTAGG
Frame 1
G G N D I Y H S V S R A R T R H L L L C L L L L T V G V G I F L L P A R * A G R
3. Patient 3
GCGGGAACGACATTTATCACAGCGTGTCACGTGCCCGAACCCGCTATTTGCTGCTTTGCCTACTCCTACTAACGGTAGGGGTAGGCATCTTCCTCCTACCAGCTCGGTGAGCTGGTAGG
Frame 1
G G N D I Y H S V S R A R T R Y L L L C L L L L T V G V G I F L L P A R * A G R
4. Patient 4
GCGGGAACGACATTTATCACAGCGTGTCGCGTGCCCGAACCCGCCATTTGCTGCTTTGCCTACTCCTACTAACGGTAGGGGTAGGCATTTTCCTCCTGCCAGCTCGGTGAGCTGGTAGG
Frame 1
G G N D I Y H S V S R A R T R H L L L C L L L L T V G V G I F L L P A R * A G R
5. Patient 5
GCGGGAACGACATTTATCACAGCGTGTCACGTGCCCGAACCCGCCATTTGCTGCTTTGCCTACTCCTACTAACGGTAGGGGTAGGCATCTTTCTCCTGCCAGCACGGTGAGCTGGTAGG
Frame 1
G G N D I Y H S V S R A R T R H L L L C L L L L T V G V G I F L L P A R * A G R
6. Patient 6
GCGGGAACGACATTTATCACAGCGTGTCACGTGCCCGAACCCGCCATTTGCTGCTTTGCCTACTCCTACTAACAGTAGGGGTAGGCATCTTCCTCCTGCCAGCGCGATGAGCTGGTAGG
Frame 1
G G N D I Y H S V S R A R T R H L L L C L L L L T V G V G I F L L P A R * A G R
7. Patient 7
GCGGGAACGACATTTATCACAGCATGTCACGTGCCCGATCCCGCTATTTGCTGCTTTGCCTACTCCTACTAACGGTAGGGGTAGGCATCTTTCTTCTGCCAGCTCGATAAGCTGGTAGG
Frame 1
G G N D I Y H S M S R A R S R Y L L L C L L L L T V G V G I F L L P A R * A G R
8. Patient 8
GCGGGAACGACATTTATCACAGCGTGTCACGTGCCCGAACCCGCTATTTGCTGCTTTGCCTACTCCTACTAACAGTAGGGGTAGGCATCTTTCTCCTGCCAGCACGGTGAGCTGGTAGA
Frame 1
G G N D I Y H S V S R A R T R Y L L L C L L L L T V G V G I F L L P A R * A G R
9. Patient 9
GCGGGAACGACATTTATCACAGCGTGTCACGTGCCCGAACCCGCTATTTGCTGCTTTGCCTACTCCTACTAACGGTAGGGGTAGGCATCTTTCTCCTGCCAGCACGGTGAGCTGGTAGG
Frame 1
G G N D I Y H S V S R A R T R Y L L L C L L L L T V G V G I F L L P A R * A G R
10. Patient 10
GCGGGAACGACATTTATCACAGCGTGTCACGTGCCCGAACCCGCCATTTGCTGCTTTGCCTACTCCTACTAACGGTAGGGGTAGGCATGGTCCTCCCGGCAGCGCGGTGAGCGGGCCAA
Frame 1
G G N D I Y H S V S R A R T R H L L L C L L L L T V G V G M V L P A A R * A G Q
11. Patient 11
GCGGGAACGACATTTATCACAGCGTGTCACATGCCCGAACCCGCTATTTGCTGCTTTGCCTACTCCTACTAACCGTAGGGGTAGGCATCTTCCTCCTGCCAGCACGGTAAGCTGGTAGG
Frame 1
G G N D I Y H S V S H A R T R Y L L L C L L L L T V G V G I F L L P A R * A G R
12. Patient 12
GCGGGAACGACATTTATCACAGCGTGTCGCGTGCCCGAACCCGCCATTTGCTGCTTTGCCTACTCCTACTAACCGTAGGGGTAGGCATTTTCCTCCTGCCAGCTCGGTGAGCTGGTAGG
Frame 1
G G N D I Y H S V S R A R T R H L L L C L L L L T V G V G I F L L P A R * A G R
13. Patient 13
GCGGGAACGACATTTATCACAGCGTGTCACGTGCCCGAACCCGCCATTTGCTGCTTTGCCTACTCCTACTAACGGTAGGGGTAGGCATTTTCCTCCTGCCAGCGCGGTGAGCTGGTAGG
Frame 1
G G N D I Y H S V S R A R T R H L L L C L L L L T V G V G I F L L P A R * A G R
14. Patient 14
GCGGGAACGACATTTATCACAGCGTGTCACATGCCCGAACCCGCTATTTGCTGCTTTGCCTACTCCTACTAACCGTAGGGGTAGGCATCTTTCTCCTGCCAGCACGGTAAGCTGGTAGG
Frame 1
G G N D I Y H S V S H A R T R Y L L L C L L L L T V G V G I F L L P A R * A G R

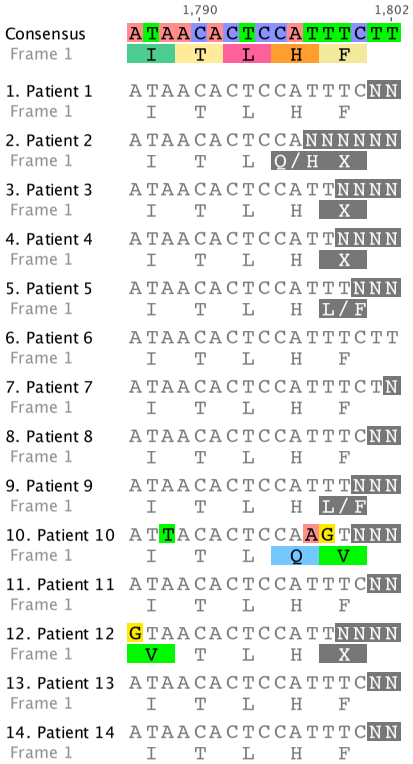
1,790
1,802
Consensus
ATAACACTCCATTTCTT
Frame 1
I T L H F
1. Patient 1
ATAACACTCCATTTCNN
Frame 1
I T L H F
2. Patient 2
ATAACACTCCANNNNNN
Frame 1
I T L Q/H X
3. Patient 3
ATAACACTCCATTNNNN
Frame 1
I T L H X
4. Patient 4
ATAACACTCCATTNNNN
Frame 1
I T L H X
5. Patient 5
ATAACACTCCATTTNNN
Frame 1
I T L H L/F
6. Patient 6
ATAACACTCCATTTCTT
Frame 1
I T L H F
7. Patient 7
ATAACACTCCATTTCTN
Frame 1
I T L H F
8. Patient 8
ATAACACTCCATTTCNN
Frame 1
I T L H F
9. Patient 9
ATAACACTCCATTTNNN
Frame 1
I T L H L/F
10. Patient 10
ATTACACTCCAAGTNNN
Frame 1
I T L Q V
11. Patient 11
ATAACACTCCATTTCNN
Frame 1
I T L H F
12. Patient 12
GTAACACTCCATTNNNN
Frame 1
V T L H X
13. Patient 13
ATAACACTCCATTTCNN
Frame 1
I T L H F
14. Patient 14
ATAACACTCCATTTCNN
Frame 1
I T L H F